

**UNDERSTANDING OF THE VARIABILITY OF PHYTOPLANKTON  
ECOSYSTEM FUNCTION PROPERTIES: A SYNERGISTIC USE OF  
REMOTE SENSING AND *IN SITU* DATA**

by

**DIONYSIOS RAITOS-EXARCHOPOULOS**

A thesis submitted to the University of Plymouth  
in partial fulfilment for the degree of

**DOCTOR OF PHILOSOPHY**

School of Earth, Ocean and Environmental Sciences  
Faculty of Science

In collaboration with  
Sir Alister Hardy Foundation for Ocean Science

**AUGUST 2006**

*To my family:*

Thanasis, Eleni, Giannis, Elena, Afroula

# Understanding of the variability of phytoplankton ecosystem function properties: a synergistic use of remote sensing and *in situ* data

Dionysios Raitsos-Exarchopoulos

The majority of the earth's surface (~71%) is covered by the aquatic environment where 97% of that is the oceanic regime. Almost every part of the aquatic regime is dominated by microscopic plants called phytoplankton. Being at the bottom of the food chain, these ecological drivers influence the earth's climate system as well as the biodiversity trends of other organisms such as zooplankton, fish, sea birds and marine mammals.

The aim of this research was to understand the ecology of phytoplankton and assess which environmental, physical, biological, and spatiotemporal factors influence their distribution and abundance. Using this information a knowledge-based expert system discriminated phytoplankton functional types. The ecological knowledge was derived from the Continuous Plankton Recorder (CPR) survey, whereas information regarding the physical regime was acquired from satellite remote sensing. The data matrix was analysed using Generalised Additive Models (GAMs) and Artificial Neural Networks (ANNs).

The significant relationships developed by the synergistic use of CPR measure of phytoplankton biomass and satellite chlorophyll a (Chl-a), allowed the production of a >50 years Chl-a dataset in the Northeast Atlantic and North Sea. It was found that the documented mid-80s regime shift corresponded to a 60% increase in Chl-a since 1948; a result of an 80% increase in Chl-a during winter alongside a smaller summer increase.

GAMs indicated that the combined effects of high solar radiation, shallow mixed layer depth and increased temperatures explained more than 89% of the coccolithophore variation. The June 1998 bloom, which was associated with high light intensity, unusually high sea-surface temperature (SST) and a very shallow mixed layer, was found to be one of the most extensive (~1 million km<sup>2</sup>) blooms ever recorded. There was a pronounced SST shift in the mid-1990s with a peak in 1998, suggesting that exceptionally large blooms are caused by pronounced environmental conditions and the variability of the physical environment strongly affects the spatial extent of these blooms.

Diatom abundance in the epipelagic zone of the Northern North Atlantic was mainly driven by SST. The ANNs indicated that higher SSTs could lead to a rapid decrease in diatom abundance; increased SST can stratify the water column for longer preventing nutrients from being available. Therefore, further increases may be devastating to diatoms but may benefit smaller plankton such as coccolithophores and/or dinoflagellates.

Finally, the knowledge gained through the developed methodological approaches was used to identify/discriminate phytoplankton functional groups (diatoms, dinoflagellates, coccolithophores and silicoflagellates) with an accuracy of greater than 70%. The most important information for phytoplankton functional group discrimination was spatiotemporal information, and for the physical environment was SST. Future research aimed at the identification of functional groups from remotely sensed data should include fundamental information on the physical environment as well as spatiotemporal information and not just based on bio-optical measurements. Further development, potential applications and future research are discussed.

# List of Contents

	Page
<b>Chapter 1: Literature Review – Aims and Objectives</b>	<b>19</b>
1.1 A Short History of the CPR Survey.....	20
1.1.1 Sampling Method.....	21
1.1.2 CPR Analysis: The Phytoplankton Colour Index and Species.....	22
1.1.3 The Value of Biological Time Series.....	23
1.1.4 Statistical Methods Overview.....	24
1.2 An Introduction to Satellite Remote Sensing.....	26
1.2.1 Ocean Colour Data.....	26
1.2.2 Ocean Colour Sensors.....	28
1.2.3 Sea Surface Temperature Data.....	30
1.2.4 Sea Surface Temperature Sensors.....	31
1.2.5 Altimetry, Wind Speed/Stress data.....	32
1.2.6 Altimetry, Wind Speed/Stress Satellites.....	35
1.3 Aims and Objectives.....	36
<b>Chapter 2: From silk to satellite: A half century of ocean colour</b>	<b>39</b>
2 Rationale.....	40
2.1 Introduction.....	40
2.2 Methodology.....	41
2.2.1 The Phytoplankton Colour Index of the CPR Survey.....	41
2.2.2 Laboratory Experiment.....	42
2.2.2.1 Sample Analysis.....	42
2.2.2.2 Assessment of Chl-a by Fluorescence.....	45
2.2.3 Synergistic Use of PCI and SeaWiFS.....	46
2.2.3.1 Satellite Data.....	47
2.2.3.2 Data Analysis.....	47
2.2.3.3 Potential Biases.....	47
2.3 Results.....	48
2.3.1 Laboratory Chl-a/PCI Intercomparison.....	48
2.3.2 PCI versus SeaWiFS.....	51
2.4 Conclusions.....	57
2.4.1 Laboratory Experiment.....	57
2.4.2 PCI versus SeaWiFS.....	57
<b>Chapter 3: Phytoplankton variations as a response to the environmental regime</b>	<b>58</b>
3.1 Introduction.....	59
3.1.1 Coccolithophores.....	59
3.1.2 Diatoms.....	61
3.2 Aims and Objectives.....	63
3.3 Methods.....	64
3.3.1 Coccolithophores.....	64
3.3.1.1 Data and Methods.....	64
3.3.1.2 Satellite Data.....	65
3.3.1.3 OCCAM Model Data.....	68

3.3.1.4 In situ Data.....	68
3.3.1.5 Data Analysis.....	69
3.3.2 Diatoms.....	69
3.3.2.1 Satellite Data.....	70
3.3.2.2 In situ Data.....	71
3.3.2.3 Methodology for Data Collation.....	71
3.3.2.4 Data Analysis Using Artificial Neural Networks.....	72
3.4 Results.....	73
3.4.1 Coccolithophores.....	73
3.4.2 Diatoms.....	81
3.5 Conclusion.....	85
3.5.1 Coccolithophores.....	88
3.5.2 Diatoms.....	89
<b>Chapter 4: Identifying phytoplankton functional groups from space: an ecological approach</b>	<b>90</b>
4.1 Introduction.....	91
4.2 Methods and Data Analysis.....	92
4.2.1 Methodological Approach.....	92
4.2.2 Phytoplankton Functional Groups.....	93
4.2.3 Potential Biases.....	94
4.2.4 Data Analysis Using Artificial Neural Networks.....	94
4.2.4.1 Probabilistic Neural Network (PNN) .....	94
4.3 Results.....	97
4.4 Conclusion.....	101
<b>Chapter 5: Discussion and future research</b>	<b>103</b>
5.1 General Discussion.....	104
5.1.1 Ocean Colour: Validation of PCI Through In situ and Satellite Chl-a.....	104
5.1.1.1 PCI versus In situ Chl-a.....	104
5.1.1.2 PCI versus Satellite Chl-a.....	105
5.1.1.3 The use of PCI to Validate the Satellite Signal in CASE II Waters.....	107
5.1.1.4 The Usage of the New Chl-a Dataset.....	109
5.1.1.4.1 Overview.....	109
5.1.2 Phytoplankton Groups and their Relation to Macroscale Factors Derived from Remotely Sensed Data.....	110
5.1.2.1 The value of Using Advanced Statistical Tools.....	111
5.1.2.2 Coccolithophores.....	112
5.1.2.3 Diatoms.....	114
5.1.2.3.1 Diatom Populations and their Relation to Climatological Changes.....	115
5.1.2.3.2 Conclusion.....	116
5.1.3 Discriminating Phytoplankton Groups from Space.....	117
5.1.4 Surface Temperatures in Relation to Phytoplankton.....	119
5.2 Future Research.....	117
5.2.1 Predicting Phytoplankton Future Distribution and Abundances.....	121

5.2.2 Coccolithophores: What is Known and What Remains still Undiscovered.....	124
5.2.3 The use of PCI Ocean Colour Data to link SeaWiFS and CZCS Sensors.....	126
<b>Appendix I.....</b>	<b>128</b>
<b>References.....</b>	<b>185</b>

## ***List of Figures***

- Figure 1.1:*** Continuous Plankton Recorder sampling routes in the Atlantic Ocean and North Sea from 1946 to 2005 (SAHFOS 2003). The letters on the map stand for the name of each route. ....21
- Figure 1.2:*** A side view of the Continuous Plankton Recorder, including the plankton filtering mechanism, and a photograph of the instrument (SAHFOS, 2003). The figure has been slightly modified by the author in order to highlight the major parts of the equipment which are addressed in the text. ....22
- Figure 1.3:*** SeaWiFS global monthly composites of Chl-a, light intensity (PAR) and normalised water leaving radiance (nLw) at 555nm. ....28
- Figure 1.4:*** An artist's side view of the SeaWiFS sensor. The figure has been taken from NASA (<http://www.nasa.gov/>) and has been slightly modified by the author. ....29
- Figure 1.5:*** Global monthly SST composite from Aqua MODIS. ....31
- Figure 1.6:*** Global Image of Sea Surface Height (*Taken from <http://www.esad.ssc.nasa.gov/>*)..... 34
- Figure 1.7:*** Global Image of wind stress taken by the European Remote Sensing Satellite (ERS). ....33
- Figure 1.8:*** Synoptic view of the data as well as the methodological approach that was used to develop the Knowledge-based Expert System to discriminate phytoplankton groups from space. ....38
- Figure 2.1:*** Positions of the CPR samples (n= 76) collected from 2004-2006 in the British Channel.....42

**Figure 2.2:** The top of the figure shows a CPR silk sample with outlined division areas used for analysis. Below is a side view of the Continuous Plankton Recorder, illustrating the entrance (where the water comes in) as well as the filtering and covering silk.....44

**Figure 2.3:** a) Location of CPR samples (n= 94,376) in the Central Northeast Atlantic Ocean and North Sea for the period 1948-2002. b) Distribution of match-ups of CPR /SeaWiFS measurements (n= 1585) for the years 1997 - 2002. ....46

**Figure 2.4:** Mean Chl-a concentration (mg per CPR sample) and distribution of Chl-a samples (n= 228) per PCI category. The PCI is a ratio scale of phytoplankton colour with four 'greenness' values: 0 (NG - no greenness), 1 (VPG - very pale green), 2 (PG - pale green) and 6.5 (G - green). Note, there is no overlap between confidence intervals for each PCI category. The mean Chl-a plot indicated that NG= 0.05, VPG= 1.68, PG= 3.98, and G= 7.72 mg/sample. ....49

**Figure 2.5:** Mean Chl-a concentration (mg per CPR sample) and distribution of Chl-a across CPR samples. Every CPR sample (n= 76) was cut into 3 equal parts (n= 228). LH= Left Hand, C= Centre and RH= Right Hand part of the CPR silks.....51

**Figure 2.6:** a) Mean Chl-a derived from SeaWiFS match-ups with CPR samples plotted against the equivalent values of PCI categories. Standard error bars represent 95% confidence intervals of the mean Chl-a. Note there is no overlap between confidence intervals for each PCI category. The number of samples (n) for each category is: No Green (NG)= 219, Very Pale Green (VPG)= 723, Pale Green (PG)= 484 and Green (G)= 162 of the 1585 match-ups. b) The seasonal cycle of Chl-a estimated from PCI and SeaWiFS for all match-ups in the area of interest. Error bars represent 95% confidence intervals. ....53



- Figure 2.7:** Time series of the new Chl-a dataset (monthly average) for the period 1948 to 2002 in the Central Northeast Atlantic and North Sea. The annual mean of Chl-a is plotted as a bold black line and the overall mean (1.678) as a horizontal line. ....55
- Figure 2.8:** Contour plot of the new Chl-a dataset (monthly average) for the period 1948 to 2002 in the Central Northeast Atlantic and North Sea. Note the seasonal changes (timing of phytoplankton) especially after the mid 80s; the spring bloom has been merged with the summer bloom.....56
- Figure 3.1:** The coccolithophore *Emiliana huxleyi* is armoured by “chalky shields” called coccoliths, which turn the blue oceanic waters milky turquoise (Landsat image of the South Western tip of the UK). ....60
- Figure 3.2:** Examples of different diatom species (<http://www.bhikku.net/archives/03/img/diatoms.jpg>) .....62
- Figure 3.3:** Study area of the subarctic North Atlantic, 51°-66°N and 11°- 40°W. The black dots represent the CPR samples taken from January 1998 to December 2002 ( $n= 3,977$ ).....65
- Figure 3.4:** (a) True colour image of the coccolithophore bloom taken by SeaWiFS on 15 June 1998, subarctic North Atlantic. Provided by the SeaWiFS Project, NASA/GSFC and ORBIMAGE. (b) Pseudo colour image presenting a monthly mean of SeaWiFS nLw\_555 for June 1998. ....66
- Figure 3.5:** Distribution of match-ups of diatom CPR data and satellite parameters for the period of 1997-2003 in the northern Atlantic Ocean.....72
- Figure 3.6:** Monthly mean of SeaWiFS nLw\_555 (solid line) and CPR coccolithophore numbers (dashed line) from January 1998 to December

2002 (3,977 samples) in the study area. The spatial distribution of the samples can be seen in Figure 3.3. ....74

**Figure 3.7:** Satellite time series of: (a) The dashed line presents the nLw\_555 (coccolithophore abundance) from September 1997 to December 2004, and the solid line presents the number of nLw\_555 pixels >0.9 (blooms areal extent), (b) solar radiation flux from September 1997 to December 2004, (c) Wind stress from September 1997 to December 2004, (d) MLD from September 1997 to December 2003. The arrows represent the Junes of every year. ....76

**Figure 3.8:** (a) SST from January 1985 to December 2004. The thin horizontal line is the overall mean and the thick line the annual mean. The open boxes surrounding the dots represent the Junes of every year, (b) SSTA from January 1985 to December 2004 (the black curve is a second order polynomial). ....78

**Figure 3.9:** GAM plots illustrate non-linear relationships between the nLw\_555 variable (lo stands for loess smoother) and each predictor. Circles represent the raw data, the connected line is the spline and the dashed lines are the 95% confidence intervals. (a) and (b) illustrate the final product of model 1 ( $r^2= 0.896$ ), which incorporated solar radiation flux (a) and SST (b). (c) and (d) illustrate the final result of model 2 ( $r^2= 0.894$ ), which incorporated solar radiation flux (c) and MLD (d).....80

**Figure 3.10:** Seasonal cycles of diatom abundance (number of cells), light intensity (PAR), sea surface temperature (SST) and wind stress. The plots are derived from the match-up data and thus the mean of every variable has been derived from the same number of data points.....82

**Figure 3.11:** The relative impact (smoothing factor) of the physical and spatiotemporal variables on diatom abundance. ....83

<b>Figure 3.12:</b> Three dimensional plot predicting diatom abundance for SST versus month.....	85
<b>Figure 3.13:</b> Three dimensional plot predicting diatom abundance for SST versus PAR.....	86
<b>Figure 3.14:</b> Three dimensional plot predicting diatom abundance for PAR versus month.....	87
<b>Figure 4.1:</b> A schematic representation of a Probabilistic Neural Network structure.....	95
<b>Figure 4.2:</b> The relative impact (smoothing factor) of the 8 variables indicating the importance of each variable in distinguishing the groups from each other as separated functional types (All groups) and discriminating one group from the others i.e. diatoms from the remaining groups. Note that the different colouration or shading separates the physical, biological, optical, temporal and spatial variables (respectively). .....	100
<b>Figure 5.1:</b> Seasonal cycle of SeaWiFS Chl-a for the open oceanic area of the Northeast Atlantic and the coastal area of the southern North Sea. The seasonal data were derived from the monthly Chl-a datasets between September 1997 and December 2005.....	107
<b>Figure 5.2:</b> Composite of CPR PCI and SeaWiFS Chl-a for the period of September 1997 to December 2005.....	108
<b>Figure 5.3:</b> Location of coastal and open North Sea areas used in Appendix I (Paper submitted) overlain by CPR samples temporally corresponding with SeaWiFS Chl-a measurements ( $n= 3695$ ).....	110
<b>Figure 5.4:</b> GAM plot illustrating the variability of diatoms in relation to fluctuations of NHT (1958-2003). .....	112

**Figure 5.5:** Annual mean of Northern Hemisphere Temperature during (data provided by Hadley Centre).....119

**Figure 5.6:** Seasonal (monthly composites) distribution and abundance of diatoms based on the CPR dataset (1958-2003). These maps can enable the validation of ANNs predicting abundance. The maps have been presented at the ASLO conference (Raitsos *et al.*, 2005 b) and also have been used to describe the seasonal variation of both groups in the Northeast Atlantic Ocean and the North Sea (Appendix I). .....123

**Figure 5.7:** SeaWiFS 7 year mean composites (1998-2004) of PAR and nLw\_555 in three major regions where *E. huxleyi* blooms have been recorded. Note that high August nLw\_555 values in the Irish Sea and off the mouth of the Thames are most likely due to resuspended sediment rather than coccolithophore blooms. ....126

## ***List of Tables***

<b><i>Table 2.1:</i></b> Chl-a concentration (mg/sample) for every PCI category.....	50
<b><i>Table 3.1:</i></b> Summary of the parameters, sources and statistical methods used to analyse them.....	64
<b><i>Table 3.2:</i></b> Summary of the parameters, sources and statistical methods used to analyse them.....	70
<b><i>Table 4.1:</i></b> Summary of the parameters, sources and statistical methods used to analyse them.....	93
<b><i>Table 4.2:</i></b> Percentage values of sensitivity, specificity and classification accuracy of the five groups, applying the PNN 5 times. Each time a random sample of 80% of cases was used as the training set and the remaining 20% as the testing set. Results are given analytically for each sample in training and testing. Mean values of the five samples are given in bold.....	99

## Acknowledgements

I would like to express my gratitude to my supervisors Samantha Lavender, Chris Reid and Martin Edwards who always readily provided invaluable support - both academically and personally – critical direction, guidance and suggestions, through stimulating discussions during these three years of effort and work. This research would not have been possible if Samantha had not provided a considerable amount of her time, especially at the beginning of the PhD, to teach me what satellite remote sensing really is. Also, I am deeply indebted to Yaswant Pradhan's steady support by teaching me how to process datasets taken from a variety of satellite sensors and solving several issues during this research; I can now say he has definitely been an unofficial supervisor of this Thesis. Finally, I would like to be grateful for the excellent collaboration with Abigail McQuatters-Gollop, which has set a strong basis for many project and ideas that we already have, and will work on.

I would like to acknowledge the assistance and co-operation of the following individuals who contributed generously to this project: Anthony Richardson, Toby Tyrrell, Christos Maravelias, John Haralambous, Tony Walne, Tony John, Gregory Beaugrand, Tim Smyth and Marian Scott. Special thanks to both the external examiner Professor Ian Robinson and the internal Dr. Tim Stevens, for their valuable input and constructive comments.

Especially, I would like to thank my close friends for their great support during the PhD! To name a few, I am grateful to: Lida, Tassos, Panagiotis, Zanna, Grigoris, Giannis, Kalia, Kostandinos, Dimitris, Patricia, Paco, Agnies, Laure, Signe, Pierre, John, Kathryn, George, Frederic, Anna, Victor, Rossana, Jeff, Vicky etc.... and of course the pub "Fisherman Arm's" that has generously contributed towards my happiness every Friday night the last 3 years.

Living and studying in UK for 8 years, I would like to thank the British educational system that gave me the opportunity, by supporting me financially and academically, to become a marine scientist. Special thanks to University of Plymouth for funding this research.

And last, but not least, I would not have achieved anything without the support of *Elena*, who has been waiting for me a few years...Don't worry *Elena*, finally I am coming back. When I left Greece 8 years ago, I was young, slim, tanned and happy, but now I am a Doctor (not a real one, but the one with a PhD).

It would be unthinkable not to mention the support offered by my family in Greece: Thanassis, Eleni, Giannis, Afrula, Elena, Lida. They were always encouraging and supported me in focussing my efforts and remaining strong during my stay in the UK.

## **Authors Declaration**

At no time during the registration for the degree of Doctor of Philosophy has the author been registered for any other University award. This study is supported by a scholarship from the University of Plymouth and carried out in collaboration with the Sir Alister Hardy Foundation for Ocean Science. This study was also supported by the UK Natural Environment Research Council through the Atlantic Meridional Transect consortium (NER/O/S/2001/00680) and Centre for Observation of Air-Sea Interactions and Fluxes (CASIX). During the PhD, advanced statistical courses were completed called “NERC/EPSRC Statistics for Environmental Evaluation”, held in Glasgow University (2004) and “PRIMER” held in Plymouth (2005).

During the second year of the PhD, *in situ* data were collected during the research cruise “Atlantic Meridional Transect” (AMT 16) that is funded through NERC. The Royal Research Ship (RRS) DISCOVERY sailed from Cape Town in South Africa on 19 May 2005 and arrived in Falmouth in the UK on 29 June.

During the PhD, several publications were published, submitted and/or presented in conferences or peer-reviewed journals.

The word count of the thesis is: 45,787

## **PUBLICATIONS**

### **Scientific papers**

**Raitsos D.E., Reid P.C., Lavender S.J., Edwards M., Richardson A.J. (2005).**  
Extending the SeaWiFS chlorophyll data set back 50 years in the northeast Atlantic. *Geophysical Research Letters*. 32: L06603 [doi:10.1029/2005 GL022484].

**Raitsos D.E.**, Lavender S.J., Pradhan Y., Tyrrell T., Reid P.C., Edwards, M. (2006). Coccolithophore Bloom Size Variation in Response to the Regional Environment of the Subarctic North Atlantic. *Limnology and Oceanography*. **51**: 2122-2130.

**Raitsos D.E.**, Lavender S.J., Walne A.W., Reid P.C., Edwards M. (Submitted). Phytoplankton Colour Index of the Continuous Plankton Recorder; a reliable >50 years ocean colour dataset. *Progress in Oceanography*.

**Raitsos D.E.**, Lavender S.J., Maravelias C.D., Haralambous J., Richardson A.J., Reid P.C. (Submitted). Identifying phytoplankton functional groups from space: an ecological approach. *Limnology and Oceanography*.

**Raitsos D.E.**, Lavender S.J., Maravelias C.D., Haralambous J., Edwards M., McQuatters-Gollop A., Reid P.C. (Submitted). Macroscale factors affecting diatom abundance: a synergistic use of Continuous Plankton Recorder and satellite remote sensing data. *Remote Sensing of Environment*.

McQuatters-Gollop A., **Raitsos D.E.**, Edwards M., Pradhan Y., Mee LD., Lavender S.J., Attrill M.J. (Submitted). A long-term chlorophyll dataset reveals a regime shift in North Sea phytoplankton biomass unconnected to increasing nutrient levels. *Limnology and Oceanography*.

McQuatters-Gollop A., **Raitsos D.E.**, Edwards M., Attrill M.J. (Submitted). Spatial patterns of diatom and dinoflagellate seasonal cycles in the North – East Atlantic Ocean. *Marine Ecology Progress Series*.



## National/International Conferences

**Raitsos D.E., Lavender S., Reid P.C., Edwards M. (2004).** A comparison of Satellite Chl-a values and *in situ* measurements of phytoplankton biomass from the CPR survey. Poster Presentation in: **NERC *Earth Observation (EO) Conference*** on 30<sup>th</sup> June-1<sup>st</sup> July, Plymouth, United Kingdom.

**Raitsos D.E., Lavender S., Edwards M., Reid P.C., Pradhan Y. (2005).** Development of a prototype system for deriving maps of phytoplankton taxa: spatial and temporal distribution of diatoms and dinoflagellates since 1950 in the North Atlantic. Poster Presentation in: **International Conference of American Society of Limnology & Oceanography (ASLO)**, Spain.

**Raitsos D.E., Lavender S., Reid P.C., Edwards M. (2005).** Discrimination of phytoplankton taxonomic groups using ocean colour data. Poster Presentation in: **NERC Earth Observation (EO) and International conference of Remote Sensing and Photogrammetry Society (RSPSoc)**, Portsmouth, United Kingdom.

**Raitsos D.E., Lavender S., Pradhan Y., Tyrrell T., Reid P.C., Edwards M. (2006).** Coccolithophore Bloom Size Variation in Response to the Regional Environment of the Subarctic North Atlantic. Oral Presentation in: **International conference of American Society of Limnology & Oceanography (ASLO)**. Honolulu, Hawaii.

Signed.....

Date..15/21/2006

# CHAPTER 1

## *Literature Review – Aims and Objectives*

This chapter is separated into three sections. Section 1.1 is a literature review that aims to briefly describe the Continuous Plankton Recorder survey and the methodological approach used to collect plankton data. It also illustrates the value of large biological databases and the previous statistical analyses used to determine spatial and temporal fluctuations in planktonic distribution and abundance. In addition, a description of the statistical/modelling tools that will be used in this thesis is briefly discussed. Section 1.2 introduces satellite remote sensing and its application to ocean colour, sea surface temperature, wind speed and altimetry. Finally, Section 1.3 summarises the aims and objectives of the thesis and briefly describes what each chapter will contain.

### ***1.1 A Short History of the CPR Survey***

The Continuous Plankton Recorder (CPR) survey is an upper-layer plankton monitoring programme that mainly operates in the North Atlantic Ocean and North Sea. The associated database is considered to be one of the largest and most valuable biological databases in the world with ~70 years of marine plankton data (Edwards *et al.*, 2001). Data has been available in paper form since 1931, while from 1946 a computerised database was created. In addition, this survey has been based on consistent methods for the sampling and analysis of plankton since 1948 (Warner and Hays 1994). Therefore, it provides unique information on geographical distribution, seasonal cycles and year-to-year changes in abundance of plankton over a large spatial area; with 181,262 plankton samples containing 2,135,072 taxonomic abundance entries (SAHFOS 2003).

The main aim of the CPR survey in the Atlantic Ocean and North Sea is to monitor the distributions and abundances of near-surface plankton on a monthly basis. In addition, a general goal of the CPR survey is to create and maintain a reliable and up to date time series database including geographical (spatial), temporal and ecological information on the pelagic ecosystem. In Figure 1.1, the Atlantic and North Sea CPR sampling area can be observed.



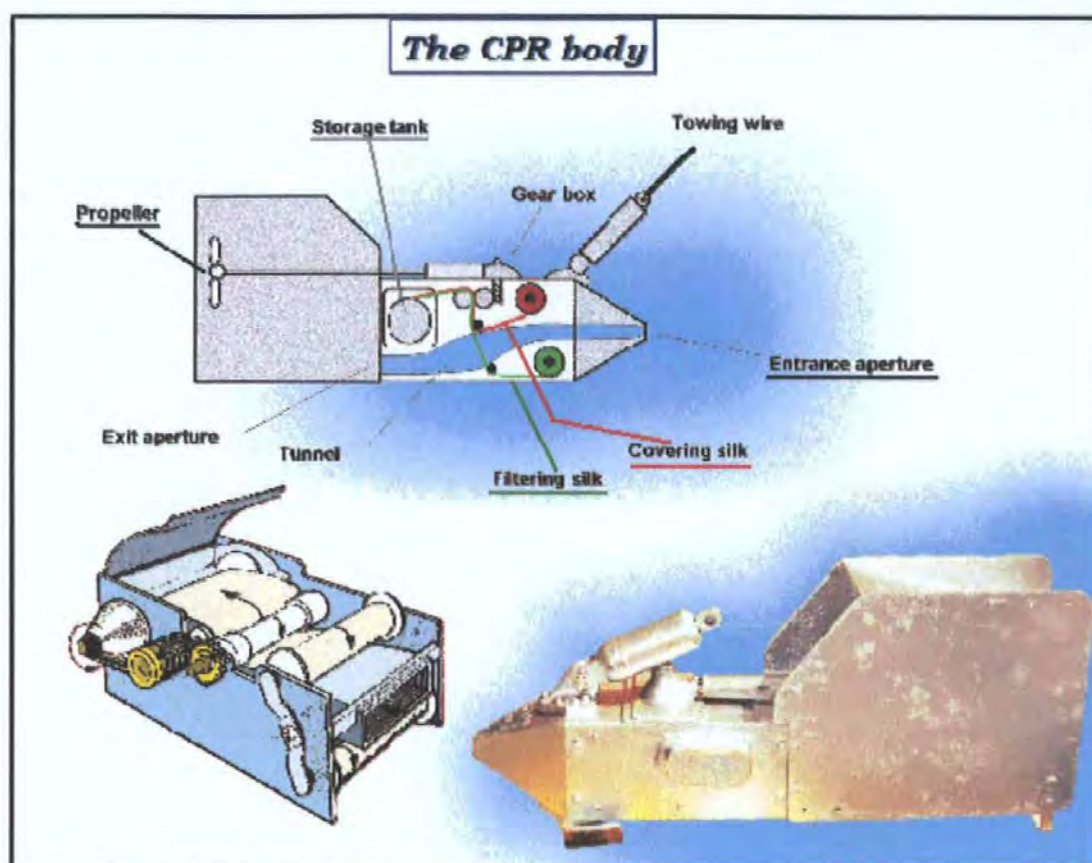


**Figure 1.2:** A side view of the Continuous Plankton Recorder, including the plankton filtering mechanism and a photograph of the instrument (SAHFOS 2003). The figure has been slightly modified by the author in order to highlight the major parts of the equipment which are addressed in the text.

### ***1.1.2 CPR Analysis: The Phytoplankton Colour Index and Species***

The routine analysis procedure is divided into three stages: *a*) phytoplankton field analysis *b*) zooplankton ‘traverse’ and *c*) zooplankton ‘eye count’ (Warner and Hays 1994). The small phytoplankton cells retained on the filtering silk, including those that disintegrate due to formaldehyde preservative, give a greenish colouration to the CPR silk (Reid 1977; Robinson *et al.*, 1986). Responsible for this colouration are the green chlorophyll pigments which are derived from chloroplasts of intact and broken cells and small unarmoured flagellates (Edwards *et al.*, 2002). The phytoplankton biomass or Phytoplankton Colour Index (PCI) is estimated by visual assessment (Colebrook 1960); further information is given in Chapter 2. After categorising the colour of the silk sample, microscopic procedures are carried out in order to identify

and count phytoplankton species presence to the highest practical extent (Batten *et al.*, 2003). Then, the number of phytoplankton cells per sample is calculated using the Robinson and Hiby (1978) equation:

$$H = -\ln(k/20)$$

Where  $k$  = the number of empty microscope fields (out of 20) observed.

The cell counts are given by multiplying  $H$  by the proportion of the sample examined and summing the different taxa (Robinson and Hiby 1978).

According to Edwards *et al.* (2001) it is not clearly known whether, and to what extent, phytoplankton colour values correspond to actual values of biomass or primary production. However, various studies in the past have clearly shown that phytoplankton colour values do strongly represent the major temporal and spatial patterns of phytoplankton (Colebrook and Robinson 1965; Robinson 1970; Gieskes and Kraay 1997; Reid *et al.*, 1998; Batten *et al.*, 2003).

### ***1.1.3 The Value of Biological Time Series***

A time series database may be defined as any long-term dataset that contains a series of values/observations collected sequentially in time. There are two major achievements of time series analysis (Statsoft 2003): identifying the nature of the phenomenon presented by the sequence of observations and predicting future values of the time series variable (forecasting). It can therefore be used to identify trends in phytoplankton biomass, which in turn can be linked with oceanic/atmospheric processes and/or physical events i.e. discriminate between natural biological responses and natural oscillations or global warming (Edwards *et al.*, 2001).

Evidence as to whether, and to what extent, anthropogenic perturbations are responsible for natural or biological changes is limited due to the lack of information

on natural variations in marine ecosystems at larger spatio-temporal scales (Edwards *et al.*, 2001). In addition, Beaugrand *et al.* (2000a) reported that conclusions regarding spatio-temporal biological trends at a regional scale cannot be drawn because of the lack of large data-sets. Various studies have tried to assess global biodiversity trends or detect effects of pollution on natural communities by extrapolating species accumulative curves or fitting models of relative abundance or using diversity indices (Beaugrand and Edwards 2001). Most of these studies were based on simulated data which, in turn, lead to a biased and inaccurate mimicry of natural communities. Long term biological datasets are therefore invaluable in identifying real biological changes. Finally, long-term biological surveys can be used to provide invaluable information on physical processes (climate change) and unusual sporadic oceanographic events (Edwards *et al.*, 2001).

Unbiased knowledge on phytoplankton ecology is highly important not only because phytoplankton organisms are ‘ecological drivers’, but also because their abundance and diversity highly influence biodiversity trends of other organisms such as fish and marine mammals. All the above statements support and emphasize the fact that long term biological databases, such as the CPR, allow the monitoring of seasonal and annual changes of plankton distribution and abundance and/or to correlate these changes with fluctuations in fisheries, taking into account oceanographic and environmental parameters.

#### ***1.1.4 Statistical Methods Overview***

Based on the aims of this study (Section 1.3), there is a need to identify which parameters are playing the most important role in phytoplankton distribution and abundance. To derive this information from concurrent *in situ* (CPR) and satellite remotely sensed data, which contains thousand of data points, a powerful statistical approach is needed. Traditional regression techniques are not adequate to explore large data matrices; therefore two methodological approaches were used, Artificial Neural Networks (ANNs) and Generalised Additive Models (GAMs). A brief description of both approaches is given in this section.

ANNs mimic the cognitive power of the human brain in problem-solving and, in the same way as learning in biological systems, involve adjustments to the synaptic connections that exist between the neurons. Therefore, the networks can accumulate knowledge gained from past experience to solve new problems under new situations using a defined set of training data. Neural networks may learn using only one type of learning: supervised (both input and output information used for training) or unsupervised (only input information is available for training). Two different types of ANNs were used in this thesis. Probabilistic Neural Networks (PNNs), are based on supervised learning, and were used to discriminate phytoplankton groups from space. Generalized Regression Neural Networks (GRNNs) proposed by Specht (1991) were used to assess the effect of physical variables on phytoplankton.

A GRNN approaches a problem on the basis of the probability density function of the observed data and thus does not require any prior assumption in the form of the regression function. ANNs are ideal for analysing complex datasets dealing with large quantities of information at the same time (as in the present study). ANNs are adaptable and can develop non-linear relationships that cannot be identified by traditional regression techniques.

GAMs can be used to investigate potential relationships between phytoplankton abundance and various independent environmental parameters. Briefly, a GAM is a flexible regression technique whose advantage over traditional regression methods, such as General Linear Models, are its ability to model nonlinearities using nonparametric smoothers (Hastie and Tibshirani 1990). However, the algorithm that fits the curve is usually iterative and so non-parametric smoothing masks a great deal of complex numerical processing. Neuro-cell and S-Plus was used for ANNs and GAMs respectively. Further information on these statistical approaches can be found in the chapters where these models were used (Chapter 3 and 4).



## ***1.2 An Introduction to Satellite Remote Sensing***

**R**emote sensing may be defined as any method used to obtain information about an object or region from a distance. This can be achieved by recording the amount of electromagnetic energy that is radiated or reflected by objects, with the most common ways involving the use of aircraft or artificial satellites that carry various types of sensors. However, satellite remote sensing is often the most beneficial and efficient way to obtain information in oceanographic science; an exception would be local studies within estuaries. Satellite based sensors can be used to obtain data about a large number of biological and physical phenomena; however, this thesis will focus on ocean colour (optical properties), sea surface temperature (SST) and wind speed/stress.

### ***1.2.1 Ocean Colour Data***

Ocean colour is determined by the interactions and dispersion of light scattered and/or absorbed when they interact with substances dissolved and suspended in the water. The amount of scattering depends on the number, size and composition of the particles (Robinson 1995); the principal constituents of which are the free-floating photosynthetic organisms (phytoplankton) and inorganic particulates. Absorption is related to both these particles and the dissolved compounds, primarily phytoplankton in the open ocean, but also their breakdown products. In coastal waters, coloured dissolved organic matter (CDOM) from terrestrial origins becomes a highly absorbing component. Coastal or optically-complex waters are characterised as Case II waters, because Chl-a is not the dominant optical constituent and so global chlorophyll algorithms (such as OC4-v4: O'Reilly *et al.*, 1998) are less reliable (IOCCG 2000).

Phytoplanktonic organisms, such as diatoms and dinoflagellates, contain photosynthetic compounds; the most common pigment is chlorophyll-a (Chl-a), making up around 75% of the chlorophyll in green plants. The chlorophyll traps light energy, absorbing mainly red and violet-blue wavelengths, and transmits in the green (Robinson 1995). Suspended Particulate Matter (SPM) can scatter and absorb light,

which in turn reduces the light transmission (clarity) of the water and can affect the colour (Muller and Austin 1995). However, its presence in the open ocean is primarily related to the phytoplankton. Species of phytoplankton contain different concentrations of chlorophyll (i.e. diatoms and coccolithophores) and this information, in addition to other parameters, may be used to differentiate phytoplankton blooms. Remote sensing images, taken over a period of time, can also provide invaluable information about changes in phytoplankton distribution and abundance at large spatial and temporal scales.

The satellite sensors obtain ocean colour imagery by recording the radiance which is back-scattered towards the sensor, often defined as normalised water leaving radiance (nLw). As this data is related to the presence of substances and/or particles, it may be used to calculate the concentration of material in the surface oceanic waters and hence biological activity. Therefore, the satellite data provides invaluable information on several aspects of oceanography i.e. marine productivity, marine optical properties, distribution and abundance of phytoplankton, interactions between currents and ocean biology, and on the anthropogenic impact regarding oceanic environments. However, the use of satellite data requires several radiometric corrections (e.g. atmospheric) in order to remove/reduce the presence of haze and clouds (Muller and Austin 1995). The corrected data can then be used in algorithms to produce parameters such as Chl-a concentration. As well as nLw and Chl-a, ocean colour data can also be used to estimate valuable parameters such as Photosynthetically Active Radiation (PAR) (Figure 1.3).

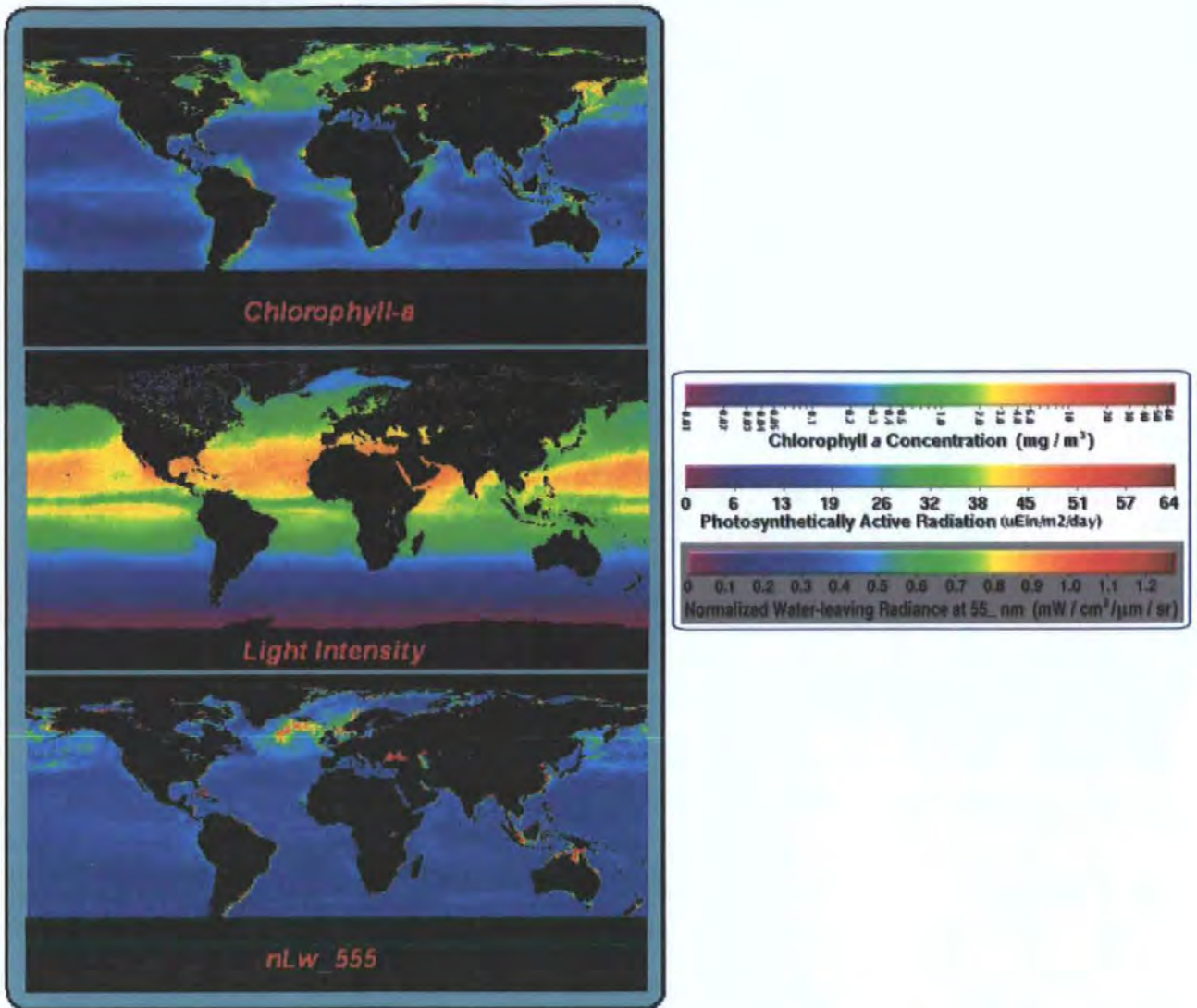


*Figure 1.3:* SeaWiFS global monthly composites of Chl-a, light intensity (PAR) and normalised water leaving radiance (nLw) at 555nm. (<http://oceancolor.gsfc.nasa.gov/>)

### *1.2.2 Ocean Colour Sensors*

**The Coastal Zone Color Scanner (CZCS)**, launched aboard NIMBUS-7 , provided Chl-a data from October 1978 to June 1986 (Robinson 2004) and was the first satellite based instrument devoted to the measurement of ocean colour. Being satellite mounted, CZCS was able to provide measurements of ocean colour over large geographic areas in short periods of time in a way that was not previously possible

with other measurement techniques i.e. research ships, buoys and aircraft. These measurements allowed oceanographers, for the first time, to observe the global distribution of phytoplankton biomass (Chl-a). NASA has recently updated the CZCS dataset by re-processing them and make the data available in a user friendly format (Hierarchical Data Format: HDF). The data (Chl-a and nLw\_550) are available via NASA's ocean colour website at 4km resolution and as daily, weekly and monthly composites.

The **Sea-Viewing Wide Field-of-view Sensor (SeaWiFS)** was initially planned to be launched in August 1993, but this action was inhibited due to technical issues until August 1997; a side view of SeaWiFS sensor can be seen in Figure 1.4. SeaWiFS is a spectroradiometer, and its primary goal is to measure radiance in specific bands of the visible light spectrum (Muller and Austin, 1995). SeaWiFS provides global information on Chl-a, light intensity and radiance estimations on a daily, 8-day, monthly and annual basis at a resolution of 9 km.

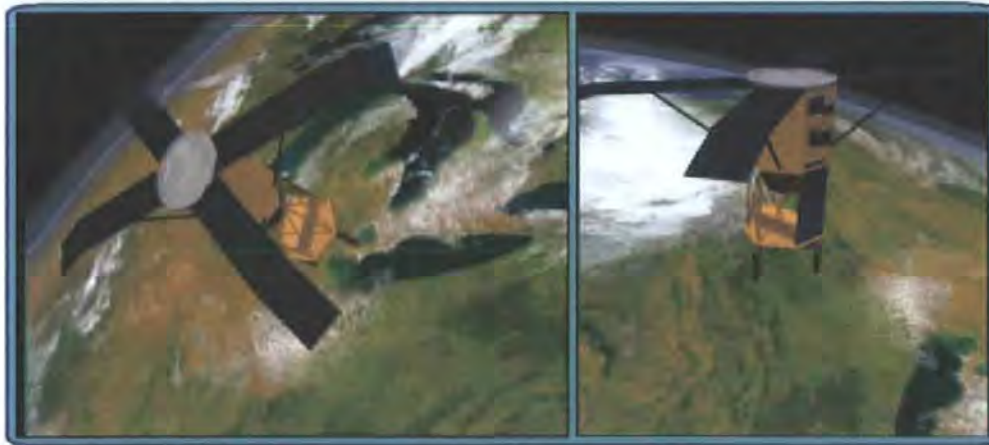


*Figure 1.4:* An artist's side view of the SeaWiFS sensor. The figure has been taken from NASA (<http://www.nasa.gov/>).

The **Moderate Resolution Imaging Spectrometer (MODIS)** was launched in December 1999, on the Terra platform, and then Aqua platform in May 2002. MODIS measures ocean colour (like SeaWiFS) on a daily basis over the globe, but can also measure chlorophyll fluorescence. This data can provide unique information not only for mapping phytoplankton distribution, but also for determining its physiological

state e.g. the more the plants fluoresce the less energy is used to photosynthesise. MODIS is considered as an advantage over SeaWiFS because the wavebands are more narrowly defined and should have a lower noise (Robinson 2004). MODIS level 3 data are freely available to the broader scientific community at a resolution of 4km (<http://oceancolor.gsfc.nasa.gov/>). Robinson (2004) reported that MODIS has a well developed programme for validating the data and inter-comparison with other sensors i.e. SeaWiFS.

The **Medium-resolution Imaging Spectrometer (MERIS)** is the European's Space Agency (ESA) first ocean colour sensor. MERIS offers ocean colour and geophysical products at a resolution of 1200m with a capability of 300m (Robinson 2004). It provides a unique European remote sensing capability for observing oceanic biology and marine water quality through global observations of ocean colour and provides continuity along with the previously mentioned ocean colour sensors. Because of its capability for 300m spatial resolution data and measurement of passive fluorescence, its major contribution to marine science (over sensors such as SeaWiFS) could be enhanced coastal monitoring.

In the thesis, only SeaWiFS was used as it provides the longest ocean colour dataset and ongoing research to create merged datasets from several ocean colour sensors is still in the preliminary stages.

### ***1.2.3 Sea Surface Temperature Data***

The Sea Surface Temperature (SST) records, obtained from earth-orbiting radiometers, have had the widest application for oceanographic science (Robinson 1995). SST measurements (Figure 1.5) are often obtained by recording the infrared radiation emitted by the ocean surface, but can also be determined using passive microwave systems.

SST can be used to identify and investigate small-scale oceanographic phenomena such as frontal regions/coastal upwelling, but also to observe currents and circulation in the oceans, monitor fisheries, identify polluted regions and monitor global changes

in climate (Robinson 1995). Robinson (1995) also stated that slight variations in SST may represent significant changes in heat energy storage, and small oscillations in large SST anomalies may influence the distribution and/or abundance of marine organisms such as phytoplankton (Reid *et al.*, 1998; Edwards *et al.*, 2001). Once more, atmospheric correction as well as comparison to *in situ* measurements is needed to produce high quality SST data.

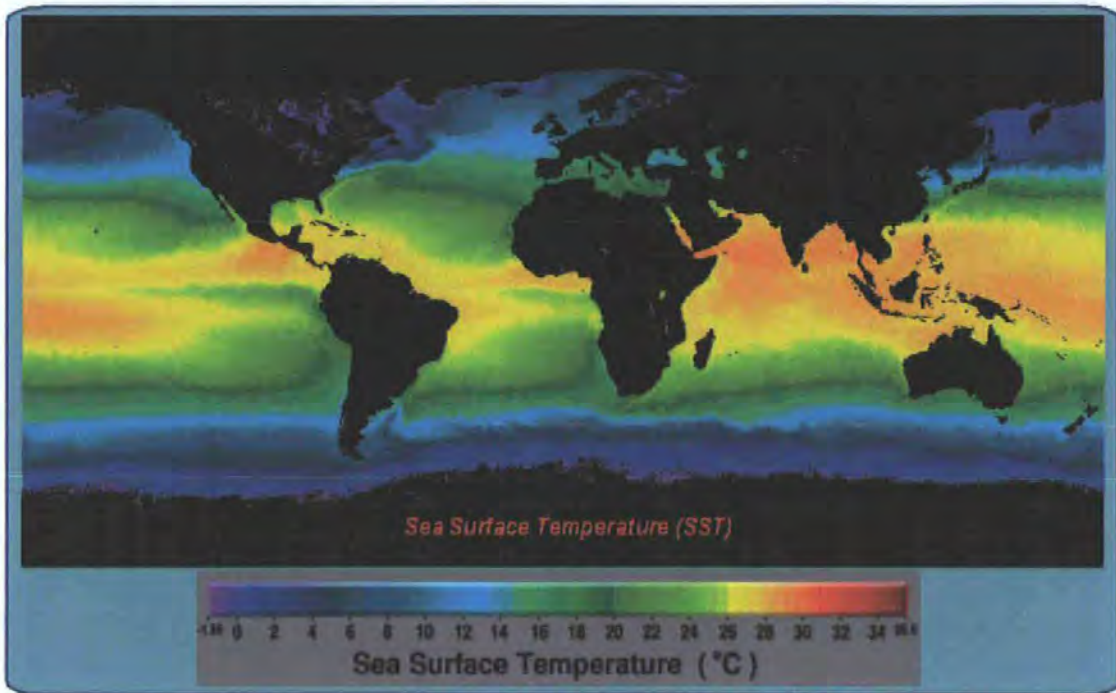


*Figure 1.5:* Global monthly SST composite from Aqua MODIS.

#### 1.2.4 Sea Surface Temperature Sensors

The **Advanced Very High Resolution Radiometer (AVHRR)** is a valuable sensor that offers more than 20 years (first launched in 1978) of data at a resolution of 1.1 km (Robinson 2004). Carried aboard the National Oceanic and Atmospheric Administration's (NOAA) polar orbiting environmental satellite series, the AVHRR sensor is a broad-band, 4 or 5 channel, scanning radiometer operating in the visible, near-infrared, and thermal infrared 'window' regions of the electromagnetic spectrum. AVHRR has been characterised as the most widely used infra-red sensor, which has had a considerable impact on oceanography (Robinson 2004). NASA has created a

useful website (<http://poet.jpl.nasa.gov/>) where high temporal and spatial resolution SST data can be obtained.

As well as providing ocean colour data, **MODIS** also provides information on SST at a global scale to an accuracy of within about 0.25°C. Global composites are available alongside the MODIS ocean colour data on NASA's ocean colour website at 4km resolution. There is also a sensor on Envisat, the Advanced Along Track Scanning Radiometer (AATSR).

AVHRR rather than MODIS or AATSR data was used, as with ocean colour, because it provides the longest SST dataset.

### *1.2.5 Altimetry, Wind Speed/Stress data*

Altimetry is primarily used to determine sea surface height (SSH), from which several other parameters can then be determined. A global image of SSHA can be seen in Figure 1.6. The microwave radar altimeter transmits high frequency signals to the earth, and the echo is reflected by the sea surface back to the satellite. Therefore, altimeters offer highly accurate information considering that the distance between the instrument and sea surface is calculated to a precision of less than 3cm (Robinson 1995), which includes a correction for the effects of water vapour in the atmosphere.

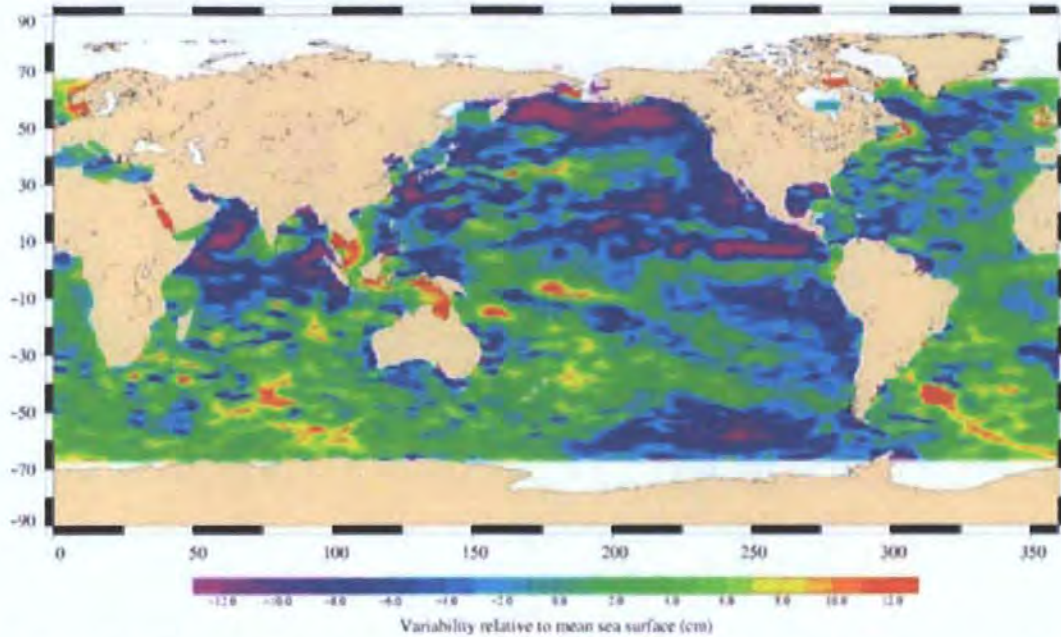


**Figure 1.6:** Global Image of Sea Surface Height Anomaly (Taken from <http://www.esad.ssc.nasa.gov/>)

The data obtained from altimeters can be used to indicate large scale patterns of ocean circulation. Measurements of wave height allow the identification and investigation of high variability areas, storms, tides and global currents. It is well known that phytoplankton are oceanic drifters, which are unable to swim against the currents, and therefore their movements depend largely on tides, currents and winds. Therefore, the phytoplankton (Chl-a) distributions can be detected and correlated to oceanic tides, eddies and currents seen by altimetry (Robinson 1995).

Specialized microwave radars (scatterometers) can measure near-surface wind speed and direction under all weather and cloud conditions over the Earth's oceans. Scatterometers transmit microwave pulses and receive backscattered power from the ocean surface. They use an indirect technique to measure wind velocity over the ocean, since the atmospheric motions themselves do not substantially affect the radiation emitted and received by the radar. Changes in wind velocity cause changes in ocean surface roughness, modifying the radar cross-section of the ocean and the magnitude of the backscattered power. They then measure this backscattered power, allowing estimation of the normalized radar cross section of the sea surface. Therefore, backscatter cross section varies with both wind speed and direction when measured at moderate incidence angles. Multiple, collocated, nearly simultaneous



cross section measurements acquired from several directions can thus be used to solve simultaneously wind speed and direction estimates.

Wind stress (Figure 1.7) is a function of wind speed, non-dimensional drag coefficient and boundary layer air density (Pickard and Pond 1978). Sea surface wind stress drives the dynamics of the boundary layer and is therefore expected, on physical grounds, to be closely related to the generation of surface waves, production of wind-driven ocean surface currents, and the stirring processes which keeps the upper ocean well mixed down to the thermocline. The spatial variation of wind stress, over the ocean, causes surface divergence of horizontal flow that in turn gives rise to vertical mass flux through Ekman pumping (Ekman 1905). Since phytoplankton are likely to be found in stratified waters, scientists use wind stress to confirm the presence of these conditions (i.e. low wind stress means shallower stratification). It is well known that both upwelling and convection jointly control the mixed-layer depth and hence phytoplankton bloom growth (Labiosa and Arrigo 2003).

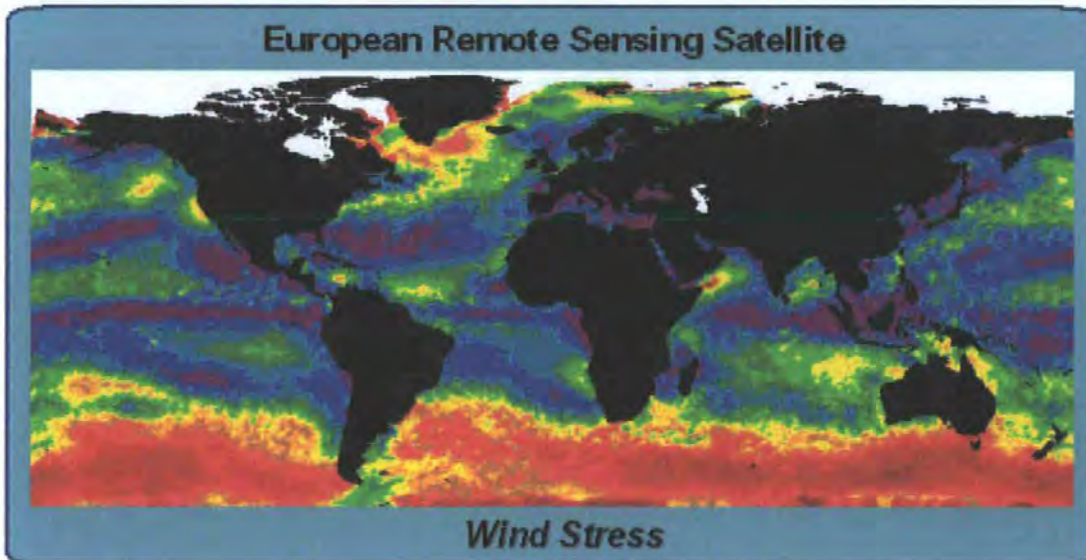


*Figure 1.7:* Global Image of wind stress taken by the European Remote Sensing Satellite (ERS).

### ***1.2.6 Altimetry, Wind Speed/Stress Sensors***

In July 1991 the European Remote-Sensing Satellite, ERS-1, was the first European satellite to be launched carrying a radar altimeter. ERS-1 has an Active Microwave Instrument (AMI) combining the functions of a Synthetic Aperture Radar (SAR) and a wind scatterometer (<http://earth.esa.int/ers/>). The radar altimeter provides accurate measurements of sea surface elevation, significant wave heights, various ice parameters and an estimate of sea surface wind speed. ERS-2, followed the ERS-1 and was launched in April 1995 (Robinson 2004).

ERS satellites offer valuable wind speed data which had a significant contribution in oceanography. Global image composites of mean wind speed and stress data ( $1^{\circ} \times 1^{\circ}$  spatial resolution) can be obtained from CERSAT, at IFREMER, Plouzané (France).

Topex/Poseidon was launched in 1992 in a joint venture between the Centre National d' Études Spatiales (CNES) and NASA. The purpose of this radar altimeter is to measure the sea surface height (SSH), with an exceptional accuracy of less than 5cm (Topex/Poseidon 2003). However, SSH values can be significantly affected by geoid variations e.g. a rocky area would warp the sea level and be visible as a small mount on the geoid. The dynamic SSH is obtained by subtracting the geoid from the altimetric observations (Wunsch and Stammer 1998). In addition, another parameter that influences SSH is sea state; due to the fact that altimeters are sensitive to sea surface elements perpendicular to the target line (electromagnetic bias). In other words, the altimeter-measured mean is shifted towards the wave trough and is altered by the wave height (Topex/Poseidon 2003). The data can be used to investigate the influence of large-scale phenomena, oceanic current oscillations and tides, on phytoplankton distribution and abundance. The signal (electromagnetic waves) is influenced by water vapour and ionisation in the atmosphere; however, this can be corrected by measuring the water absorption bands in the microwave region (Topex/Poseidon 2003).

### 1.3 Aims and Objectives

Recently, remote sensing has been used to derive maps of phytoplankton taxa by using ocean colour data (Sathyendranath *et al.*, 2004). However, this is a developing area of research and improved results can be obtained with some additional knowledge (e.g. phytoplankton ecology) and lead to a more robust interpretation. For instance, ocean colour satellite images show an increasing chlorophyll concentration in April-May indicating that the spring bloom is underway. The optical properties can be determined from satellite data by resolving the spectral absorption and backscattering coefficients e.g. coccolithophore blooms produce significant scattering (in their coccolith stage) and have been routinely followed in SeaWiFS and AVHRR images. However, ocean colour algorithms cannot provide information regarding the functional group or species present in the examined waters (Sathyendranath *et al.*, 2004).

Satellite remote sensing and *in situ* datasets (biomass, productivity, species characteristics) were used synergistically to achieve the aims of this research (for aims see below). Figure 1.8 presents a synoptic view of the data as well as the statistical/modelling methods used.

The general aim is to understand the variability of the functional properties of the phytoplankton ecosystem from satellite remotely sensed data by making use of ecological/biological and geographical knowledge derived from a >50 year plankton survey. The combined information was used to develop a prototype Knowledge-based Expert System (KES), incorporating the ecological, physical, geographical, temporal knowledge and the phytoplankton bio-optical characteristics. This prototype system was used to identify and discriminate phytoplankton functional groups from satellite remotely sensing data (Figure 1.8). The objectives were achieved by the following steps:

- a) Validating SeaWiFS data with CPR results to allow extrapolation.

- b) Understanding the ecology of the phytoplankton biomass and major phytoplankton functional groups.
- c) Assess which environmental, physical, biological, and spatiotemporal factors influence the distribution and abundance of phytoplankton.
- d) Using the valuable information derived from objectives a and b, develop KES which ultimately attempts to discriminate phytoplankton functional types using satellite remotely sensed data.

A brief summary of the chapters and how the objectives were met throughout the thesis is given below:

**Chapter 2** (objective a & b): presents a laboratory experiment, which assesses the quality of CPR phytoplankton biomass (PCI) in relation to *in situ* Chl-a. In addition, the relationship between PCI and SeaWiFS Chl-a is presented for concurrent match ups. This information is valuable as the thesis results are based on the methodological approach derived from this study. The synergistic use of PCI and SeaWiFS allowed the retrospective calculation of Chl-a back to 1948 in the Northeast Atlantic and North Sea.

**Chapter 3** (objectives b and c): identifies the environmental (physical/ biological) as well as spatiotemporal variables that influence coccolithophores, diatoms and phytoplankton biomass (PCI).

**Chapter 4** (objective d): demonstrates the use of ecological knowledge to identify phytoplankton groups from space. Using the information derived from previous chapters, an analysis that led to the discrimination of four major phytoplankton groups (diatoms, dinoflagellates, coccolithophores and silicoflagellates) was performed.

**Chapter 5:** discusses the major findings of the thesis while revealing limitations of the methodologies used and how this could be improved in future research.

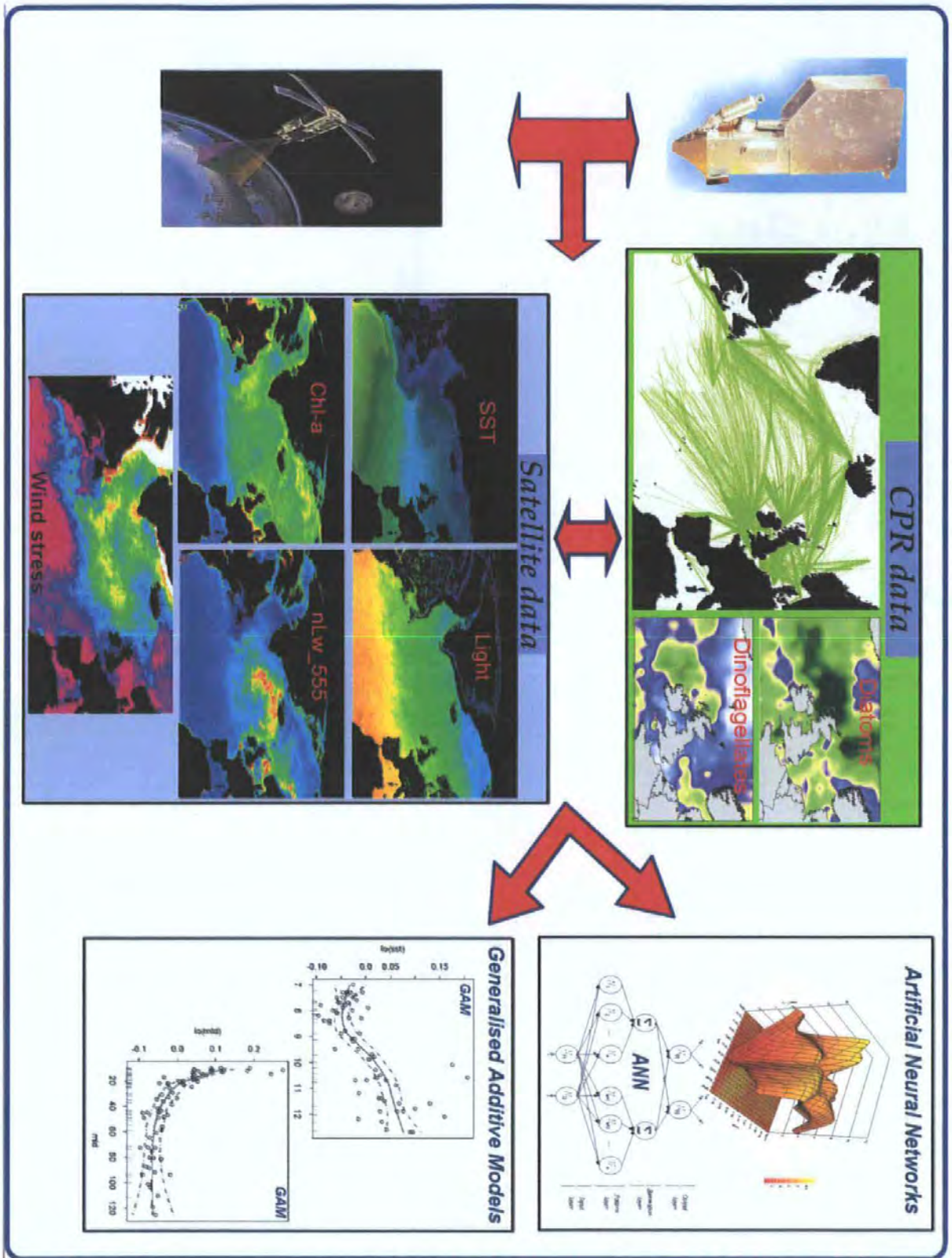


**Figure 1.8:** Synoptic view of the data as well as the methodological approach that was used to develop the Knowledge-based Expert System to discriminate phytoplankton groups from space.

## CHAPTER 2

### *From silk to satellite: A half century of ocean colour*

This chapter demonstrates two approaches in order to convert the CPR PCI to a quantitative measure using: a) *in situ* determinations of Chl-a concentration and b) satellite ocean colour data values for Chl-a concentration. The synergistic use of PCI and SeaWiFS Chl-a led to the production of a new >50 year Chl-a dataset, which is used to explain changes seen in the ecology of the Northeast Atlantic Ocean and North Sea.

Aspects of this chapter are included in the following publications:

**Raitsos D.E., Reid P.C., Lavender S.J., Edwards M., Richardson A.J.** (2005). Extending the SeaWiFS chlorophyll data set back 50 years in the northeast Atlantic. *Geophysical Research Letters*. 32: L06603 [doi:10.1029/2005 GL 022484].

**Raitsos D.E., Lavender S.J., Walne A.W., Reid P.C., Edwards M.,** (Submitted). Phytoplankton Colour Index of the Continuous Plankton Recorder; a reliable >50 years ocean colour dataset. *Progress in Oceanography*.

**McQuatters-Gollop A., Raitsos D.E., Edwards M., Pradhan Y., Mee LD., Lavender S.J., Attrill M.J.** (Submitted). A long-term chlorophyll dataset reveals a regime shift in North Sea phytoplankton biomass unconnected to increasing nutrient levels. *Limnology and Oceanography*.

**Raitsos D.E., Lavender S., Reid P.C., Edwards M.** (2004). A comparison of Satellite Chl-a values and *in situ* measurements of phytoplankton biomass from the CPR survey. Poster Presentation in: *NERC Earth Observation (EO) Conference* on 30<sup>th</sup> June-1<sup>st</sup> July, Plymouth, United Kingdom.

## 2.1 Introduction

Phytoplankton, the plants of the oceans, exist in almost every aquatic environment, produce >45% of the primary production of plants on Earth (Falkowski *et al.*, 2004), absorb the greenhouse gas carbon dioxide (CO<sub>2</sub>) from the atmosphere, and contribute to the biological pump, which ensures that the climate of the world is much cooler than would otherwise be the case (Reid and Edwards 2001). As they transfer energy to higher levels of the marine food web (Miralto *et al.*, 1999; Irigoien *et al.*, 2002) they influence the biodiversity trends of other organisms such as zooplankton, fish, seabirds and marine mammals (Nybakken 1997; Paerl *et al.*, 2003). Despite the significant role of algal production in the oceans, the short time series of large-scale chlorophyll patterns from satellites limits our understanding of the impact of global change on primary productivity and vice versa. Acquiring this information is essential for the further development of global climate change models.

Precise quantitative measurements of Chl-a, a measure of phytoplankton biomass, have only been available globally since 1997 from SeaWiFS. In the North Atlantic, semi-quantitative measurements of chlorophyll (PCI) for >50 years have been collected by the CPR survey. However, both of the measurements have limitations. SeaWiFS cannot assess decadal changes of phytoplankton due to its limited lifespan. Although the PCI is a unique measurement of *in situ* ocean colour data, with approximately 200,000 samples taken since 1948, the lack of an adequate experiment testing the PCI's quantitative validity is a concern; PCI is a semi-quantitative measurement that is based on an arbitrary scale of four categories of greenness. However, PCI measurements of the CPR survey has been extensively used to describe the major temporal and spatial patterns of phytoplankton (Colebrook and Robinson 1965; Robinson 1970; Gieskes and Kraay 1997; Reid *et al.*, 1998; Reid *et al.*, 2003), and as an indicator of phytoplankton standing stock (Batten *et al.*, 2003).

This chapter aims to test the validity of the CPR ocean colour index (PCI), to identify what is the equivalent averaged value of Chl-a for each category of the PCI using a laboratory based fluorometer and to assess the numerical values assigned by previous

studies (Colebrook and Robinson 1961 and 1965). The laboratory experiment also examined if the Chl-a was distributed equally across each CPR sample.

In addition, the relationship between SeaWiFS Chl-a measurements in the Central Northeast Atlantic and North Sea (1997-2002) and simultaneous *in situ* measurements of PCI was investigated by combining data from both instruments. Finally, the use of a new, combined, greater than 50 year Chl-a dataset was used to explain documented changes in the North Sea.

## 2.2 Methodology

### 2.2.1 The Phytoplankton Colour Index of the CPR Survey

The preliminary analysis of CPR samples, prior to species specific analysis, involves the visual estimation of the green colour of the silk mesh that filters the surface waters. Small phytoplankton cells retained on the filtering silk, including those that disintegrate, give a greenish colouration to the CPR silk (Reid 1977; Robinson *et al.*, 1986). For training and quality control purposes, the phytoplankton biomass or PCI is estimated by reference to a standard colour chart; whereas during the standard procedure, PCI is recorded by visual assessment (Colebrook 1960). There are four different 'greenness' values: 0 (no greenness), 1 (very pale green), 2 (pale green) or 6.5 (green). For mathematical purposes the four rank order categories of phytoplankton colour have been assigned numerical values on a ratio scale based on acetone extracts (Colebrook and Robinson 1965). PCI is a unique estimate of phytoplankton biomass, as small phytoplankton cells that cannot be counted under the microscope contribute to the colouration of the filtering silk (Batten *et al.*, 2003).



### 2.2.2 Laboratory Experiment

For this experiment, CPRs that did not contain formalin (preservative), were towed from Plymouth to Roscoff on a monthly basis for 8 months enabling 76 samples to be taken (Figure 2.1). These tows were approximately 18km long and the points in Figure 2.1. are at the middle of every tow. Once the samples were collected, they were stored in a freezer (below 18°C) to preserve the samples until analysis could take place. The CPR silk underwent the PCI visual assessment for greenness before being analysed for Chl-a.

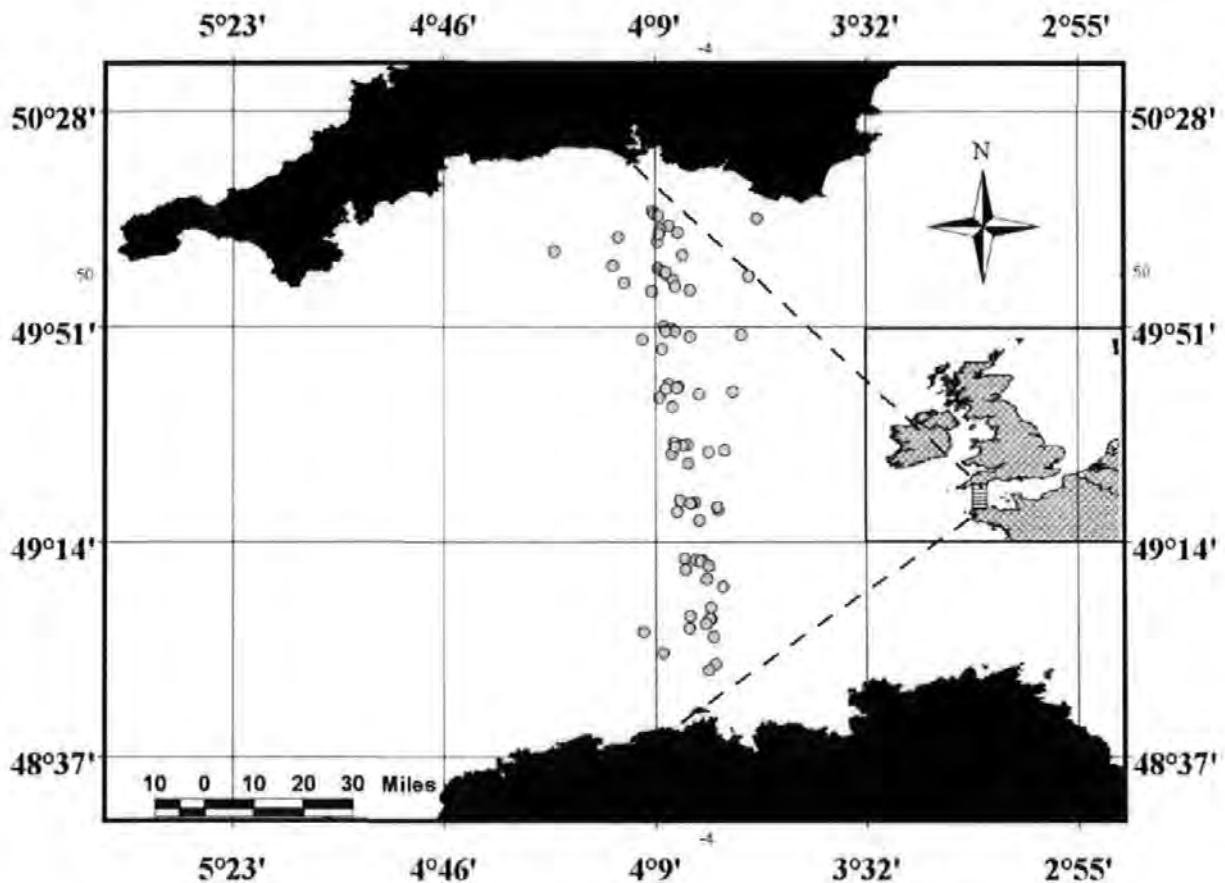


*Figure 2.1:* Positions of the CPR samples (n= 76) collected from 2004-2006 in the British Channel.

### 2.2.2.1 Sample Analysis

Two previous studies (Colebrook and Robinson 1961 and 1965) describe an experimental procedure for producing numerical values for each PCI category. Thus, the PCI is corrected to an ratio scale (not  $\text{mg m}^{-3}$ ) where Very Pale Green (VPG) varied between 0.6 and 1.5, Pale Green (PG) between 1.4 and 2.8 and Green (G) between 4.5 and 9.6. The average values of 1 for VPG, 2 for PG and 6.5 for G were then assigned (Colebrook and Robinson 1961). In other words, category four is 6.5 times higher than category one and category three is 2 times higher than category one. However, these values were derived for a small number of samples and the extracts were diluted using acetone to give extracts of similar intensity by visual assessment; fluorometry was not used to measure fluorescence. In this research, a greater number of samples was analysed and a rigorous approach was implemented.

Every sample, of the 76 collected, was cut into 3 equal (LH= Left Hand, C= Centre, and RH= Right Hand) parts (Figure 2.2). This allowed the experiment to *a*) repeat the Chl-a assessment 3 times per sample and then take the average in order to avoid any potential bias, and *b*) examine if there was any significant difference in Chl-a concentration within the CPR samples (to assess if Chl-a is equally distributed across the silk). Thus 228 (76 x 3) samples had their Chl-a concentration measured. The edges of the silk (Figure 2.2) were removed as they contained negligible concentrations of Chl-a (0.005 mg/sample) and the visual assessment is based only on the actual filtering and covering silk (LH+C+RH), see Figure 2.2.

From each sample, a piece (one third of the total sample) of filtering and covering silk was cut and placed into a test tube along with 10ml of 90% buffered (with 10% distilled water) acetone and left to be extracted in a fridge for approximately 20 hours.

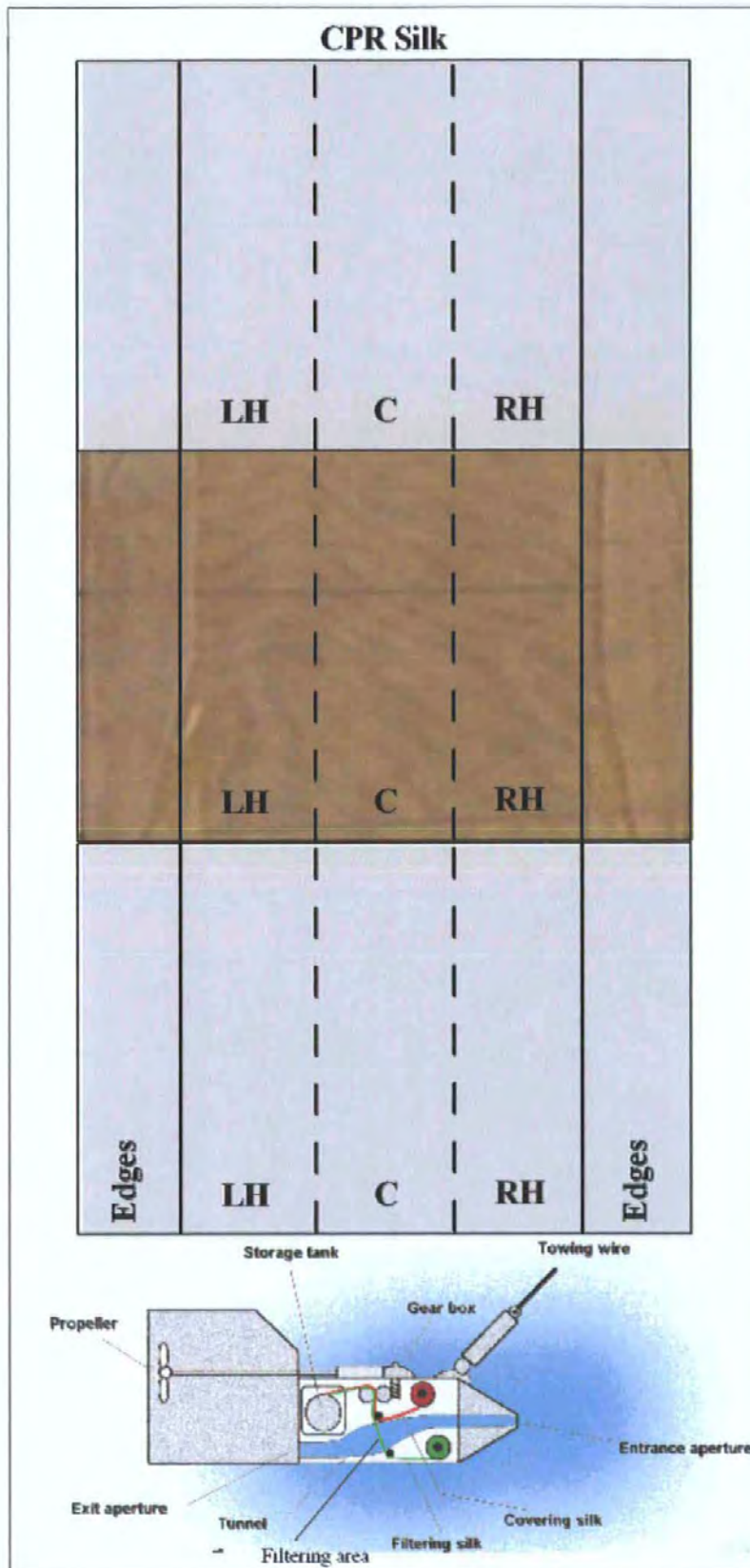


*Figure 2.2:* The top of the figure shows a CPR silk sample with outlined division areas used for analysis. Below is a side view of the Continuous Plankton Recorder, illustrating the entrance (where the water comes in) as well as the filtering and covering silk.

### 2.2.2.2 Assessment of Chl-a by Fluorescence

An F-4500 Fluorescence Spectrophotometer (Hitachi) was used to measure the concentration of Chl-a according to the procedure detailed by Strickland and Parson (1972). A stock solution of 20 mg/l of Chl-a was made from an ampoule containing 1mg of Chl-a (standard extracted from spinach leaves); stored in a freezer (below 18°C). Six Chl-a stock solutions were used to calibrate the fluorometer, which covered the whole range of samples: 0.2, 2.0, 5.0, 20.0, 50.0, 200.0 and 1000.0 mg m<sup>-3</sup>. The instrument was turned on and allowed to warm up for more than 15 minutes before each calibration, and was always calibrated before usage and every standard was run 5 times to gain a mean value. The fluorescence was recorded and plotted against the standard concentration to create a mean calibration curve; the coefficient of regression was always around 0.9998.

A sample of the stock solution was placed in a cuvette and a spectrum taken to detect the excitation (436 nm) and emission (680 nm) wavelengths. Each CPR sample (acetone extracted) was examined in the fluorometer and the Chl-a concentration was calculated using the calibration curve. The Chl-a concentration (mg/sample) for each of the 228 samples was examined 3 times and the average taken to avoid instrument bias. Knowing the concentration in the acetone and the volume of acetone, the chlorophyll concentration as mg per CPR sample was calculated.

Units of mg/sample, rather than mg m<sup>-3</sup>, were used as the volume of water filtered by the silk is not precisely known. Batten *et al.* (2003) mentioned that approximately 3 m<sup>3</sup> of seawater goes through each CPR sample. Therefore, as each piece of silk was cut into 3 equal parts, each of the 228 samples had filtered approximately 1m<sup>3</sup> of seawater.

Once the Chl-a concentration has been recorded, an acidification procedure took place. Two drops of 2<sub>N</sub> (roughly 8% conc. HCl by volume) were added and the fluorescence was measured again after 30 seconds (Strickland and Parson 1972) The acidification step enabled the contribution of pigments other than Chl-a to be assessed; HCl eliminates chlorophyll and what is left is carotenoids. Note that all the

test tubes, cuvettes or any other laboratory equipment, were rinsed 3 times with the buffered acetone solution (90%). The acidified values per sample were recorded and subtracted from the original Chl-a values to avoid any potential bias.

Finally, a blank CPR silk was also analysed in order to see if chemicals within the silk affected the results. No fluorescence response was detected by the fluorometer, which indicated that no substance leached from the silks that could have affected the fluorescence readings.

### 2.2.3 Synergistic use of PCI and SeaWiFS

PCI data were extracted from the CPR database for the Central Northeast Atlantic and North Sea. For the period 1948-2002, the CPR survey collected more than 94,000 samples (Figure 2.3a).

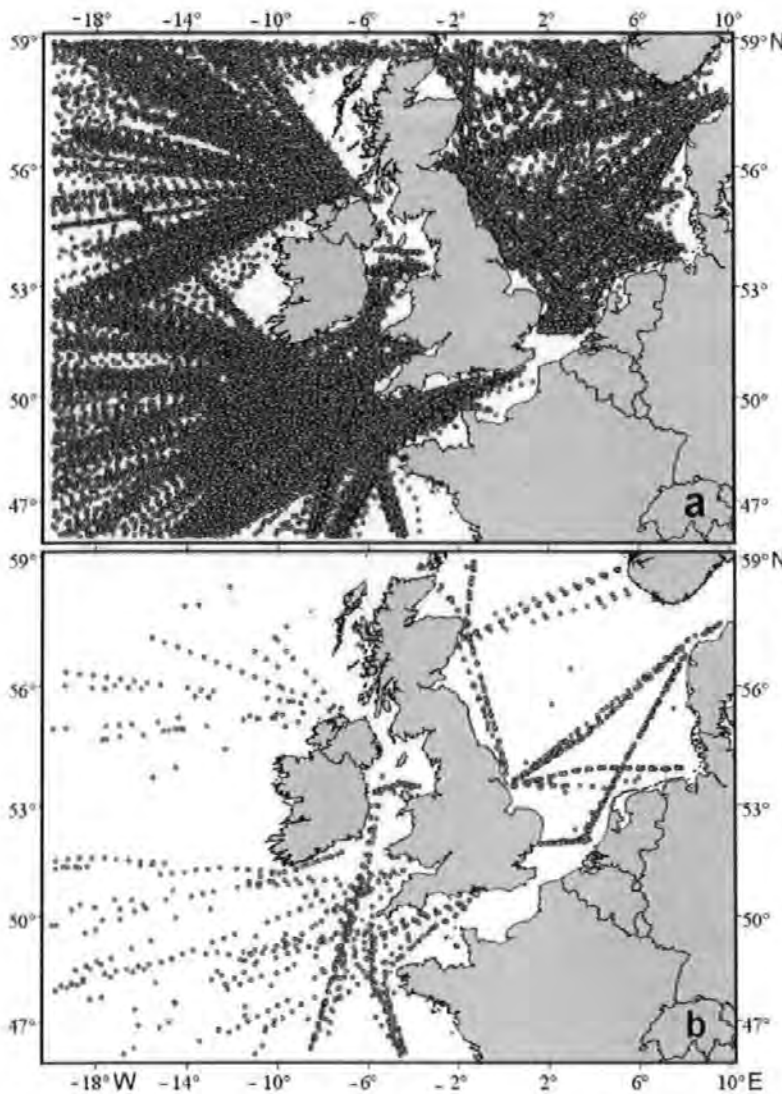


**Figure 2.3:** a) Location of CPR samples ( $n= 94,376$ ) in the Central Northeast Atlantic Ocean and North Sea for the period 1948-2002. b) Distribution of match ups of CPR/SeaWiFS measurements ( $n= 1585$ ) for the years 1997 - 2002.

### 2.2.3.1 Satellite Data

SeaWiFS data were acquired from the NASA GES DAAC and processed using SeaDAS version 4.4. Data used were Level 3 daily products (9x9 km<sup>2</sup> resolution) of the near-surface Chl-a concentration (mg m<sup>-3</sup>), estimated using the Ocean Chlorophyll 4 - version 4 (OC4-v4) algorithm (O'Reilly *et al.*, 1998):

$$\text{Chl - a} = 10^{(0.366 - 3.067x + 1.930x^2 + 0.649x^3 - 1.532x^4)},$$

where  $x = \log_{10} \left( \frac{(R_{rs} 443 > R_{rs} 490 > R_{rs} 510)}{R_{rs} 555} \right)$

### 2.2.3.2 Data Analysis

Sixty-four months (September 1997-December 2002) of *in situ* PCI and satellite Chl-a values were compared for the area of the Central Northeast Atlantic and North Sea. Concurrent SeaWiFS and CPR measurements were compared for the same spatial and temporal (daily) coverage. In the area of study, the CPR survey collected 11,149 different samples for the 5-year period. After screening the SeaWiFS dataset for CPR match-ups, only 1,585 samples could be used for comparison (86.7 % of the data did not have a SeaWiFS match-up, primarily due to cloud coverage); see Figure 2.3b.

PCI data is on a ratio scale i.e. not only can PCI categories be ranked, but differences are quantified. Thus, Pearson correlation (or linear regression) is appropriate to assess the strength of the relationship between SeaWiFS and PCI data (StatSoft 2004). SeaWiFS data were log-transformed to improve homogeneity of variance and normality (Zar 1984).

### 2.2.3.3 Potential Biases

Consistency and comparability of the methodology used in the CPR survey has been studied in some depth (Batten *et al.*, 2003; Reid *et al.*, 2003). Although standard methods have been used for more than 50 years in the survey, the PCI has been measured by a number of different analysts during this time. However, measuring

greenness is a simple task that is typically undertaken by 2 to 3 people in a year, many of whom have done this work for more than a decade. As well as referring to a standard colour chart, apprentices are trained in assessing PCI for a year before they undertake the task on their own.

The study area includes both Case I and Case II waters. In optically-complex Case II waters, Chl-a can not readily be distinguished from particulate matter and/or yellow substances (dissolved organic matter) and so global chlorophyll algorithms (such as OC4-v4) are less reliable (IOCCG 2000). As the majority of the area included in this study comprises Case I water this bias influences only a small proportion of the data points (Figure 2.3b).

## 2.3 Results

### 2.3.1 Laboratory Chl-a/PCI Intercomparison

Firstly, the overall relationship between PCI and *in situ* Chl-a concentrations (mg per CPR sample) was examined. Figure 2.4 presents the mean Chl-a concentration and Chl-a sample distribution for each PCI category with the 95% confidence intervals (CI) for each category. There is a relatively small variation in the CI of Chl-a for the first 3 categories with maximum variation in the fourth category; possibly due to the lower number of cases in that category (see Table 2.1). Overall, a clear relationship can be seen as the Chl-a concentration increases as the PCI categories increase. In addition, a significant positive relationship was found between the four PCI categories and Chl-a ( $r^2 = 0.73$ ,  $df = 226$ ,  $p < 0.0001$ ). From Figure 2.4 it can also be clearly observed that there is an apparent differentiation in Chl-a among PCI categories (95% CI do not overlap), as Chl-a increases gradually along with PCI categories.

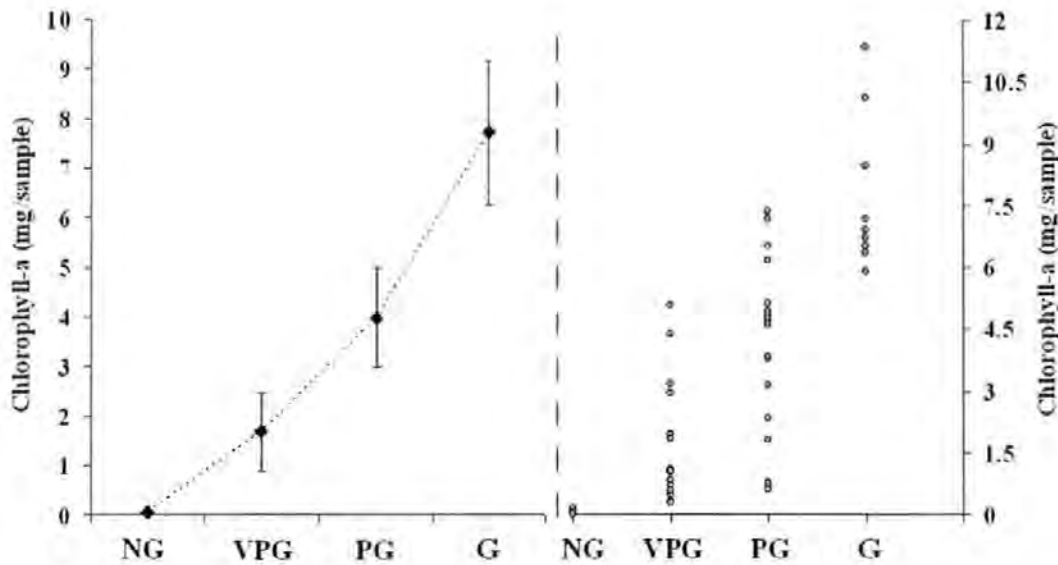


**Figure 2.4:** Mean Chl-a concentration (mg per CPR sample) and distribution of Chl-a samples (n= 228) per PCI category. The PCI is a ratio scale of phytoplankton colour with four 'greenness' values: 0 (NG - no greenness), 1 (VPG - very pale green), 2 (PG - pale green) and 6.5 (G - green). Note, there is no overlap between confidence intervals for each PCI category. The mean Chl-a plot indicated that NG= 0.05, VPG= 1.68, PG= 3.98, and G= 7.72 mg/sample.

Table 1 also demonstrates the descriptive statistics of the Chl-a (mg/sample) for each PCI category; the mean, minimum and maximum values of Chl-a progressively increase as the PCI category increases, which supports the differentiation and the significant relationships seen in Figure 2.4.



**Table 2.1:** Chl-a concentration (mg/sample) for every PCI category.

	Mean	Median	Minimum	Maximum	N
<b>NG</b>	0.05	0.05	0	0.18	32
<b>VPG</b>	1.68	1.06	0.29	5.11	16
<b>PG</b>	3.98	4.61	0.63	7.37	19
<b>G</b>	7.72	6.91	5.9	11.34	9

Figure 2.5 shows the differences between the different parts of the samples, in order to examine if the Chl-a is distributed equally across the CPR silk. Overall, it seems that the three parts vary slightly, as the Left Hand (LH) part is almost always higher than Central (C) and Right Hand (RH) part. However, an analysis of variance (ANOVA) indicated that there is no significant difference between the three parts ( $f=0.38$ ,  $df=226$ ,  $p=0.68$ ). In addition, it is clear from Figure 2.5 that the CI of the mean Chl-a overlap, indicating that the true mean population of the three parts is not significantly different from each other. Therefore, the across silk differences could be due to a surface area size bias as the cutting was approximate, however the difference is consistent as it exists in 79% of the cases; LH slightly higher than RH. Another possible reason is the CPR sampling mechanism; in order to negate the effects of bias within a single unit, 6 different CPR units were used and the error existed in all of them. This bias does not affect the PCI CPR quality or species specific counts as the manual examination is representative across all parts of the CPR sample (*pers. comms.* Tony John). For detailed methods see Reid *et al.* (2003).

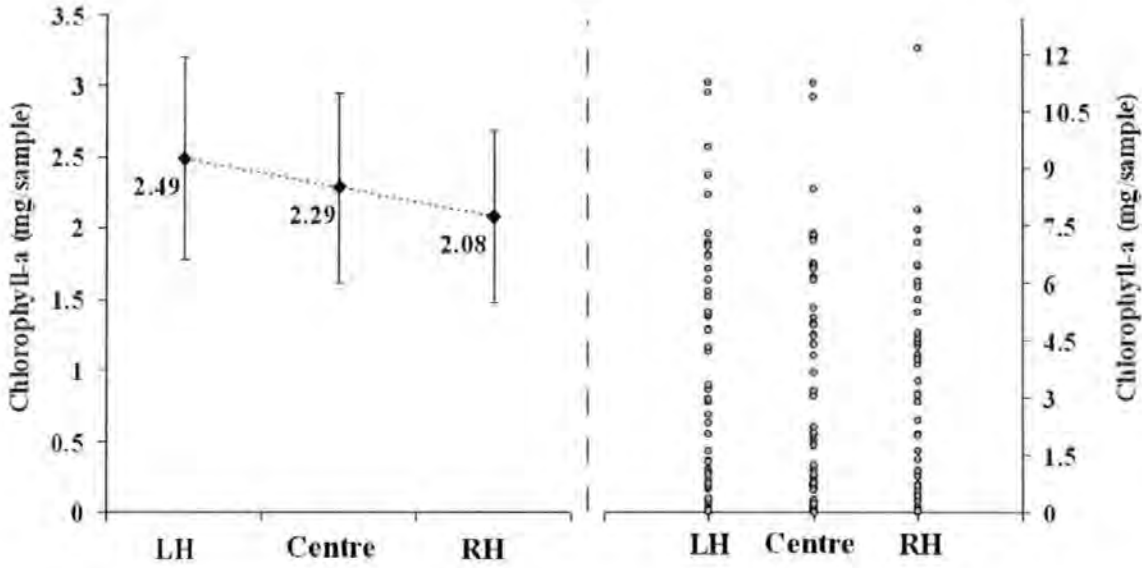


**Figure 2.5:** Mean Chl-a concentration (mg per CPR sample) and distribution of Chl-a across CPR samples. Every CPR sample ( $n=76$ ) was cut into 3 equal parts ( $n=228$ ). LH= Left Hand, C= Centre and RH= Right Hand part of the CPR silks.

### 2.3.2 PCI versus SeaWiFS

The overall relationship between PCI and SeaWiFS Chl-a was first examined for the whole study area (Figure 2.6a). There is a significant positive relationship ( $r=0.33$ ,  $p<0.001$ ) confirmed and strengthened when spatial and temporal autocorrelation are considered ( $r=0.47$ ,  $F=15.38$ , Adjusted  $df=53$ ,  $p=0.0003$ ). Spatial autocorrelation was removed by calculating the monthly average for the entire area of interest for PCI and matched SeaWiFS data. The Pearson correlation between these monthly time series was then calculated, and the degrees of freedom and thus the significance level of this test procedure were adjusted (Pyper and Peterman 1998).

As the relationship between SeaWiFS Chl-a and PCI is non-linear, the mean of SeaWiFS Chl-a for each PCI category was calculated (Figure 2.6a). There is a relatively small variation in the confidence intervals of Chl-a for the first three PCI categories; no green (NG)=  $1.03 \pm 0.21 \text{ mg m}^{-3}$ , very pale green (VPG)=  $1.65 \pm 0.16 \text{ mg m}^{-3}$ , pale green (PG)=  $2.61 \pm 0.29 \text{ mg m}^{-3}$  with maximum variation in the fourth

category (green (G))=  $4.25 \pm 0.98 \text{ mg m}^{-3}$ . There is clear differentiation in mean Chl-a among PCI categories (95% confidence intervals do not overlap), so these values can be used retrospectively to estimate Chl-a from PCI values.

To explore the seasonal patterns of PCI and SeaWiFS, the monthly means of both datasets were plotted (Figure 2.6b). Seasonal cycles for both show similar patterns, with a peak during late spring (spring bloom) and a decline during autumn and winter. The correlation coefficient implies a significant positive relationship ( $r= 0.79$ ,  $p<0.01$ ). For all months except July, the 95% confidence intervals overlap, indicating good agreement between the two Chl-a measures. It is possible that an increase of dinoflagellates in CPR samples in summer may have contributed to the difference in July, as they are the dominant phytoplankton at this time and give a brownish colour to the CPR silks and so could potentially lead to overestimates of Chl-a from PCI.

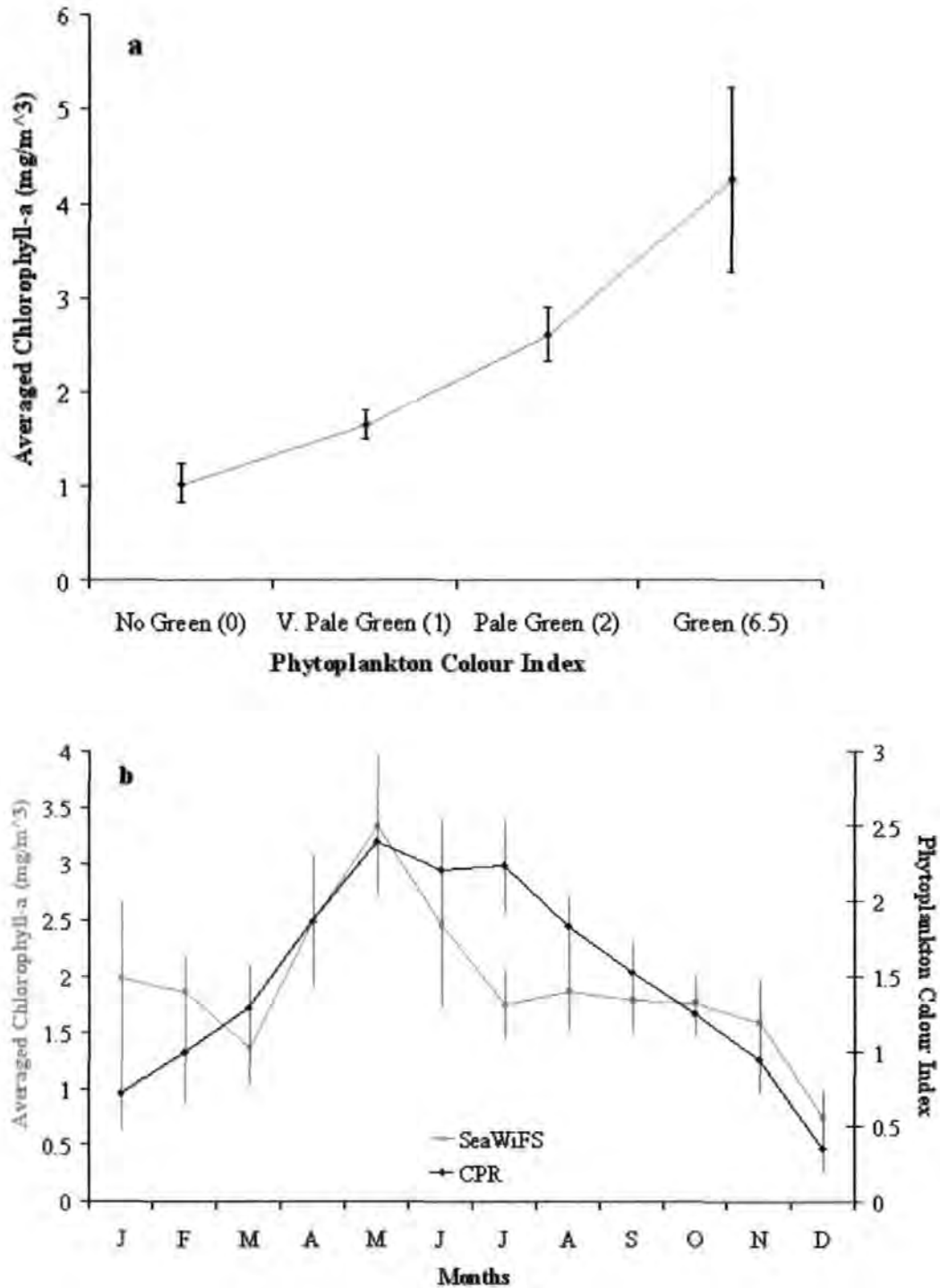


**Figure 2.6:** a) Mean Chl-a derived from SeaWiFS match-ups with CPR samples plotted against the equivalent values of PCI categories. Standard error bars represent 95% confidence intervals of the mean Chl-a. Note there is no overlap between confidence intervals for each PCI category. The number of samples (n) for each category is: No Green (NG)= 219, Very Pale Green (VPG)= 723, Pale Green (PG)= 484 and Green (G)= 162 of the 1585 match-ups. b) The seasonal cycle of Chl-a estimated from PCI and SeaWiFS for all match-ups in the area of interest. Error bars represent 95% confidence intervals.

Using the significant relationship between the PCI and Chl-a (Figure 2.6a) and the results of the >94,000 CPR samples analysed in the period 1948-2002 (Figure 2.3a), a retrospective calculation of Chl-a averaged for the Central Northeast Atlantic and North Sea has been produced (Figure 2.7). While the changes shown have been demonstrated previously in a semi-quantitative manner for the PCI (Reid *et al.*, 1998), the current results confirm and quantify the observations. An increasing trend is apparent in mean Chl-a for the area of study over the period 1948-2002 (Figure 2.7). There is clear evidence for a stepwise increase after the mid-1980s, with a minimum of  $1.3 \text{ mg m}^{-3}$  in 1950 and a peak annual mean of  $2.1 \text{ mg m}^{-3}$  in 1989 (62% increase). Post 1986 levels of Chl-a have increased systematically during winter (80% increase), with generally higher values in summer as well (Figure 2.8). The marked increase in chlorophyll seen in the mid 1980s is part of what has been termed a regime shift, a stepwise alteration in the composition and productivity of the whole ecosystem at a regional scale that reflects major hydrographic change (Reid *et al.*, 2001; Beaugrand 2004). Changes through time in the PCI are significantly correlated with both sea surface temperature and Northern Hemisphere Temperature (NHT, air and surface temperatures provided by Hadley Centre) (Beaugrand and Reid 2003). A climate signal is strongly evident in all trophic levels of the marine system in the North Atlantic and North Sea, although the mechanisms underlying such relationships are not fully understood (Richardson and Schoeman 2004).

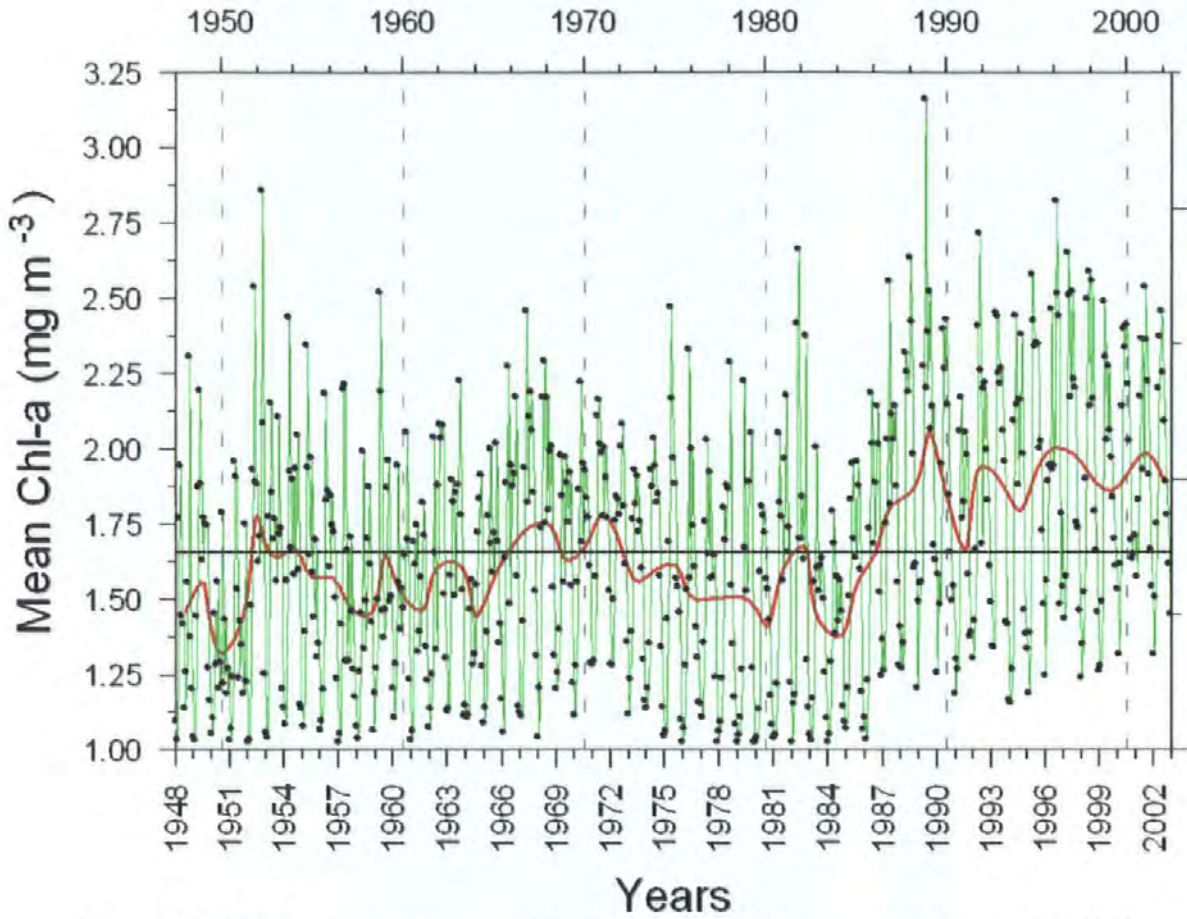


**Figure 2.7:** Time series of the new Chl-a dataset (monthly average) for the period 1948 to 2002 in the Central Northeast Atlantic and North Sea. The annual mean of Chl-a is plotted as a bold red line and the overall mean (1.678) as a horizontal line.

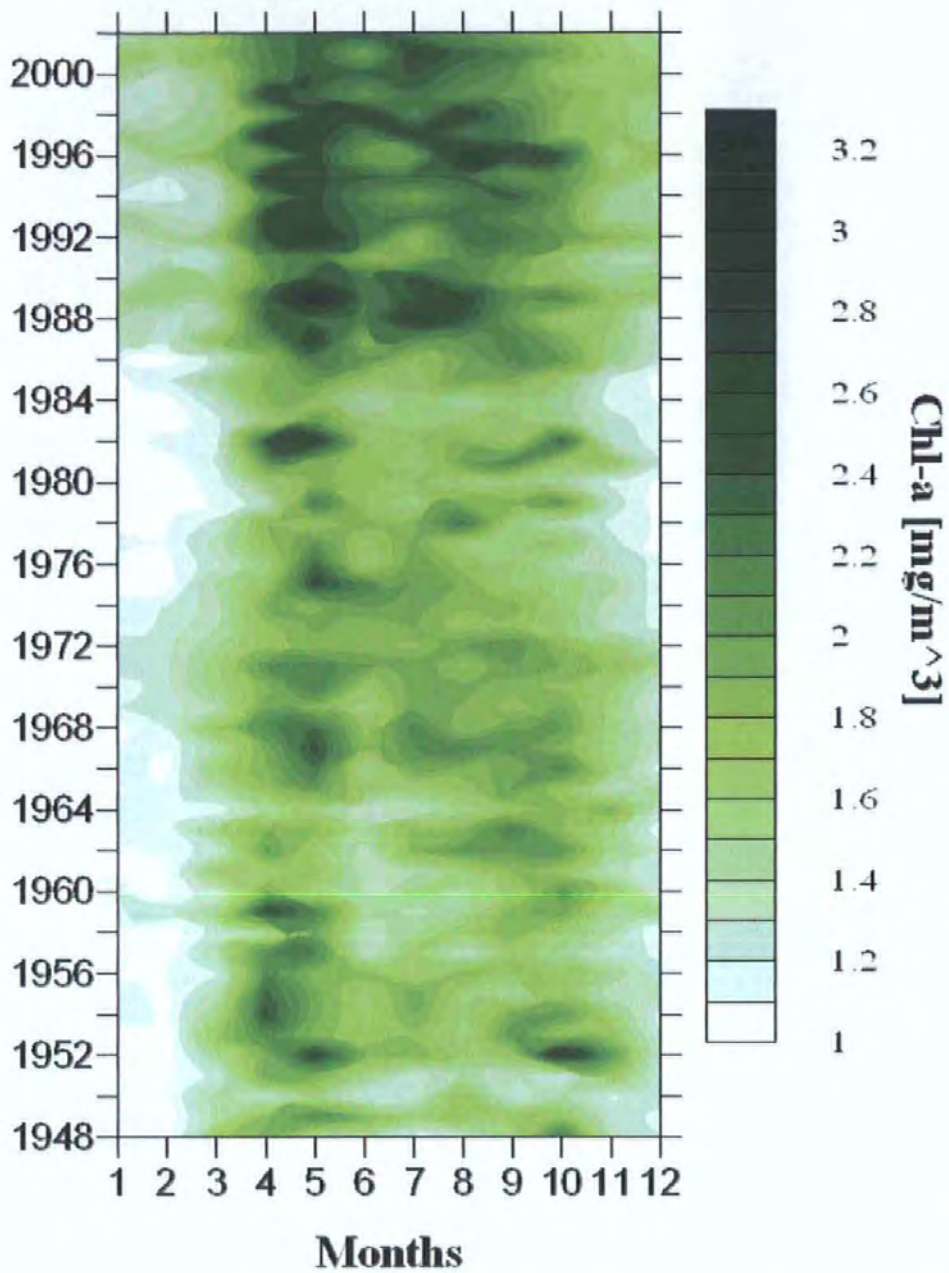


**Figure 2.8:** Contour plot of the new Chl-a dataset (monthly average) for the period 1948 to 2002 in the Central Northeast Atlantic and North Sea. Note the seasonal changes (timing of phytoplankton) especially after the mid 80s; the spring bloom has been merged with the summer bloom.

## 2.4 Conclusions

### 2.4.1 Laboratory Experiment

Similar values were found to those of Colebrook and Robinson (1965); however, based on the same way of creating an arbitrary ratio scale the new values are: NG= 0, VPG= 1, PG= 2.3 and G= 6.04. As the current results are based on a more robust methodological approach, it is suggested that future research should use the Chl-a concentration (mg/sample) mean values derived from this experiment. Although PCI is a visual assessment that can be characterised as a crude approach to identify ocean colour from a silk, the current results as well as those of Batten *et al.* (2003) indicate that PCI is a good index of phytoplankton standing stock. Further discussion can be seen in Chapter 5.

### 2.4.2 PCI versus SeaWiFS

The results make available for the first time, Chl-a data (since 1948) on the monthly variation of plant biomass in the Northeast Atlantic and North Sea. This allows a quantification of the stepwise increase in plant biomass in the mid-1980s; the regime shift corresponded to a 60% increase in Chl-a that is mainly due to the 80% increase in Chl-a during winter since the mid-1980s, alongside a smaller increase during summer. Discussions on the results as well as further applications are given in Chapter 5. Finally, this methodological approach was used to explain whether the changes observed in the North Sea were based on climatic changes or eutrophication (see paper in Appendix 1 and discussion in Chapter 5).



## CHAPTER 3

### *Phytoplankton variations as a response to the environmental regime*

This chapter illustrates two different methodological approaches to identify the key environmental, physical and spatiotemporal variables influencing the distribution and abundance of phytoplankton. For the purpose of this study, GAMs and ANNs were used to investigate which parameters influence coccolithophores and diatoms blooms.

Aspects of this chapter are included in the following publications:

**Raitsos D.E.**, Lavender S.J., Pradhan Y., Tyrrell T., Reid P.C., Edwards, M. (2006). Coccolithophore Bloom Size Variation in Response to the Regional Environment of the Subarctic North Atlantic. *Limnology and Oceanography*. **51**: 2122-2130.

**Raitsos D.E.**, Lavender S.J., Maravelias C.D., Haralambous J., Edwards M., McQuatters-Gollop A., Reid P.C. (Submitted). Macroscale factors affecting diatom abundance: a synergistic use of Continuous Plankton Recorder and satellite remote sensing data. *Remote Sensing of Environment*.

**Raitsos D.E.**, Lavender S., Pradhan Y., Tyrrell T., Reid P.C., Edwards M. (2006). Coccolithophore Bloom Size Variation in Response to the Regional Environment of the Subarctic North Atlantic. Oral Presentation in: **International conference of American Society of Limnology & Oceanography (ASLO)**. Honolulu, Hawaii.

### 3.1 Introduction

Literature has reported that coccolithophore abundances are increasing whereas diatoms are decreasing in the North Atlantic Ocean. In order to understand the impact of climate variability and physical environmental change on their abundance, as well as their potential reaction to future changes, it is important to understand the key factors influencing their spatial and temporal variability. Relationships between the synergistic satellite-CPR data matrix were built and analysed using GAMs and ANNs for coccolithophores and diatoms respectively.

#### 3.1.1 Coccolithophores

*Emiliana huxleyi* is a relatively small (circa 5-10  $\mu\text{m}$  diameter) phytoplankton species belonging to the taxonomic group of coccolithophores, which is capable of forming spatially extensive blooms. As this species can be visually detected, by turning dark blue oceanic waters milky-turquoise in colour (Figure 3.1) due to scattering caused by the coccoliths, the extensive blooms that it forms are visible from space (via satellite based sensors). That is why more is known about the spatial distribution of this phytoplankton species than any other (Tyrrell and Merico 2004). Blooms exceeding 250,000  $\text{km}^2$  in size, like the 1991 North Atlantic bloom (based on AVHRR, Holligan *et al.*, 1993), may have significant effects on the oceanic as well as atmospheric environment (Tyrrell and Merico 2004). Also, coccolithophores are major producers of several substances, e.g. dimethyl-sulphide (DMS), calcium carbonate and organic carbon, that are thought to affect the climate (Holligan 1993).

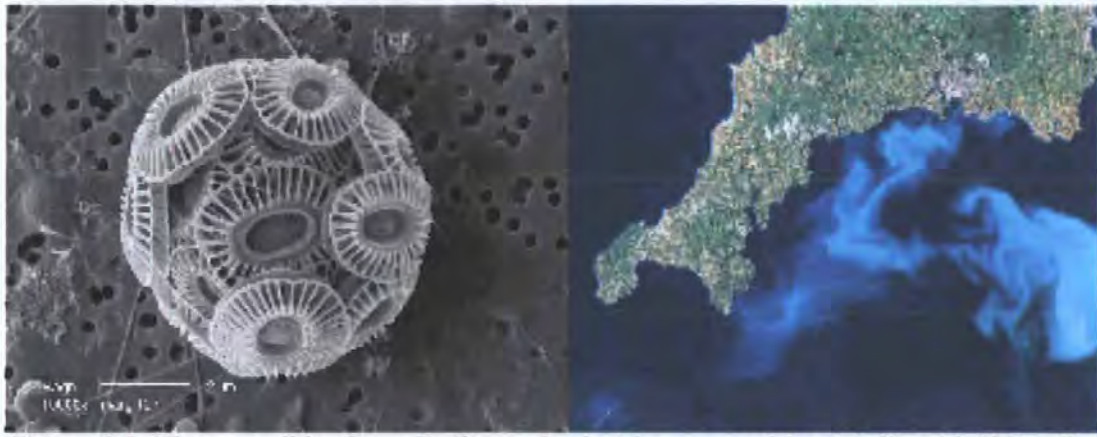


**Figure 3.1:** The coccolithophore *Emiliana huxleyi* is armoured by “chalky shields” called coccoliths, which turn the blue oceanic waters milky turquoise (Landsat image of the South Western tip of the UK). (<http://www.soes.soton.ac.uk/staff/tt/eh/index.html>)

Although satellites have been characterized as excellent tools for detecting and mapping *E. huxleyi* (Tyrrell and Merico 2004), several cases have shown that not all bright waters are caused by this species. Examples of water conditions that mimic *E. huxleyi*, or in other words mimic the highly reflective characteristics of coccolithophore blooms with significant numbers of liths, include broken-up diatom frustules (Broerse *et al.*, 2003), shallow carbonate shelves (Brown and Yoder 1994) and suspended sulphur particles (Weeks *et al.*, 2002). Generally, it is only very infrequently that open ocean turquoise waters should be ascribed to species other than *E. huxleyi* (Weeks *et al.*, 2004); however, it is essential that *in situ* verification is obtained before significant conclusions are drawn (Tyrrell and Merico 2004). This *in situ* verification can be acquired from the CPR survey.

Several environmental, physical and chemical factors can induce *E. huxleyi* blooms; although one factor alone is unlikely to trigger a bloom. Briefly, this coccolithophore species inhabits the sub-surface layer (mixed layer depth ~20m, Balch *et al.*, 1991) in highly stratified waters (caused by sunny and calm weather) where light intensity is high (Nanninga and Tyrrell 1996). An environmental parameter that may have an indirect effect on coccolithophores (through stratification) is wind stress; responsible for vertical mixing in the water column. It was thought (Tyrrell and Taylor 1996) that *E. huxleyi* blooms are favoured when inorganic phosphate is more limiting than nitrate, but a recent review showed that the Bering Sea and other blooms have

occurred in nitrate-scarce, phosphate-replete waters (Lessard *et al.*, 2005). *E. huxleyi* is also found in waters where carbonate saturation is high (Tyrrell and Merico 2004), silicate concentration is low (Brown and Yoder 1994) and iron concentration is low (Brand *et al.*, 1983). In addition, positive temperature and negative salinity anomalies (associated with strong haline stratification) have been correlated with coccolithophore blooms in the Barents Sea (Smyth *et al.*, 2004). Iglesias-Rodriguez *et al.* (2002) reported that water temperature combined with other factors, such as high light intensity, critical irradiance (stratification relative to light level) and declining nitrate concentrations appeared to be a good predictor of *E. huxleyi*. However, it is thought to be due to secondary effects i.e. water stratification (Tyrrell and Merico 2004). Although many attempts have been made to study the biogeochemistry of these blooms, little information is known on the effect of the physical environment in the subarctic North Atlantic.

### 3.1.2 Diatoms

Diatoms (Figure 3.2) are responsible for ~20% of global carbon fixation (Armbrust *et al.* 2004 and references within), ~25% of global primary production and a large amount of the carbon exported to the deep sea via sinking particles (Milligan and Morel 2002). Because their cell walls are impregnated with silica, diatoms are major contributors to the biogeochemical cycling of silicon (Falciatore *et al.*, 2000); the second most abundant element on Earth (Basile-Doelsch *et al.*, 2005). This major group of marine plants prospers in almost every aquatic environment (Armbrust *et al.*, 2004; Strzpek and Harrison 2004) and they are considered a key food for copepods and other zooplankton, which are subsequently consumed by larger predators such as fish and marine mammals (Irigoien *et al.*, 2002; Jones and Flynn 2005), thereby transferring energy to higher levels of the marine food web (Miralto *et al.*, 1999). Therefore, as primary producers diatoms play a key role in some of the most productive and economically important marine ecosystems (Irigoien *et al.*, 2002,).

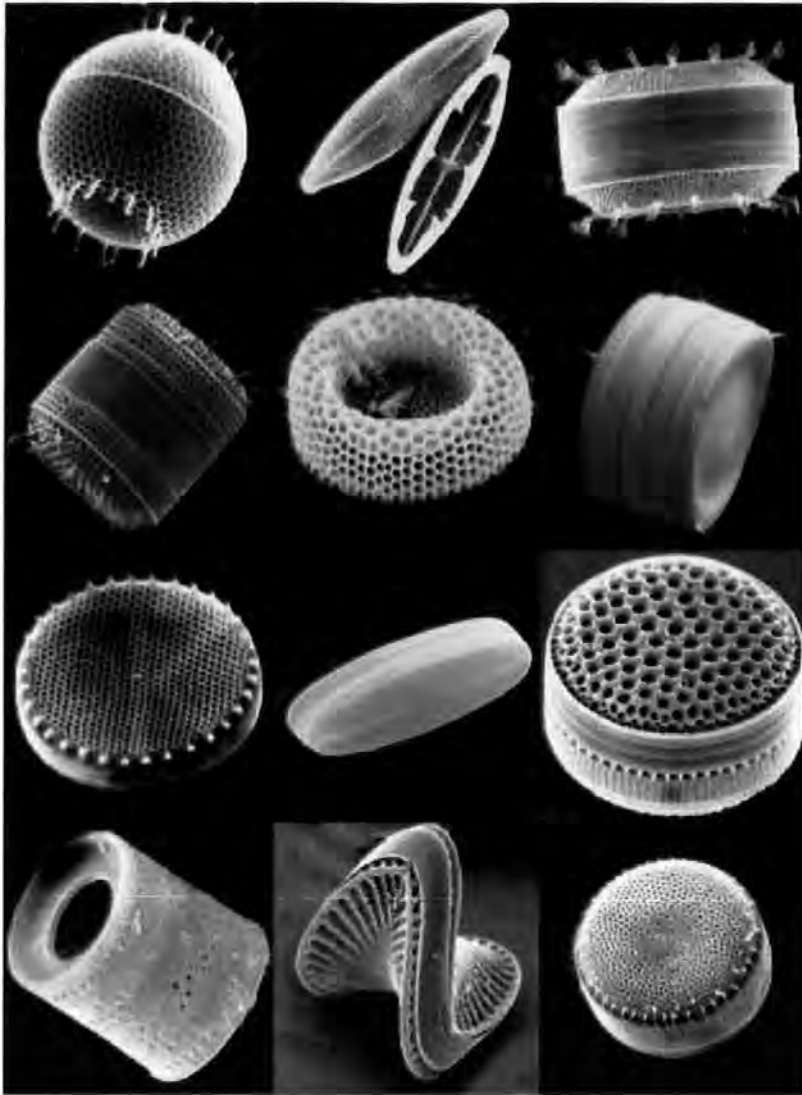


**Figure 3.2:** Examples of different diatom species (<http://www.bhikku.net/archives/03/img/diatoms.jpg>)

The vulnerability of phytoplankton in relation to climatic changes in the North Atlantic Ocean has been reported previously (Edwards and Richardson 2004; Richardson and Schoeman 2004). Decreasing patterns of diatoms have been repeatedly reported based on past *in situ* data (Leterme *et al.*, 2005) and modelled data (Bopp *et al.*, 2005). Bopp *et al.* (2005) reported that climate change is likely to lead to an increasingly nutrient depleted epipelagic surface zone that will lead to a relative reduction in diatom populations in favour of other smaller phytoplankton. Information linking global climatic variability to changes in biological communities is a matter of concern (Richardson and Schoeman 2004 and references within).

In order to understand the impact of climate and physical environmental variability on diatoms, as well as the potential reaction of diatom blooms to environmental change, it is important to understand the key factors dictating the spatial variability of this functional group. Despite the importance of this information, knowledge on large spatial scales, especially in open oceanic waters, is limited due to poor data availability. The CPR has been used to examine decadal-scale diatom phenology (Edwards and Richardson 2004), changes in abundance (Leterme *et al.*, 2005), species specific spatial variability (Barnard *et al.*, 2004) and the significant role of mesoscale anticyclonic eddies on diatom distribution (Batten and Crawford 2005). However, the high spatial coverage of the CPR dataset does not include physical parameters that regulate diatom abundance; therefore satellite remote sensing provides a complementary dataset.

### ***3.2 Aims and Objectives***

**Coccolithophores:** Examine the causative physical factors and/or environmental extremes that induce extensive coccolithophore blooms, detected by SeaWiFS, in the subarctic North Atlantic. The physical variables used in the analysis are: solar radiation flux; SST and its anomaly; mixed layer depth (MLD); wind stress. Particular attention was paid to a massive *E. huxleyi* bloom that occurred in June 1998.

**Diatoms:** Understanding diatom variability and identify the key spatiotemporal and physical environmental factors influencing diatom abundance in the open oceanic area of the Northeast Atlantic. A data matrix composed of concurrent satellite remote sensing and CPR *in situ* measurements was collated for the same spatial and temporal coverage; a >6 year period (Sep 1997-Dec 2003) in the Northeast Atlantic. While previous studies have used annual variations of phytoplankton linked with SST, here (although only 6 years of data were available) a more robust increased spatial and temporal resolution analysis was performed to derive relationships between the physical/spatiotemporal regimes and diatom abundance.

### 3.3 Methods

#### 3.3.1 Cocolithophores

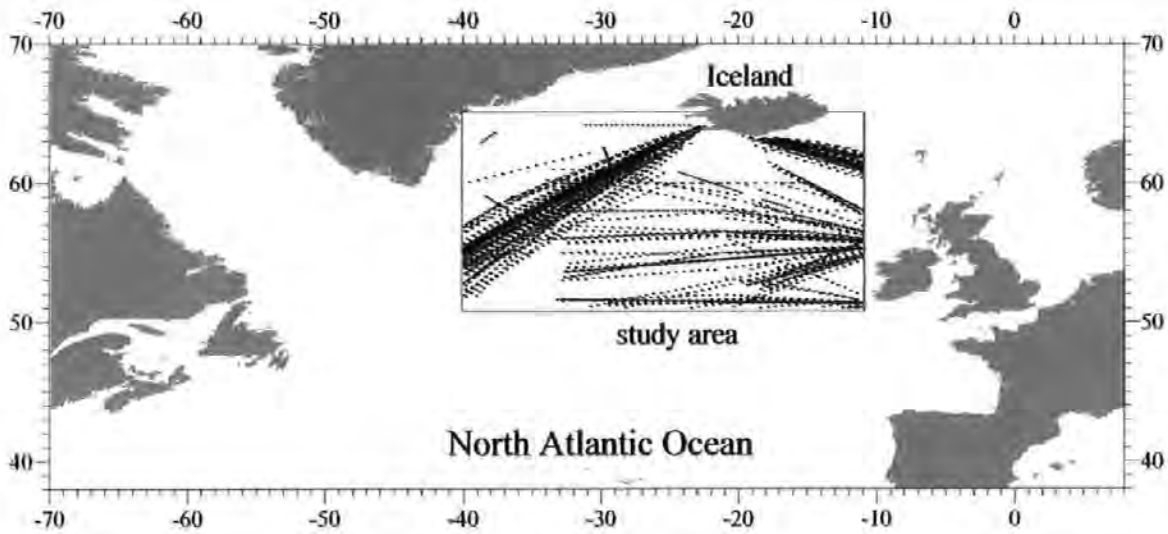
This part outlines the methodological approach used to identify which parameters drive the coccolithophore blooms in the subarctic North Atlantic; an area which has been characterised as the most abundant coccolithophore area in the world. Table 3.1 summarise the physical parameters used in this study as well as their sources and the statistical modelling approach used to derive relationships between coccolithophores and the independent variables.

Table 3.1: Summary of the parameters, sources and statistical methods used to analyse them.

<b>Coccolithophores study</b>		
<b>Parameters</b>	<b>Source</b>	<b>Statistics</b>
nLw_555	SeaWiFS	
SST	AVHRR	
SSTA	AVHRR	GAMs
Wind stress	NCEP/NCAR	
light intensity	NCEP/NCAR	

##### 3.3.1.1 Data and methods

All satellite, *in situ* and modelled datasets were for the same study area; the subarctic North Atlantic defined by 51°N - 66°N and 40°W - 11°W (Figure 3.3).



**Figure 3.3:** Study area of the subarctic North Atlantic, 51°-66°N and 11°- 40°W. The black dots represent the CPR samples taken from January 1998 to December 2002 ( $n=3,977$ ).

### 3.3.1.2 Satellite data

**SeaWiFS:** Version 5.1 data produced by Ocean Biology Processing Group (OBPG) was acquired from the NASA Oceancolor website (<http://oceancolor.gsfc.nasa.gov/>). The data were Level 3 monthly composite products ( $9 \times 9$  km<sup>2</sup> resolution) of the normalized water-leaving radiance (nLw) at 555 nm ( $\text{mW cm}^{-2} \mu\text{m}^{-1} \text{sr}^{-1}$ ) for the period from September 1997 to December 2004 (>7 years of data). It was used to indicate the temporal and spatial variability of coccolithophore blooms, which has been routinely assessed using SeaWiFS imagery (Cokacar *et al.*, 2004). The size of the 1998 coccolithophore bloom detected by SeaWiFS (see Figure 3.4) was calculated by recording the number of pixels where nLw<sub>555</sub> was greater than  $0.9 \text{ mW cm}^{-2} \mu\text{m}^{-1} \text{sr}^{-1}$  (Cokacar *et al.*, 2004).



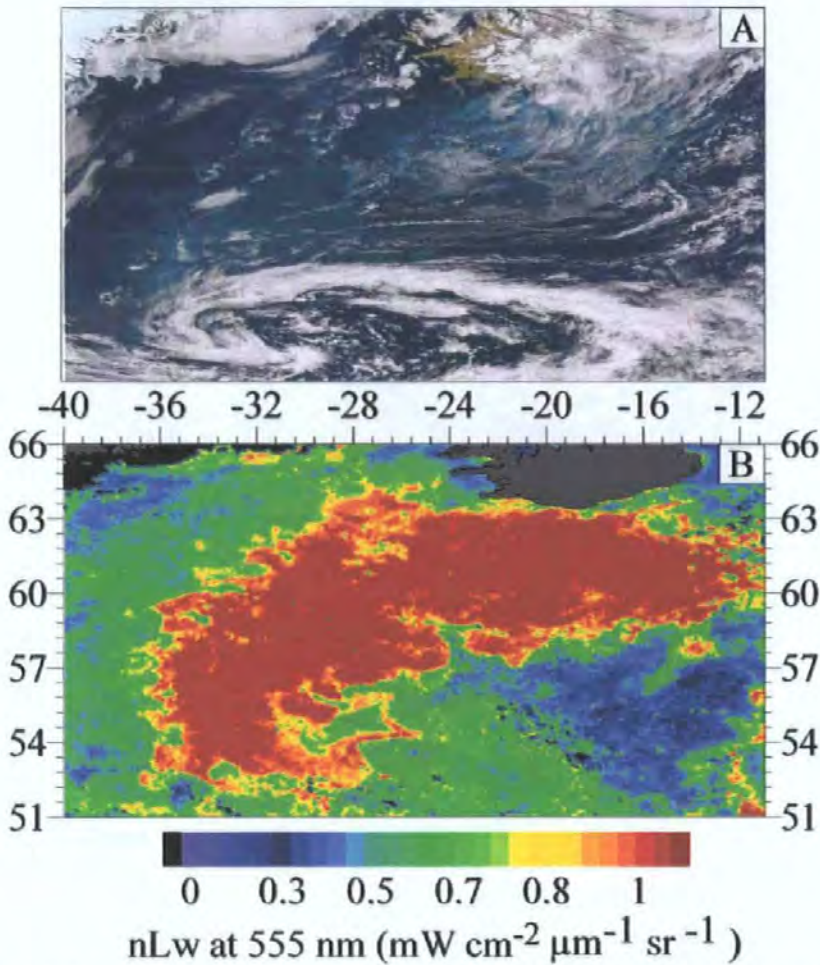


**Figure 3.4:** (a) True colour image of the coccolithophore bloom taken by SeaWiFS on 15 June 1998, subarctic North Atlantic. Provided by the SeaWiFS Project, NASA/GSFC and ORBIMAGE. (b) Colour contour image presenting a monthly mean of SeaWiFS nLw<sub>555</sub> for June 1998.

**AVHRR:** The night-time AVHRR Pathfinder 5 (P5) monthly mean SST at  $9 \times 9 \text{ km}^2$  resolution were obtained from the NASA PO.DAAC website at <http://poet.jpl.nasa.gov/>. Then, the monthly mean climatologies were computed from 1985-2004 and the monthly Sea Surface Temperature Anomaly (SSTA) was the deviation of the SST from the mean climatology. The night-time SST products were used so that the solar radiation bias (the diurnal fluctuation in SST) that can occur during the day-time could be avoided.

**The NCEP/NCAR Reanalysis data:** a) Monthly composites of mean wind speed ( $\text{m s}^{-1}$ ) data were obtained ( $2.5^\circ \times 2.5^\circ$  spatial resolution) from which the wind stress (Pa) was calculated (September 1997 to December 2004). The stress exerted by the surface wind (at 10 m above the sea surface) is derived as a function of wind speed, non-dimensional drag coefficient and boundary layer air density (Pickard and Pond 1978):

$$\tau = \rho_a C_D |W|W$$

Where,  $\rho_a$  is the average air density ( $\sim 1.3 \text{ kg m}^{-3}$ ),  $W$  is the wind speed over the sea surface (for most practical purpose a 10 m height wind speed,  $W_{10}$ , is acceptable) and  $C_D$  is the dimensionless drag coefficient that varies with wind speed as (Yelland and Taylor 1996):

$$C_D = \left( 0.29 + \frac{3.1}{W_{10}} + \frac{7.7}{W_{10}^2} \right) 10^{-3} \quad \text{for } (3 \leq W_{10} < 6 \text{ m s}^{-1})$$

$$C_D = (0.60 + 0.07 W_{10}) 10^{-3} \quad \text{for } (6 \leq W_{10} \leq 26 \text{ m s}^{-1})$$

Sea surface wind stress drives the dynamics of the boundary layer and is therefore expected, on physical grounds, to be closely related to the generation of surface waves, production of wind-driven ocean surface currents and the stirring processes that keep the upper ocean well mixed down to the thermocline. The spatial variation of wind stress, over the ocean, causes surface divergence of horizontal flow that in turn gives rise to vertical mass flux through Ekman pumping (Ekman 1905). Since coccolithophores are likely to be found in highly stratified waters, the wind stress (as well as MLD, see below) was used to confirm the presence of these conditions (stratification).

b) Monthly composites of mean downward solar radiation flux ( $\text{W m}^{-2}$ ) data were obtained for the period of 1997-2004 ( $2.5^\circ \times 2.5^\circ$  spatial resolution). The NCEP/NCAR reanalysed 'surface' downward solar radiation flux was used, which is estimated at the bottom of the atmosphere (Kalnay *et al.*, 1996), and is therefore considered as the solar radiation received at the earth's surface. Reanalysis data were provided by the NOAA-CIRES Climate Diagnostics Center, Boulder, Colorado, USA, from their website at <http://www.cdc.noaa.gov/>.

### 3.3.1.3 OCCAM Model Data

The MLD dataset was obtained from the Ocean Circulation and Climate Advanced Modelling Project (OCCAM) that runs a high resolution global ocean model. The monthly mean MLD (m) product ( $0.25^\circ \times 0.25^\circ$  resolution) for the North Atlantic and Arctic Ocean model domain was used. Then, an averaged time series was created for the period from September 1997 to December 2003.

Generally, the modelled MLDs are based on a variety of physical variables such as wind speed, wind stress and latent heat fluxes, thus the estimation of MLDs are most consistent with a large number of data sources. For instance, the primary OCCAM model variables were potential temperature, horizontal velocity and sea surface elevation (Webb *et al.*, 1998). More technical details of the OCCAM model can be found elsewhere (Webb *et al.*, 1998). The data were ordered from the official website address of the OCCAM model: <http://www.noc.soton.ac.uk/JRD/OCCAM/EMODS/>.

### 3.3.1.4 In situ Data

Although *E. huxleyi* is only 5-10  $\mu\text{m}$  in diameter, it is reported that this species has been identified repeatedly in CPR samples (Hays *et al.*, 1995). Hays *et al.* (1995) suggested two possible reasons why this small coccolithophore species is present on CPR samples; plankton clogging up the filter and its capture on the finer threads of silk that constitute the mesh-weave.

The CPR analysis does not identify coccolithophores to the species level, but the archived samples are available for re-examination. Therefore, archived samples were re-analysed to confirm if the bloom observed from satellite was *E. huxleyi*. Data (number of coccolithophore cells per tow) for the North Atlantic were extracted from the CPR database between 1998 and 2002 (Figure 3.3). The CPR took 95 samples within 6 days (1, 20, 21, 27, 28, and 29) in June 1998, and 30 of those appeared to be dominated by coccolithophores. These archived CPR samples (preserved in buffered formalin) were re-examined and *E. huxleyi* was identified.

### **3.3.1.5 Data Analysis**

Generalised Additive Models (GAMs) were used to investigate potential relationships between an index of coccolith abundance (nLw\_555) and various environmental parameters (solar radiation flux, SST, SSTA, MLD and wind stress). GAM is a flexible regression technique whose advantage over traditional regression methods, such as General Linear Models, are its ability to model nonlinearities using nonparametric smoothers. A detailed description of GAMs can be found elsewhere (Hastie and Tibshirani 1990).

Seventy six (number of monthly averages) data points were employed to develop the relationships for each parameter. The least squared weighted smoothers (loess) was used to estimate the non-parametric function, and the Gaussian error distribution was assumed after consideration of diagnostic residual plots (Hastie and Tibshirani 1990; Maravelias 2001). In order to construct the GAM, a forward and backward stepwise model fitting approach was used, based on the Akaike's Information Criterion (AIC) statistic (Chambers and Hastie 1992). All predictors in the model were included as smoothed terms and by using the AIC, the significance of each term in the model could be assessed. Also, the stepwise approach enabled the removal of the non significant variables (predictors) from the final model. Hence, the final models showed the combined effect of each predictor (physical variable) on the response (nLw\_555).

### **3.3.2 Diatoms**

This part outlines the methodological approach and data used to identify which parameters drive the diatom blooms in the North Atlantic Ocean. The parameters used are summarised in Table 3.2.

Table 3.2: Summary of the parameters, sources and statistical methods used to analyse them.

<b>Diatoms study</b>		
<b>Parameters</b>	<b>Source</b>	<b>Statistics</b>
PAR	SeaWiFS	
SST	AVHRR	
wind stress	ERS2-QS	Neural Networks
In situ diatoms	CPR	GRNN
longitude-latitude	CPR	
Month	CPR	

### 3.3.2.1 Satellite Data

**SeaWiFS:** solar radiation product was acquired from the NASA Oceancolor website (<http://oceancolor.gsfc.nasa.gov/>); reprocessing version 5.1 produced by the Ocean Biology Processing Group. The data were Level-3 8-day composite products (9×9 km<sup>2</sup> resolution) of the Photosynthetically Active Radiation (PAR) (E/m<sup>2</sup>/Day), which is the incoming solar radiation or insolation that can generally be defined as the light intensity received at the surface of the Earth. Further information/documentation regarding the PAR algorithm and its calculation can be found at [http://oceancolor.gsfc.nasa.gov/DOCS/seawifs\\_par\\_algorithm.pdf](http://oceancolor.gsfc.nasa.gov/DOCS/seawifs_par_algorithm.pdf).

The AVHRR Pathfinder 5 (P5) SST weekly mean products at a resolution of 4×4 km<sup>2</sup> were used (further details can be seen in section 3.3.1.2).

**ERS-2 and NASA-QuikSCAT (QS):** weekly composites of mean wind stress data (0.5°×0.5° spatial resolution) were obtained from CERSAT, IFREMER (<http://www.ifremer.fr/cersat/en/index.htm>). A preliminary inter-sensor comparison between ERS-2 and QS wind speeds indicated that both sensors are compatible with each other ([http://www.ifremer.fr/cersat/en/research/validation/qscat\\_vs\\_topex](http://www.ifremer.fr/cersat/en/research/validation/qscat_vs_topex)

\_ers.htm). Wind stress, which is responsible for vertical mixing in the water column, may have an indirect effect on phytoplankton biomass through nutrient availability. The spatial variation of wind stress over the ocean causes surface divergence of horizontal flow that in turn gives rise to vertical mass flux through Ekman pumping (Pond and Pickard 1983).

### **3.3.2.2 *In situ Data***

CPR analysis involves microscopic procedures in order to identify and count phytoplankton species presence to the highest practical extent (Batten *et al.*, 2003). The total number of diatoms (sum of all species found) for each sample was used; the full species list can be seen elsewhere (Reid *et al.*, 2003). In the area of study, the CPR survey collected 14,001 different samples for the >6 year period. After screening the satellite dataset for spatial and temporal CPR match-ups, only 3,732 concurrent samples could be used for comparison (primarily due to cloud coverage affecting the satellite data).

### **3.3.2.3 *Methodology for Data Collation***

The methodological approach used match-ups between satellite derived physical parameters and CPR total diatom measurements which were collated for the same spatial and temporal coverage. The area of study is defined by: 46°N - 66°N, 52°W - 4°W (Figure 3.5) and were processed between September 1997 to December 2003. Note that all the figures and plots are based only on CPR match-ups that have a corresponding occurrence with every satellite variable used in the study (Figure 3.5).

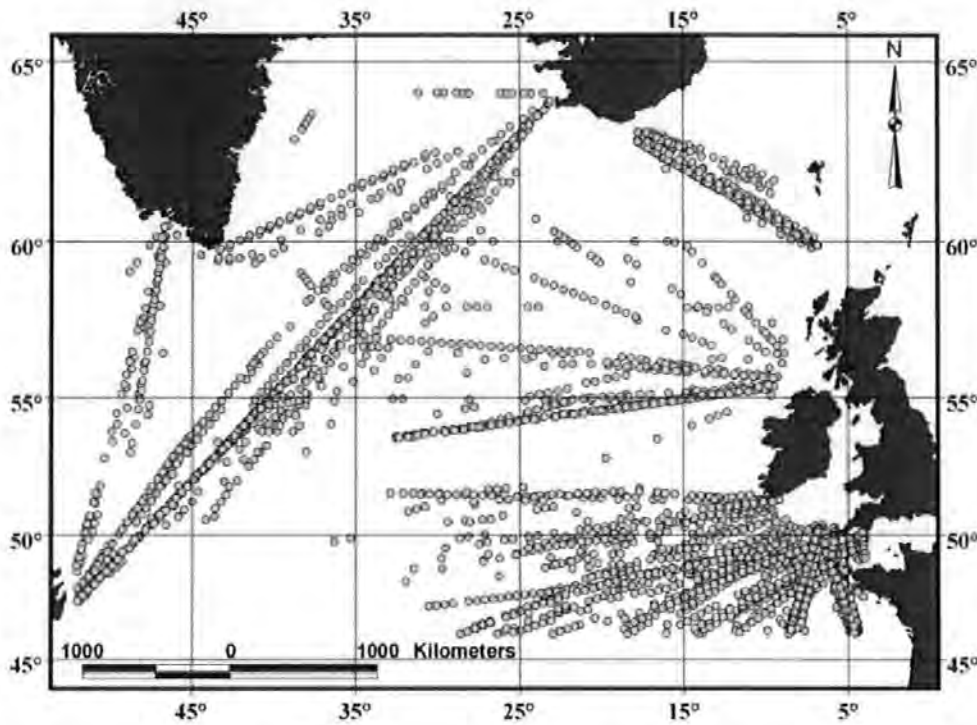


Figure 3.5: Distribution of match-ups of diatom CPR data and satellite parameters for the period of 1997-2003 in the northern Atlantic Ocean.

#### 3.3.2.4 Data Analysis using Artificial Neural Networks

A typical GRNN structure consists of 4 interconnected layers of ‘nodes’ or ‘neurons’. The input layer contains one neuron per independent variable. The pattern layer (first hidden layer) contains the radial base function (RBF) units. The summation layer (second hidden layer) contains units that help to estimate the weighted average; the only weights that need to be learned by the network are the widths of the RBF units. These widths (often a single width is used) are called ‘smoothing parameters’ or ‘bandwidths’ and are usually chosen by cross-validation. Each output has a special unit assigned in this layer that forms the weighted sum and to get the weighted average, the weighted sum must be divided throughout by the sum of the weighting factors. The output layer then performs the actual divisions (using special division units). Hence, the second hidden layer always has exactly one more unit than the output layer.

The GRNNs were implemented on a random subset of the available data (training set) and then applied to the remaining data (validation or testing set). In this research, the training set consisted of a random 4/5ths of the available data set (2986 cases) with the remaining random 1/5<sup>th</sup> of the data (746 cases) being used as the testing set. This holdout partitioning technique (Kohavi 1995) was repeated five times to ensure the validity of the model. The testing set was used for calibration which prevented overtraining the networks thereby enabling them to generalise well on new data. Calibration adjusted the weight of each neuron by computing the distance metric between a given classification and the network results for all outputs over all patterns. The genetic adaptive algorithm (Specht 1991) was applied during this process to test a whole range of smoothing factors. At the end, the individual smoothing factors were used as a sensitivity analysis tool: the larger the smoothing factor for a given input, the more important that input variable was to the model, at least, as far as the test set was concerned.

### 3.4 Results

#### 3.4.1 Coccolithophores

To explore the seasonal cycle of coccolithophores, the monthly means of both time series data (CPR and SeaWiFS nLw\_555) were plotted against time for the period 1998 to 2002 (Figure 3.6). A clear visual agreement can be seen and the results suggest that both patterns exhibit seasonal cycles with similar trends; increasing during early summer (both peaked during June) and gradually decreasing during autumn/winter. However, there is a noticeable difference from July to September when the CPR values drop off rapidly while the nLw\_555 values remain high. Once the coccolithophore bloom starts to decline, the coccoliths are detached from the cells and float separately in the water. Therefore, the satellite still detects the reflectance resulting from these blooms (for optical properties of coccoliths see Voss *et al.*, 1998), whereas the CPR is counting only the live cells and not the coccoliths. It has been reported that when the coccolithophore bloom of 1991 aged, the number of the



detached coccoliths increased (Balch *et al.*, 1996a) and that suspended coccoliths were causing up to 80% of the total backscattering in the centre of the bloom (Balch *et al.*, 1996b). However, Figure 3.6 clearly shows that in the subarctic North Atlantic the favourable month for coccolithophores is June.

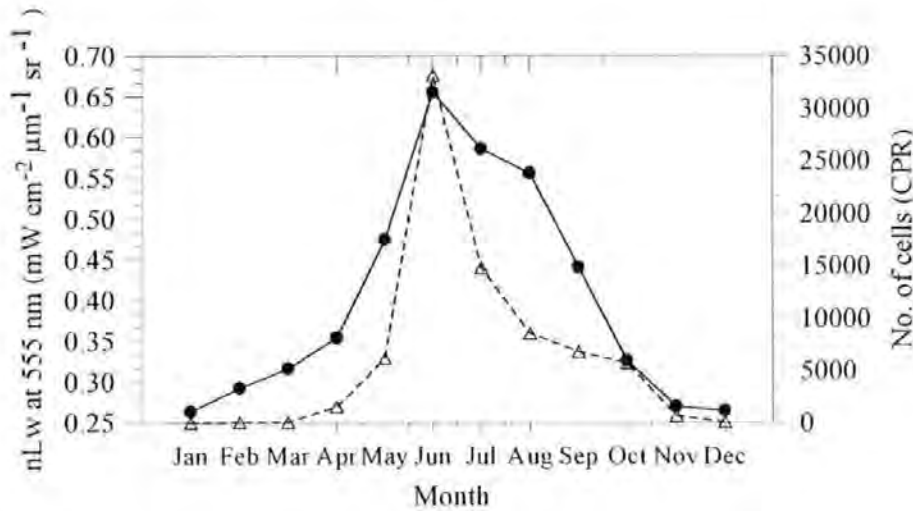


**Figure 3.6:** Monthly mean of SeaWiFS nLw\_555 (solid line) and CPR coccolithophore numbers (dashed line) from January 1998 to December 2002 (3,977 samples). The spatial distribution of the samples can be seen in Figure 3.3.

The >7 year time series of nLw\_555 indicated that the highest values (primarily from coccolithophores) occurred during the summer months and specifically June (Figure 3.7a). The highest nLw annual mean occurred during 1998, and June appeared to have the highest nLw mean ( $\sim 0.8 \text{ mW cm}^{-2} \mu\text{m}^{-1} \text{ sr}^{-1}$ ); it showed an increase of  $\sim 25\%$  when compared to the overall mean of the remaining Junes. In addition, June 1998 appeared to occupy the largest aerial extent. Figure 3.4b shows that the spatial extent of the June 1998 coccolithophore bloom, and the calculated size (based on SeaWiFS) of this extensive bloom was  $>995,000 \text{ km}^2$  (15 June 1998). Also, an analysis of the archived *in situ* samples confirmed that this bloom was primarily composed of coccolithophores; *E. huxleyi* was present in almost all the samples. Coccolithophore blooms also occur in the other years, but their spatial extent appeared to be less pronounced (Figure 3.7a).

Several environmental/physical parameters were plotted in order to examine their importance on coccolithophores (Figure 3.7). The solar radiation flux time series

indicated that the highest values occurred during the summer months and peaked in June every year (mean of  $477 \text{ W m}^{-2}$ ), whereas the lowest light occurred during the winter months with the lowest values during the December months (mean of  $35 \text{ W m}^{-2}$ ), Figure 3.7b.

Figure 3.7c shows that overall, July appeared to have had the lowest wind stress every year. The wind stress shows the opposite pattern (negatively related) to SST (Figure 3.8a); it is high during the autumn and winter months and decreases rapidly during the summer months enabling summer stratification (favourable conditions for *E. huxleyi*). June 1998 and 2001 appeared to have the lowest mean wind stress (0.08 Pa) in comparison with the Junes of other years. However, the overall average for all Junes (0.095 Pa) does not differ considerably from the monthly mean of June 1998.

Figure 3.7d indicates that during autumn-winter months the MLD reaches the highest values, whereas during the summer months the MLD is decreasing rapidly (lowest in July). During Junes (highest nLw\_555 values), the overall MLD mean for the study area is 14.6 m, while the shallowest MLD of this time series appeared during June 1998 (11.6 m). These results confirm the presence of highly stratified and shallow mixed layer depth waters within the study area (during Junes) that favour *E. huxleyi*.

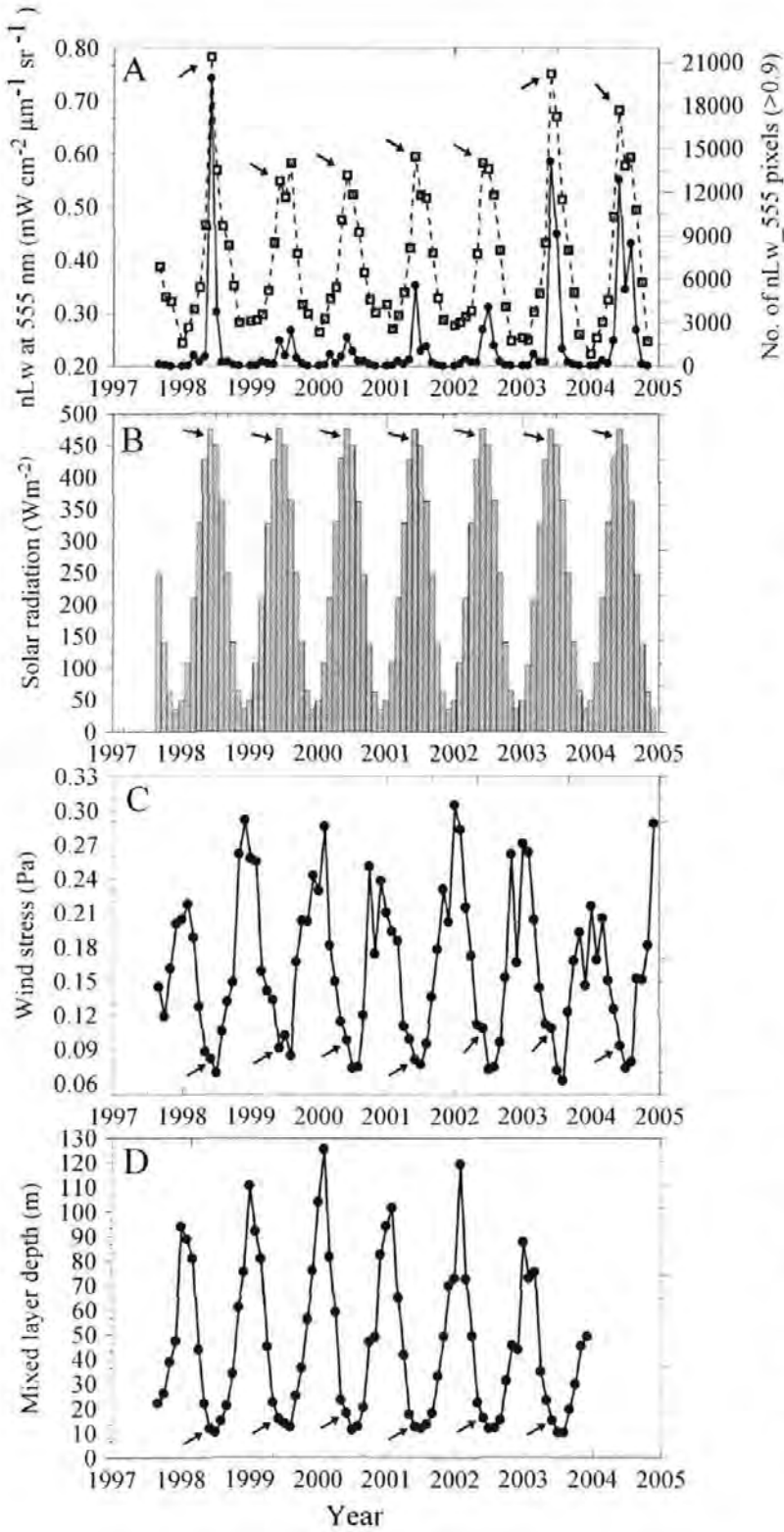


**Figure 3.7:** Satellite time series of: (a) The dashed line presents the nLw<sub>555</sub> (coccolithophore abundance) from September 1997 to December 2004, and the solid line presents the number of nLw<sub>555</sub> pixels >0.9 (blooms areal extent), (b) solar radiation flux from September 1997 to December 2004, (c) Wind stress from September 1997 to December 2004, (d) MLD from September 1997 to December 2003. The arrows represent the Junes of every year.

Figure 3.8a shows AVHRR SST (1985-2004) that has a pronounced change in this 20 year time series with evidence for a stepwise increase in 1996. It can be clearly seen that after this year the annual SST mean remains above the overall mean, whereas the opposite occurred before 1996. The annual mean showed that 1998 was the warmest year (9.6 °C) and June 1998 (when the extensive coccolithophore bloom occurred) along with June 1995, appeared to be the warmest Junes of the 20 year time series. Overall, the average temperature during all Junes was 9.6 °C whereas in 1998 the monthly mean was 10.6 °C (1 °C above the mean).

It should be noted that *E. huxleyi* may trap light near to the surface layer; consequently, surface waters that are dominated with this species tend to have increased temperatures. In other words, the temperature might be increased due to the presence of *E. huxleyi* rather than the bloom benefiting from an already present increased temperature. The subarctic North Atlantic 1998 monthly SST data was warmer than the monthly SST data from other years for both the area within and outside of the bloom, which suggests that the temperature influenced the size of the bloom rather than the other way around in this particular case. In addition, it has been reported that 1998 was the warmest year in the record of instrumental measurements (Lu 2005). SST anomaly (SSTA) confirmed the SST observations and also showed that 1998 was the most anomalous SST year, with June 1998 and 1995 being the most positively anomalous Junes of the time series (Figure 3.8b); note that the spike in 2001 is the month July. In the study area, another extensive bloom was reported (based on AVHRR) during the summer of 1991 (Holligan *et al.*, 1993). In Figure 3.8 it can be seen that this year was relatively warm, with a high positive temperature anomaly and generally higher than average temperature (July 1991).

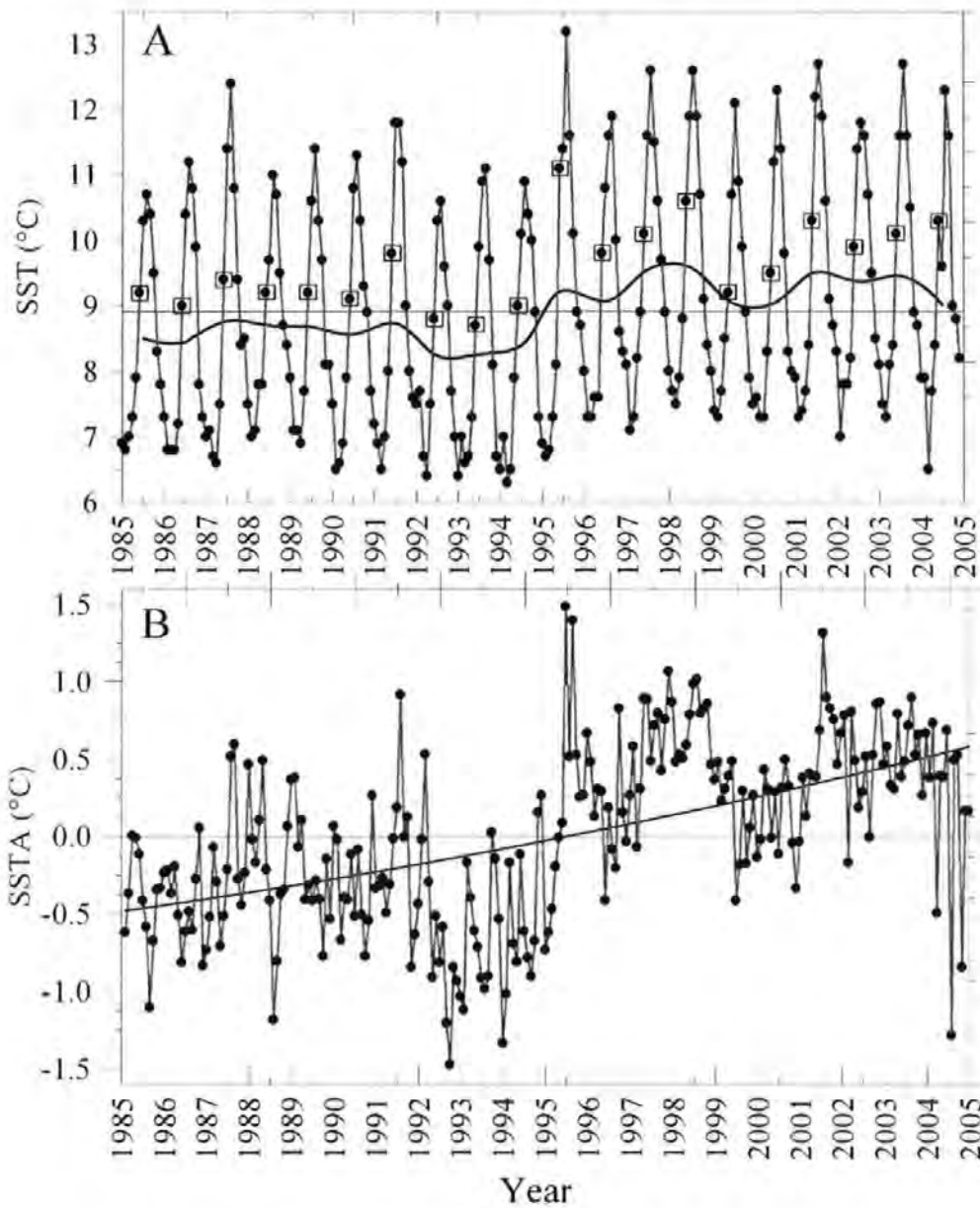


**Figure 3.8:** (a) SST from January 1985 to December 2004. The thin horizontal line is the overall mean and the thick line the annual mean. The open boxes surrounding the dots represent the Junes of every year, (b) SSTA from January 1985 to December 2004 (the black curve is a second order polynomial).

GAMs were also used to identify relationships between nLw\_555 and the environmental/physical parameters. It has to be noted that if two predictors (parameters) are highly correlated with each other, i.e. are not independent, then they

can cause a problem in fitting a model involving both of them. The problem is usually that the parameter estimates are unstable and the model cannot be fitted (Marian Scott *pers. comm.*). In order to avoid this, two different models should be used that will have all the independent variables. In our case, MLD and SST were highly negatively correlated (Spearman rank order correlation coefficient:  $r_s = -0.85$ ,  $p < 0.0001$ ); probably due to the fact that MLD was derived from temperature (see 3.3.1.3). Consequently, model 1 (Figure 3.9 a and b) incorporated solar radiation flux, SST, SSTA and wind stress, whereas model 2 (Figure 3.9 d and c) incorporated solar radiation flux, MLD, SSTA and wind stress.

Using a stepwise approach, which enabled the removal of non-significant variables, model 1 indicated that the parameters to predict coccolithophore abundance (nLw\_555) should be solar radiation flux and SST (Figure 3.9 a and b). Both parameters were highly significant and explained 89.6% of the variation in coccolithophore abundance. Figure 3.9a indicated that coccolithophore abundance increased as the solar radiation flux (insolation) increased with this significant relationship ( $p < 0.00001$ ) exhibiting an early exponential increase that became linear after  $370 \text{ W m}^{-2}$  of solar radiation flux. For SST (Figure 3.9b), the significant model ( $p = 0.0185$ ) showed that the coccolithophore abundance was low and reasonably constant until  $\sim 8.5^\circ\text{C}$  of SST, after which it increased rapidly as SST increased and then reached an optimal reflectance (nLw\_555) at  $12.5^\circ\text{C}$ . Although both parameters appeared to be significant, solar radiation flux explained the nLw\_555 variability more than SST.

Model 2 indicated that coccolithophore abundance should be predicted using solar radiation flux and MLD (Figure 3.9 d and c), and that the other factors were not significantly related to bloom formation; the combination of these two parameters explained 89.4% of the variation in coccolithophore abundance. As it was expected, solar radiation flux ( $p = 0.0002$ ) in Figure 3.9c exhibited a similar pattern to model 1 where it increased progressively along with coccolithophore abundance until the relationship increased rapidly and became linear after  $370 \text{ W m}^{-2}$  of solar radiation flux. The MLD appeared to be highly significant negatively related ( $p < 0.00001$ ) with coccolithophore abundance. As can be seen from Figure 3.9d, the coccolithophore

abundance increased as the MLD values decreased. Specifically, below 20 m of MLD (shallow mixed layer) the relationship was linearly negative whereas after that an exponential decay can be observed until it became stable below 65 m of MLD. In terms of significance, model 2 indicated that MLD was the most important parameter as it explained the nLw\_555 variability more than solar radiation.

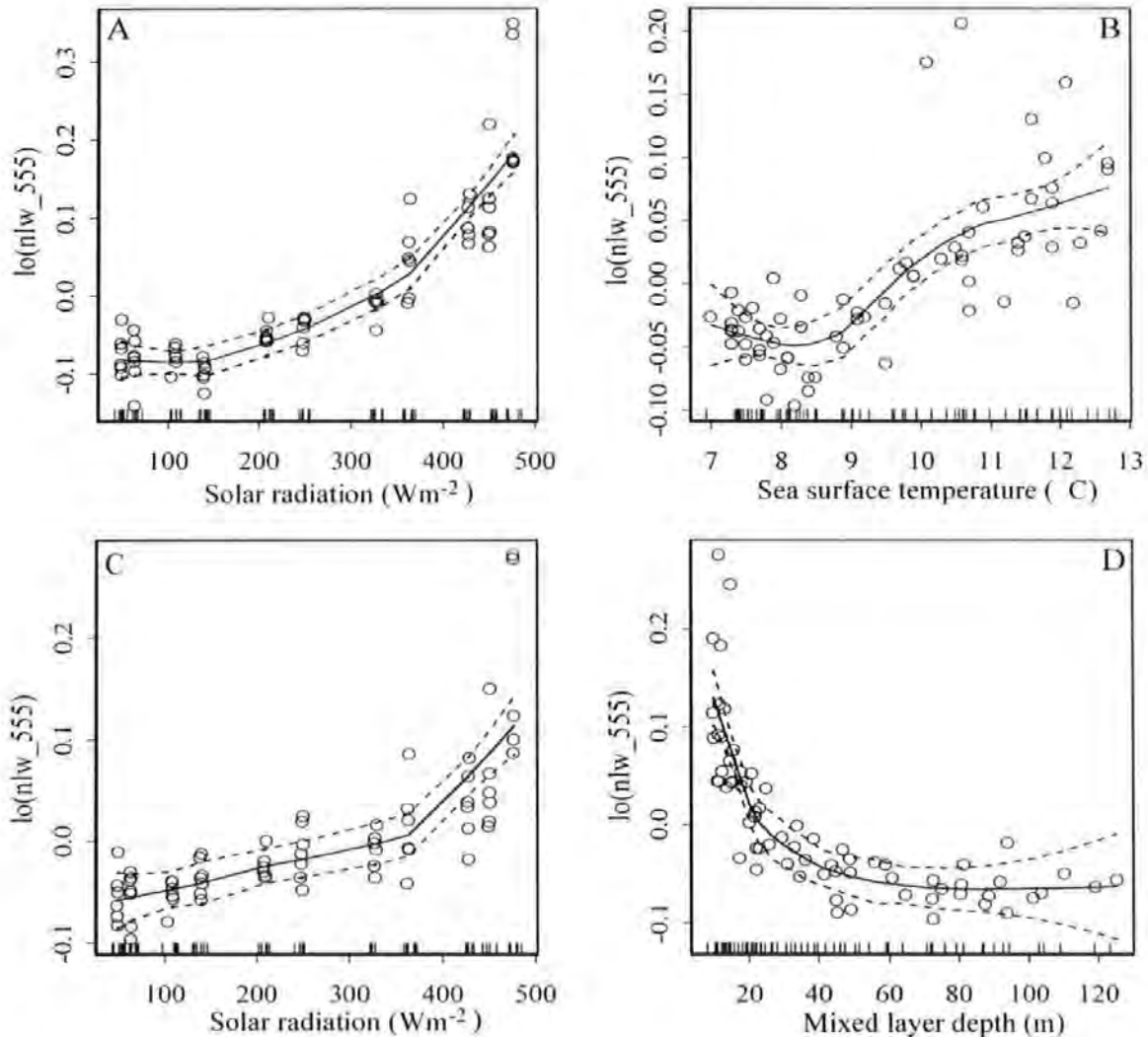


**Figure 3.9:** GAM plots illustrate non-linear relationships between the nLw\_555 variable (lo stands for loess smoother) and each predictor. Circles represent the raw data, the connected line is the spline and the dashed lines are the 95% confidence intervals. (a) and (b) illustrate the final product of model 1 ( $r^2 = 0.896$ ), which incorporated solar radiation flux (a) and SST (b). (c) and (d) illustrate the final result of model 2 ( $r^2 = 0.894$ ), which incorporated solar radiation flux (c) and MLD (d).

### 3.4.2 Diatoms

Plotting the seasonal cycles of the variables offers the opportunity for a rapid assessment of the environmental conditions occurring in relation to diatom abundance (Figure 3.10). Because the ANNs were built upon these CPR-environmental parameter match-up data points, it is important to assess if the ANNs truly represent the environmental/biological variability in the northern North Atlantic and if the results are in agreement with the current literature (see Chapter 5).

Figure 3.10 illustrates the seasonal cycles of diatom abundance, light intensity (PAR), SST and wind stress. In the area of study, diatom cell numbers exhibit a peak during late spring, corresponding with the diatom spring bloom and a clear gradual decline during the autumn months before reaching minimum abundance in December and January. PAR follows a standard seasonal cycle where it is low during the winter and autumn months and high in the late spring and summer months. After winter, May is the first month that PAR reaches  $40 \text{ E/m}^2/\text{day}$ ; the value at which light penetrates the epipelagic zone and enables diatoms to photosynthesise. SST shows a similar pattern to PAR, however the highest SSTs appear during late summer. The sudden peak of SST in May (at least  $1.5^\circ\text{C}$  higher than the winter and spring months) enables stratification to occur. Wind stress demonstrates the opposite pattern to PAR; wind stress is lowest during spring and summer, and higher during autumn and winter. Overall, during May, the sudden change of all the physical parameters results in a shallowing of the mixed layer depth (stratification), which triggers the large diatom spring blooms. Although the seasonal plots suggest conditions that could lead to maximum diatom abundance, they cannot specifically identify the most important key parameters affecting diatom distribution and abundance; thus GRNNs were used for this purpose.



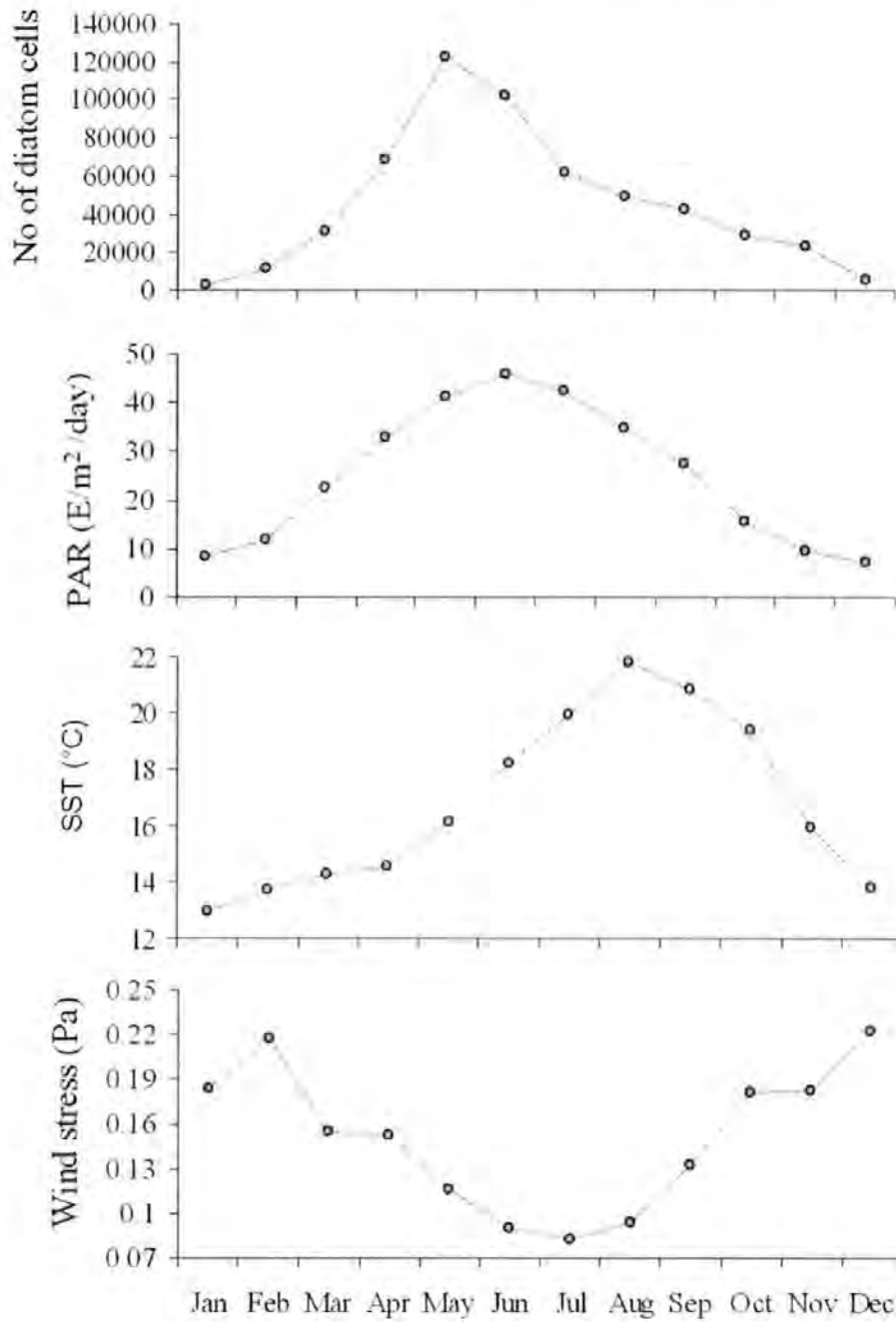


**Figure 3.10:** Seasonal cycles of diatom abundance (number of cells), light intensity (PAR), sea surface temperature (SST) and wind stress. The plots are derived from the match-up data and thus the mean of every variable has been derived from the same number of data points.

The model indicated that the combination of both spatiotemporal and physical variables explains 65% of diatom variability. Figure 3.11 presents the level of contribution of each predictor (variable) on the response (diatoms). Overall, it appears that all of the parameters play important roles in predicting diatom abundance. The

lowest relative impact appeared to be 1.34 (maximum possible value is 3). Regarding the physical information, SST (2.271) appeared to be the key factor, followed by PAR (1.929) and wind stress (1.753). The seasonal information (month) had the second highest contribution in predicting diatom abundance (Figure 3.10). Although the spatial information, longitude (1.341) and latitude (1.412) did contribute to the overall prediction, they appeared to be of less importance than the other parameters. However, it has to be mentioned that the high level of prediction performance (65%) comes from the combination of all variables and not just the one that had the highest contribution.

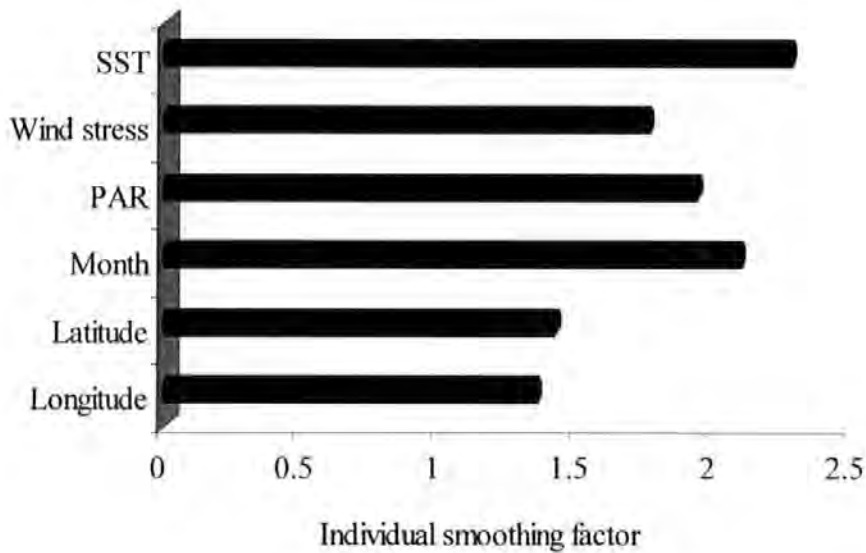


**Figure 3.11:** The relative impact (smoothing factor) of the physical and spatiotemporal variables on diatom abundance.

Three dimensional (3D) plots were used to predict the effect of the three most important variables (SST, PAR and month) on diatom abundance (Figure 3.12, 3.13 and 3.14). The 3D plots, based on the training set of GRNNs, predict the possible reaction of diatoms in relation to the combinations of these parameters. Although the 3D plots demonstrate only two parameters, the effect of all the parameters are taken into account by keeping the rest in a stable average (mean value) condition. As the model attempts to predict the response of diatoms in almost every possible condition,

some of the conditions may not be realistic. For instance, during January it is not possible to have conditions of 26 °C (Figure 3.12), however the model is testing this possibility and finds that diatom abundance would be minimal.

Figure 3.12 shows the effect of SST combined with calendar month on diatom abundance. For almost every SST scenario, diatom abundance remains low during January and February, while during April and May diatom abundance increases rapidly between a SST temperature range of 14 and 23 °C. The pattern of abundance decreases during late summer and early autumn. The model also predicts an increase in diatom abundance during late autumn and the early winter months (November-December) when the SST is high (14-20 °C); however it decreases rapidly in a scenario where SST exceeds 21 °C.

Figure 3.13 represents the combined effect of SST and PAR on diatom abundance. When PAR is low (4-25 E/m<sup>2</sup>/day) diatom abundance remains very low regardless of the SST fluctuation. Once PAR exceeds 40 E/m<sup>2</sup>/day, diatom abundance increases rapidly especially at SST values of between 11 and 21 °C. However, if SST exceeds 23 °C diatom abundance decreases rapidly regardless of the high PAR. The highest abundance can therefore be reached at temperatures of between 10-14 °C and PAR 40-45 E/m<sup>2</sup>/day.

Figure 3.14 indicates the relationship between PAR and month. It can clearly be seen that during the winter months (December-February), diatom abundance remains low regardless of the PAR; whereas abundance peaks during spring (April-June) when PAR exceeds 40 E/m<sup>2</sup>/day.

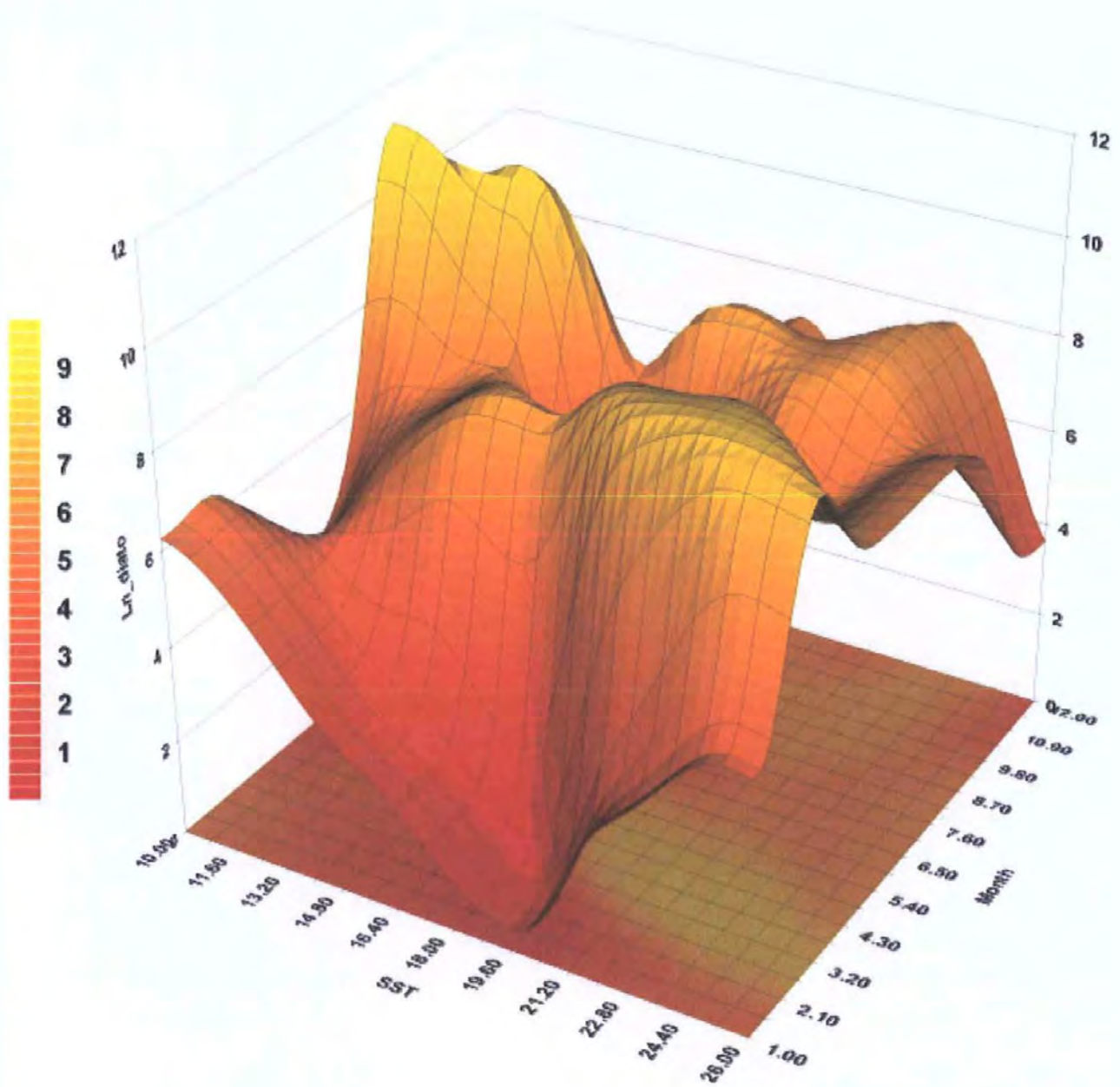


Figure 3.12: Three dimensional plot predicting diatom abundance for SST versus month.

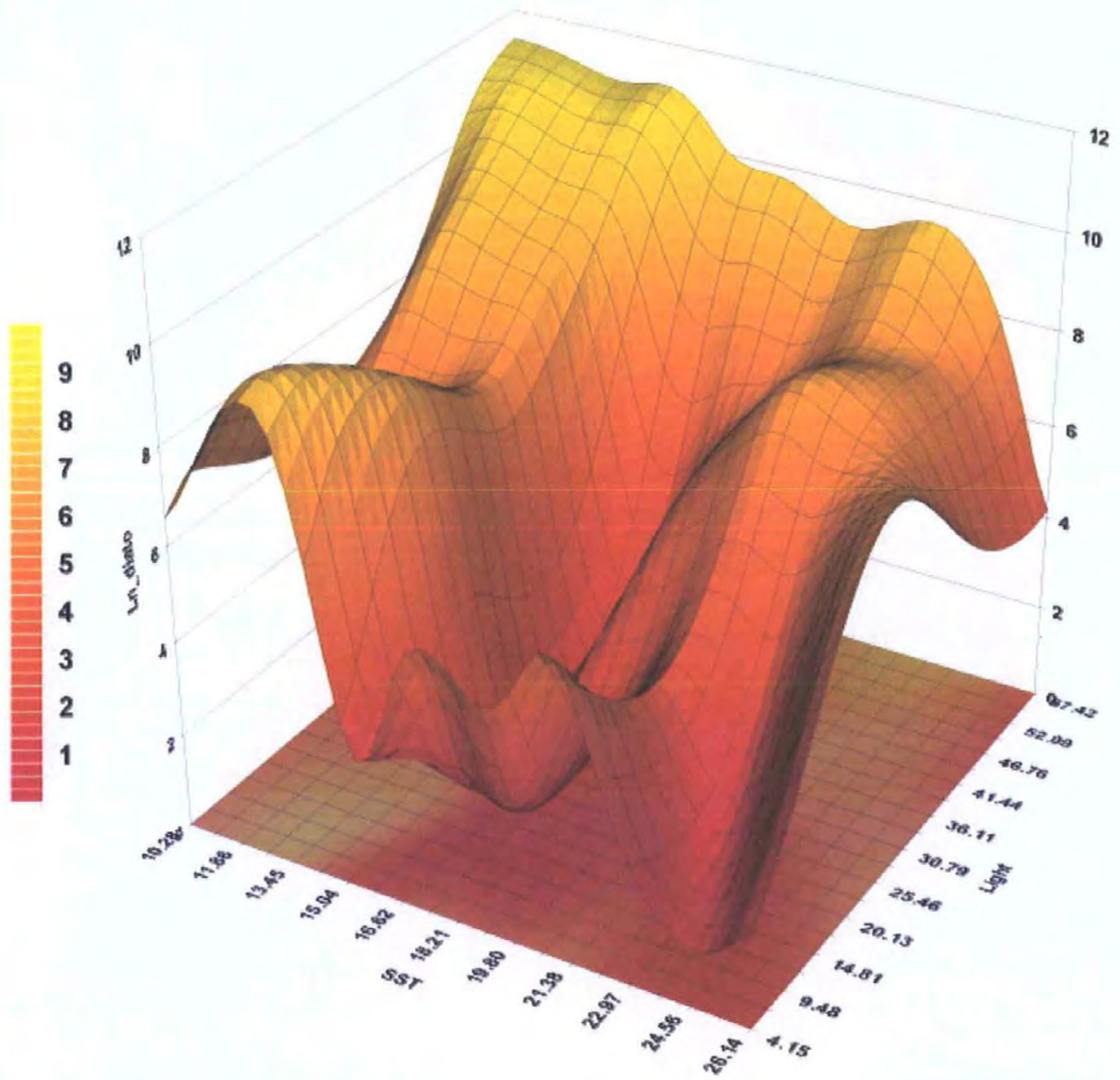


Figure 3.13: Three dimensional plot predicting diatom abundance for SST versus PAR.

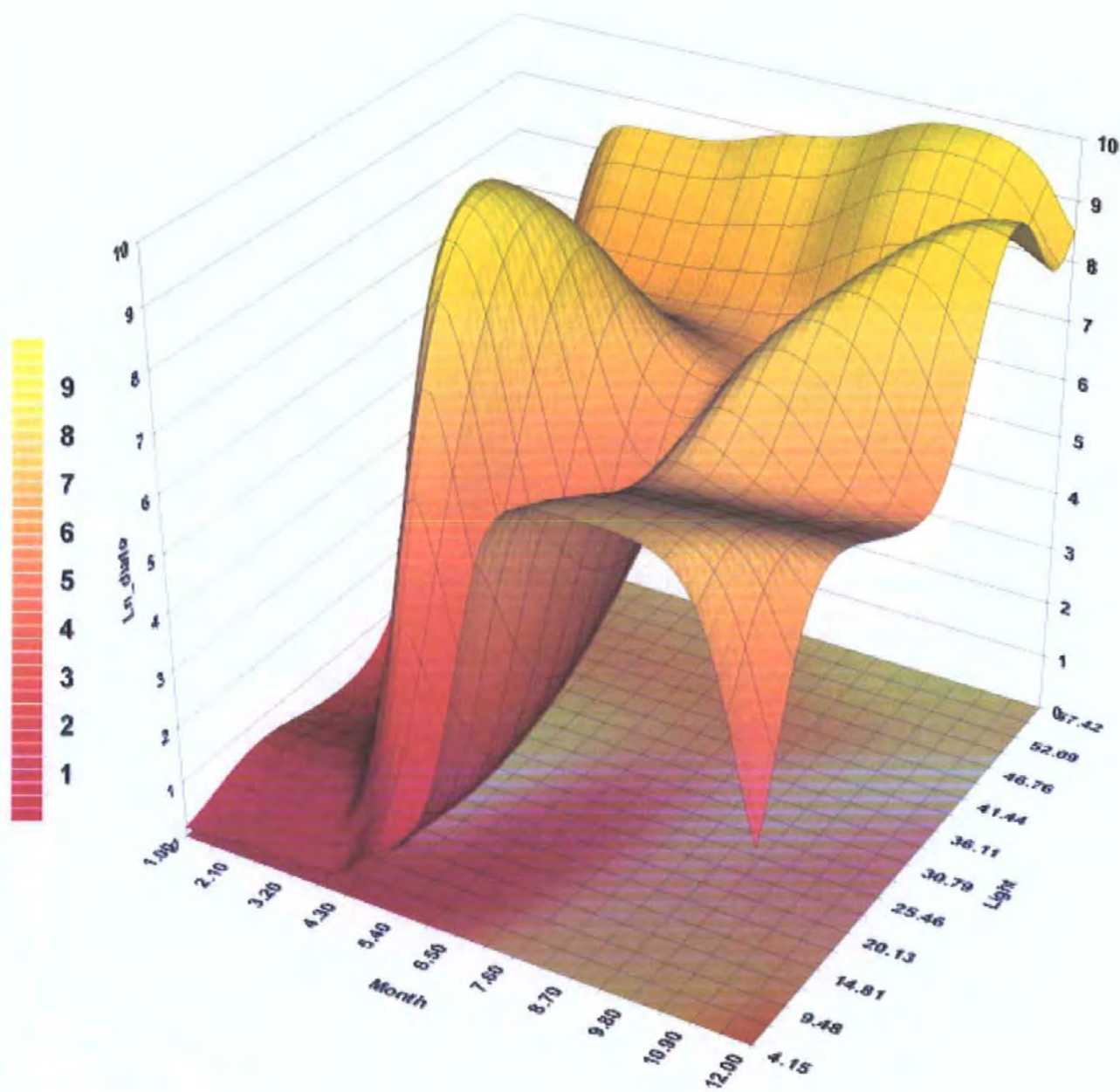


Figure 3.14: Three dimensional plot predicting diatom abundance for PAR versus month.

### 3.5 Conclusion

#### 3.5.1 Coccolithophores

During June 1998 an extensive coccolithophore bloom occurred in the North Atlantic and, according to this research, this bloom is the extensive coccolithophore bloom recorded by SeaWiFS (>995,000 km<sup>2</sup>). The bloom has been compared to blooms reported in the literature and exceeds their size by a considerable margin, but these were analysed with AVHRR (at least until 1997) that has a reduced sensitivity and broad waveband in the visible region of the electromagnetic spectrum.

*In situ* and satellite measurements indicated that coccolithophores in the subarctic North Atlantic occur at their highest abundance during late spring/early summer and peak in June. The environmental variables used in the analysis suggested that the solar radiation flux was very high during June 1998 (as it was during every June), while the MLD was shallow (11.6 m). These results are in agreement with those of Balch *et al.* (1991) who mentioned that the MLD within coccolithophore blooms is shallow (~20 m). In addition, June 1998 together with 1995 were the warmest and most positively anomalous Junes of the last 20 years.

Using the results of the time series, GAMs were used to identify which environmental/physical parameters were the most important for the formation of coccolithophore blooms. The two GAM models supported the observations and indicated that the combined effect of high solar radiation flux, shallow MLD and increased SST were highly correlated with coccolithophore abundance (nLw\_555). Compared to other phytoplankton groups, such as diatoms, this coccolithophore species has an unusual tolerance for high light intensity, i.e. lacks photoinhibition (Nanninga and Tyrrell 1996). Both models also indicated that wind stress was not a major factor contributing to bloom formation.

The 7 year time series (Figure 3.7c) indicated that there are no anomalous fluctuations (relatively stable seasonal cycle, at least during Junes) that can be related to the bloom occurrence; nevertheless, it is suggested that the typical low wind stress (vertical

mixing) during all Junes indirectly benefits bloom formation as it contributes to water-column stability. However, it must be noted that whenever high SST anomalies occur it does not mean that a bloom will be formed, but when it co-occurs with the timing of coccolithophores it will probably benefit the bloom. For instance, November 1997 (Figure 3.8b) appeared to be the most positively anomalous month during 1997, but the nLw was very low as it was the wrong time of the year in terms of other parameters (Figure 3.7a).

### 3.5.2 Diatoms

Constructing a time series of *in situ* monthly or annual averages of the areas of interest has proven to be very effective in identifying decadal changes in phytoplankton populations (Reid *et al.*, 1998; Edwards *et al.*, 2001). However, to understand the extent to which physical, spatial, and temporal parameters influence diatom populations in the epipelagic zone a different approach is needed. This research used individual *in situ* CPR samples without the interpolation or averaging of datasets and enables effective utilization of the *in situ* samples together with satellite remote sensing data, revealing the relative importance of those parameters which regulate diatom abundance according to satellite derived physical information.

Based on satellite information, it was found that although all of the parameters play important roles in diatom abundance, the physical environmental parameters appeared to be more important than spatiotemporal factors. SST was found to be the key factor most influencing diatom abundance, followed by light intensity and wind stress. This is in agreement with Platt *et al.* (2005) who reported that the growth, size structure and community composition of phytoplankton groups is controlled by physical forcing. However, it must be noted that the level of importance of each physical/spatiotemporal variable may depend on the geographical area. For instance, sea surface warming is associated with an increase in phytoplankton abundance in cooler areas, whereas a decrease has been reported in warmer regions (Richardson and Schoeman 2004). It is also important to mention that our results provide ecological information on diatoms that were sampled in the first 10 metres and not in the deeper water column.



## CHAPTER 4

### *Identifying phytoplankton functional groups from space: an ecological approach*

This chapter demonstrates the use of satellite remote sensing data to discriminate phytoplankton groups. Several environmental and biological parameters are known to affect the distribution and abundance of phytoplankton. The ecological knowledge needed to discriminate phytoplankton taxonomic groups from space was identified, using ANNs. ANNs aimed to assess the importance of each parameter, as well as developing a model, which used all the parameters (satellite and *in situ*) to predict the presence/absence of diatoms, dinoflagellates, coccolithophores and silicoflagellates.

*Aspects of this chapter are included in the following publications:*

**Raitsos D.E., Lavender S.J., Maravelias C.D., Haralambous J., Richardson A.J., Reid P.C.** (Submitted). Identifying phytoplankton functional groups from space: an ecological approach. *Limnology and Oceanography*.

**Raitsos D.E., Lavender S., Edwards M., Reid P.C., Pradhan Y.** (2005b). Development of a prototype system for deriving maps of phytoplankton taxa: spatial and temporal distribution of diatoms and dinoflagellates since 1950 in the North Atlantic. Poster Presentation in: **International Conference of American Society of Limnology & Oceanography (ASLO)**, Spain.

**Raitsos D.E., Lavender S., Reid P.C., Edwards M.** (2005). Discrimination of phytoplankton taxonomic groups using ocean colour data. Poster Presentation in: **NERC Earth Observation (EO) and International conference of Remote Sensing and Photogrammetry Society (RSPSoc)**, Portsmouth, United Kingdom.

McQuatters-Gollop A., **Raitsos D.E.**, Edwards M., Attrill M.J. (Submitted). Spatial patterns of diatom and dinoflagellate seasonal cycles in the North – East Atlantic Ocean. *Marine Ecology Progress Series*.

## 4.1 Introduction

Discrimination of phytoplankton functional types is of major importance as they influence the oceanic regime in various different ways and magnitudes. The importance of diatoms and coccolithophores has been covered in Chapter 3, thus only the importance of dinoflagellate and silicoflagellates are mentioned here. Photosynthetic dinoflagellates are important aquatic primary producers, however they are less nutritious (compared to diatoms which are a key food for copepods) and are often considered trophic dead ends and can result in food webs culminating in non-fodder gelatinous organisms instead of fish (Verity and Smetacek 1996; Sommer *et al.*, 2002). Certain species that cause toxic 'red tides', may impact fisheries, aquaculture, marine mammals and human health by introducing toxins into the food chain (Nixon 1995; Flewelling *et al.*, 2005). Silicoflagellates represent a minor fraction in the total micro-plankton assemblage in the pelagic environment (Takahashi 1991), however they can be considered as a major components in coastal and estuarine waters (Jochem and Babenerd 1989). Silicoflagellates have also been considered as indicators of water masses and applied to reconstructions of the paleoenvironment (Onodera and Takahashi 2005). Nejstgaard *et al.* (2001) reported that certain bloom-forming silicoflagellate species may affect copepod reproduction negatively.

Despite the significant role of marine phytoplankton, knowledge of the spatio-temporal distribution and abundance of their functional groups is limited, especially in the open oceans. Research is restricted in time and space as it is often from relatively expensive ship-based *in situ* measurements. Deriving maps of phytoplankton functional groups from remote sensing data is a potentially important and new technological application, which can offer high spatio-temporal coverage. Although studies have provided promising results for discriminating phytoplankton functional groups from space (Sathyendranath *et al.*, 2002; Alvain *et al.*, 2005), they have acknowledged weaknesses. One of the major issues is the limitation of *in situ* data to develop concrete relationships needed for building accurate models. These data are not only restricted to those collected by ship, but also most of the *in situ* data (~85%) are not matched with satellite data, primarily due to cloud coverage (Sathyendranath

*et al.*, 2002; section 2.2.3.2). In addition, published research attempts to separate phytoplankton groups using only bio-optical properties (spectral absorption and backscattering) without using information on the environmental regime. Improved and more robust interpretations can be obtained by including additional information, such as ecological knowledge of the physical, chemical and biological regime that different functional groups prefer.

A system was developed based on satellite remotely-sensed data that discriminated four major phytoplankton functional groups: diatoms, dinoflagellates, coccolithophores and silicoflagellates. To discriminate between these functional groups an ANN was developed, that uses as inputs ecological and geographical knowledge together with ocean colour bio-optical characteristics and remotely-sensed physical parameters. The dominance of these different groups was determined from CPR samples. The physical and optical variables used in the analysis were derived from satellite sources and include Chl-a, solar radiation, SST, wind stress, and normalised water-leaving radiances. These were supplemented by spatiotemporal variables of longitude, latitude and season.

## **4.2 Methods and Data Analysis**

### **4.2.1 Methodological Approach**

**S**atellite and *in situ* datasets were processed for the northern North Atlantic (46°N - 66°N and 52°W - 4°W) between September 1997 and December 2003. Within this region concurrent match-ups between SeaWiFS and *in situ* CPR samples (phytoplankton biomass) were compared. The methodological approach used is covered in Chapter 3 (section 3.3.2). A summary of the data, source as well as statistical analysis is summarised in Table 4.1.

Table 4.1: Summary of the parameters, sources and statistical methods used to analyse them.

<b>KES study</b>		
<b>Parameters</b>	<b>Source</b>	<b>Statistics</b>
Chl-a	SeaWiFS	
PAR	SeaWiFS	
SST	AVHRR	Neural Networks
wind stress	ERS2-QS	GRNN
<i>In situ</i> plankton	CPR	
longitude-latitude	CPR	
month	CPR	

#### 4.2.2 Phytoplankton Functional Groups

Measurements of phytoplankton abundance (cell counts) were derived from the CPR survey. The total number (sum of all species) for diatoms, dinoflagellates, coccolithophores and silicoflagellates for each sample was used; each group is composed of many species (see list in Richardson *et al.*, 2006 for details).

The dominant phytoplankton group for each sample was estimated using the  $Z$  factor standardised method:

$$Z_i = \frac{n_i - \bar{x}_i}{s_i}$$

Where  $n_i$  is the cell count for phytoplankton group  $i$  in a sample,  $\bar{x}_i$  is the overall mean of all cell counts for each group  $i$ , and  $s_i$  is the standard deviation of all samples for group  $i$ . The largest  $Z_i$  for each sample was used as the dominant species.

This standardised method was used to derive the dominant group because the number of cells between each of the four groups varied significantly. For instance, diatoms form more concentrated blooms than silicoflagellates (mean cell counts 140,000 and 34,000 respectively). Whenever CPR samples indicated that there were no phytoplankton cells, this category was named as “no-dominance”; in other words this is a category that the CPR sample had no phytoplankton presence. This category was used in the models in order to acquire the information of the conditions when no phytoplankton was present in the surface waters (as indicated from CPR samples).

### ***4.2.3 Potential Biases***

Weekly mean satellite data (for the Chl-a, 8-day standard NASA product) was used to establish CPR match-ups. When daily satellite data were used, ca. 85% of CPR data were unusable, but with weekly mean composites the loss was reduced to 73%. Results of a daily comparison indicated that they were not statistically different from the weekly comparison. However, the weekly relationship was more robust (based on more samples), and the 95% confidence limits were reduced considerably, improving the correlations. In summary, the weekly products do not lose the essential information needed to build the relationships. For statistical models limitations see 4.4 section.

### ***4.2.4 Data Analysis using Artificial Neural Networks***

#### ***4.2.4.1 Probabilistic Neural Network (PNN)***

PNNs were used to discriminate the four phytoplankton functional groups based on the environmental, optical and spatio-temporal variables. The PNN is in essence a combination of neural networks and Bayesian statistics (Specht 1988 and 1990). Bayes theory takes into account the relative likelihood of events and uses *a priori* information to improve prediction. The network paradigm uses Parzen estimators and spheres of influence that were developed to construct the probability density functions required by Bayes theory.

The most common choice of kernel is the basic Gaussian kernel, which involves only the Gaussian function and one sphere of influence parameter  $\sigma$ . A schematic representation of a typical PNN structure is given in Figure 4.1. As Bayesian approximators, the basic Gaussian kernel PNN built to map  $x_k$  as function of  $x_1; x_2; \dots; x_{k-1}$  will have  $k - 1$  neurons in the input layer, one neuron in the first hidden layer (pattern layer) for each case in the training set,  $k - 1$  neurons in the second hidden layer (summation layer), and one neuron in the output layer (decision layer).

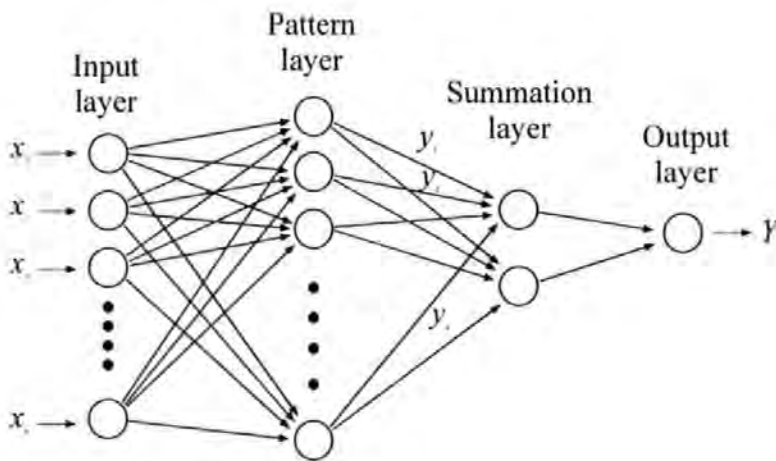


Figure 4.1: A schematic representation of a Probabilistic Neural Network structure.

The current PNN was implemented on a random subset of available data (training set) and then applied to the remaining data (validation or testing set). The training set consisted of a random 80% of the available data (2986 cases) with the remaining random 20% (746 cases) used as the testing set. This holdout partitioning technique (Kohavi 1995) was repeated five times to test the validity of the model. As can be seen from Table 4.2, after the 5 repetitions the mean is taken as an overall result (the  $s_i$  is also reported). The testing set was used for calibration, which prevented overtraining the networks, making them generalise well on new data. Calibration adjusted the weight of each neuron by computing the distance metric between a given classification and the network results for all outputs over all patterns. The genetic adaptive algorithm (Specht 1991) was applied during this process to test a range of

smoothing factors. Individual smoothing factors were used as a sensitivity analysis tool, as the larger the factor for a given input, the more important that input was to the model, at least, as far as the test set was concerned.

The following performance criteria were evaluated: (1) sensitivity, the percentage of true presences correctly identified; (2) specificity, the percentage of true absences correctly identified; and (3) accuracy, the total fraction of the sample correctly identified. When applied to training sets, the accuracy provides a measure of the recognition performance, whereas when applied to testing sets it gives a measure of prediction performance.

An important property of Neural Networks (NNs) is that they are adaptive, i.e. they can take data and learn from them. This ability does not depend upon the prior knowledge of rules. There are no conditions put on the predicted variables i.e. they can be True/False, continuous values and so forth. Moreover, with only a few exceptions, NN are essentially non-linear, and they are capable of learning complex interactions among the input variables in a system even when they are difficult to find and describe. Consequently, NN can provide solutions for problems that do not have an algorithmic solution or for which an algorithmic solution is too complex to be found. NNs have the ability of extracting essential process information from data. As new training data become available, the network can be updated to represent the process more accurately. A further important advantage of NNs is that they are capable of generalisation, i.e. they can correctly process information that only broadly resembles the original training data. They are also fault tolerant by being capable of properly handling noisy or incomplete data.

There are several advantages of using a PNN in addition to its non-linear and multi-modal properties. First, a PNN network structure is dictated by the dimensionality of the samples as opposed to a multi-layer perceptron whose network structure is determined either by a trial-and-error or rule-of-thumb approach. Second, the training process only takes one pass of the training set to compute the optimal smoothing factor. Last, it works well on small training sets and when the sample size increases it provides a very close approximation to the real density function. Nevertheless, its

major drawback is on the need to store all training cases in the pattern layer for future classifications.

### 4.3 Results

Table 4.2 illustrates the discrimination results of PNN for the training, testing and overall datasets. Training outcomes (percentages) can be considered an indication of the quality of the data used to develop the relationships for the final discrimination model. Sensitivity analysis in the training stage performed well, as each functional phytoplankton group was classified with a precision of >83% and dinoflagellates had the highest percentage (>89.7%). Regarding the true absences (specificity), the PNN model outcome had a performance of >93%, with coccolithophores and silicoflagellates having the highest percentages. The classification accuracy had a recognition performance of >92%, again with coccolithophores and silicoflagellates coming out highest (Table 4.2).

Using the training relationships derived from the 80% of the dataset, the ability of the PNN model to discriminate the groups within the remaining (random) 20% of the samples was examined (testing). The sensitivity results showed that the true presences were correctly identified with a precision of >68%; the highest mean discrimination performance was for the no-dominance (76.4%), diatom (74.6%) and coccolithophore (72.8%) groups, whereas the dinoflagellate and silicoflagellate groups performed slightly lower (72.0% and 68.1% respectively). From Table 4.2 it can also be clearly observed that the specificity performed considerably better; every group was >82%, with the silicoflagellate and coccolithophore groups (95.1% and 92.6% respectively) performing better, followed by the dinoflagellate (85.3%), diatom (83.2%) and non-dominance (82.5%) groups. Although silicoflagellates and dinoflagellates had the lowest sensitivity performance in testing, the opposite pattern was observed for specificity.



The accuracy for the total fraction of the functional groups correctly identified indicated the final prediction ability of the PNN model had an accuracy of >80%. The order of performance was: silicoflagellates, coccolithophores, dinoflagellates, diatoms and no-dominance (92.7 %, 90.5 %, 82.5 %, 81.1 % and 80.4 % respectively).

The contribution of each predictor used for discrimination varies within and among phytoplankton functional groups. Thus, the analysis is made up of two approaches: a) distinguishing the groups from each other as separate functional types (Figure 4.2: all groups plot) and b) discriminating one group from the others i.e. diatoms from the remaining groups (Figure 4.2).

The relative impact (smoothing factor) of the eight predictors is shown in Figure 4.2, with the first plot (all groups) indicating the importance of each variable in distinguishing the functional types. Spatio-temporal information such as longitude, month and latitude made an important contribution to the discrimination of the phytoplankton functional groups (2.9, 2.3 and 1.9 respectively). Regarding the effect of the physical regime, SST was found to be the key factor (2.3), followed by PAR (1.4) and wind stress (1.3). Chl-a and nLw\_555 did contribute to the overall discrimination, but were of lesser importance compared to other parameters (1.1 and 0.8 respectively).

In terms of diatoms, latitude along with PAR and SST (3.0, 2.2 and 1.9 respectively) were the key factors for discriminating this functional group from other groups (Figure 4.2). In addition, wind stress and Chl-a seem to play an important discriminatory role (1.4 and 1.4 respectively), whereas longitude (0.6) had the lowest impact. Dinoflagellates were distinguished mostly based on spatiotemporal information i.e. latitude, month and longitude (3.0, 3.0 and 2.5 respectively). In terms of physical variables, PAR (2.9) is the key discriminator, followed by nLw\_555 and wind stress. SST and Chl-a contributed less to the dinoflagellate discrimination (Figure 4.2). Discrimination of coccolithophores appeared to be modulated by the seasonal cycle (month, 2.9), with PAR (1.9), wind stress (1.8) and nLw\_555 (1.7) playing a key role while SST (0.2) appeared not to make a significant contribution. Longitude (2.9) and nLw\_555 (2.8) had the highest impact for discriminating

silicoflagellates, followed by month, SST and PAR, although Chl-a and wind stress contributed to the final discrimination, their impact appeared to be less significant (Figure 4.2). Finally, for the no-dominant group almost all parameters played a key role, but contributions of Chl-a and nLw\_555 (0.2 and 0.1 respectively) were smaller.

**Table 4.2:** Percentage values of sensitivity, specificity and classification accuracy of the five groups, applying the PNN 5 times. Each time a random sample of 80% of cases was used as the training set and the remaining 20% as the testing set. Results are given analytically for each sample in training and testing. Mean values of the five samples are given in bold.

Group	sample	Set					
		Training			Testing		
		Sensitivity	specificity	Accuracy	sensitivity	specificity	Accuracy
No-Dominance	1	86.7	96.2	93	75.6	83.1	80.4
	2	86.6	96.3	93	76	82.9	80.4
	3	87	96.2	93.1	76.3	82.6	80.4
	4	87.4	96	93.1	77.1	81.6	80
	5	86.8	96.1	93	77.1	82.4	80.6
	$\bar{x}$	<b>86.9</b>	<b>96.2</b>	<b>93</b>	<b>76.4</b>	<b>82.5</b>	<b>80.4</b>
	$s$	0.3	0.1	0.1	0.7	0.6	0.2
Diatom	1	83.8	96.3	93.3	74	83.1	81
	2	83.9	96.2	93.3	75.1	83.7	81.6
	3	84.1	96.5	93.5	75.1	83.3	81.4
	4	84.1	96.5	93.6	73.5	82.8	80.6
	5	83.2	96.1	93.1	75.1	83	81.1
	$\bar{x}$	<b>83.8</b>	<b>96.3</b>	<b>93.4</b>	<b>74.6</b>	<b>83.2</b>	<b>81.1</b>
	$s$	0.4	0.2	0.2	0.8	0.3	0.4
Dinoflagellate	1	90.1	93.7	92.9	73.6	85.4	82.8
	2	90	93.9	93.1	72.3	85	82.3
	3	89.7	93.5	92.7	71.1	85.5	82.4
	4	89.8	93.6	92.8	72.3	85.7	82.8
	5	88.9	93.8	92.7	70.4	85	81.9
	$\bar{x}$	<b>89.7</b>	<b>93.7</b>	<b>92.8</b>	<b>72</b>	<b>85.3</b>	<b>82.5</b>
	$s$	0.5	0.2	0.2	1.2	0.3	0.4
Coccolithophore	1	83.5	98.1	96.2	72.8	92.5	90.4
	2	83.2	98.2	96.3	71.6	92.6	90.4
	3	85.1	98	96.4	75.3	92.9	91
	4	82.4	98	96.1	74.1	92.3	90.4
	5	82.7	98.1	96.2	70.4	92.6	90.2
	$\bar{x}$	<b>83.4</b>	<b>98.1</b>	<b>96.2</b>	<b>72.8</b>	<b>92.6</b>	<b>90.5</b>
	$s$	1	0.1	0.1	2	0.2	0.3
Silicoflagellate	1	85	98.1	96.9	70.2	95.1	92.9
	2	84.3	98.1	96.8	67.2	94.9	92.4
	3	86.1	98.2	97.1	74.6	95	93.2
	4	83.9	98.1	96.8	62.7	95.3	92.4
	5	84.7	98	96.8	65.7	95.1	92.5
	$\bar{x}$	<b>84.8</b>	<b>98.1</b>	<b>96.9</b>	<b>68.1</b>	<b>95.1</b>	<b>92.7</b>
	$s$	0.8	0.1	0.1	4.6	0.2	0.4

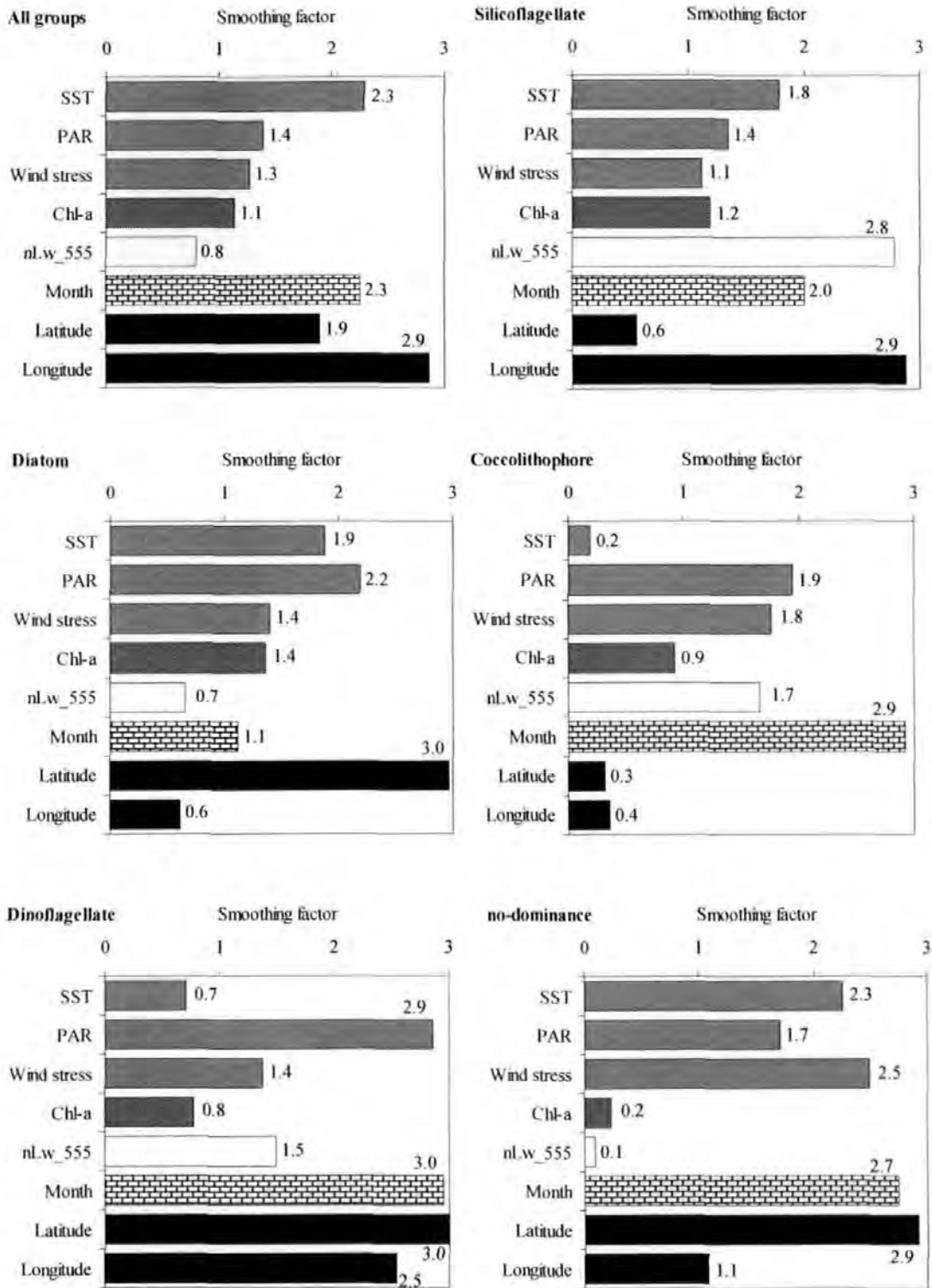


**Figure 4.2:** The relative impact (smoothing factor) of the 8 variables indicating the importance of each variable in distinguishing the groups from each other as separated functional types (All groups) and discriminating one group from the others i.e. diatoms from the remaining groups. Note that the different colouration or shading separates the physical, biological, optical, temporal and spatial variables (respectively).

#### 4.4 Conclusion

The neural networks appeared to be able to discriminate and identify the four phytoplankton functional types used in the study with high performance (>70%). It has to be mentioned that an important property of successful presence/absence ecological models, when applied to independent datasets, is their ability to predict presence accurately. Hence, sensitivity is considered of primary importance compared to specificity (and overall accuracy) as the latter can suffer from the groups' prevalence effect, i.e. frequency of occurrence (Maravelias *et al.*, 2003). In the current study, true absence outnumbered true presence. Therefore, prevalence effect was reflected in every section of the analysis (training and testing) as the PNN model predicted true absence better than true presence. However, in the testing section, the ability of the model to successfully discriminate and identify the true cases was ~70%. Discussion of results and potential applications of the results are given in Chapter 5.

Here, it has to be mentioned that statistically predictive models have acknowledged limitations in demonstrating causality in an ecological sense. This is because these models attempt to correlate the parameters and/or to find which parameter is the most important for causing blooms, without testing if this causality has an ecological sense. For instance, if an x-parameter fluctuates similarly to diatoms abundance, the model will predict that this factor is probably causing/influencing the diatoms to grow; although in reality or in an ecological sense, this parameter may never have a direct or indirect effect on diatoms. That is why one should use only parameters that are well known to be able to affect phytoplankton such as in this study: wind, temperature, light, stratification measures etc. However, in addition to that knowledge, prior to any use of statistical models, one must be able to explain the outcome of these models and be able to reject a model if the results are wrong or in other words not making an ecological sense. For instance, in chapter 3, I used two different GAM models. Reasons for that are detailed in that chapter, however briefly there were two parameters that were autocorrelated (SST and MLD) and that is why 2 separated models were created. This decision was taken after observing that the outcome of the initial model (which included all the parameters) was ecologically wrong. Statistical

models have been widely used to explain patterns of a biological variable (i.e. Chl-a) in relation to several different variables (physical, biological and/or chemical), but the results should be treated with caution as they can be miss-leading, as with every statistical analysis.

## CHAPTER 5

### *Discussion and Future Research*

This chapter discusses the major findings of the thesis, as well as identifying methodological limitations and providing information of what could be done to improve current knowledge. In addition, a future research section outlines potential future projects regarding: a) predicting phytoplankton future distribution and abundance, b) coccolithophores: what is known and what remains still undiscovered, and c) the use of the PCI ocean colour data to link SeaWiFS and CZCS sensors.

## 5.1 General Discussion

**I**n *situ* measurements of phytoplankton were obtained from the CPR survey, which provided high spatial and temporal data (at least compared with other *in situ* datasets). However, although the CPR provides a good estimate of the microscopic biological communities of the upper surface layer, it does not provide any environmental, physical or chemical variables that might affect the phytoplankton. Satellite remote sensing can provide high spatial and temporal data of biological as well as physical parameters at a global scale. Satellite sensors such as SeaWiFS were used synergistically with CPR data to fulfil the lack of physical CPR parameters and thus attempt to understand the variability of phytoplankton ecosystem function properties.

### 5.1.1 Ocean Colour: Validation of PCI through *In situ* and Satellite Chl-a

#### 5.1.1.1 PCI versus *In situ* Chl-a

The PCI is a unique measurement of *in situ* ocean colour data, however the lack of an adequate experiment testing the PCI's quantitative validity was of concern. The CPR's measure of phytoplankton biomass was quantified/validated by fluorescence ( $r^2 = 0.73$ ,  $p < 0.0001$ ). This allowed the substitution of the arbitrary old scale (greenness) with the Chl-a values derived from this experiment.

At the present time, simple devices exist in industry that can be used to identify changes in CPR silk colour, quickly, reliably and may also identify more categories than the four currently used. Such an instrument could be run for a few years in parallel with the visual assessment to validate it and ensure that both visual and instrumental assessments are in agreement; ultimately the device could replace the visual assessment. However, this could happen only if the device is able to identify unusual features on the silk such as sand. Although the results of this experiment confirm the quality of PCI, there were occasional circumstances (assuming Chl-a concentrations were correct) that the PCI category PG could be G or *vice versa*.

However, Figure 2.4 indicated that for at least 95% of the samples the visual assessment was correct.

At present the CPR tows are operating in the Atlantic and Pacific Oceans, and North Sea. This experiment could be repeated with samples taken from different oceanic as well as coastal areas to assess Chl-a concentration, and so examine a greater number of samples equally distributed in time.

### 5.1.1.2 PCI versus Satellite Chl-a

In order to test the compatibility of the two different ocean colour datasets, *in situ* and satellite derived ones, it was attempted to correlate the CPR phytoplankton biomass (PCI) with the SeaWiFS Chl-a. The outcome demonstrated a compatibility between the two different measures of ocean colour (Figure 2.6). This significant relationship was then used to drive the SeaWiFS dataset back 50 years in the Northeast Atlantic and North Sea and enabled, for the first time, a quantification of changes that have been documented in the past (Figure 2.7 and 2.8). Briefly, it was found that the mid-80s regime shift (Beaugrand 2004) corresponded to a 60% increase in Chl-a since 1948; this was the result of an 80% increase in Chl-a during winter alongside a smaller summer increase.

New insights into decadal changes in phytoplankton standing stock can be developed by combining data from SeaWiFS Chl-a and PCI, although each have strengths and acknowledged weaknesses. The strength of satellite remote sensing (e.g. SeaWiFS) is its ability to obtain information on phytoplankton distribution and abundance over large spatial scales. For instance, SeaWiFS has been used extensively to assess the role that global oceanic photosynthesis plays in climate and fisheries (McClain *et al.*, 1998). The PCI is an alternative way of assessing the major temporal and spatial patterns of phytoplankton biomass over almost 60 years in the North Atlantic (Colebrook and Robinson 1965; Reid *et al.*, 1998). However, both the PCI and SeaWiFS have limitations. The PCI provides a visual (semi-quantitative) estimate of phytoplankton biomass, which has only previously been coarsely calibrated with chlorophyll acetone extracts (Colebrook and Robinson 1965), and its coverage is



restricted to shipping routes (Reid *et al.*, 2003). By contrast, SeaWiFS has limitations due to its limited lifespan, making it impossible to investigate decadal changes in phytoplankton. Problems with SeaWiFS data associated with restricted coverage due to clouds (McClain *et al.*, 1998) are also highlighted in the present study where only 13% of the *in situ* PCI data could be used for comparison with SeaWiFS, and in a recent comparative study where only about 2-3% could be used (Hooker and McClain 2000).

The oceans are increasingly recognised as a key component of the climate system (Bigg *et al.*, 2003) and have recently been shown to be the only true sink for anthropogenic CO<sub>2</sub> over the last 200 years (Sabine *et al.*, 2004). The same study showed that this oceanic sink of the key greenhouse gas CO<sub>2</sub> may well be declining at the same time as the strength of the terrestrial biosphere sink remains constant. If true, this result implies that concentrations of atmospheric CO<sub>2</sub> are likely to increase at a more rapid rate over the next 100 years than currently predicted. Primary production and phytoplankton composition play a key role in the modulation of radiatively-important gases such as CO<sub>2</sub> and also produces reactive gases that contribute to the formation of clouds and affect albedo. Increasing levels of atmospheric CO<sub>2</sub>, which consequently causes significant changes in surface ocean pH and carbonate chemistry, impact phytoplankton with calcareous body parts such as coccolithophores (Riebesell *et al.*, 2000). Given this background and the fact that primary production is at present not included in global climate models emphasises the importance of obtaining appropriate spatiotemporal data on phytoplankton.

This new Chl-a dataset (based on >94,000 stations), along with physical, biological and chemical parameters, can now be assimilated into the next generation of climate models. This will not only open up new possibilities for modelling marine ecosystems on a regional and oceanic scale, but should also advance our understanding of biogeochemical cycling and improve our predictive capability of the impacts of climate change.

### 5.1.1.3 The use of PCI to Validate the Satellite Signal in CASE II Waters

PCI can also be used to explain phytoplankton variability in areas where remote sensing cannot easily distinguish between phytoplankton absorption and or absorption/scattering by additional optically active substances i.e. in CASE II waters. For example, it was commonly believed that the wintertime Chl-a concentrations observed via satellite in the southern North Sea were mainly the result of suspended sediment and not actually due to the presence of phytoplankton (IOCCG 2000).

A brief example of the seasonal cycle derived from SeaWiFS for the southern North Sea and open oceanic waters of the Northeast Atlantic can be seen in Figure 5.1. As can be clearly seen, the open oceanic waters demonstrate the typical increase of Chl-a during the spring bloom (May) and then gradually lower in the winter and autumn. Whereas from the southern North Sea, an area dominated by CASE II optically complex waters, this typical seasonal cycle is not clear, as the Chl-a in January and November is as high as the spring bloom indicating the lack of an ability to distinguish between substances/sediments and Chl-a. Note that the scale of the open oceanic areas is significantly lower than that of the coastal ones (Figure 5.1).

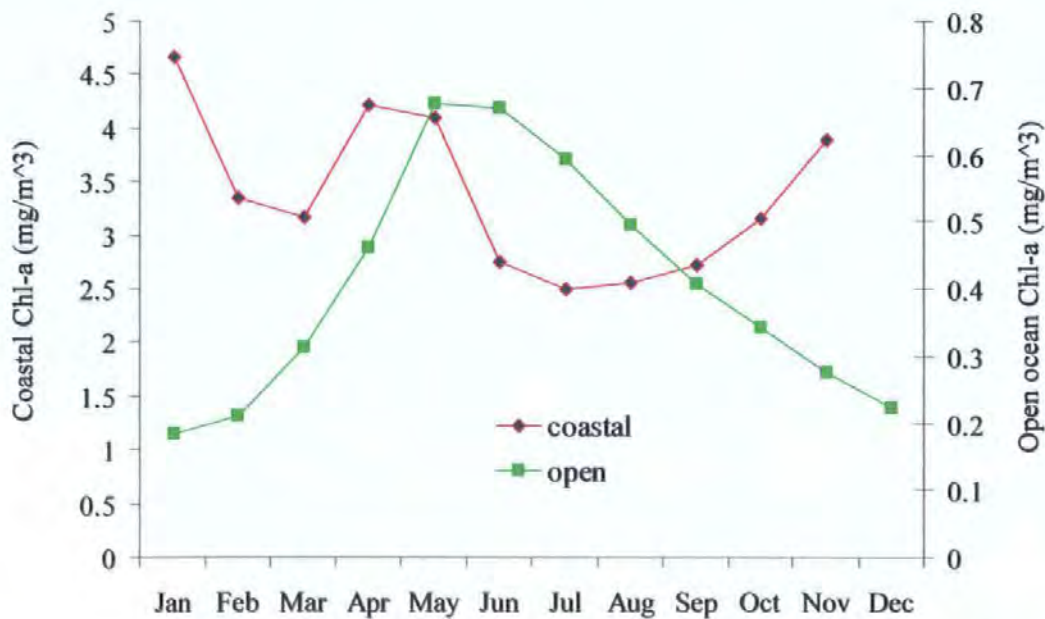


**Figure 5.1:** Seasonal cycle of SeaWiFS Chl-a for the open oceanic area of the Northeast Atlantic and the coastal area of the southern North Sea. The seasonal data were derived from the monthly Chl-a datasets between September 1997 and December 2005.

However, this is not necessarily wrong as the coastal North Sea is a nutrient rich area (Clark and Frid 2001) and as was expected, the amount of Chl-a is much greater than in the oligotrophic oceanic areas. This is where PCI can be particularly useful by mapping the *in situ* ocean colour data as well as SeaWiFS derived ones and compare them, in order to see if this high abundance is an artefact (see Figure 5.2). As high Chl-a values are clearly observed in both of the ocean colour datasets, indicates that the southern North Sea is an area with high phytoplankton concentrations. Thus, by braking down the total composite images to seasonal plots, SeaWiFS misinterpretation of Chl-a (in time and space), can be assessed.

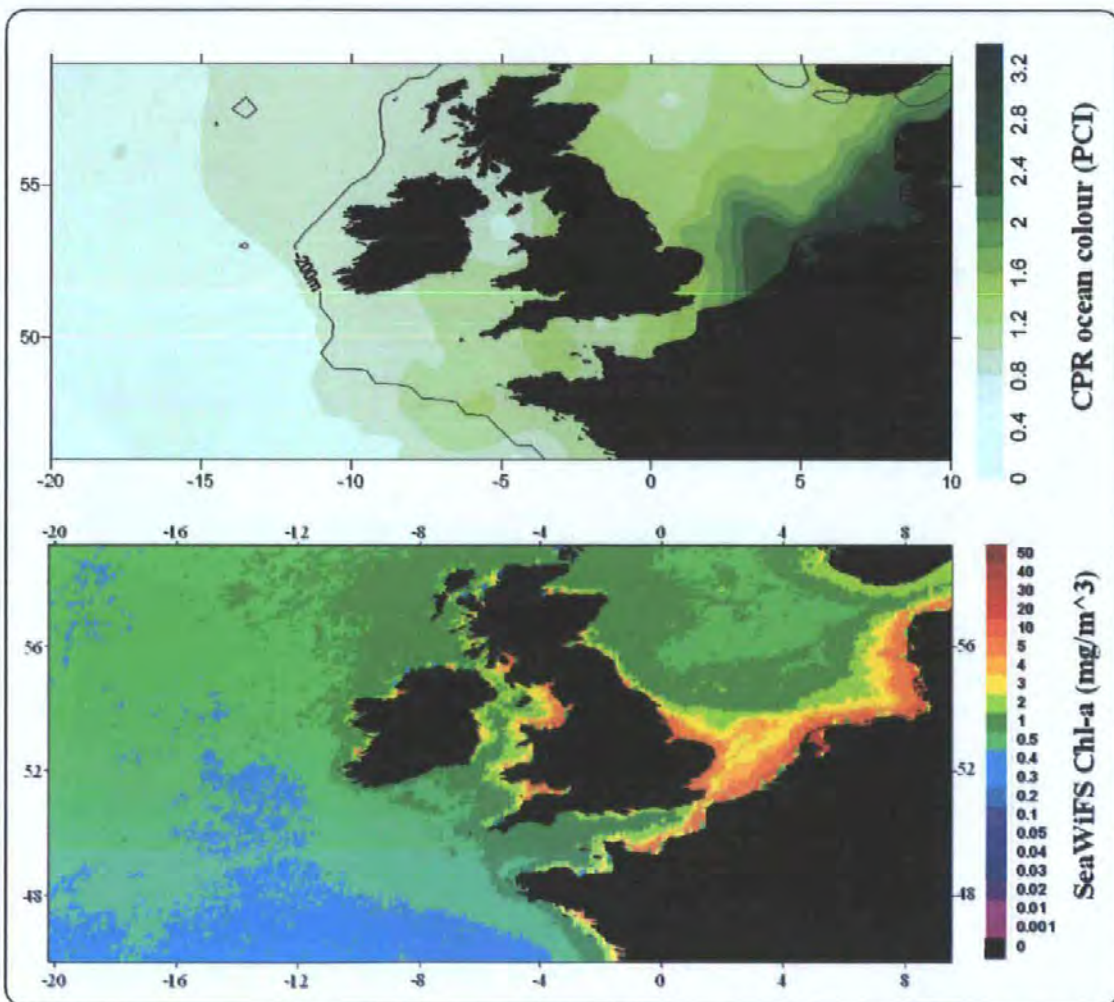


**Figure 5.2:** Composite of CPR PCI and SeaWiFS Chl-a for the period of September 1997 to December 2005. The PCI map was produced using Kriging interpolation methods.

#### 5.1.1.4 The Usage of the New Chl-a Dataset

##### 5.1.1.4.1 Overview

This section briefly outlines the conclusions of the usage of the new Chl-a dataset to explain changes seen in the North Sea (the full document can be seen in Appendix I). The North Sea is an area rich in natural resources, thus much of it has been affected by anthropogenic impacts including fishing, nutrient runoff, and oil, gas, and aggregate extraction (Clark and Frid 2001). Because of its proximity to land, the degree of impact on the coastal area is more likely to be greater than that affecting the open North Sea. Two new Chl-a datasets, but this time based on coastal and open oceanic waters of North Sea, were created (Figure 5.3) in order to quantify differences in the previous and current regimes of both the anthropogenically impacted coastal North Sea and the comparatively unaffected open North Sea.

It was found that the open North Sea region has the typical stepwise increase that happened in the mid 80s; whereas in the coastal region a new regime was revealed. The new coastal regime maintains a 13% higher Chl-a concentration in the open North Sea and a 21% higher concentration in the coastal North Sea waters. However, the current regime has lower total nitrogen and total phosphorus concentrations than the previous regime, although the molar Nitrogen : Phosphorous (N:P) ratio in coastal waters is now well above the Redfield ratio and continually increasing. Although nutrient concentrations in the coastal North Sea have decreased significantly since the regime shift algal biomass has continued to increase. While there is a strong relationship between algae and nutrients, it is thought to be non-linear in coastal North Sea waters, i.e. a reduction in nutrient load does not lead to an equivalent reduction of phytoplankton biomass (Lenhart 2001). A similar pattern in turbidity changes was also observed in the Western Wadden Sea (De Jonge *et al.*, 1996), although the explanation behind the increase in water clarity is still unclear. However, the reduction in turbidity does not seem to be enough to explain the increase in Chl-a, coincident with the decrease in nutrients. One possible explanation may be that after the regime shift, coastal waters have become more vulnerable to fluxes in nutrient concentrations. The warmer SST and increased light of the new coastal regime

provide environmental conditions well suited to phytoplankton growth, which allow algae to utilize lower concentrations of nutrients more efficiently. Because coastal phytoplankton are light limited, the cooler more turbid state of the previous regime may have acted as a buffer, preventing algae from reaching the high biomass that is now possible. The enhanced response by the algal community to changes in nutrients is a characteristic of the new alternate state of the North Sea (Appendix I).

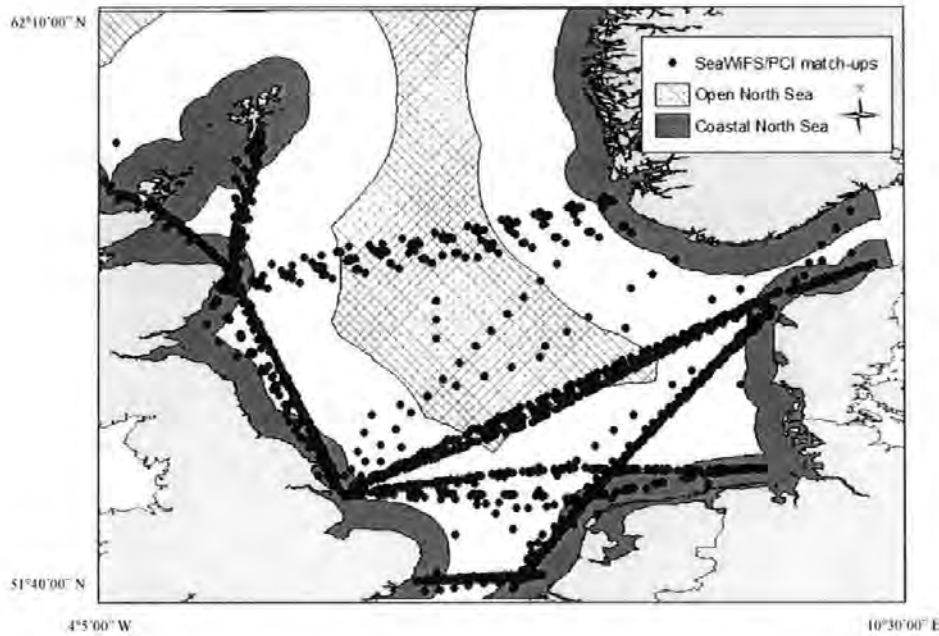


**Figure 5.3:** Location of coastal and open North Sea areas used in Appendix I (Paper submitted) overlain by CPR samples temporally corresponding with SeaWiFS Chl-a measurements ( $n=3695$ ).

### ***5.1.2 Phytoplankton Groups and their Relation to Macroscale Factors Derived from Remotely Sensed Data***

The second stage was to identify which environmental variables are the most important influencing the distribution and abundance of phytoplankton; the importance of phytoplankton and relevant information can be seen in Chapter 3.

### 5.1.2.1 The Value of Using Advanced Statistical Tools

Generalised Additive Models and Artificial Neural Networks were used; both approaches offer the advantage of dealing with non-linearity and complex data matrices in a way that standard linear regression techniques cannot be used. For instance, the Pearson correlation coefficient can be used to assess whether, for instance, diatoms are correlated with SST. Briefly, for the purpose of this example, the annual mean of CPR diatom abundance was used from 1958 to 2003 and NHT for the Northeast Atlantic. The Pearson correlation coefficient indicated a non significant relationship between the two variables ( $r^2 = -0.05$ ,  $p = 0.733$ ). However, the opposite result was indicated by the GAM model (Figure 5.4), which not only supports that there is a high correlation but also a positive one ( $r^2 = 0.33$ ,  $p = 0.0233$ ). From Figure 5.4 it can be observed (bell shape distribution) that diatoms prefer mid temperatures and whenever temperatures are low diatoms abundance is lower, whereas if NHT is in a positively higher phase ( $>0.3$ ) diatom abundance is decreasing rapidly. This result is also confirmed in Chapter 3 where ANNs were used to develop relationships between SST and diatoms. Explanations of why diatoms react negatively to higher temperatures (i.e. higher stratification = lack of nutrients) has been covered in Chapter 3 and will also be discussed in section 5.1.4. It was demonstrated that Pearson or standard regression techniques could not identify the significant association because the relationship was not linear (increase or decrease as NHT fluctuates). Therefore, advanced statistical tools were used only when appropriate because the Pearson correlation coefficient proved particularly useful in Chapter 2 (to identified relationships between PCI and SeaWiFS Chl-a).

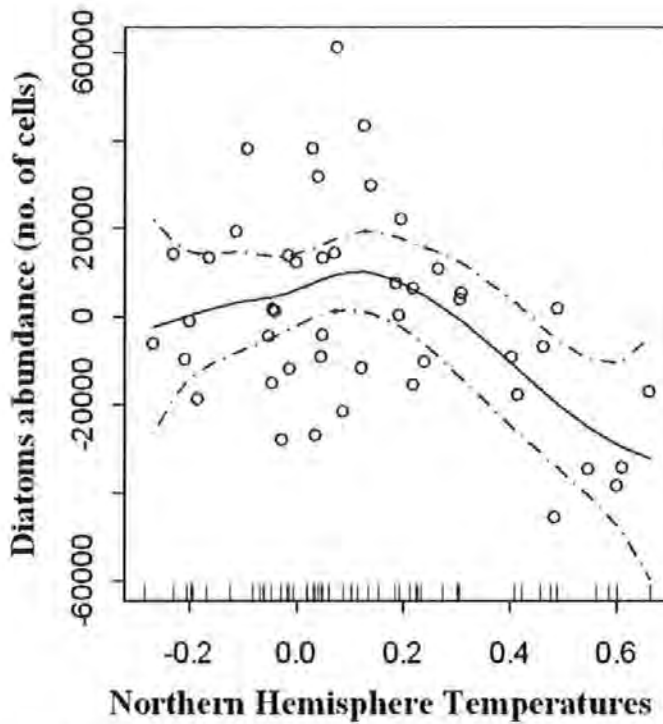


*Figure 5.4:* GAM plot illustrating the variability of diatoms in relation to fluctuations of NHT (1958-2003).

#### 5.1.2.2 Coccolithophores

Coccolithophores were highly correlated with solar radiation flux, high temperatures and shallow mixed-layer depth ( $r^2 = 0.89$ ). GAMs also indicated that as temperature increases, coccolithophore abundance increases as well.

The *in situ* measurements (CPR) confirmed that the 1998 bloom was *E. huxleyi*, and the area of study is a well known region where large coccolithophore blooms and their relationships to the biogeochemical environment have been reported in the past (Holligan *et al.*, 1993). Although the subarctic North Atlantic can be characterised as ideal for studying *E. huxleyi* blooms, information regarding the link between the extensive blooms of this species and the physical environment are limited.

The use of physical/environmental data-sets suggested that large coccolithophore blooms may be caused by distinct environmental conditions i.e. high solar radiation flux, very shallow MLDs and positive SST anomalies. Also, our understanding of the coccolithophore bloom distribution pattern can be improved by learning more about their ecology. Knowing the effect of the physical as well as of biogeochemical environment on this species, additional knowledge on the potential impact of climate change on coccolithophores may be conveyed.

It is thought that increasing levels of atmospheric CO<sub>2</sub>, which consequently causes significant changes in surface ocean pH (acidification), will be responsible for a reduction in calcifying phytoplankton such as coccolithophores (Riebesell *et al.*, 2000). An indirect effect of climate warming is that increasing temperatures alone, or by contributing to ice melting (freshwater runoff) and consequently decreased salinity, can lead to increased stratification in surface waters and stabilise the water column for longer (favourable conditions for *E. huxleyi*). Positive temperature and negative salinity anomalies have been correlated with *E. huxleyi* bloom occurrence in the Barents Sea (Smyth *et al.*, 2004). In addition, a potential *E. huxleyi* bloom was detected in the Barents Sea in June 1998 that was less intense than other years. In the same study it was reported that the frequency of coccolithophore blooms in the Barents Sea may be increased if global warming persists and stimulates warming and increased run off. The results of this study, based on a 20 year time series (AVHRR), showed that there was a pronounced temperature shift from 1996 to 2004 in the subarctic North Atlantic. The results also suggested that coccolithophores are probably favoured by anomalously warm temperatures, when this increase co-occurs with their seasonal peak (usually June in the area of study). A possible reaction of coccolithophore blooms to this warmth is an increase in their abundance. If the latter is true, it can have a major effect on the oceanic and atmospheric environment of the North Atlantic as these blooms are thought to play a key role in biogeochemical cycling and contribute in a major way to climatic processes (Holligan *et al.*, 1993; Westbroek *et al.*, 1993; Tyrrell *et al.*, 1999). However, the short time series of SeaWiFS (1997-present) does not allow us to draw any significant conclusions on decadal changes of coccolithophores. Nevertheless, if their spatial extent varies significantly then their contribution to these cycles or the impacts on the environment will vary too.



### 5.1.2.3 Diatoms

Regarding diatoms, ANNs reported that SST and PAR were the most important factors explaining 65% of their abundance (along with the less important variables). Also, it was found that whenever SST reached high temperatures there was an instant plummet in diatom abundance; no matter how high light levels were and/or the month. Therefore, SST was found to be the key factor influencing diatoms' abundance. The results also indicated that seasonal information plays an important role in diatom abundance; diatoms have a strong standard seasonal cycle, which is modulated by the physical conditions favouring this group. During winter, strong wind stress and winter convection (resulting in well mixed waters), along with low SST and low light intensity maintains the diatom abundance at a minimum level. Wintertime mixing in oceanic waters brings nutrients towards the photic zone that diatoms can utilise in spring once light intensity increases and stratification occurs (Townsend *et al.*, 1994).

As observed from the results of this study, the diatom spring bloom occurs once warming temperatures (solar heating) and weakening winter winds induces shallow stratification (Townsend *et al.*, 1994). In late spring, and especially May, diatoms are at their maximum abundance. Edwards (2000) reported that this sudden increase is predominantly controlled by light availability in the euphotic zone because the day length and light intensity increases as the degree of mixing gradually declines. However, in open oceanic areas, as temperature increases, stratification increases as well and nutrient availability in surface waters declines. Across the Northeast Atlantic, during summer the marine vegetation community composition changes from diatom to dinoflagellate dominance. Due to shallow stratification, phytoplankton deplete upper layer nutrients and diatoms (opportunists) give way to flagellates (competitors) and eventually dinoflagellates (stress-tolerators) and coccolithophores, which are adapted to survive in low nutrient, stable waters (Margaleff 1978). As was observed from Figure 3.10, during autumn, the sudden cooler SST and increased wind stress caused the erosion of the thermocline allowing the mixing of cold, nutrient rich

bottom waters with warm, nutrient depleted surface waters (Holligan 1987; Cushing 1990).

#### ***5.1.2.3.1 Diatom Populations and their Relation to Climatological Changes***

In addition to climatological conditions, nutrients are also key regulators of diatom abundance (Redfield *et al.*, 1963). In this study, the importance of the spatiotemporal and physical regime was assessed while the effect of the chemical (i.e. nutrient) regime on diatom populations was not considered due to a lack of adequate nutrient data; only satellite remotely sensed data was used. However, Redfield *et al.* (1963) reported that diatoms require Si:N:P in the ratio of 16:16:1 and diatoms are Si limited. Usually, as long as sufficient light and Si are available, increased N and P results in an increase in phytoplankton biomass and primary production as phytoplankton cease to be nutrient limited (Cloern 2001).

Increasing temperatures have been repeatedly reported in the northeast Atlantic (Reid *et al.*, 2001) and the subarctic northeast Atlantic, where a pronounced SST shift in the mid-1990s took place (Chapter 3). The results of this study are in agreement with the outcomes of other research indicating a tight coupling between diatom abundance and SST (Edwards and Richardson 2004); the GRNN models found SST to be the most important of the tested factors contributing to diatom abundance. Also, the 3D graphs (Figure 3.12) indicated a negative relationship between SST and diatoms, whenever SST was significantly increased, no matter the adequate light and/or ideal month.

SST is predicted to increase as climate change continues (Houghton *et al.*, 2001), a situation which will further alter the phytoplankton ecosystem of the northeast Atlantic. While the exact mechanisms underlying such relationships are tentative, the regional climate warming signal is strongly evident at all trophic levels of the marine system in the Northeast Atlantic (Edwards and Richardson 2004). The level of response of marine vegetation to climate forcing varies in different areas and between phytoplankton functional groups; however, it was recently reported that climate change has a strong impact on marine pelagic phenology and led to a mismatch

between trophic levels (Edwards and Richardson 2004; Richardson and Schoeman 2004).

Recently, it was also reported that climatic changes lead to an increasingly nutrient depleted state of the epipelagic surface zone that causes diatom populations to decrease (Bopp *et al.*, 2005). Also, Bopp *et al.* (2005) showed that these changes are most apparent in the North Atlantic Ocean and subantarctic Pacific; where in a modelling scenario featuring 4 times the current CO<sub>2</sub> level a 60% decrease in diatom populations was predicted. In addition, based on *in situ* datasets, decadal trends of total diatom abundance from 1958-2002 have appeared to decrease significantly in the North Atlantic Ocean (Leterme *et al.*, 2005).

An indirect effect of climate warming is that increasing temperatures can contribute to ice melting (freshwater runoff) and consequently decreased salinity; these changes are especially apparent in high latitudes (Gregg *et al.*, 2003). Both higher temperatures and lower salinities lead to a decreased density of shallow water, and hence to stronger stratification, which, due to prolonged warmer temperatures, may allow the water column to remain in a stratified state for longer. These conditions lead to further nutrient depleted zones which favour nanoplankton (Bopp *et al.*, 2005) and coccolithophores such as *E. huxleyi* (Chapter 3), but can be detrimental to diatom abundance. The increase of less nutritious and palatable phytoplankton at the expense of diatoms is likely to resonate upwards through the food web, as diatoms are a major dietary food source for many zooplankton species (Verity and Smetacek 1996).

#### **5.1.2.3.2 Conclusion**

Robinson (1995) stated that slight variations in SST may represent significant changes in heat energy storage within the ocean. Also, small oscillations in large SST anomalies may influence the timing or even spatiotemporal distribution and abundance of phytoplankton (Reid *et al.*, 1998; Edwards *et al.*, 2001). The consequence of increasing SST may lead to changes in higher trophic levels, since plankton are at the base of the marine food web and thus have implications for the ecological 'food chain', biological pump, carbon fixation, productivity and fisheries of the North Atlantic (Richardson and Schoeman 2004). The process of how oceanic

planktonic organisms respond to climate change is still largely unknown, at least in part due to a lack of adequate datasets.

By examining the relationships between a major phytoplankton functional group with spatiotemporal and physical variables obtained from the synergistic use of *in situ* and satellite remote sensing data, it was found that diatoms have a regular seasonal cycle with their abundance most strongly influenced by SST and light intensity. Therefore, this research presents information on the ecology of diatoms that may enable an improved understanding of the potential response of diatoms to climatic change. As the *in situ* as well as satellite data used in this study are freely available to the scientific community, this methodological approach can give further insights at a broader scale if the study is repeated for several different environments and for finer scales where *in situ* data is available i.e. North Pacific, Mediterranean Sea, North Atlantic and North Sea. Additionally, the methodological approach presented here, with some modifications, brings the possibility of discerning phytoplankton functional groups from remote sensing imagery one step closer, which may enable the cost effective large scale monitoring of phytoplankton community composition as an indicator of ecosystem change (see section 5.2.1).

### ***5.1.3 Discriminating Phytoplankton Groups from Space***

From the information derived from the different studies of the thesis as well as the methodological approach, developed gradually in Chapters 2 and 3, the ultimate goal of the thesis was attempted; the discrimination of different phytoplankton functional groups using remotely sensed variables.

The discrimination of phytoplankton functional types from remotely sensed data is usually based on bio-optical properties and does not incorporate spatiotemporal and environmental knowledge (Sathyendranath *et al.*, 2005; Alvain *et al.*, 2005). In this research, this approach was extended by incorporating geographical, temporal, biological, physical and bio-optical information. Phytoplankton optical properties (light absorption and backscattering) have been found to vary significantly among different phytoplankton groups, thus the nLw product was used as a proxy for

backscattering in the discrimination procedure (Platt *et al.*, 2002). Light intensity is a major variable that generally enables phytoplankton to photosynthesise; details of the importance of light on phytoplankton can be seen elsewhere (Nanninga and Tyrrell 1996). Generally temperature has major direct (i.e. metabolism) and indirect (stratification) effects on phytoplankton (Edwards and Richardson 2004)

The results (section 4.3) demonstrated that neural networks were able to discriminate and identify four major functional groups (diatoms, dinoflagellates, coccolithophores and silicoflagellates) with an accuracy of >70%. There are several studies that deal with the ecological/physical importance as well as the identification of key processes controlling the growth of phytoplankton functional groups (Platt *et al.*, 2005 and references within), but the results of this study (Chapter 4) present the parameters' importance regarding the discrimination of species. Although species discrimination and identification of key processes might seem similar, they are not. For example, a parameter such as SST might be vital for a particular group such as coccolithophores (Chapter 3), however this study found that light intensity, wind stress and seasonal information were more important than SST when discriminating and separating coccolithophores group from the others. Based on the results (section 4.3), it is suggested that future research concerning the discrimination and identification of functional groups from remote sensing data should include fundamental information about the physical environment.

Although all predictors played a role, the variables responsible for the highest percentages of discrimination accuracy were physical information such as SST, PAR (light intensity) and wind stress (vertical mixing), with spatiotemporal variables such as longitude, latitude and month generally less important. Platt *et al.*, (2005) argued that growth, as well as community and size structure of phytoplankton assemblages are under the control of physical factors. Physical parameters are sometimes reflecting the habitat of the epipelagic zone as they have a significant direct/indirect impact on the phytoplankton. Therefore, one factor alone was not sufficient to identify/separate the phytoplankton functional types. Alvain *et al.*, (2005) reported that Chl-a alone will never be able to discriminate phytoplankton functional groups; however, using this factor in combination with other variables may lead to the ultimate goal of deriving maps of these groups using remote sensing data. This insight into the factors

influencing the spatiotemporal patterns of phytoplankton functional groups may enable the production of predictive presence/absence maps in areas and at times when *in situ* data are limited. It may also be useful for global climate change and carbon cycle modellers, as the resulting data will enable improved climate change scenarios and the degree of carbon fixation by the oceans to be better established.

#### 5.1.4 Surface Temperatures in Relation to Phytoplankton.

The earth's increasing temperature due to global climate warming is generally widely accepted as evident in terrestrial (Vinnikov and Grody 2003; Fu 2004) as well as marine ecosystems (Richardson and Schoeman 2004). Figure 5.5 presents the annual time series of NHT since 1948, which is representative for the areas of study used in this thesis. It can be seen that NHT is continuously and gradually increasing since 1978. Note that the highest temperature of this 50 year time series was found to be 1998 when one of the largest coccolithophore blooms was recorded (Chapter 3).

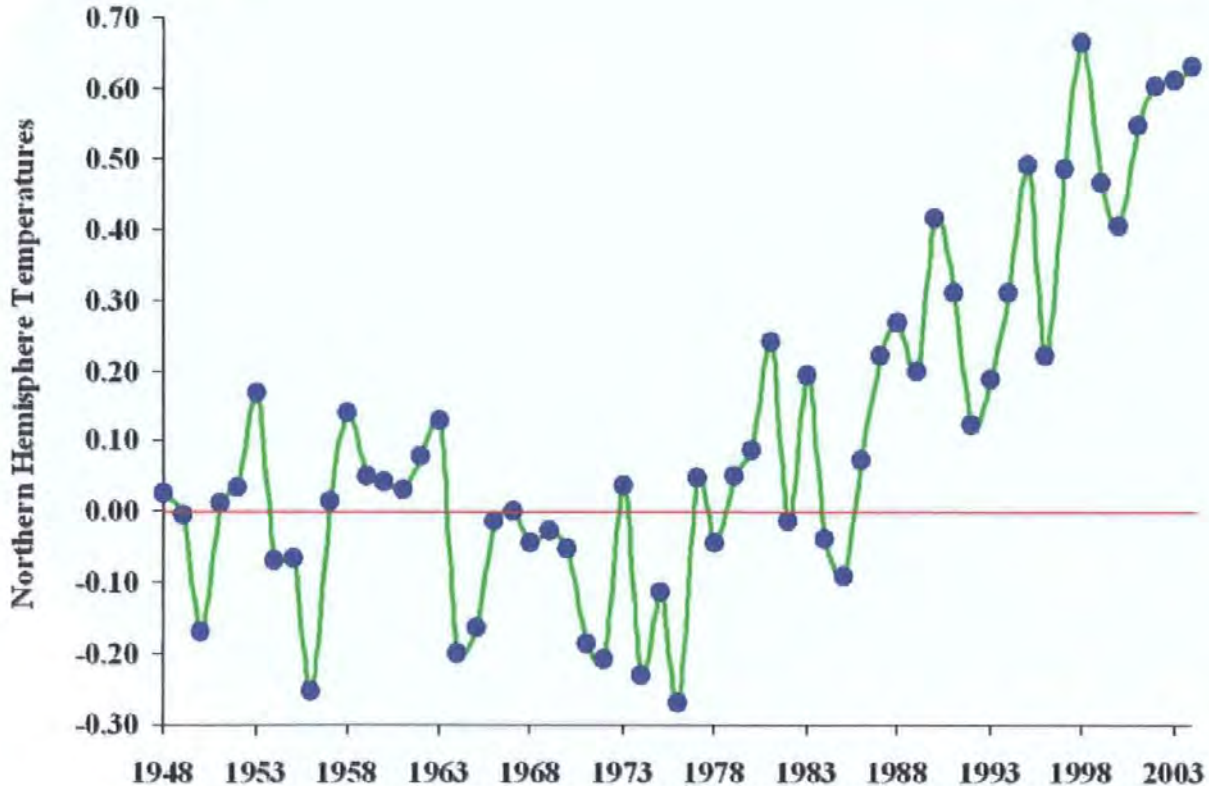


Figure 5.5: Annual mean of Northern Hemisphere Temperature during (data provided by Hadley Centre).

SST can have direct effects on the phytoplankton's physiology i.e. metabolism (Richardson and Schoeman 2004). Indirect effects of climate warming include increasing temperatures, which contribute to ice melting and consequently decreased salinity, which in turn leads to increased stratification. It is well known that highly stratified waters are ideal for coccolithophores such as *Emiliana huxleyi* (Holligan *et al.*, 1993) and other small phytoplankton; however they can be detrimental to diatoms (Bopp *et al.*, 2005). Different phytoplankton groups react differently to fluctuations of SST, and they also do not respond the same way to increasing SST in all areas. For instance, Richardson and Schoeman (2004) reported that warming temperatures can cause phytoplankton to increase in cooler areas and decrease in warmer ones; similar patterns have also been documented in cod recruitment (O'Brien *et al.*, 2000). Climate patterns may affect the timing of phytoplankton growth as well as their distribution and abundance, which in turn have a strong influence on other trophic levels (Edwards and Richardson 2004). Since phytoplankton are at the base of the marine food web, significant changes in their spatiotemporal abundance may have implications on the ecological 'chain', CO<sub>2</sub> fluxes, biological pump, carbon fixation and the productivity of the North Atlantic.

It has been predicted that ocean temperatures are likely to be further increased in the future; for instance, by the year 2100 the temperature in the northeast Atlantic may rise between 2° to 4°C (Houghton *et al.*, 2001). The process of how planktonic organisms respond to climatic changes is still largely unknown. This approach may lead to an improved understanding of the phytoplankton response to climatic changes.

The methodological approach used in this study has acknowledged limitations. Firstly all the biological phytoplankton data used were sampled from the first 10 meters of the water column; as these obtained from the CPR, thus the vertical profile distribution and abundance of phytoplankton could not be assessed. However, the benefit of using the CPR dataset is its high spatial and temporal coverage (at least regarding *in situ* data). An additional limitation is that the chemical regime was not taken into account (directly at least), due to the fact that there are no long-term datasets with a spatial and temporal coverage that would enable sufficient match-ups with satellite or CPR data. Although there are climatological nutrient datasets, these

offer only low resolution and 12 monthly composites (each month), whereas the methodological approach followed treated every month of every year as a separate case allowing the local variability and/or extreme phenomena to be assessed.

## 5.2 Future Research

### 5.2.1 Predicting Phytoplankton Future Distribution and Abundances

Based on the results of this thesis and particularly on the valuable information obtained from the training stage of the ANN (used to develop the relationships with a classification accuracy of >83%), neural networks can be used to derive maps of phytoplankton functional groups without using *in situ data*. This approach can have enormous applications, such as mapping the spatial and temporal (seasonal cycles) trends of these functional groups using only remote sensing data for the areas that have not been sampled by CPR, at a resolution of 4km. The predicted maps can be firstly validated with existing CPR maps, based on >50 year data (Appendix I). This would give us the opportunity to assess the likely influence of global warming scenarios on phytoplankton and on their bloom timing (phenology). For instance, increase the temperature by 1°- 4°C and hence forecast the potential effect of warming on the spatiotemporal distribution of these phytoplankton functional groups. Alvain *et al.* (2005) mentioned that distinguishing phytoplankton groups from space is not only a major challenge of ocean colour research, but will also enable better understanding of biogeochemical processes such as carbon fixation.

Satellites will hardly ever substitute ship-based collections, not only because *in situ* verification is always needed to improve/confirm satellite data quality, but also because satellites only describe the physical/biological regime activity in the first few meters of depth (influenced by the clarity of the water). However, Uitz *et al.* (2006) inferred phytoplankton biomass, its vertical distribution, and the community composition (microplankton, nanoplankton and picoplankton), from the near-surface satellite derived Chl-a concentrations. The results of this thesis indicate, that satellites can be used to discriminate phytoplankton groups from space with an adequate discrimination performance.



This research may offer new possibilities for modelling ocean ecosystems on a regional and oceanic scale; the applicability of this new methodology can be examined in a wider set of ocean basins using other areas where the CPR is currently sampling or has sampled in the past such as the Mediterranean, North Pacific, North Sea, and Northwest Atlantic.

The proposed approach also has considerable potential application in the mapping of spatial and temporal (seasonal cycle) trends in functional groups using only remote sensing data, for areas with minimal *in situ* data. This methodological advance will also give us the opportunity to assess the likely influence of global warming scenarios on phytoplankton and on their bloom timing (phenology). The future predictions deriving from the ANNs models of this study could be validated using CPR maps of phytoplankton abundance. An example of monthly composites of two functional groups (diatoms and dinoflagellates) based on CPR dataset, that could be used for this purpose, are given in Figure 5.6.

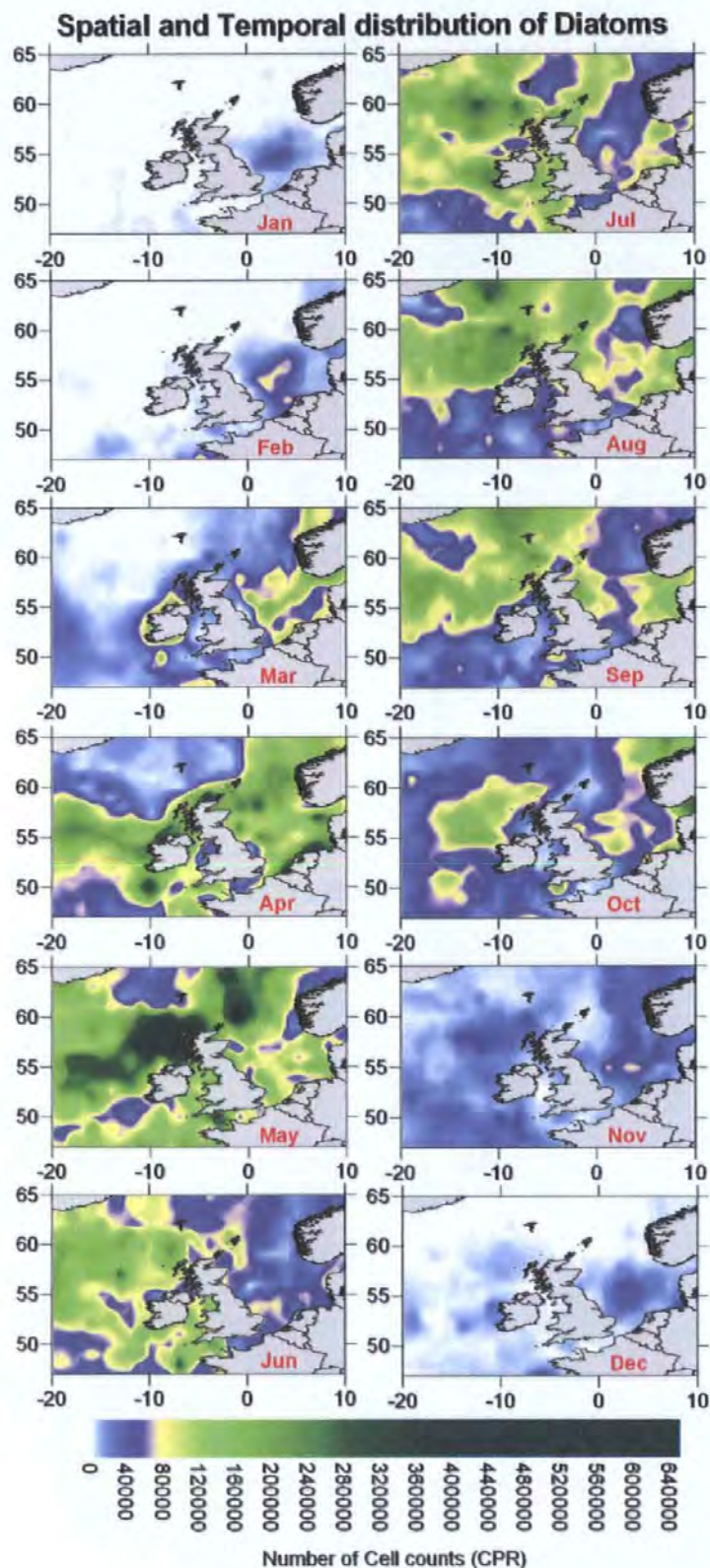


**Figure 5.6:** Seasonal (monthly composites) distribution and abundance of diatoms based on the CPR dataset (1958-2003). These maps can enable the validation of ANNs predicting abundance. The maps have been presented at the ASLO conference (Raitsos *et al.*, 2005 b) and also have been used to describe the seasonal variation of both groups in the Northeast Atlantic Ocean and the North Sea (Appendix I). The methodology used to derive those maps can be seen in both: Raitsos *et al.*, 2005b and Appendix I.

### ***5.2.2 Coccolithophores: What is known and What Remains Still Undiscovered***

Results relating the physical regime with coccolithophore abundance (Chapter 3), has provided important information regarding the ecology of this phytoplankton group as well as its potential reaction to future environmental change. However, every methodological approach has acknowledged limitations and so this section gives a brief explanation of what should be done in the future in order to improve our knowledge on global coccolithophore abundance and its relation to the physical regime.

To assess the importance of the physical environment on *E. huxleyi* blooms, initially, the identified blooms could be characterised as resulting primarily from *E. huxleyi* by running test criteria (Iglesias-Rodriguez *et al.*, 2002). Then, the physical variables (SST, incoming solar radiation, wind stress, MLD and average light within the mixed layer) obtained from satellite/model reanalysis datasets could be correlated with the temporal and spatial distribution of *E. huxleyi* blooms all over the globe (where this species occurs).

Even if one factor, i.e. high light intensity, proves to be an essential requirement for *E. huxleyi* blooms one factor alone is doubtfully sufficient enough to evoke a bloom. Also, the level of importance of each physical variable may depend on the geographical area. For instance, oceanic areas such as the subarctic North Atlantic are going through significant changes; anomalously high SSTs since 1996 (Chapter 3). Therefore, every geographical area would be treated as a separate case.

Nanninga and Tyrrell (1996) indicated that high light intensities and shallow mixed layers are a requirement for *E. huxleyi* blooms with later work on blooms in individual areas corroborating this (Cokacar *et al.*, 2001; Stabeno *et al.*, 2001). However, this hypothesis has previously been investigated only on a case-by-case basis with a limited number of *in situ* datasets. Also, it has never been investigated globally using satellite datasets that offer the advantage of high spatial and temporal coverage and a consistent methodological approach across different areas. The only

similar attempt was carried out by Iglesias-Rodriguez *et al.* (2002), who used global climatologies and limited *E. huxleyi* data (2 years) that restricted significant conclusions on the effect of extreme events or sudden variations of the physical regime.

In Chapter 3 it was reported that the most important physical factor inducing blooms in the subarctic North Atlantic was light intensity (solar radiation arriving at the sea-surface). However, information regarding this variable and its relationship to coccolithophore blooms over the globe needs to be carefully evaluated. For instance, in high latitudes solar radiation might be the primary requirement whereas in mid latitudes it may play a secondary role. In other words, does light intensity play an equally important role in high latitudes, where light levels are seasonally low, in comparison to lower latitude coccolithophore dominated areas such as the Black Sea? Figure 5.7 represents PAR and nLw\_555 seven year mean composite images. During June (when the light intensity is high) the subarctic North Atlantic and Black Sea are dominated by coccolithophores, whereas the blooms almost disappear during August when the light is somewhat less. However, a different pattern is observed in the Barents Sea, where coccolithophores dominate during July and August when the light intensity is lower than in June. So, which physical parameter is the most important in the Barents Sea and if it is also solar radiation then which parameters force the blooms to appear in August rather than June?

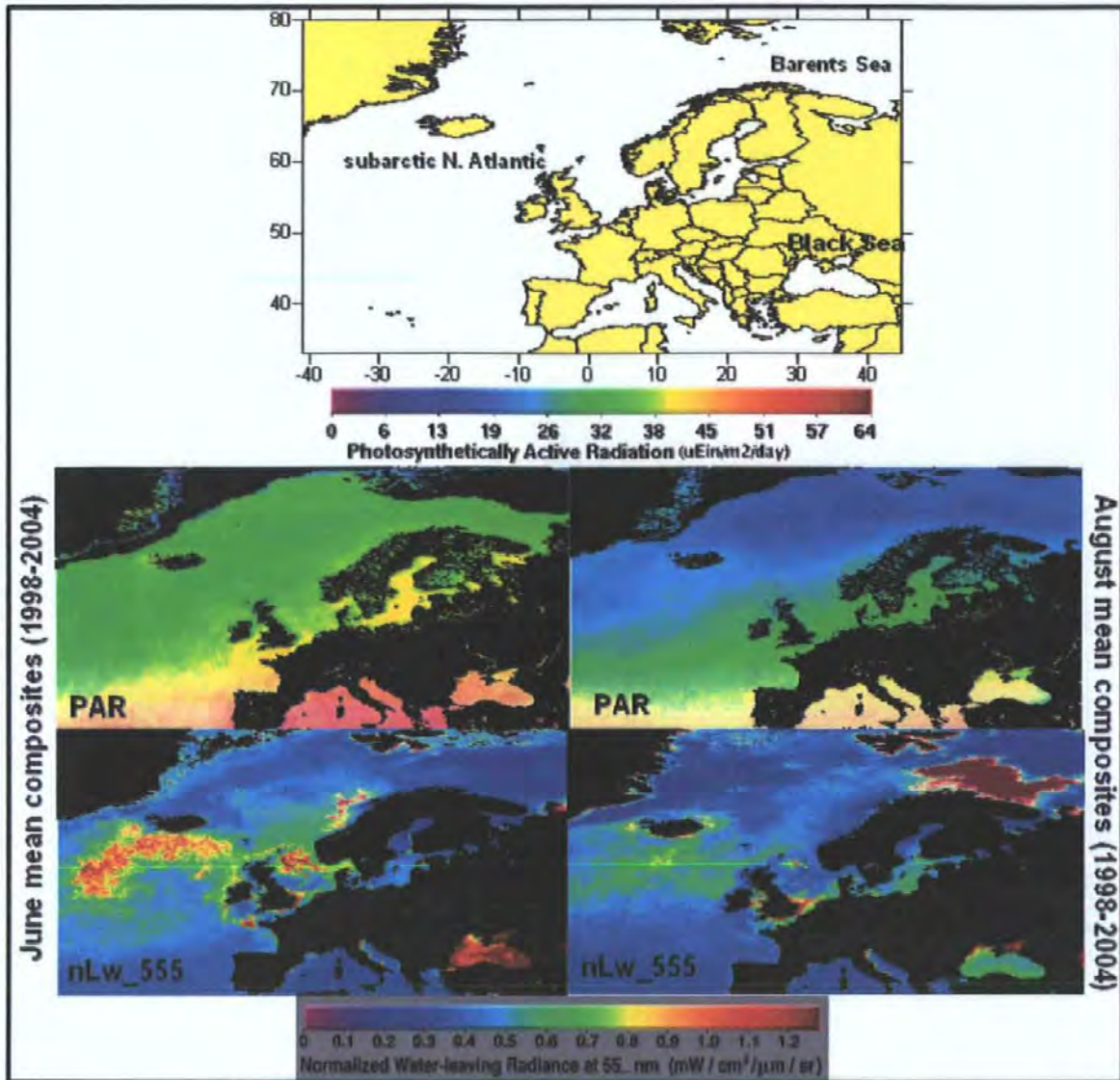


**Figure 5.7:** SeaWiFS 7 year mean composites (1998-2004) of PAR and nLw\_555 in three major regions where *E. huxleyi* blooms have been recorded. Note that high August nLw\_555 values in the Irish Sea and off the mouth of the Thames are most likely due to resuspended sediment rather than coccolithophore blooms.

### 5.2.3 The Use of PCI Ocean Colour Data to Link SeaWiFS and CZCS

#### Sensors

The CZCS sensor was providing data of Chl-a from October 1978 to June 1986 (~8 years). The SeaWiFS Chl-a dataset is available from September 1997 until present. However, there is no other satellite providing global images of Chl-a that can link the

two sensors, in order to be able to assess the decadal changes of the phytoplankton biomass.

In Chapter 2 the validity of the *in situ* ocean colour (CPR PCI) dataset was demonstrated. The new Chl-a dataset is probably the longest as well as most specially extended *in situ* ocean colour dataset in the Northeast Atlantic and North Sea. This new ocean colour dataset obtained from the synergistic use of SeaWiFS and PCI can serve as a link between the two sensors (SeaWiFS and CZCS). For instance, the same methodological approach can be used as seen in Chapter 2, but with CZCS data. Once both of the relationships, SeaWiFS and CZCS Chl-a against PCI, are obtained for each PCI category for the same area of study, then the PCI can be used to link the two sensors and the decadal change of phytoplankton to be assessed. This approach, linking the two satellites, has been performed in the past but by using modelled datasets or very patchy *in situ* data. The use of PCI has the advantage of utilizing more than 100,000 *in situ* data points and also the fact that its relationship with satellites has been demonstrated previously (Chapter 2). One of the biggest problems with conducting such research was the fact that the two sensors were highly incompatible. However, very recently, NASA has provided through the ocean colour website (<http://oceancolor.gsfc.nasa.gov/>) the whole CZCS data in a user friendly HDF format (the same as for SeaWiFS) allowing the comparison of the two sensors.

## Appendix I

This appendix contains the two papers that have been In Press/submitted to peer-reviewed journals but have not been extensively mentioned/analysed within the thesis. The editing, i.e. reference format, of both manuscripts is made according to the journals submitted.

McQuatters-Gollop A., **Raitsos D.E.**, Edwards M., Pradhan Y., Mee LD., Lavender S.J., Attrill M.J. (In Press). A long-term chlorophyll dataset reveals a regime shift in North Sea phytoplankton biomass unconnected to increasing nutrient levels. *Limnology and Oceanography*. xx-xx.

McQuatters-Gollop A., **Raitsos D.E.**, Edwards M., Attrill M.J. (Submitted). Spatial patterns of diatom and dinoflagellate seasonal cycles in the North – East Atlantic Ocean. *Marine Ecology Progress Series*.

These two papers have been derived after two years of collaboration with Abigail McQuatters-Gollop. Both of the projects started by putting down our ideas and testing different hypothesis. My contribution to the first manuscript involved the extraction, ordering, processing and analysing the satellite data; correlating satellite data with CPR data to derive the relationship; and statistical testing of the robustness of the CPR-SeaWiFS relationship in open and coastal North Sea waters. The Results and Discussion sections which interpreted the data are a result of an iterative discussion process between myself, Abigail, and, to a lesser extent, the other authors of the paper.

The second manuscript was largely based on the work I presented at ASLO 2005 (Raitsos et al., 2005b); therefore I extracted and processed the data, using interpolation methods. Abigail, because GIS is her area of expertise, created the maps based on that data. We worked together to interpret the finished products and to speculate on the usefulness of such maps in research and management.

Abigail and I worked together to outline the formats of both manuscripts. Although she wrote the initial drafts, we passed them back and forth between ourselves to make additions and changes to each version of the manuscripts, before finally passing suitable versions to the other co-authors.

## **A long-term chlorophyll dataset reveals a regime shift in North Sea phytoplankton biomass unconnected to increasing nutrient levels**

Abigail McQuatters-Gollop<sup>1,2,3</sup>, Dionysios E. Raitsos<sup>1,2</sup>, Martin Edwards<sup>2</sup>, Yaswant Pradhan<sup>1</sup>, Laurence D. Mee<sup>1</sup>, Samantha J. Lavender<sup>1</sup>, and Martin J. Attrill<sup>3</sup>

<sup>1</sup>School of Earth, Ocean and Environmental Sciences, University of Plymouth, Drake Circus, Plymouth, PL4 8AA, United Kingdom

<sup>2</sup>Sir Alister Hardy Foundation for Ocean Science, The Laboratory, Citadel Hill, Plymouth, PL1 2PB, United Kingdom

<sup>3</sup>Marine Biology and Ecology Research Centre, School of Biological Sciences, University of Plymouth, Drake Circus, Plymouth, PL4 8AA, United Kingdom

Short title: Regime shift unrelated to nutrients



**Acknowledgements**

The authors would like to thank past and present SAHFOS workers and the international funding consortium supporting the CPR survey. Their dedication has made this unique time-series possible. Abigail McQuatters – Gollop is supported by the University of Plymouth as well as SAHFOS. We also thank the anonymous reviewers for their helpful comments and suggestions

**Abstract**

During the 1980s, a stepwise increase in Phytoplankton Colour, a semiquantitative visual estimate of algal biomass, was observed in the North Sea as part of a region-wide regime shift. Two new datasets created from the relationship between Phytoplankton Colour and SeaWiFS chlorophyll a (Chl-a) quantify differences in the previous and current regimes in both the anthropogenically impacted coastal North Sea and the comparatively unaffected open North Sea. The new regime maintains a 13% higher Chl-a concentration in the open North Sea and a 21% higher concentration in coastal North Sea waters. However, the current regime has lower total nitrogen and total phosphorus concentrations than the previous regime, although the molar N:P ratio in coastal waters is now well above the Redfield ratio and continually increasing. Besides becoming warmer, North Sea waters are also becoming clearer (i.e. less turbid), thereby allowing the normally light-limited coastal phytoplankton to more effectively utilize lower concentrations of nutrients. Thus, despite decreasing nutrient concentrations, Chl-a continues to increase, suggesting that climatic variability and water transparency are more important than nutrient concentrations to phytoplankton production at the scale of this study.

## Introduction

Phytoplankton are the primary producers of pelagic marine waters, the base of the marine food web and thus an integral part of the ecosystem, affecting trophic dynamics, nutrient cycling, habitat condition and fishery resources (Paerl et al. 2003). Additionally, plankton are closely coupled to environmental change (Hays et al. 2005), making them sensitive indicators of environmental disturbance.

Between 1983 and 1988 a stepwise change occurred in many biological and ecosystem processes and individual species in the North Atlantic region (Beaugrand 2004). A shift in the proportion of cold and warm water species of *Calanus* (Reid et al. 2003a), phenological changes in production resulting in trophic mismatch (Edwards and Richardson 2004), an influx of oceanic species (Lindley et al. 1990) and changes in zooplankton community structure and salmon abundance (Beaugrand and Reid 2003) occurred in the North Sea during the mid to late 1980s. Additionally, phytoplankton production demonstrated a marked increase across the North Atlantic and North Sea regions during that period (Edwards et al. 2001; Reid et al. 1998). These changes, observable across multiple trophic levels, are linked to what has been described as a regime shift, a stepwise alteration in the composition and productivity of the whole ecosystem at a regional scale that reflects major hydrographic change (Beaugrand 2004; Reid et al. 2001).

The cause of the late 1980s North Sea regime shift may have been a response to an increase in the winter North Atlantic Oscillation Index (NAO) from a negative phase to its longest ever positive phase (Alheit et al. 2005; Beaugrand 2004; Weijerman et al. 2005). A positive phase NAO influences the North Sea ecosystem through regional climate effects including increased sea surface temperature, strong westerly winds (Alheit et al. 2005; Beaugrand 2004; Weijerman et al. 2005), and increased inflow of warm, salty water from the Atlantic Ocean (Beaugrand 2004; Edwards et al. 2001).

Although oceanic algal production is an important component of the marine system, few long-term biological datasets exist for European waters. The lack of time-series data has made it difficult to identify trends in phytoplankton production dynamics and establish linkages to natural variability or anthropogenic change (Edwards et al. 2001). The Continuous Plankton Recorder (CPR) survey, an upper-layer plankton monitoring program

operated since 1931, provides the only long-term biological plankton dataset with spatial coverage across coastal and open North Sea waters (Edwards et al. 2001). The first level of analysis the CPR offers is the Phytoplankton Colour Index (PCI), a semiquantitative in situ measurement of phytoplankton biomass (see Methods section). The PCI was recently used in conjunction with phytoplankton chlorophyll-a data estimated by the Sea-viewing Wide Field-of-view Sensor (SeaWiFS) satellite to extrapolate a new 50 year Chl-a dataset for the Northeast Atlantic and North Sea (Raitsos et al. 2005).

As an area rich in natural resources, much of the North Sea has been affected by anthropogenic impacts including fishing, nutrient runoff and oil, gas and aggregate extraction (Clark and Frid 2001). Because of its proximity to land, the degree of impact on the coastal area is likely to be greater than that affecting the open North Sea. The aim of this paper is to separately extrapolate the SeaWiFS dataset back 50 years for the open and coastal North Sea in order to assess the long-term variability of Chl-a within and between these two regions and to relate the Chl-a time series to environmental and climatic variation. In this paper we will attempt to explain trends observed in phytoplankton biomass based on environmental, climatic and nutrient related factors and processes. We also examine the biological, environmental and climatic differences between the pre- and post- regime shift North Sea system and investigate factors generating change, including nutrient concentrations, water transparency, sea surface temperature (SST), sea level pressure (SLP), precipitation, wind stress and climatic variability.

## **Methods and Materials**

### *Area of study*

The North Sea is bordered by some of the most densely populated and highly industrialized Western European countries; its catchment covers an area of 850,000 km<sup>2</sup> and contains 184 million people (OSPAR Commission 2000). The North Sea has been a productive fishing ground and is heavily exploited for oil, gas and aggregates. Additionally, the North Sea is extensively used for transport as well as for the dumping of dredged material. From an environmental perspective, the North Sea is an ecologically rich and diverse environment; a number of endangered species and important habitats, some of which are now protected, are found within the North Sea ecosystem (OSPAR Commission 2000).

For the purpose of this study, we defined the limit of the coastal North Sea as a standard 30 nm (56 km) distance from land (Fig. 1). In order to minimize the impact of land-based activities, the open North Sea was designated as the area greater than 125 nm (231 km) from the shore. Polygons representing the open and coastal North Sea study areas were constructed with ESRI ArcMap 9.0. These polygons were used to select the corresponding data points for each geographically referenced dataset used in this analysis (PCI, SeaWiFS, PCI – SeaWiFS match-ups, SST, nutrient concentrations and transparency measurements).

### *Data extraction*

#### *Environmental data*

Annual surface nutrient concentration data for the North Sea and Elbe and Rhine rivers were obtained from the European Environment Agency's Waterbase (EEA) via their website (<http://dataservice.eea.eu.int/dataservice/>). Waterbase contains reliable and validated data collected from EEA member countries' national monitoring programs and therefore comprehensively covers a large geographical area, a requirement which is paramount to our study. To assess variability of nutrient input, Elbe and Rhine River discharge data were obtained from the Global Runoff Data Centre, a digital world-wide repository of discharge data and associated metadata (Global Runoff Data Centre 2005).

Coastal water transparency data were extracted from the Secchi Disk Data Collection for the North Sea and Baltic Sea (available at <http://www.ices.dk/ocean/project/secchi/>) compiled by Thorkild Aarup (Aarup 2002). While the transparency dataset contains a considerable number of samples ( $n = 5057$ ) with a wide spatial and temporal resolution, they are not uniformly distributed in time or space. Temporally, the nineties were the most heavily sampled decade ( $n = 3056$ ) followed by the eighties ( $n = 1188$ ) and the seventies ( $n = 758$ ); thus, the accuracy of trend in Secchi depth increases with time. The majority of samples were taken in the Dutch, German, Danish and Norwegian waters of the southern North Sea ( $n = 2730$ ) and Kattegat ( $n = 2116$ ). The remaining samples are from the coastal areas of the UK and western Norway. Water transparency is dependent on phytoplankton biomass, dissolved particulate organic matter (POM), suspended sediments and yellow substances in the water column (Sanden and Hakansson 1996) as well as water column stability.

The North Atlantic Oscillation (NAO) is the principal form of climatic variability affecting the North Sea and influences its ecology through SST, wind direction and

magnitude, and precipitation (Ottersen et al. 2001) and is strongly linked to oceanic inflow into the North Sea (Reid et al. 2003a). The winter (December through March) NAO index was acquired from the website of Jim Hurrell at the National Center for Atmospheric Research. The NAO index is based on the difference in normalized sea level pressure between Lisbon, Portugal, and Stykkisholmur, Iceland (Hurrell 1995). Mean annual SST data were obtained from the Hadley Center, UK Met Office (HadISST v1.1). Monthly mean precipitable water content (as a measure of precipitation) and sea level pressure data were obtained from the NCEP/NCAR Reanalysis Project at the NOAA-CIRES Climate Diagnostics Center (<http://www.cdc.noaa.gov/cdc/reanalysis/>). Wind speed data, also obtained from the NCEP/NCAR Reanalysis Project, were converted into wind stress data. Wind stress is a function of wind speed, non-dimensional drag coefficient and boundary layer air density (Pickard and Pond 1978). Wind stress regulates the dynamics of the boundary layer and is connected to the production of wind-driven surface currents, the generation of surface waves and upper-ocean mixing (Raitzos et al. 2006). Therefore, low wind stress is associated with highly stratified waters.

Data on the influx of Atlantic waters entering the North Sea between the Orkney Island and Utsira were obtained from the NORWECOM 3-D hydrodynamic model (Iversen et al. 2002). Model generated data were used as no long-term measured time-series exist.

#### *Primary production data*

PCI data were extracted from the CPR database for the North Sea. During the period 1948-2003, the CPR survey collected approximately 52,000 samples. Although the CPR has been sampling in the North Sea since 1931, we used data from 1948 onwards as the methodology of sampling and measurement of PCI has remained consistent since 1948 (Reid et al. 2003b). Samples are collected by a high-speed plankton recorder (~15-20 knots [ $28 - 37 \text{ km hr}^{-1}$ ]) that is towed behind 'ships of opportunity' in the surface layer of the ocean (~10 m depth); one sample represents 18 km of tow. Accumulation of phytoplankton cells on the silk gives it a greenish color (Batten et al. 2003); the Phytoplankton Colour Index (PCI) is based on a relative scale of greenness and determined on the silk by reference to a standard color chart. There are four different 'greenness' values: 0 (no greenness), 1 (very pale green), 2 (pale green) or 6.5 (green). Categories of PCI are assigned numerical values based on acetone extracts (Colebrook and Robinson 1965). PCI is a unique measurement of phytoplankton

biomass, as small phytoplankton cells that cannot be counted under the microscope contribute to the coloration of the filtering silk (Batten et al. 2003).

SeaWiFS current reprocessed version (v5.1) data produced by Ocean Biology Processing Group (OBPG) were acquired from the NASA Ocean Color website (<http://oceancolor.gsfc.nasa.gov/>). The data were Level 3, 8-day products (9 km x 9 km square resolution) of the near-surface Chl-a concentration ( $\text{mg m}^{-3}$ ), estimated using the ocean Chlorophyll 4 - version 4 (OC4-v4) algorithm (O'Reilly et al. 1998):

$$\text{Chl-a} = 10^{(0.366 - 3.067x + 1.930x^2 + 0.649x^3 - 1.532x^4)},$$

where  $x = \log_{10}((R_{rs\ 443} > R_{rs\ 490} > R_{rs\ 510})/R_{rs\ 555})$  and  $R_{rs}$  is the satellite calculated remote sensing reflectance

NASA processed these data using a series of radiometric corrections (e.g. atmospheric) to eliminate the presence of clouds, haze and water vapor (Mueller and Austin 1995). The 8-day data products were used in order to increase the number of CPR – SeaWiFS match-ups, as the daily data were highly obscured by cloud cover.

### *Data analysis*

#### *Matching SeaWiFS and PCI data*

Seventy-six months (September 1997 - December 2003) of in situ measurements of PCI and satellite Chl-a values were compared for the North Sea. Concurrent SeaWiFS and CPR measurements were collated for the same spatial and temporal coverage. Then, refining the technique developed and used on a larger scale by Raitsos et al (2005), coastal and open North Sea samples were selected based on the areas shown in Fig 1. The finer geographical scale helped us to establish more accurate relationships between Phytoplankton Colour and SeaWiFS Chl-a for the open and coastal North Sea study areas. In the North Sea, the CPR survey collected 6294 different samples for the 6-year period; 2311 of which fell within 30 nm (56 km) of the coast and 723 of which were located in the defined open North Sea area. After screening the SeaWiFS dataset for CPR match-ups, only 1272 samples could be used for comparison in the coastal North Sea (44.96 % of coastal data did not have a SeaWiFS match-up, primarily due to cloud coverage) and only 412 could be used in the open North Sea. As we considered 412 too small a sample size to establish a reliable relationship, all

available non-coastal North Sea match-ups (3695) were used to construct the relationship to be applied to the open North Sea (Fig. 1). PCI data are on a ratio scale (i.e. not only can PCI categories be ranked but differences are quantified). Thus, Pearson correlation (or linear regression) is appropriate to assess the strength of the relationship between SeaWiFS and PCI data (Raitsos et al. 2005; Zar 1984). SeaWiFS data were log-transformed to improve homogeneity of variance and normality (Zar 1984). Simple correlation analysis (Pearson) and multiple linear regression were used to determine the existence and strength of possible relationships between environmental and biological variables. For multiple regression modeling, data were first assessed for normality (Kolmogorov-Smirnov test) and transformed if necessary. Models were estimated using forward selection stepwise regression procedures with Chl-a (coastal or open) as the dependent variable and a suite of environmental parameters as candidate independent variables. Robustness of resulting models ( $\alpha$  set at 0.05) was assessed by testing the residuals for normality (K-S test) and homoscedasticity (scrutinizing plots of standardized residuals). All significant analyses conformed to these regression assumptions. Standardized regression coefficients were used to infer the relative importance of model variables for explaining variations in Chl-a data.

The PCI and SeaWiFS datasets demonstrate an overall increase in chlorophyll during the study period. Significant positive relationships exist between PCI and SeaWiFS data for the entire North Sea ( $r = 0.26, p < 0.001$ ) and for the coastal area ( $r = 0.30, p < 0.001$ ). As these relationships are non-linear, the mean SeaWiFS Chl-a value was calculated for each PCI category in each North Sea region (Fig. 2). Using the significant relationships between PCI and SeaWiFS Chl-a for each region (Fig. 2) and the total number of CPR samples analyzed (approximately 52000) for the period 1948 – 2003, retrospective calculations of Chl-a for the coastal and open North Sea could be produced.

#### *Potential biases*

Consistency and comparability of the methodology used in the CPR survey has been studied in depth (Reid et al. 2003b). Although standard methods have been used for more than 50 years in the survey, the PCI has been measured by a number of different analysts during this time. However, evaluating greenness is a simple task that is typically undertaken by 2 to 3 people in a year, many of whom have done this work for more than a decade. As well as referring to a standard color chart, apprentices are trained in assessing PCI for a year before performing the task on their own (Raitsos et al. 2005).



We used the 8-day SeaWiFS Chl-a data for the establishment of PCI match-ups, because when using daily images of Chl-a, approximately 90% of CPR in situ data were unusable due to high cloud coverage. Thus, the 8-day Chl-a mean composite images were used, thereby increasing the amount of usable CPR data to >45%. It has to be mentioned that final results of the daily SeaWiFS data – PCI relationships were not significantly different from the relationships presented in this paper (data not shown). However, we used the 8-day relationship as it was statistically more significant (more samples), and the 95% confidence limits were reduced for each PCI category.

The study area includes both Case I (open ocean) and Case II (optically complex coastal) waters (IOCCG 2000). In Case II waters, Chl-a is difficult to distinguish from particulate matter and/or yellow substances (dissolved organic matter) and so global chlorophyll algorithms (such as OC4-v4) are less reliable (IOCCG 2000). Previous work applying the Phytoplankton Colour/SeaWiFS Chl-a relationship has occurred primarily in Case I waters (Raitsos et al. 2005). This is the first time the relationship has been used to create a Chl-a time-series for a substantial geographic area featuring optically complex Case II waters.

## Results

### *Environmental measures*

Since 1958, annual mean SST in the North Sea demonstrates an increasing trend which is most pronounced during the late 1980s, and continues through to the present (Fig. 3) (Edwards et al. 2002). Across the North Sea, mean SST increased an average of 0.48 °C per decade between the 1960s and 1990s; locally, the increase was greatest in the southern North Sea waters (0.75°C) and least in the northern North Sea (0.18°C). The increasing trend in SST is related to changes in the NAO (Ottersen et al. 2001). During the 1950s and 1960s the NAO was in a negative period, but since 1972 has been in its longest ever positive phase, reaching its highest recorded value in 1989. The phytoplankton growing season has been lengthened by the resulting warmer SST in the North Sea (Reid et al. 1998).

Secchi depth data ( $n = 5057$ ) showed that, after a major decline during the early 1970s, water transparency in coastal North Sea waters has been improving (Fig. 3). Improvement during both summer and winter has been greatest since the mid seventies, with a mean summer Secchi depth of 2.6 m and a mean winter depth of 1.8 m during the 1975-1979 period in contrast to a summer mean of 6.1m and a winter mean of 5.7 m between 1991 and 1995.

Inflow of oceanic waters to the North Sea from the Atlantic Ocean displayed an increasing trend throughout the 1960s and early 1970s before decreasing from 1976 through 1980 (Fig. 3). During the early and mid 1980s inflow continued to increase, reaching a maximum volume of more than 2.5 standard deviations above the mean in 1989. From 1988 to 1995, influx of Atlantic waters remained consistently above the long-term mean, although volume of inflow began to decline in 1990. Inflow is significantly positively correlated with the NAO ( $r = 0.63$ ,  $p < 0.001$ ) and SST ( $r = 0.32$ ,  $p = 0.035$ ) as well as significantly negatively correlated with Rhine ( $r = -0.32$ ,  $p = 0.03$ ) and Elbe ( $r = -0.42$ ,  $p < 0.001$ ) river discharge (Table 1 displays full details of correlation results).

Until 1974, wind stress in the North Sea was predominantly below average for the study period (Fig. 3). After 1974, wind stress began to show an increasing trend, and reached its highest value in 1990. Although, like Secchi depth, wind stress displays an overall increasing trend throughout the late 1970s and 1980s, only a weak negative relationship exists between the two variables (see Table 1). Wind stress is however strongly correlated with

Atlantic inflow ( $r = 0.70$ ,  $p < 0.001$ ) and NAO ( $r = 0.64$ ,  $p < 0.001$ ) but not with SST or precipitation.

Unlike SST, NAO, wind stress, Atlantic inflow and Secchi depth, precipitation did not show an increasing trend during the 1980s but instead showed considerable variability during that period (Fig. 3). Precipitation decreased during our period of study with the 1970s being the driest decade and the 1950s the wettest. Precipitation shows strong positive relationships with SST ( $r = 0.48$ ,  $p < 0.001$ ) and summer Secchi depth ( $r = 0.43$ ,  $p = 0.02$ ), but no other environmental variables considered in this study.

Sea level pressure (SLP) is variable throughout the entire time-series but shows a period of slight increase during the 1980s and early 1990s (Fig. 3). SLP is correlated only with winter Secchi depth ( $r = 0.47$ ,  $p = 0.03$ ).

When examining nutrient data from the coastal and open North Sea regions, it is clear that the coastal zone was much richer than the open North Sea in total nitrogen (TN) and total phosphorus (TP) (Fig. 4a). Significantly decreasing trends in annual mean TN ( $r^2 = 0.65$ ,  $p < 0.001$ ,  $n = 23$ ) and TP ( $r^2 = 0.57$ ,  $p < 0.001$ ,  $n = 23$ ) were observed in coastal North Sea waters, TN and TP following very similar patterns (but note the difference in scales), with visible peaks in the late-eighties followed by dramatic decreases in TN and TP from 1988 - 2002. These are general trends, observable for nutrients in the coastal North Sea as a whole, and may not reflect local variability. For example, when examined at a finer scale, nutrient concentrations showed a significantly decreasing trend in the Southern Bight area since 1980 (TN:  $r^2 = 0.57$ ,  $p < 0.001$ ,  $n = 23$ ; TP:  $r^2 = 0.74$ ,  $p < 0.001$ ,  $n = 23$ ), but although TP has been decreasing in Norwegian coastal waters ( $r^2 = 0.33$ ,  $p < 0.01$ ,  $n = 20$ ), TN displays an increasing trend in that area ( $r^2 = 0.38$ ,  $p = 0.01$ ,  $n = 17$ ). However, because the concentrations of both TN and TP in the Southern Bight are up to 10 times richer than those in Norwegian coastal waters (data not shown), the general decreasing nutrient trends observable for the coastal North Sea as a whole are heavily weighted by nutrient dynamics occurring in the Southern Bight.

The open North Sea time-series of both nutrients have a much narrower range than their coastal counterparts; although the open North Sea lacks adequate data to distinguish any trend, there is no indication at all of a temporal change in nutrient levels. As the

concentrations of TN and TP decreased in coastal North Sea waters, the molar ratio of N:P rose far above the Redfield ratio of 16:1, the molecular ratio at which diatoms require the two elements (Redfield et al. 1963). The N:P ratio continued to increase in coastal waters (Fig. 4c), while in the open North Sea N:P remained below Redfield. Nutrient concentrations in coastal waters are negatively correlated to SST (TN coast:  $r = -0.59$ ,  $p < 0.001$ ; TP coast:  $r = -0.53$ ,  $p = 0.01$ ) while N:P in coastal waters is positively to correlated to SST ( $r = 0.61$ ,  $p < 0.001$ ). Possibly due to lack of nutrient data, open North Sea nutrients and N:P show no significant relationship with SST or any other environmental variable.

Since the start of our time-series in 1982 annual mean nutrient concentrations have decreased in both the Elbe (TN:  $r^2 = 0.94$ ,  $p < 0.001$ ,  $n = 21$ ; TP:  $r^2 = 0.71$ ,  $p < 0.001$ ,  $n = 21$ ) and Rhine rivers (TN:  $r^2 = 0.84$ ,  $p < 0.001$ ,  $n = 14$ ; TP:  $r^2 = 0.91$ ,  $p < 0.001$ ,  $n = 21$ ) (Fig. 4b). Data from the International Commission on the Protection of the Rhine indicate that Rhine TP has displayed a decreasing trend since 1973 and Rhine  $\text{NO}_3$  (data on Rhine TN was not available) increased steadily from 1954 before peaking in 1989 and declining thereafter (ICPR - International Commission for the Protection of the Rhine 2006). Similarly to coastal North Sea waters, the difference in scale between the concentration of TN and that of TP in the Elbe and Rhine rivers has caused an increase in the riverine N:P (Fig. 4d). Concentrations of TN and TP in Elbe and Rhine waters are strongly correlated with TN (Elbe TN:  $r = 0.76$ ,  $p < 0.001$ ; Rhine TN:  $r = 0.67$ ,  $p = 0.009$ ) and TP (Elbe TP:  $r = 0.56$ ,  $p = 0.012$ ; Rhine TP:  $r = 0.64$ ,  $p = 0.002$ ) concentrations in the coastal North Sea. Nutrient concentrations in both rivers demonstrate negative relationships with winter (Elbe TN:  $r = -0.64$ ,  $p = 0.01$ ; Elbe TP:  $r = -0.58$ ,  $p = 0.04$ ; Rhine TN:  $r = -0.72$ ,  $p = 0.02$ ; Rhine TP:  $r = -0.54$ ,  $p = 0.04$ ) and summer Secchi depth (Elbe TN:  $r = -0.63$ ,  $p = 0.01$ ; Elbe TP:  $r = -0.63$ ,  $p = 0.02$ ; Rhine TN:  $r = -0.42$ ,  $p = 0.23$ ; Rhine TP:  $r = -0.66$ ,  $p = 0.01$ ). SST is also negatively related to Elbe TN ( $r = -0.62$ ,  $p < 0.001$ ), Elbe TP ( $r = -0.62$ ,  $p < 0.001$ ), Rhine TN ( $r = -0.21$ ,  $p = 0.47$ ) and Rhine TP ( $r = -0.64$ ,  $p < 0.001$ ). Note that the correlations between Rhine TN and summer Secchi depth and SST are not statistically significant (Table 1); this may be due to the short time-series of Rhine TN (Fig. 4b). Furthermore, data for the Elbe river indicated no significant change in annual quantity of water discharged into the North Sea between 1948 and 2001, while output from the Rhine increased slightly ( $r^2 = 0.09$ ,  $p < 0.05$ ,  $n = 54$ ) (Fig. 5). Additional analysis also revealed that there has been no seasonal change in discharge pattern for either river. Thus, the absence of change in quantity of river discharge in conjunction with the decline in

riverine nutrients indicate that the Elbe and Rhine rivers have reduced their input of nutrients to North Sea waters.

In general, coastal North Sea and riverine nutrient concentrations, have been decreasing since the early 1980s, while open North Sea nutrient concentrations show no clear trend. Since the early 1980s, SST, Secchi depth, wind stress and Atlantic inflow have also displayed decreasing trends, while precipitation and SLP remain variable.

#### *Phytoplankton production data*

The newly created Chl-a time-series shows considerable variability in both the open and coastal North Sea until the mid-1980s when a rapid increase in Chl-a began to occur (Fig. 6). This increase resulted in a chlorophyll peak in 1989, observable in both the coastal ( $3.92 \text{ mg m}^{-3}$ ) and open ( $3.15 \text{ mg m}^{-3}$ ) North Sea. After 1990, the coastal and open North Sea have both sustained Chl-a concentrations well above those maintained before the regime shift rather than returning to pre-phase shift levels (Fig. 6). As mentioned earlier, this pattern of change for the North Sea as a whole has been observed and described as a regime shift (Reid et al. 1998). The changes in Chl-a observed in coastal waters have occurred throughout the coastal North Sea. The regime shift and subsequent increased level of Chl-a are visible in the northern ( $> 58^\circ$  latitude), central ( $55^\circ - 58^\circ$  latitude), and southern ( $< 55^\circ$  latitude) coastal regions of the North Sea (Figs. 7a-c). SST is significantly correlated with both open Chl-a ( $r = 0.32, p < 0.05$ ) and coastal Chl-a ( $r = 0.42, p < 0.01$ ). Also, winter NAO is significantly correlated with Chl-a in the open North Sea ( $r = 0.28, p = 0.036$ ) but not with coastal Chl-a. Wind stress, however, is significantly positively correlated with both open Chl-a ( $r = 0.30, p = 0.03$ ) and coastal Chl-a ( $r = 0.26, p = 0.05$ ). Coastal Chl-a also has a strong significant relationship with winter Secchi depth ( $r = 0.63, p = 0.002$ ) while open Chl-a is positively correlated with Atlantic inflow ( $r = 0.36, p = 0.01$ ). Most interestingly, coastal Chl-a was found to have a significant negative relationship with both TN ( $r = -0.65, p = 0.001$ ) and TP ( $r = -0.45, p = 0.029$ ) in coastal waters but an insignificant relationship with molar N:P ( $r = 0.27, p = 0.216$ ). In addition to nutrients in coastal waters, Coastal Chl-a is negatively correlated with riverine nutrients as well (Elbe TN:  $r = -0.69, p < 0.001$ ; Elbe TP:  $r = -0.84, p < 0.001$ ; Rhine TN:  $r = -0.36, p < 0.21$ ; and Rhine TP:  $r = -0.77, p < 0.001$ ). Notice that the correlation between coastal Chl-a and Rhine TN is not statistically significant; again this may be due to the short time-series of Rhine TN.

Separate multiple linear regression analyses were performed on the coastal and open Chl-a datasets. In the coastal North Sea model, winter Secchi depth (standardized regression coefficient,  $\beta$ , = 0.564,  $p$  = 0.017) and SST ( $\beta$  = 0.455,  $p$  = 0.045) were the most important predictors of Chl-a ( $r^2$  = 0.51,  $p$  = 0.015,  $n$  = 15) while in the open North Sea model no significant predictor was identified. Although no variable was significant when performing the multiple linear regression on the open North Sea, the exclusion of nutrients (due to their short time-series,  $n$  = 12) showed that Atlantic inflow ( $\beta$  = 0.364,  $p$  = 0.14) is the best predictor of Chl-a in the open North Sea ( $r^2$  = 0.112,  $p$  = 0.014,  $n$  = 45). Neither model featured nutrients (TN, TP, or N:P) as significant predictors of Chl-a.

In summary, Chl-a across the entire North Sea displayed a rapid increase since the mid 1980s, culminating in the regime shift peak in 1989. After 1989, Chl-a concentrations remain higher than in the pre-regime shift period in both the open and coastal North Sea. Our results indicate that coastal Chl-a is strongly negatively correlated with coastal nutrient concentrations, but positively correlated with winter Secchi depth and SST. Open North Sea Chl-a shows no significant relationship with nutrients and is most closely correlated with Atlantic inflow, wind stress and SST.

## Discussion

It is well documented that in 1989 the North Sea experienced a strong peak in phytoplankton abundance (Reid et al. 1998) that has been correlated with warmer than average SST, a positive phase in the NAO and increased oceanic inflow from the North Atlantic (Beaugrand 2004). This same peak, preceded by a stepwise increase in Chl-a, can be clearly observed in the new coastal and open North Sea Chl-a time-series (Fig. 6). The rapid increase in Chl-a beginning during the mid-1980s and peaking in 1989 are part of what is now thought to be a regime shift, a stepwise modification in the composition and productivity of an entire ecosystem at a regional scale, reflecting substantial hydrographic change (Beaugrand 2004; Reid et al. 2001). At that point, the system converted to an alternate resilient state. As this sequence of events is non-linear, a reduction of pressures on the system does not necessarily mean that the system will recover to a previous alternate state (Scheffer et al. 2001), a clear example of hysteresis.

Because riverine input is the primary vector through which anthropogenic nutrients enter the North Sea, nutrient concentrations in coastal North Sea waters are fundamentally linked to riverine nutrient concentrations and discharge (de Vries et al. 1998; van Bennekom and Wetsteijn 1990). Nutrient concentration data from the Elbe and Rhine rivers, important sources of nutrients to coastal waters, demonstrated a significant decrease in TN and TP since the early 1980s, while quantity of water discharged changed little (Figs. 4b, 4d, 5). This suggests that the decreased anthropogenic nutrient loads to the North Sea have not occurred due to decreased river discharge but more likely due to declining riverine nutrient levels. This is further supported by the positive correlations between riverine nutrients and coastal nutrient concentrations and negative relationship between riverine nutrients and coastal Chl-a as well as the lack of relationships between coastal Chl-a and Elbe and Rhine discharge (Table 1). Surprisingly, Elbe and Rhine discharge do not appear to be related to precipitation. This could be because our precipitation data is for the North Sea itself and not the river catchments. However, Elbe discharge is significantly negatively related to SST ( $r = -0.32$ ,  $p = 0.02$ ), although Rhine discharge is not ( $r = -0.18$ ,  $p = 0.19$ ).

The declining riverine nutrient load is reflected in the decreasing nutrient concentrations observed in coastal waters and causing the current regime in the North Sea to be lower in coastal nutrient concentrations than the previous regime. Decadal means of TP

and TN in coastal waters were nearly 50% higher in the 1980s (TN = 110.48  $\mu\text{Mol l}^{-1}$ , TP = 3.43  $\mu\text{Mol l}^{-1}$ ) compared to the post-regime shift 1990s (TN = 56.03  $\mu\text{Mol l}^{-1}$ , TP = 1.97  $\mu\text{Mol l}^{-1}$ ). Other workers have also observed declining concentrations of phosphorus (de Vries et al. 1998; Hickel 1998; Nixon et al. 2003; OSPAR Commission 2000) and, to a lesser extent, nitrogen (de Vries et al. 1998; Nixon et al. 2003) in areas of the coastal North Sea in recent years. Agriculture is currently the main anthropogenic contributor of both N (63%) and P (45%) to North Sea waters (Anonymous 2005; Nixon et al. 2003). Since 1985, pollution from agricultural nitrates has been reduced by 21% (Nixon et al. 2003); part of this reduction can be attributed to the Nitrates Directive which was adopted by the EU in 1991 (European Union 1991a). Since 1985, agricultural P has been reduced by just 5% (Nixon et al. 2003). In 1991 the EU also implemented the Urban Waster Water Treatment Directive (European Union 1991b). This directive has been partially responsible for the 42% decrease of N and the 78% decrease of P from urban waste water treatment works since 1980 (Nixon et al. 2003). Since 1985 there have also been significant reductions in N and P loads from industry (81% P reduction, 79% N reduction) and other sectors (62% P reduction, 43% N reduction) (Nixon et al. 2003).

As concentrations of TN and TP have decreased, the molar ratio between N and P has steadily increased in coastal (Fig. 4c) and riverine (Fig. 4d) waters; the change in N:P is potentially an artifact of this similar rate of decline in the two contrasting scales of concentrations. Since 1983, N:P has remained above the Redfield ratio of 16:1 in the coastal North Sea while in the open North Sea, the ratio has stayed consistently below Redfield. Throughout our time-series, both Elbe and Rhine waters have had an N:P greater than Redfield. Unlike the coastal North Sea, an increase in the N:P ratio is probably not observable for the open North Sea because a trend in nutrient concentrations cannot be found due to insufficient data (Fig. 4a). However, as nutrient concentrations in the open North Sea are predominantly influenced by natural variability and not anthropogenic (riverine) sources (Lenhart et al. 1997), we would not expect to see as rapid a change in nutrient concentrations for open waters as we see for coastal and riverine waters. Therefore as open North Sea nutrient concentrations change little, so does the N:P ratio. This suggests that P is presently the limiting nutrient in coastal North Sea waters while the open North Sea is N limited (Pätsch and Radach 1997). Studies in the Marsdiep (Philippart et al. 2000) and Helgoland (Hickel et al. 1992; Radach et al. 1990) have shown that a strong relationship exists between N:P and phytoplankton community composition, while laboratory experiments have demonstrated that



a high N:P creates favorable conditions for *Phaeocystis*, a harmful algal bloom (HAB) causing species (Riegman 1991). Thus, further investigation is needed to determine the effects of change in the N:P on the wider coastal phytoplankton community composition.

As consequence of the regime shift, biological changes to new alternate states are revealed in the new Chl-a datasets. The datasets are in good agreement with changes observed previously for the PCI (Reid et al. 2001) and then later confirmed and quantified based on the PCI/SeaWiFS relationship for the North Atlantic and North Sea as a whole (Raitsos et al. 2005). As mentioned previously, the regime shift is evident as a rapid increase followed by a consistently high level of Chl-a in both coastal and open North Sea waters, but these changes cannot be explained by nutrients alone as nutrient concentrations in the open North Sea have not changed significantly (Fig. 4a). Our multiple linear regression models confirm this as they too indicate that nutrients are not good predictors of Chl-a in either region of the North Sea. After the regime shift, neither coastal nor open North Sea Chl-a returned to its pre-regime shift level, but instead the time-series indicates that the current North Sea regime maintains an average Chl-a level 21% higher in the coastal zone and 13% higher in the open zone than that of the pre-1980 regime (Fig. 6). Additionally, Chl-a in coastal waters appears to be increasing still further, particularly in the southern North Sea. Post regime shift alterations to the North Sea ecology have also been observed, such as a change in the proportion of warm and cold water species of *Calanus* (Reid et al. 2003a), trophic mismatch due to changes in phenology (Edwards and Richardson 2004) and changes in distribution of horse mackerel (Reid et al. 2001). The current North Sea regime has fewer piscivorous top predators (Heath 2005; Reid and Edwards 2001), and a lower mean trophic level of fisheries landings (Pauly et al. 1998).

At a regional scale, the increase in coastal Chl-a appears to be most linear in the northern coastal North Sea; this may be a response to increased SST or changing environmental conditions. The southern coastal North Sea exhibits the most variability in Chl-a of the three regions. This is expected, as the southern North Sea is not only subject to greater anthropogenic stress (very high levels of nutrients, direct river input, etc) and therefore experiences more variability in nutrient concentrations and water clarity than the northern and central coastal regions, it is also more susceptible to climate variation than the other coastal regions due to its comparatively shallow waters (Edwards 2000). Finer scale climate and

environmental data are needed in order to perform a more in depth investigation into the exact causes of the regional variations in coastal North Sea Chl-a.

Although nutrient concentrations in the coastal North Sea have decreased significantly since the regime shift, algal biomass has continued to increase. The coincident decrease in nutrients and increase in Chl-a is surprising as traditionally, increases in plankton production are triggered by increasing nutrients and are a symptom of eutrophication (Cloern 2001; Nixon 1995). In fact, areas of the coastal North Sea are commonly considered to be eutrophic (Cadee 1986; de Jonge et al. 1996; de Jonge and Essink 1991; Hickel et al. 1993; Philippart et al. 2000; van Beusekom and de Jonge 2002) and eutrophication was identified as a key issue affecting the North Sea in the 1987 North Sea Quality Status Report (Reid and Edwards 2001).

While there is a strong relationship between algae and nutrients, it is considered to be non-linear in coastal North Sea waters (i.e. a reduction in nutrient load does not lead to an equivalent reduction of phytoplankton biomass) (Lenhart 2001). Furthermore, as North Sea nutrient concentrations have decreased, water transparency has improved (Fig. 3), allowing the light-limited coastal phytoplankton (Pätsch and Radach 1997) to make better use of available nutrients. A similar increase in phytoplankton biomass was also documented in the Scheldt estuary where the construction of a storm surge barrier caused reduced river flow with a corresponding increase in water transparency and decrease in nutrient concentrations (Westetyn and Kromkamp 1994). Improvement in water transparency has been observed in the Western Wadden Sea (de Jonge et al. 1996) and Marsdiep (Bot and Colijn 1996). Although the explanation behind the increase in North Sea water transparency is still unclear, it may be linked to the increased inflow of warm, clear, oceanic water entering the North Sea (Reid et al. 2003a). Additionally, multiple linear regression showed that Atlantic inflow is the best predictor of Chl-a in the open North Sea when nutrient data are excluded from the analysis. The transparency minima (Fig. 3) occurring during the mid to late 1970s is coincident with a period of reduced Atlantic inflow (Corten 1999) and low Chl-a values in both the open and coastal North Sea datasets (Fig. 6). This is in agreement with work performed by Edwards et al (2001) who also attributed low Phytoplankton Colour values in the late 1970s and early 1980s to a period of reduced Atlantic inflow. Additionally, the increasing water transparency that occurred throughout the 1980s and 1990s coincides with a proposed increase in Atlantic inflow during that period (Corten 1999; Edwards et al. 2002;

Edwards et al. 2001). The increase of indicator species with a southerly origin in the mid 1980s and sustained abundance thereafter in the North Sea (Corten 1999; Edwards et al. 2001), may indicate a change in current patterns, thereby increasing the volume of warm, clear, southerly water entering the North Sea from the North Atlantic (Edwards et al. 2001).

However, the reduction in turbidity alone does not seem to be enough to explain the increase in Chl-a, coincident with the decrease in nutrients. One possible explanation may be that after the regime shift, coastal waters have become more vulnerable to fluxes in nutrient concentrations. Because coastal phytoplankton are light limited, the cooler, more turbid state of the previous regime may have acted as a buffer, preventing algae from reaching the high biomass that is now possible. Multiple linear regression analysis supports this, indicating that while winter Secchi depth is the best single predictor of coastal Chl-a, it only explains 30% ( $p = 0.035$ ,  $n = 15$ ) of the variability. Together SST and winter Secchi depth form the best model, explaining 51% of the variation in coastal Chl-a. As mentioned previously, significant correlations exist between both open and coastal Chl-a and mean annual SST. This result is in agreement with the previously established positive relationship between Phytoplankton Colour and SST (Beaugrand and Reid 2003). The low Chl-a values occurring in the late 1970s (Fig. 6) and the exceptionally high Chl-a values observed in the late 1980s correspond to two hydroclimatic anomalies: the previously mentioned cold-boreal event in the late 1970s associated with lower than average SST and a warm-temperate event in the late 1990s associated with warmer than average SST (Edwards et al. 2002). Phytoplankton are closely linked to the temperature of their environment and respond to increased SST directly (physiologically), indirectly (enhanced or earlier stratification of the water column result in changes in phytoplankton succession) and phenologically (certain species are now experiencing earlier spring blooms) (Edwards and Richardson 2004; Richardson and Schoeman 2004). Additionally, warmer SST in the North Sea has created a longer growing season, thereby resulting in increased phytoplankton biomass, particularly during summer (Reid et al. 1998) and winter (Raitsos et al. 2005). The enhanced response by the algal community to changes in nutrients is a characteristic of the new alternate state of the North Sea and may have triggered the other documented changes to the pelagic system. If, due to increased SST and clearer water, coastal waters are indeed more sensitive to changes in nutrients, it is more important than ever that the quantity of anthropogenic nutrients entering the North Sea is reduced.

Alternatively, or additionally, to bottom-up (resource limited) control, it is also important to consider the top-down (consumer regulated) control of phytoplankton biomass. Fishing is an important industry in the North Sea and the last few decades have seen changes in the catch of the top predators such as cod, haddock, and mackerel (Heath 2005; Reid and Edwards 2001). The decrease in piscivorous predators and the subsequent dominance of planktivorous fishes (sprat, sandeel, herring, and Norway pout) in the North Sea indicate that we are fishing down the food web (Heath 2005; Pauly et al. 1998). In theory, the resulting trophic cascade may have increased the consumption of zooplankton (Heath 2005) and therefore may also effect a subsequent lessening of grazing pressure on phytoplankton leading to an increase in algal biomass (Reid et al. 2000). However, data suggest that the top-down control of North Sea phytoplankton is only important during times of ecosystem stress (Reid et al. 2000; Riegman 1995). Additionally, Richardson and Schoeman (2004) suggest that bottom up control dominates the North Sea plankton community. More research is needed to further quantify the importance of top down control on North Sea phytoplankton biomass.

We suggest changes in large-scale climatological forcing (possibly exacerbated by anthropogenic pressures such as overfishing) gradually eroded the resilience of the North Sea system until a critical threshold was reached. The North Sea is now in an alternate state with its own characteristic ecological and environmental features. The present regime, though lower in nutrient concentrations, maintains a higher (and possibly still increasing) Chl-a level in both coastal and open North Sea waters, this level of phytoplankton biomass in North Sea waters being more closely related to climatic variability and water transparency than nutrient concentrations.

---

**References**

- Aarup, T. 2002. Transparency of the North Sea and Baltic Sea - a Secchi Depth data mining study. *Oceanologia* **44**: 323-337.
- Alheit, J., C. Møllmann, J. Dutz, G. Kornilovs, P. Loewe, V. Mohrholz, and N. Wasmund. 2005. Synchronous ecological regime shifts in the central Baltic and the North Sea in the late 1980s. *ICES J Mar Sci* **62**: 1205-1215.
- Anonymous. 2005. Source apportionment of nitrogen and phosphorus inputs into the aquatic environment, p. 48. European Environment Agency.
- Batten, S. D., A. W. Walne, M. Edwards, and S. B. Groom. 2003. Phytoplankton biomass from continuous plankton recorder data: An assessment of the phytoplankton colour index. *J Plankton Res* **25**: 697-702.
- Beaugrand, G. 2004. The North Sea regime shift: Evidence, causes, mechanisms and consequences. *Prog Oceanogr* **60**: 245-262.
- Beaugrand, G., and P. C. Reid. 2003. Long-term changes in phytoplankton, zooplankton and salmon related to climate. *Global Change Biology* **9**: 801-817.
- Bot, P. V. M., and F. Colijn. 1996. A method for estimating primary production from chlorophyll concentrations with results showing trends in the Irish Sea and the Dutch coastal zone. *ICES J Mar Sci* **53**: 945-950.
- Cadee, G. C. 1986. Increased phytoplankton primary production in the Marsdiep area (western Dutch Wadden Sea). *Neth. J. Sea Res.* **29**: 285 - 290.
- Clark, R. A., and C. L. J. Frid. 2001. Long-term changes in the North Sea ecosystem. *Environmental Reviews* **9**: 131-187.
- Cloern, J. E. 2001. Our evolving conceptual model of the coastal eutrophication problem. *Mar Ecol Prog Ser* **210**: 223-253.
- Colebrook, J. M., and G. A. Robinson. 1965. Continuous plankton records: seasonal cycles of phytoplankton and copepods in the north-eastern Atlantic and North Sea. *PSZN I: Mar Ecol* **6**: 123-139.
- Corten, A. 1999. Evidence from plankton for multi-annual variations of Atlantic inflow in the northwestern North Sea. *J Sea Res* **42**: 191-205.
- de Jonge, V. N., J. F. Bakker, and M. van Stralen. 1996. Recent changes in the contributions of river Rhine and North Sea to the eutrophication of the western Dutch Wadden Sea. *Aquat Ecol* **30**: 27-39.

- de Jonge, V. N., and K. Essink. 1991. Long-term changes in nutrient loads and primary and secondary producers in the Dutch Wadden Sea. *In* M. E. a. J. P. Ducrotoy [ed.], *Estuaries and Coasts: Spatial and Temporal Intercomparisons*. Olsen and Olsen.
- de Vries, I., R. N. M. Duin, J. C. H. Peeters, F. J. Los, M. Bokhorst, and R. W. P. M. Laane. 1998. Patterns and trends in nutrients and phytoplankton in Dutch coastal waters: comparison of time-series analysis, ecological model simulation, and mesocosm experiments. *ICES J Mar Sci* **55**: 620-634.
- Edwards, M. 2000. Large-scale temporal and spatial patterns of marine phytoplankton and climate variability in the North Atlantic. PhD dissertation. University of Plymouth.
- Edwards, M., G. Beaugrand, P. C. Reid, A. A. Rowden, and M. B. Jones. 2002. Ocean climate anomalies and the ecology of the North Sea. *Mar Ecol Prog Ser* **239**: 1-10.
- Edwards, M., P. Reid, and B. Planque. 2001. Long-term and regional variability of phytoplankton biomass in the Northeast Atlantic (1960-1995). *ICES J Mar Sci* **58**: 39-49.
- Edwards, M., and A. J. Richardson. 2004. Impact of climate change on marine pelagic phenology and trophic mismatch. *Nature* **430**: 881-884.
- European Union. 1991a. Nitrates Directive. Directive 91/676/EEC.
- . 1991b. Urban Waste Water Treatment Directive. Directive 91/271/EEC.
- Global Runoff Data Centre. 2005. Rhine River Discharge Data. Global Runoff Data Centre, D - 56002 Koblenz, Germany.
- Hays, G. C., A. J. Richardson, and C. Robinson. 2005. Climate change and marine plankton. *Trends Ecol Evol* **20**: 337-344.
- Heath, M. R. 2005. Changes in the structure and function of the North Sea fish foodweb, 1973-2000, and the impacts of fishing and climate. *ICES J Mar Sci* **62**: 847-868.
- Hickel, W. 1998. Temporal variability of micro- and nanoplankton in the German Bight in relation to hydrographic structure and nutrient changes. *ICES J Mar Sci* **55**: 600-609.
- Hickel, W., J. Berg, and K. Treutner. 1992. Variability in phytoplankton biomass in the German Bight near Helgoland, 1980-1990. *ICES Mar Sci Symp* **195**: 249-259.
- Hickel, W., P. Mangelsdorf, and J. Berg. 1993. The Human Impact in the German Bight - Eutrophication During 3 Decades (1962-1991). *Helgol Meeresunters* **47**: 243-263.
- Hurrell, J. W. 1995. Decadal trends in the North Atlantic Oscillation: regional temperatures and precipitation. *Science* **169**: 676-679.
- ICPR - International Commission for the Protection of the Rhine. 2006. Water Quality Data. ICPR.

- IOCCG. 2000. Remote sensing of ocean color in coastal, and other optically complex waters. In S. Sathyendranath [ed.], Reports of the International Ocean-Color Coordinating Group, No. 3.
- Iversen, S. A., M. D. Skogen, and E. Svendsen. 2002. Availability of horse mackerel (*Trachurus trachurus*) in the north-eastern North Sea, predicted by the transport of Atlantic water. *Fish Oceanogr* **11**: 245-250.
- Lenhart, H. J. 2001. Effects of river nutrient load reduction on the eutrophication of the North Sea, simulated with the ecosystem model ERSEM. *Senckenb Marit* **31**: 299-311.
- Lenhart, H. J., G. Radach, and P. Ruardij. 1997. The effects of river input on the ecosystem dynamics in the continental coastal zone of the North Sea using ERSEM. *J Sea Res* **38**: 249-274.
- Lindley, J. A., J. Roskell, A. J. Warner, N. C. Halliday, H. G. Hunt, A. W. G. John, and T. B. Jonas. 1990. Doloids in the German Bight in 1989: evidence for exceptional inflow into the North Sea. *J Mar Biol Ass U K* **70**: 679-702.
- Mueller, J. L., and R. W. Austin. 1995. Ocean optics protocols for SeaWiFS validation, revision 1. NASA Technical Memorandum - SeaWiFS Technical Report Series **25**.
- Nixon, S. W. 1995. Coastal marine eutrophication: A definition, social causes and future concerns. *Ophelia* **41**: 199-219.
- Nixon, S. W., Z. Trent, C. Marcuello, and C. Lallana. 2003. Europe's water: an indicator-based assessment, p. 97. European Environment Agency.
- O'Reilly, J. E., S. Maritorena, B. G. Mitchell, D. A. Siegel, K. L. Carder, S. A. Garver, M. Kahru, and C. McClain. 1998. Ocean color chlorophyll algorithms for SeaWiFS. *J Geophys Res C* **103**.
- OSPAR Commission. 2000. Quality Status Report 2000, p. 136 + xiii. OSPAR Commission.
- Ottersen, G., B. Planque, A. Belgrano, E. Post, P. C. Reid, and N. C. Stenseth. 2001. Ecological effects of the North Atlantic Oscillation. *Oecologia* **128**: 1-14.
- Paerl, H. W., L. M. Valdes, J. L. Pinckney, M. F. Piehler, J. Dyble, and P. H. Moisander. 2003. Phytoplankton photopigments as indicators of estuarine and coastal eutrophication. *BioScience* **53**: 953-964.
- Pätsch, J., and G. Radach. 1997. Long-term simulation of the eutrophication of the North Sea: Temporal development of nutrients, chlorophyll and primary production in comparison to observations. *J Sea Res* **38**: 275-310.
- Pauly, D., V. Christensen, J. Dalsgaard, R. Froese, and F. J. Torres. 1998. Fishing down marine food webs. *Science* **279**: 860 - 863.

- Philippart, C. J. M., G. C. Cadee, W. Van Raaphorst, and R. Riegman. 2000. Long-term phytoplankton-nutrient interactions in a shallow coastal sea: Algal community structure, nutrient budgets, and denitrification potential. *Limnol Oceanogr* **45**: 131-144.
- Pickard, G. L., and S. Pond. 1978. *Introductory Dynamic Oceanography*, 2nd edition ed. Pergamon Press.
- Radach, G., J. Berg, and E. Hagmeier. 1990. Long-term changes of the annual cycles of meteorological, hydrographic, nutrient and phytoplankton time-series at Helgoland and at Lv Elbe 1 in the German Bight. *Cont Shelf Res* **10**: 305-328.
- Raitsos, D. E., S. J. Lavender, Y. Pradham, T. Tyrell, P. Reid, and M. Edwards. 2006. Coccolithophore bloom size variation in response to the regional environment of the subarctic North Atlantic. *Limnol Oceanogr* **in press**.
- Raitsos, D. E., P. C. Reid, S. J. Lavender, M. Edwards, and A. J. Richardson. 2005. Extending the SeaWiFS chlorophyll data set back 50 years in the northeast Atlantic. *Geophys Res Lett* **32**.
- Redfield, A. C., B. H. Ketchum, and F. A. Richards. 1963. The influence of organisms on the composition of sea water, p. 26-77. *In* M. N. Hill [ed.], *The Sea*. John Wiley.
- Reid, P. C., E. J. V. Battle, S. D. Batten, and K. M. Brander. 2000. Impacts of fisheries on plankton community structure. *ICES J Mar Sci* **57**: 495-502.
- Reid, P. C., M. De Fatima Borges, and E. Svendsen. 2001. A regime shift in the North Sea circa 1988 linked to changes in the North Sea horse mackerel fishery. *Fish Res* **50**: 163-171.
- Reid, P. C., and M. Edwards. 2001. Long-term changes in the pelagos, benthos and fisheries of the North Sea. *Senckenb Marit* **31**: 107-115.
- Reid, P. C., M. Edwards, G. Beaugrand, M. Skogen, and D. Stevens. 2003a. Periodic changes in the zooplankton of the North Sea during the twentieth century linked to oceanic inflow. *Fish Oceanogr* **12**: 160-169.
- Reid, P. C., M. Edwards, H. G. Hunt, and A. J. Warner. 1998. Phytoplankton change in the North Atlantic. *Nature* **391**: 546.
- Reid, P. C., J. B. L. Matthews, and E. M. A. Smith. 2003b. Achievements of the Continuous Plankton Recorder survey and a vision for its future. *Prog Oceanogr* **58**: 115-358.
- Richardson, A., and D. S. Schoeman. 2004. Climate impact on planktonic ecosystems in the Northeast Atlantic. *Science*.



- Riegman, R. 1991. Mechanisms behind eutrophication induced novel algal blooms, p. 52. Nederlands Inst. voor Onderzoek der Zee.
- . 1995. Nutrient-related selection mechanisms in marine phytoplankton communities and the impact of eutrophication on the planktonic food web. *Water Sci Technol* **32**: 63-75.
- Sanden, P., and B. Hakansson. 1996. Long-term trends in Secchi depth in the Baltic Sea. *Limnol Oceanogr* **41**: 346-351.
- Scheffer, M., S. Carpenter, J. A. Foley, C. Folke, and B. Walker. 2001. Catastrophic shifts in ecosystems. *Nature* **413**: 591-596.
- van Bennekom, A. J., and F. J. Wetsteijn. 1990. The winter distribution of nutrients in the Southern Bight of the North Sea (1961-1978) and in the estuaries of the Scheldt and the Rhine/Meuse. *Neth. J. Sea Res.* **25**: 75-87.
- van Beusekom, J., and V. de Jonge. 2002. Long-term changes in Wadden Sea nutrient cycles: importance of organic matter import from the North Sea. *Hydrobiologia* **475**: 185-194.
- Weijerman, M., H. Lindeboom, and A. F. Zuur. 2005. Regime shifts in marine ecosystems of the North Sea and Wadden Sea. *Mar Ecol Prog Ser* **298**: 21-39.
- Westetyn, L. P. M. J., and J. C. Kromkamp. 1994. Turbidity, nutrients and phytoplankton primary production in the Oosterschelde (The Netherlands) before, during and after a large-scale coastal engineering project (1980-1990). *Hydrobiologia* **282-283**: 61-78.
- Zar, J. H. 1984. *Biostatistical Analysis*, 2nd ed. Prentice-Hall.

**Table 1.** Results of correlation analysis between the coastal and open Chl-a time-series and climatic and environmental variables. Significant ( $p < 0.05$ ) results are in bold.

	open	coast	coast	coast	coast	open	open	open	Flow	Flow	TN	TP	N:P	TN	TP	N:P	NAO	SST	Inflow	Secchi	Secchi	taion	Stress
Chl-a coast	<b>0.74</b>																						
TN coast	-0.25	<b>-0.65</b>																					
TP coast	-0.08	<b>-0.45</b>	<b>0.80</b>																				
N:P coast	0.07	0.27	<b>-0.63</b>	<b>-0.65</b>																			
TN open	-0.16	-0.18	0.51	-0.01	<b>-0.42</b>																		
TP open	-0.09	0.38	-0.22	-0.34	0.03	0.10																	
N:P open	0.00	-0.03	-0.21	0.06	0.34	<b>-0.55</b>	0.05																
Elbe Flow	-0.06	-0.12	<b>0.43</b>	<b>0.59</b>	-0.33	0.12	0.24	<b>0.48</b>															
Rhine Flow	0.15	0.12	0.34	0.23	0.06	0.33	0.05	0.35	<b>0.71</b>														
Elbe TN	-0.22	<b>-0.69</b>	<b>0.76</b>	<b>0.73</b>	<b>-0.58</b>	0.22	-0.26	-0.34	0.10	-0.02													
Elbe TP	<b>-0.75</b>	<b>-0.84</b>	<b>0.63</b>	<b>0.56</b>	-0.44	0.12	-0.37	-0.32	-0.21	-0.15	<b>0.93</b>												
Elbe N:P	<b>0.70</b>	<b>0.77</b>	<b>-0.50</b>	-0.41	0.37	-0.18	0.46	0.35	0.43	0.27	<b>-0.79</b>	<b>-0.93</b>											
Rhine TN	0.36	-0.36	<b>0.67</b>	<b>0.68</b>	-0.39	0.19	-0.16	-0.37	-0.14	-0.47	<b>0.90</b>	<b>0.71</b>	-0.46										
Rhine TP	-0.30	<b>-0.77</b>	<b>0.76</b>	<b>0.64</b>	<b>-0.52</b>	0.28	-0.31	-0.28	0.08	0.01	<b>0.97</b>	<b>0.94</b>	<b>-0.82</b>	<b>0.88</b>									
Rhine N:P	-0.29	0.07	<b>-0.55</b>	<b>-0.61</b>	0.27	-0.34	-0.01	0.38	0.26	0.47	<b>-0.72</b>	<b>-0.62</b>	0.48	<b>-0.56</b>	<b>-0.87</b>								
Winter NAO	<b>0.28</b>	0.15	0.13	0.01	0.04	0.00	-0.17	-0.19	-0.16	-0.03	0.11	0.07	-0.11	<b>0.54</b>	0.11	<b>-0.52</b>							
SST	<b>0.32</b>	<b>0.42</b>	<b>-0.59</b>	<b>-0.53</b>	<b>0.61</b>	-0.25	-0.10	-0.08	<b>-0.32</b>	-0.18	<b>-0.62</b>	<b>-0.62</b>	0.54	-0.21	<b>-0.64</b>	0.16	<b>0.50</b>						

*Appendix I*

Inflow	<b>0.36</b>	0.22	-0.01	-0.12	0.14	0.02	-0.19	-0.34	<b>-0.42</b>	<b>-0.32</b>	0.15	0.13	-0.28	<b>0.80</b>	0.13	<b>-0.73</b>	<b>0.63</b>	<b>0.31</b>					
Summer																							
Secchi	0.19	0.35	<b>-0.60</b>	<b>-0.44</b>	-0.09	-0.10	0.11	-0.11	-0.04	-0.06	<b>-0.63</b>	<b>-0.63</b>	<b>0.59</b>	-0.42	<b>-0.66</b>	0.47	-0.03	0.24	-0.16				
Winter																							
Secchi	0.27	<b>0.63</b>	<b>-0.55</b>	<b>-0.48</b>	-0.11	-0.10	0.36	-0.15	-0.17	-0.15	<b>-0.64</b>	<b>-0.58</b>	0.45	<b>-0.72</b>	<b>-0.54</b>	0.19	0.06	0.17	0.02	<b>0.53</b>			
Precipitation	-0.05	-0.09	-0.01	-0.04	0.17	-0.17	-0.49	-0.26	-0.19	-0.21	-0.05	-0.05	0.08	-0.15	-0.10	0.24	0.24	<b>0.48</b>	0.01	<b>0.43</b>	-0.08		
Wind																							
Stress	<b>0.30</b>	<b>0.26</b>	0.20	0.05	-0.12	0.28	0.03	-0.38	-0.11	-0.01	0.14	0.09	-0.13	<b>0.67</b>	0.09	<b>-0.57</b>	<b>0.64</b>	0.23	<b>0.70</b>	-0.18	-0.14	-0.02	
SLP	-0.11	0.12	0.07	0.18	-0.29	-0.06	0.32	-0.19	-0.21	<b>-0.40</b>	0.18	0.17	-0.19	0.16	0.14	-0.18	-0.15	0.01	-0.04	0.02	<b>0.47</b>	-0.08	-0.19

**Figure 1.** Location of coastal and open North Sea areas used in study overlain by CPR samples temporally corresponding with SeaWiFS chlorophyll measurements ( $n=3695$ ).

**Figure 2.** Equivalent SeaWiFS – PCI values for coastal and whole North Sea areas with 95% confident limits. This relationship was applied to the PCI dataset to extrapolate the new Chl-a time-series. The PCI is a ratio scale of Phytoplankton Colour with four 'greenness' values: 0 (NG - no greenness), 1 (VPG - very pale green), 2 (PG - pale green) and 6.5 (G - green). Note there is no overlap between confidence intervals for each PCI category.

**Figure 3.** Time-series of environmental variables with 5-year running means. With the exception of precipitation and sea level pressure, all of the environmental variables considered in this study demonstrated a rapidly increasing trend during the 1980s. SST and summer and winter Secchi depth continue to show increasing trends.

**Figure 4.** (a) Annual total nitrogen (TN) and total phosphorus (TP) concentrations in coastal and open North Sea waters and (b) Elbe and Rhine rivers during the period 1980 – 2002. Both datasets show similar decreasing trends in TN and TP in coastal North Sea and riverine waters, despite the differences in scale. As TN and TP concentrations decrease, the molar ratio of N to P is increasing in both (c) coastal North Sea and (d) Elbe and Rhine waters.

**Figure 5.** Annual mean discharge (1948 – 2001) of Elbe and Rhine rivers. There is no trend in Elbe discharge and a slight increase in Rhine discharge, indicating that the decrease in coastal nutrients can most likely be attributed to the decline in nutrient concentrations in both rivers rather than decreased discharge.

**Figure 6.** Time-series of the new Chl-a data set (annual means) for the period 1948 to 2003 in the coastal and open North Sea. The regime shift is evident as a rapid increase in Chl-a between 1982 and 1989 followed by mean annual Chl-a concentration that is consistently higher than that observed prior to the regime shift. Both open and coastal North Sea time-series show a higher level of Chl-a in the period after the regime shift than in the period before.

**Figure 7.** The regime shift and subsequently increased Chl-a level are observable in the northern (a), central (b), and southern (c) coastal regions of the North Sea.

Figure 1.

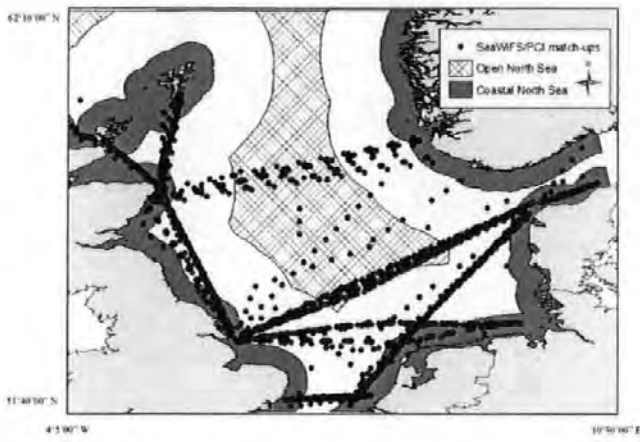


Figure 2.

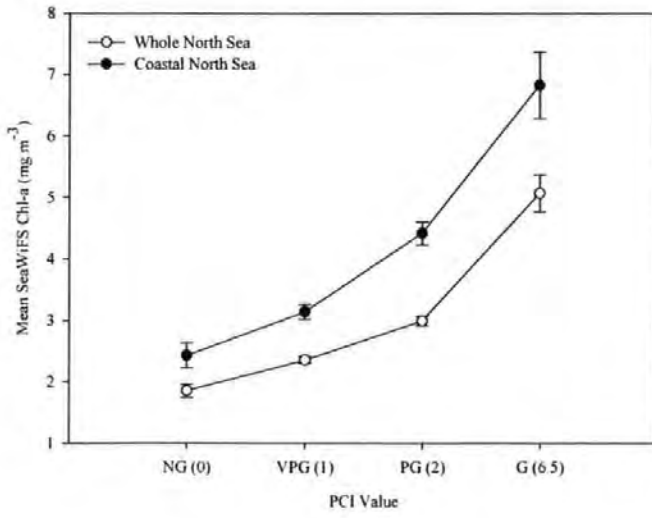


Figure 3.

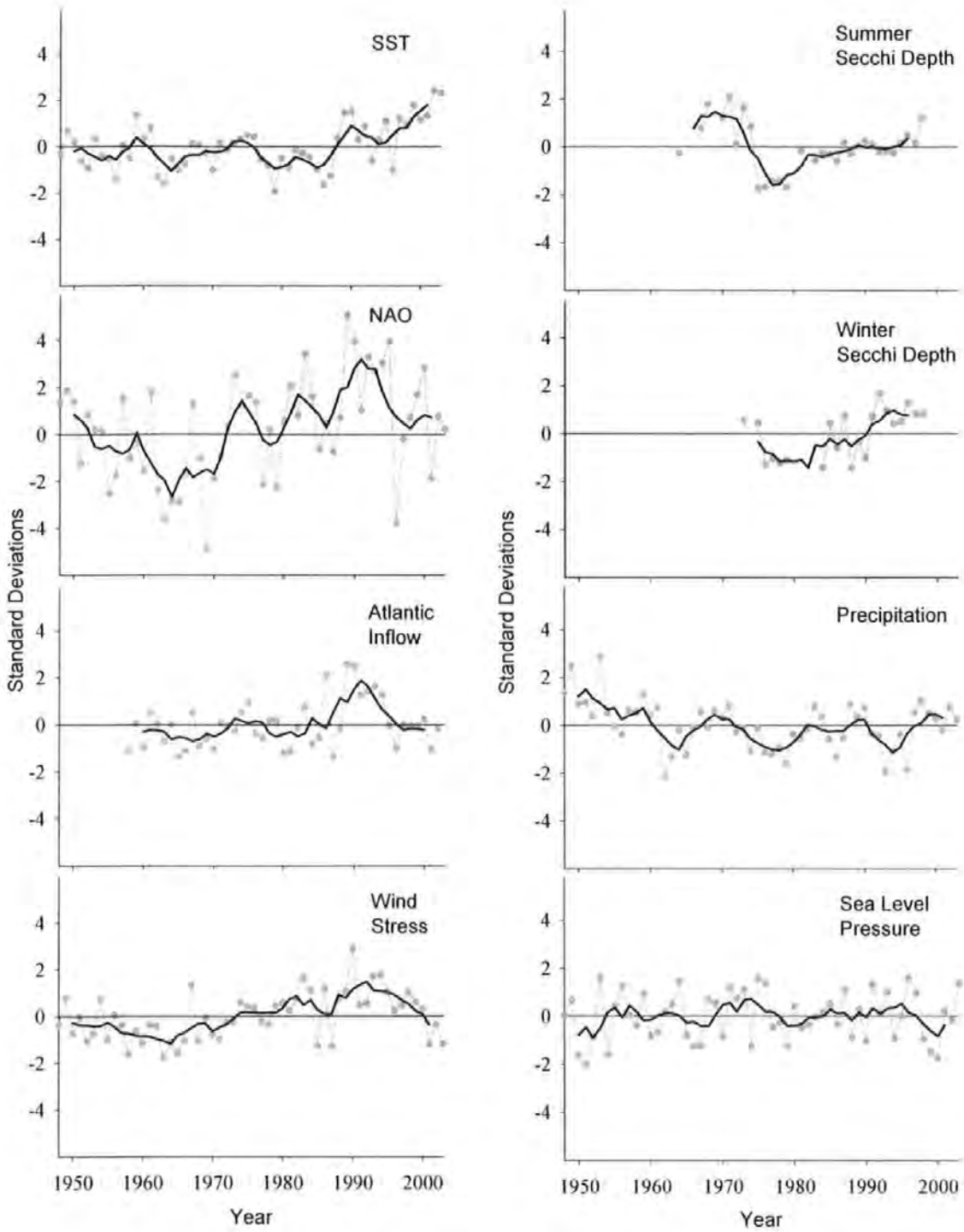




Figure 4.

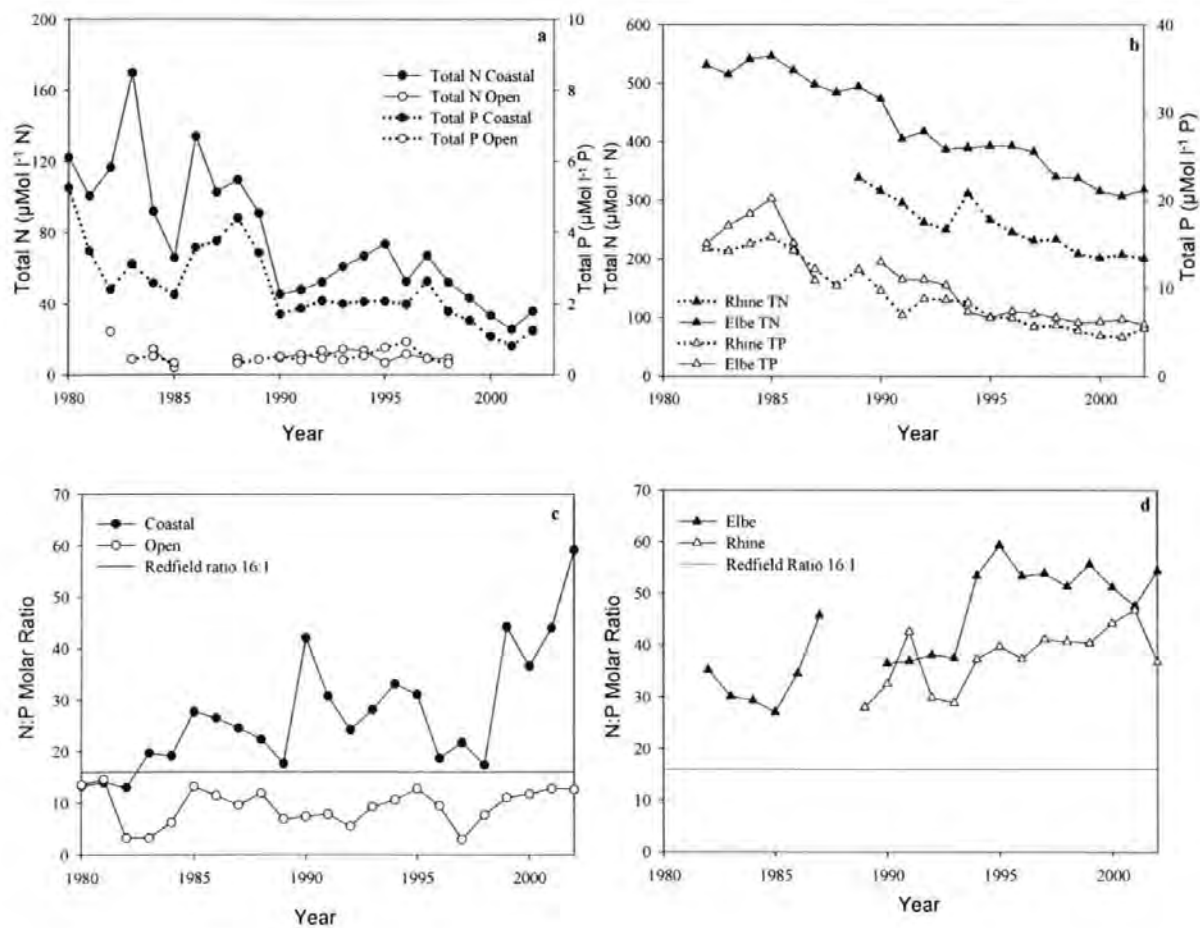


Figure 5.

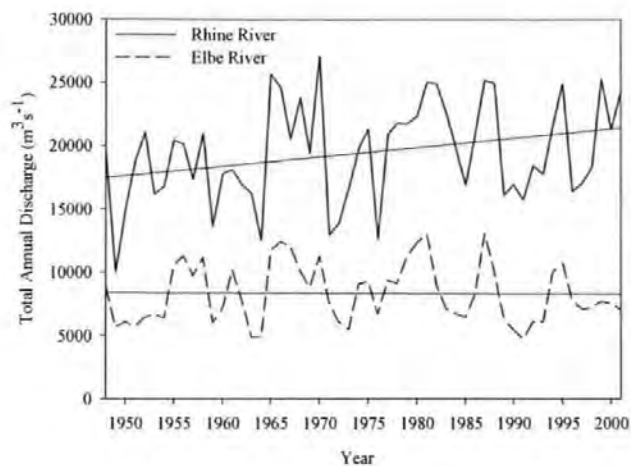


Figure 6.

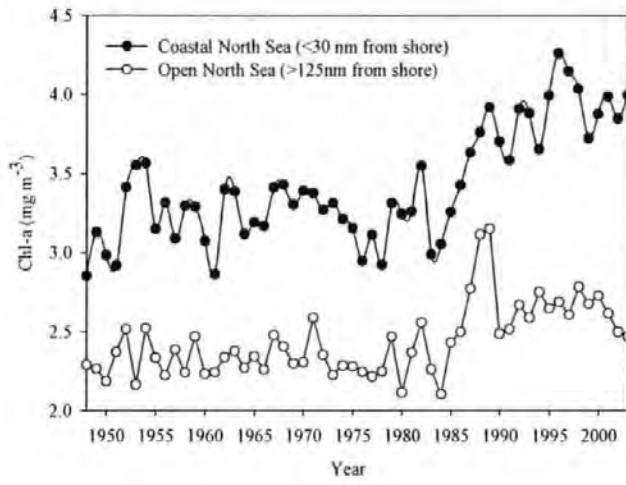
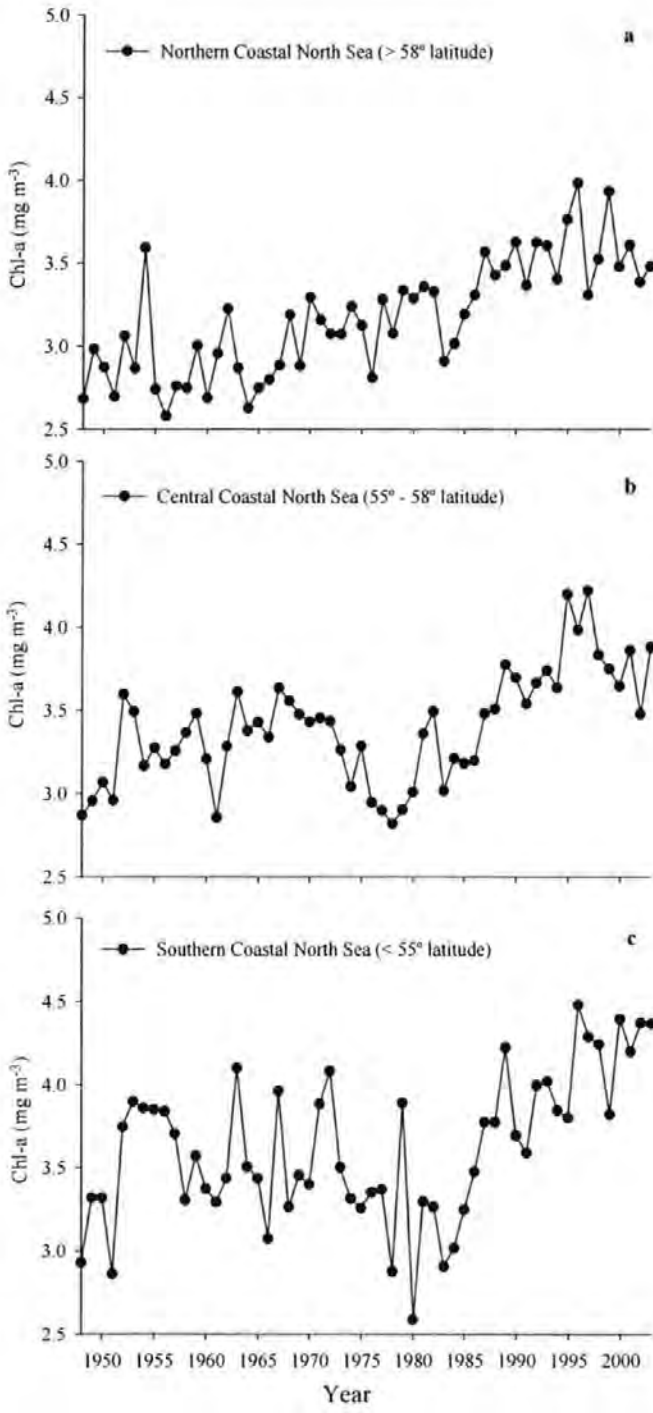


Figure 7.



## Spatial patterns of diatom and dinoflagellate seasonal cycles in the North – East Atlantic Ocean

Abigail McQuatters-Gollop<sup>1,2,3\*</sup>, Dionysios E. Raitsos<sup>1,2</sup>, Martin Edwards<sup>2</sup>, and  
Martin J. Attrill<sup>1</sup>

<sup>1</sup>Marine Institute, University of Plymouth, Drake Circus, Plymouth, PL4 8AA, United Kingdom

<sup>2</sup>Sir Alister Hardy Foundation for Ocean Science, The Laboratory, Citadel Hill, Plymouth, PL1 2PB, United Kingdom

\* E-mail: abigail.mcquatters-gollop@plymouth.ac.uk

### ABSTRACT

As the base of the marine food web, phytoplankton community composition significantly influences the pelagic ecosystem; thus the seasonal and spatial distribution of phytoplankton taxonomic groups is important to higher trophic levels. Within the phytoplankton, diatoms and dinoflagellates have diverse roles and different spatial patterns. Here we present spatial and temporal patterns of diatom and dinoflagellate seasonal cycles in the North-East Atlantic Ocean based on >100,000 Continuous Plankton Recorder (CPR) samples. This analysis is presented in the form of monthly composite maps of the spatial distribution of diatoms and dinoflagellates and their relative abundances from 1958 – 2003, whose unique monthly time scale allows the biogeographical exploration of seasonal cycle patterns for each group. The blooms of both phytoplankton functional groups commence in the North Sea and spread outward across the region. Diatoms exhibit a spring bloom, peaking in May, followed by an autumnal bloom during late summer. Dinoflagellates bloom in summer with a peak in August. The abundances of both groups are lowest during the winter months across the entire region, with the highest winter abundances occurring in the southern North Sea. These data are not available from remote sensing sources

and may be used for the validation of current models and research as well as coastal and resource management.

### **KEY WORDS**

North Atlantic phytoplankton, seasonal cycles, spatial patterns

### **RUNNING HEAD**

Phytoplankton seasonal cycles in north-east Atlantic

### **INTRODUCTION**

Variations in phytoplankton community composition impact the pelagic ecosystem through changes in trophic transfer efficiency (Nagata et al. 1996), food web structure and nutritional content provided to higher trophic levels (Pedersen et al. 1999). Diatoms and dinoflagellates play unique roles in ecosystem processes. Within the phytoplankton, diatoms form the base of the copepod-fish food web while the smaller, unpalatable, and less nutritious dinoflagellates are often considered trophic dead ends and can result in food webs culminating in non-fodder gelatinous organisms instead of fish (Verity & Smetacek 1996, Sommer et al. 2002). Thus the spatial distributions of diatoms and dinoflagellates, and their relative abundances, throughout the year may influence the seasonal distributions of higher trophic organisms.

Shifts in phytoplankton group dominance have been tentatively linked to causes such as eutrophication (Radach et al. 1990, Micheli 1999) and climate change (Bopp et al. 2005, Leterme et al. 2006). In order for these links to be confirmed and for these environmental changes to be assessed and monitored, some indication of 'typical' community dominance throughout the year is first needed. Although community dominance data is available for some local near-shore areas this information is less common for the wider open ocean.

The spatial distribution of phytoplankton taxonomic groups is also of concern for coastal managers. Approximately half of all harmful algal bloom (HAB) causing species and 75% of toxic algal species are dinoflagellates (Sournia 1995) and HABs can cause both negative economic (caged and wild fish kills, beach closures) and

human health (fish and shellfish poisoning) impacts (Richardson 1997, Smayda 1997). The identification of areas commonly inhabited by large populations of potentially HAB causing dinoflagellate phytoplankton may influence the placement and management of aquaculture and tourist facilities. Additionally, if standard area group abundances are known, anomalous phytoplankton group abundances may indicate an underlying anthropogenically caused phenomenon.

Despite the significant roles of phytoplankton functional groups in our world oceans, information about their distribution and comparative seasonal cycles in the open oceanic areas is limited due to the lack of comprehensive datasets (Reid 1997, Beaugrand et al. 2000, Edwards et al. 2001). The Continuous Plankton Recorder (CPR) survey, an upper layer plankton monitoring program, is unique in providing comprehensive data on the spatial and temporal distributions of diatoms and dinoflagellates in the North-East Atlantic Ocean and North Sea. Because it is not yet possible to differentiate diatom and dinoflagellates from space, the CPR survey is able to provide large scale information not available through remote sensing (Sathyendranath et al. 2004, Alvain et al. 2005).

Recently, Beaugrand et al (2004) published a comprehensive CPR plankton atlas detailing the abundance and presence of various phytoplankton species in the North-East Atlantic. Whilst the atlas is an invaluable reference illustrating the spatial distribution of individual phytoplankton taxa, it does not explore the distribution of diatoms and dinoflagellates at the functional group scale. Reid et al. (1987) mapped the abundances of diatoms and dinoflagellates using point data; however point data, unlike continuous data developed via grid based interpolation, leaves gaps between sample locations. Temporal variation of major phytoplankton groups across large areas of the North-East Atlantic has also recently been investigated (Leterme et al. 2005, Leterme et al. 2006), but this was done at a large scale and seasonal cycles were not examined.

Here we present spatial and temporal patterns of diatom and dinoflagellate seasonal cycles in the North-East Atlantic Ocean based on >100,000 CPR samples. This analysis is presented in the form of monthly composite maps of the spatial distribution

of both major taxonomic groups from 1958 – 2003, as well as maps of their relative abundances throughout the calendar year. These are the first maps of this kind to be developed in the North-East Atlantic and the unique monthly time scale allows the biogeographical exploration of seasonal cycle patterns for each group.

## METHODS

The CPR has been operating in the North-East Atlantic and North Sea since 1931 (Fig. 1a in Raitsos et al. 2005). Full details of the operation of the CPR have been published elsewhere (e.g. Warner & Hays 1994) but are summarized here. The CPR collects samples using a high-speed plankton recorder (~15-20 knots [28 – 37 km hr<sup>-1</sup>]) that is towed behind ‘ships of opportunity’ in the surface layer of the ocean (~10 m depth). Water passes through the recorder, filtering plankton onto a 270 µm mesh silk; one sample represents 18 km of tow. Abundance of each phytoplankton species is then quantified for each sample. The collection and analysis of CPR samples have been carried out using a consistent methodological approach since 1958, making the CPR survey the longest continuous dataset of its kind in the world (Edwards & Richardson 2004). The CPR survey measures the abundance of approximately 200 phytoplankton taxa (and species) and has been used to describe the seasonal and long-term variations of phytoplankton abundance in the North Atlantic since 1958 (Warner & Hays 1994). Because phytoplankton cells are recorded as either present or absent across transects spanning each section of silk, CPR phytoplankton abundance is a semiquantitative estimate. However, the proportion of cells captured by the silk reflects the major changes in abundance, distribution, and community composition of the phytoplankton (Robinson 1970), and is consistent and comparable over time. For more information on CPR sampling methods see Reid et al (1987).

The diatom and dinoflagellate abundances are standard CPR products. Abundance data were  $\log_{10}(x + 1)$  transformed to ensure the data fit a normal distribution. Monthly composite maps of diatoms and dinoflagellates were produced using the kriging method of interpolation on a 1°×1° data grid (Caruso & Quarta 1998) thereby creating a continuous distribution of phytoplankton group abundances. Kriging, like all geostatistical methods, assumes that spatial structures are stable in time, at least for



the duration of the sampling period (Simard et al. 1992). However, this cannot be assumed of CPR data due to its 45 year sampling period. This problem has been resolved by portioning the data into shorter temporal periods and treating each temporally-partitioned dataset individually (Edwards 2000). Thus, the period of study was refined into nine shorter time periods of generally five years each (1958-1962, 1963-1967, 1968-1972, 1973-1977, 1978-1982, 1983-1987, 1988-1992, 1993-1997, and 1998-2003). Next, twelve monthly-averaged maps were created for each of the five-year intervals using the kriging method described above. For each calendar month, all nine of the five-year maps of that month were then averaged at each grid node and kriging was used to create monthly composite maps showing the mean spatial distribution for each month over the entire study period. This process was performed separately for diatoms and dinoflagellates. Each monthly composite map is made up of approximately 8,000 in situ CPR samples taken between 1958 and 2003. In order to explore phytoplankton community composition, the monthly composite maps of diatoms and dinoflagellates were then used to calculate the relative abundance (measured as percent diatoms) for each calendar month.

## **RESULTS AND DISCUSSION**

To explore the seasonal patterns of diatoms and dinoflagellates, the monthly means of both datasets were plotted (Fig. 1). The seasonal cycles show dissimilar bloom patterns. The diatom spring bloom peaks during May, abundance then gradually declines through summer before a weaker peak occurs in late summer. Dinoflagellates bloom during late summer, peaking in August, then progressively decline throughout autumn. Both groups maintain only a minimum abundance during winter months. The 95% confidence interval calculated for each month is very small, indicating that the measured abundances are consistent (Zar 1984). The spatial patterns of abundance during the seasonal cycle and the relative percent composition of the functional groups were further examined using the monthly abundance (Fig. 2) and monthly percent diatom composition (Fig. 3) composite maps.

Across the survey time period, the spring diatom bloom commences in the shallow areas of the North Sea in March. Its timing is predominantly controlled by light

penetration, the amount of light available in the euphotic zone being determined by day length, strength of solar radiation, cloudiness (most notably in winter), degree of mixing and amount of suspended matter in the water column (Edwards 2000). In March, the Dogger Bank (Fig. 4) and the Southern and German Bights showed an increase in diatom abundance. The low levels of suspended matter present in these shallow areas during early spring allow for increased light penetration and the early onset of the spring diatom bloom (Horwood et al. 1982, van Beusekom & Diel-Christiansen 1994). The diatom bloom also began in March in the Skagerrak, but more as a result of haline stratification due to Baltic inflow rather than because of shallow depth and low suspended matter (Richardson & Christoffersen 1991).

By April, the diatom bloom spreads outwards from shallow to deeper waters, encompassing nearly the entire main shelf area. During April, the diatom bloom was most intense in the North Sea and the shelf area west of Scotland, while diatom abundance to the south of Iceland remained somewhat lower, possibly due to colder water and deep vertical mixing in that region (Edwards 2000). In deep waters the spring bloom is usually initiated when the temperature rises and winter winds weaken, resulting in stratification (Townsend et al. 1994). In the open North-East Atlantic, depth generally increases with latitude while solar radiation decreases (Otto et al. 1990). Thus, stratification, and therefore the spring bloom, occurs later at higher latitudes. In summary, the spring diatom bloom occurs earlier, and the growing season is longer, in shallow neritic waters compared with deeper offshore waters (Edwards 2000).

By May, the diatom bloom was at its peak, covering nearly the entire North-East Atlantic, although a reduction in abundance in the Skagerrak and Norwegian Trench indicated the end of the diatom spring bloom in those areas. At that time, the bloom was most intense to the west and north of Scotland and around the Rockall Trough. During May, the dinoflagellate bloom began in the Skagerrak, the Rockall Trough and Porcupine Bank. In late spring and summer, the phytoplankton community composition across most of the North-East Atlantic changed from one of diatom dominance to one of dinoflagellate dominance. Because the water column is stratified, phytoplankton deplete upper layer nutrients and diatoms (opportunists) give

way to flagellates (competitors) and eventually dinoflagellates (stress-tolerators), both of which are adapted to survival in low nutrient, stable waters (Margaleff 1978, Drinkwater et al. 2003).

During June, the spring diatom bloom gradually continued to recede across the region while the dinoflagellate bloom spread throughout most of the North-East Atlantic, except for the coastal area around the southern United Kingdom and Ireland, which remains well mixed and unstratified due to tidal turbulence (Pingree & Griffiths 1978). Diatom abundance again increased across the entire region in July, and by August diatom abundance was especially high in the Skagerrak, the German Bight, the waters north of Norway as well as those to the northwest of Ireland. The dinoflagellate bloom peaked during July and August, with particularly high abundances persisting in the Skagerrak, German Bight and the Shetland and Orkney Island areas of Scotland. Oceanic inflow from the North Atlantic to the Shetland/Orkney Island area, and tidal fronts occurring between the stratified and mixed water masses of both areas, may contribute to the high productivity of those regions (Lee 1970, Otto et al. 1990, Edwards 2000). After August, the blooms of both taxonomic groups began to retreat, starting in the Celtic Sea and continuing northwards throughout the autumn months.

During autumn, cooler water temperatures and increased storms cause the thermocline to start to erode, allowing the mixing of cold, nutrient rich bottom waters with warm, nutrient depleted surface waters (Holligan 1987, Cushing 1990). Thus, as stratification decreased, autumn diatom and dinoflagellate blooms occurred in parts of the North Sea, Norwegian Trench and deeper shelf waters. During September, the diatom bloom continued to gradually recede in the Celtic Sea, Irish Sea, the Norwegian Trench and south of Iceland, although it remained strongest around the Faroe Islands and Rockall Plateau. The dinoflagellate bloom also still covered much of the North-East Atlantic, though abundance continued to decline compared to previous months, especially in the Celtic Sea, Irish Sea and to the south of Iceland.

By October, the diatom and dinoflagellate blooms remained only in the Rockall Trough, shallow areas of the North Sea, the Porcupine Bank and north of Norway.

Strengthening wind and wave action result in increased turbidity, which along with decreasing solar radiation causes the blooms of both phytoplankton groups to come to an end by November. North-East Atlantic waters are light limited in winter, remaining cool, turbulent, and well-mixed throughout the winter months (OSPAR Commission 2000). Thus, abundance of both phytoplankton groups continued to decline, with diatoms reaching a minimum in January and dinoflagellates reaching a minimum in February. However, even during winter months, the abundance of both groups was highest in the shallow areas of the Dogger Bank and southern areas of the North Sea. These areas are the first to bloom in March when the seasonal cycle begins again.

Like the monthly abundances of diatoms and dinoflagellates, the relative community composition of each functional group (measured as percent diatoms) is patchy across both space and time (Fig. 3). However, some definite seasonal patterns can be observed. During winter and spring months the North-East Atlantic is generally dominated by diatoms, while the phytoplankton community is dinoflagellate dominated in summer and autumn. The North Sea, particularly the shallow areas in the southern region and around Dogger Bank, is more weakly dominated by diatoms throughout the year than are most other regions of the study area including the English Channel, Celtic Seas, Porcupine Bank and the areas to the south and east of Iceland. The North Sea, Norwegian Trench, Skagerrak and Rockall regions show the lowest percentage of diatoms during summer months, while relative diatom abundance remains much higher throughout the summer in the English Channel, the Celtic Sea and to the south and east of Iceland. Hydrographic explanations for the variations in diatom and dinoflagellate abundance have been provided above, but additional research is required to rule out influence by anthropogenic factors.

## **CONCLUSION**

The analysis presented here provides a description of phytoplankton seasonal cycles across the North-East Atlantic and North Sea and their relationships to the hydrographical characteristics of the region based on > 50 years of data. These maps contribute information intended to help us better understand the mechanisms through

which phytoplankton community composition can influence ecosystem structure and functioning as well as to illustrate the patchy nature of phytoplankton distribution in the North-East Atlantic.

These maps provide information that is not yet available from remote sensing, as satellites currently lack the ability to distinguish between diatoms and dinoflagellates (Sathyendranath et al. 2004, Alvain et al. 2005). Thus, the abundance distribution maps (Fig. 2) may be particularly valuable resources for model validation, especially in Case II (optically complex coastal) waters where global chlorophyll algorithms are less reliable (IOCCG 2000). For example, until recently, it was commonly believed that the wintertime chlorophyll concentrations observed via satellite in the Case II English Channel were mainly the result of suspended sediment and not actually due to the presence of phytoplankton (IOCCG 2000). However, our maps clearly show that diatoms are present in the English Channel all year. Additionally, because phytoplankton comprise the foundation of the marine food web, these maps may be of particular value to researchers studying pelagic distribution patterns of higher trophic species, particularly in the open ocean where there are few wide scale datasets illustrating phytoplankton group distribution and relative abundance.

The relative abundance maps (Fig. 3) highlight the differences between diatom-dominated and dinoflagellate-dominated areas of the North-East Atlantic. Throughout the year relative diatom abundance is least pronounced in the coastal areas of the North Sea, Skagerrak and Norwegian Trench while off-shore regions to the west and north of the British Isles are more strongly diatom dominated. The abundance distribution maps also show abundances of both diatoms and dinoflagellates in the North Sea, Skagerrak, and Norwegian Trench areas that are higher than those occurring in most other regions of the North-East Atlantic. Finer scale investigation is required to determine if the elevated abundance of phytoplankton, particularly dinoflagellates, in those coastal areas is due to purely hydrographical reasons or is also augmented by anthropogenic causes such as eutrophication or climate change.

Besides their value to the scientific community, these maps may be used as a reference for coastal and resource managers. Diatoms, dinoflagellates and their relative community abundances are useful monitoring indicators already employed in various coastal regions throughout the North-East Atlantic (Hickel et al. 1992, Philippart et al. 2000). The seasonal cycle maps provide a baseline indication of 'typical' diatom and dinoflagellate distributions while the relative abundance maps illustrate 'typical' phytoplankton community dominance in the North-East Atlantic region throughout the year. These maps may serve to help interpret current and future monitoring data and research. For example, significant deviations from expected abundances (or relative abundances) may help to identify unusual local phytoplankton activity which could indicate an underlying anthropogenic problem (e.g. a sewage leak). Additionally, the identification of areas strongly dominated by dinoflagellates, which are more likely to cause HABs than diatoms, may influence the placement and management of aquaculture and tourist facilities. Also, the maps presented here have the unique ability to put local monitoring data into context. For example, a new local area monitoring scheme may have data showing a very high relative abundance of dinoflagellates throughout all months over several recent years. It is very difficult to determine if the observed community dominance is a local or widespread phenomenon from data gathered at a single location. If widespread, the local data may confirm a naturally occurring regional hydrographic condition or it could signify a large scale anthropogenically caused problem that may need inquiry; if surrounding communities are not dinoflagellate dominated, the local data may indicate a locally occurring problem.

These general trends provide the framework for more detailed exploration of spatial and temporal trends in smaller geographic areas and across more refined time periods in order to explore finer scale changes. We believe that additional knowledge regarding trends in long-term spatial and temporal variation in phytoplankton functional group distribution can provide insights into the effects of climate change and anthropogenic pressures on primary productivity in the North-East Atlantic.

**LITERATURE CITED**

- Alvain S, Moulin C, Dandonneau Y, Breon FM (2005) Remote sensing of phytoplankton groups in case 1 waters from global SeaWiFS imagery. *Deep-Sea Res Part I* 52:1989-2004
- Beaugrand G (2004) Continuous plankton records: Plankton atlas of the North Atlantic Ocean (1958-1999). I. Introduction and methodology. *Mar Ecol Prog Ser* CPR:3-10
- Beaugrand G, Ibanez F, Reid PC (2000) Spatial, seasonal and long-term fluctuations of plankton in relation to hydroclimatic features in the English Channel, Celtic Sea and Bay of Biscay. *Mar Ecol Prog Ser* 200:93-102
- Bopp L, Aumont O, Cadule P, Alvain S, Gehlen M (2005) Response of diatoms distribution to global warming and potential implications: A global model study. *Geophys Res Lett* 32:1-4
- Caruso C, Quarta F (1998) Interpolation methods comparison. *Computers and Mathematics with Applications* 35:109-126
- Cushing DH (1990) Recent studies on long-term changes in the sea. *Freshw Biol* 23:71-84
- Drinkwater KF, Belgrano A, Borja A, Conversi A, Edwards M, Greene CH, Ottersen G, Pershing AJ, Walker H (2003) The response of marine ecosystems to climate variability associated with the North Atlantic Oscillation. *Geophysical Monograph* 134:211-234
- Edwards M (2000) Large-scale temporal and spatial patterns of marine phytoplankton and climate variability in the North Atlantic. PhD dissertation, University of Plymouth
- Edwards M, Reid P, Planque B (2001) Long-term and regional variability of phytoplankton biomass in the Northeast Atlantic (1960-1995). *ICES J Mar Sci* 58:39-49
- Edwards M, Richardson AJ (2004) Impact of climate change on marine pelagic phenology and trophic mismatch. *Nature* 430:881-884
- Hickel W, Berg J, Treutner K (1992) Variability in phytoplankton biomass in the German Bight near Helgoland, 1980-1990. *ICES Mar Sci Symp* 195:249-259

- Holligan PM (1987) The physical environment of exceptional phytoplankton blooms in the northeast Atlantic. *Rapport et Proces-Verbaux des Reunions ICES* 187:8-18
- Horwood JW, Nichols JH, Harrop R (1982) Seasonal changes in net phytoplankton of the west-central North Sea. *J Mar Biol Ass U K* 62:15-23
- IOCCG (2000) Remote sensing of ocean color in coastal, and other optically complex waters. In: Sathyendranath S (ed) *Reports of the International Ocean-Color Coordinating Group*, No 3, Dartmouth, N.S., Canada
- Lee A (1970) The currents and water masses of the North Sea. *Oceanogr Mar Biol Annu Rev* 8:33-71
- Leterme SC, Edwards M, Reid PC, John AWG, Attrill MJ, Seuront L (2005) Decadal basin-scale changes in diatoms, dinoflagellates, and phytoplankton color across the North Atlantic. *Limnol Oceanogr* 50:1244-1253
- Leterme SC, Seuront L, Edwards M (2006) Differential contribution of diatoms and dinoflagellates to phytoplankton biomass in the NE Atlantic Ocean and the North Sea. *Mar Ecol Prog Ser* 312:57-65
- Margaleff R (1978) Life forms of phytoplankton as survival alternatives in an unstable environment. *Oceanol Acta* 1:493-509
- Micheli F (1999) Eutrophication, fisheries, and consumer-resource dynamics in marine pelagic ecosystems. *Science* 285
- Nagata T, Takai K, Kawabata KI, Nakanishi M, Urabe J (1996) The trophic transfer via a picoplankton-flagellate-copepod food chain during a picocyanobacterial bloom in Lake Biwa. *Archiv fur Hydrobiologie* 137:145-160
- OSPAR Commission (2000) *Quality Status Report 2000*, OSPAR Commission, London
- Otto L, Zimmerman JTF, Furnes GK, Mork M, Saetre R, Becker G (1990) Review of the physical oceanography of the North Sea. *Neth J Sea Res* 26:161-238
- Pedersen L, Jensen HM, Burmeister A, Hansen BW (1999) The significance of food web structure for the condition and tracer lipid content of juvenile snail fish (*Pisces: Liparis* spp.) along 65-72°N off West Greenland. *J Plankton Res* 21:1593-1611
- Philippart CJM, Cadee GC, van Raaphorst W, Riegman R (2000) Long-term phytoplankton-nutrient interactions in a shallow coastal sea: Algal community



- structure, nutrient budgets, and denitrification potential. *Limnol Oceanogr* 45:131-144
- Pingree RD, Griffiths DK (1978) Tidal fronts on the shelf seas around the British Isles. *J Geophys Res* 83:4615-4622
- Radach G, Berg J, Hagmeier E (1990) Long-Term Changes of the Annual Cycles of Meteorological, Hydrographic, Nutrient and Phytoplankton Time-Series at Helgoland and at Lv Elbe 1 in the German Bight. *Cont Shelf Res* 10:305-328
- Reid PC (1997) Phytoplankton and anthropogenic influences: a review. In: Earll RC (ed) *Marine environmental management: Review of events in 1996 and future trends*, Kempsey, p 113-118
- Reid PC, Robinson GA, Hunt HG (1987) Spatial and temporal patterns of marine blooms in the Northeastern Atlantic and North Sea from the Continuous Plankton Recorder survey. *Rapp P V Reun Cons Int Explor Mer* 187:27-37
- Richardson K (1997) Harmful or exceptional phytoplankton blooms in the marine ecosystem. In: *Adv Mar Biol*, Vol 31, p 301-385
- Richardson K, Christoffersen A (1991) Seasonal distribution and production of phytoplankton in the southern Kattegat. *Mar Ecol Prog Ser* 78:217-227
- Robinson GA (1970) Continuous Plankton Records: variation in the seasonal cycle of phytoplankton in the North Atlantic. *Bull Mar Ecol* 6:333-345
- Sathyendranath S, Watts L, Devred E, Platt T, Caverhill C, Maass H (2004) Discrimination of diatoms from other phytoplankton using ocean-colour data. *Mar Ecol Prog Ser* 272:59-68
- Simard Y, Legendre P, Lavoie G, Marcotte D (1992) Mapping, estimating biomass, and optimizing sampling programs for spatially autocorrelated data: case study of the northern shrimp. *Can J Fish Aquat Sci* 49:32-45
- Smayda TJ (1997) What is a bloom? A commentary. *Limnol Oceanogr* 42:1132-1136
- Sommer U, Stibor H, Katschakis A, Sommer F, Hansen T (2002) Pelagic food web configurations at different levels of nutrient richness and their implications for the ratio fish production: primary production. *Hydrobiologia* 484:11-20
- Sournia A (1995) Red tide and toxic marine phytoplankton of the world ocean: an inquiry into biodiversity. In: Lassus P A, G., E. Erad, P. Gebtien, C. Marcaillou (ed) *Harmful Marine Algal Blooms*. Lavoisier, Inc, Paris, p 103-112

- Townsend DW, Cammen LM, Holligan PM, Campbell DE, Pettigrew NR (1994) Causes and consequences of variability in the timing of spring phytoplankton blooms. *Deep-Sea Res Part I* 41:747-765
- van Beusekom JEE, Diel-Christiansen S (1994) Alterations of the North Sea plankton due to changes of the regional climate, nutrient input and contaminant load: a hypothesis In: *North Sea Quality Status Report*. Danish Environmental Protection Agency, p 64-71
- Verity PG, Smetacek V (1996) Organism life cycles, predation, and the structure of marine pelagic systems. *Mar Ecol Prog Ser* 130:277-293
- Warner AJ, Hays GC (1994) Sampling by the Continuous Plankton Recorder survey. *Prog Oceanogr* 34:237 - 256
- Zar JH (1984) *Biostatistical Analysis*, 2nd ed., Vol. Prentice-Hall, Upper Saddle River, NJ

**FIGURE LEGENDS**

Fig. 1. Averaged seasonal cycles of diatoms and dinoflagellates between 1958 and 2003 in the North-East Atlantic and North Sea (ninety-five percent confidence intervals are indicated but are very small). Diatoms bloom strongly in spring and more weakly in late summer while dinoflagellates reach maximum abundance in late summer.

Fig. 2. The mean monthly spatial patterns of diatoms and dinoflagellates in the North-East Atlantic during the period 1958 – 2003.

Fig. 3. The mean monthly spatial patterns of the relative community abundance of diatoms in the North-East Atlantic during the period 1958 – 2003.

Fig. 4. Bathymetric map with detailed location names of the North-East Atlantic and North Sea regions mentioned in the text.

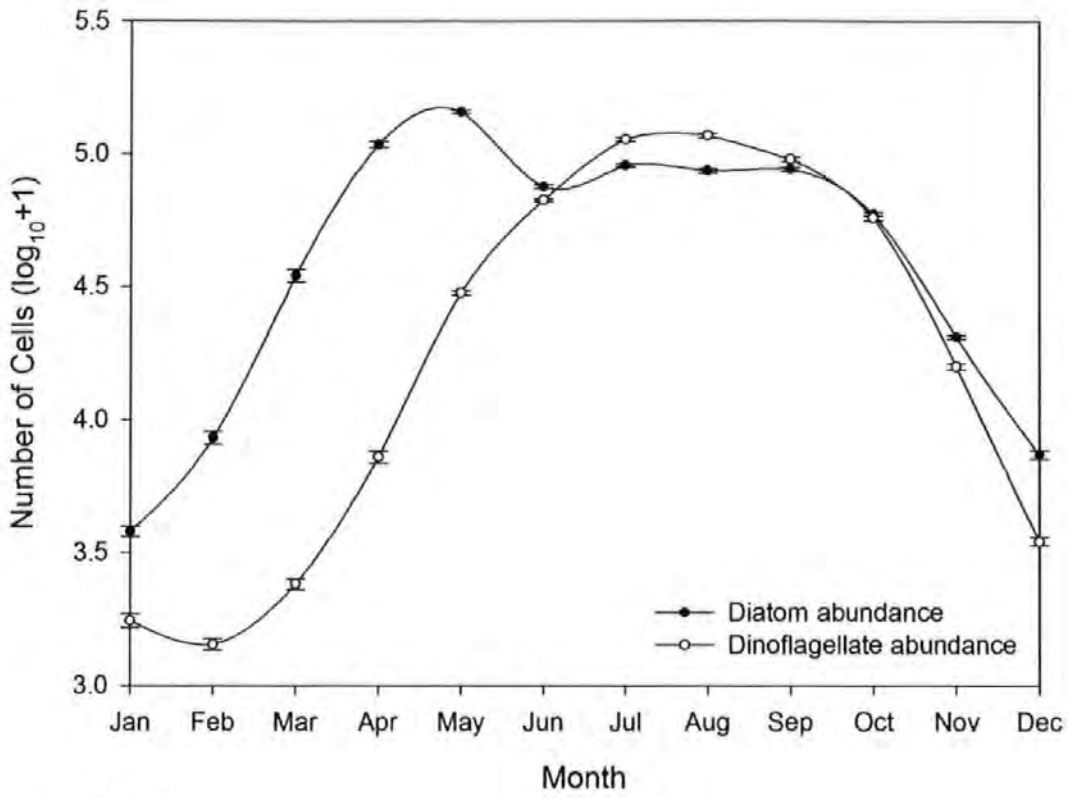


Fig. 1

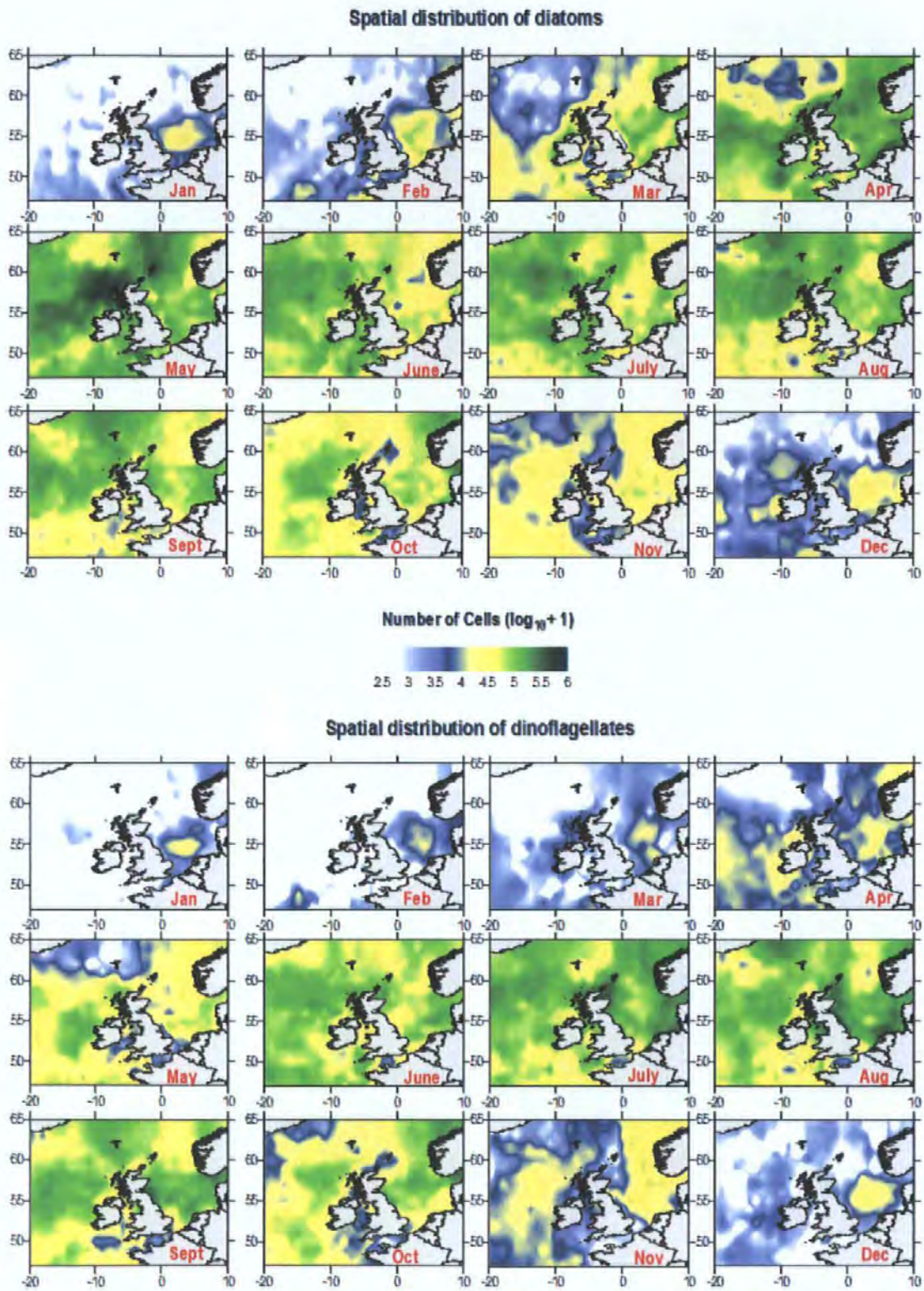


Fig. 2

Relative abundance of diatoms and dinoflagellates

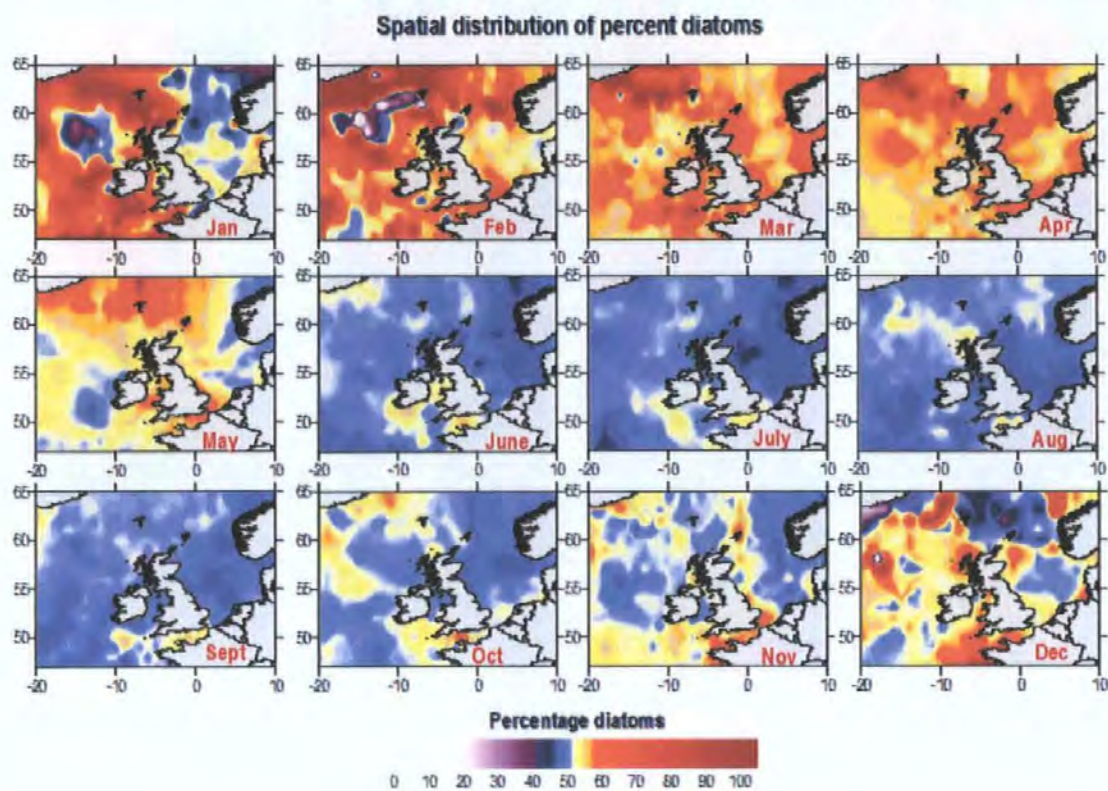


Fig. 3

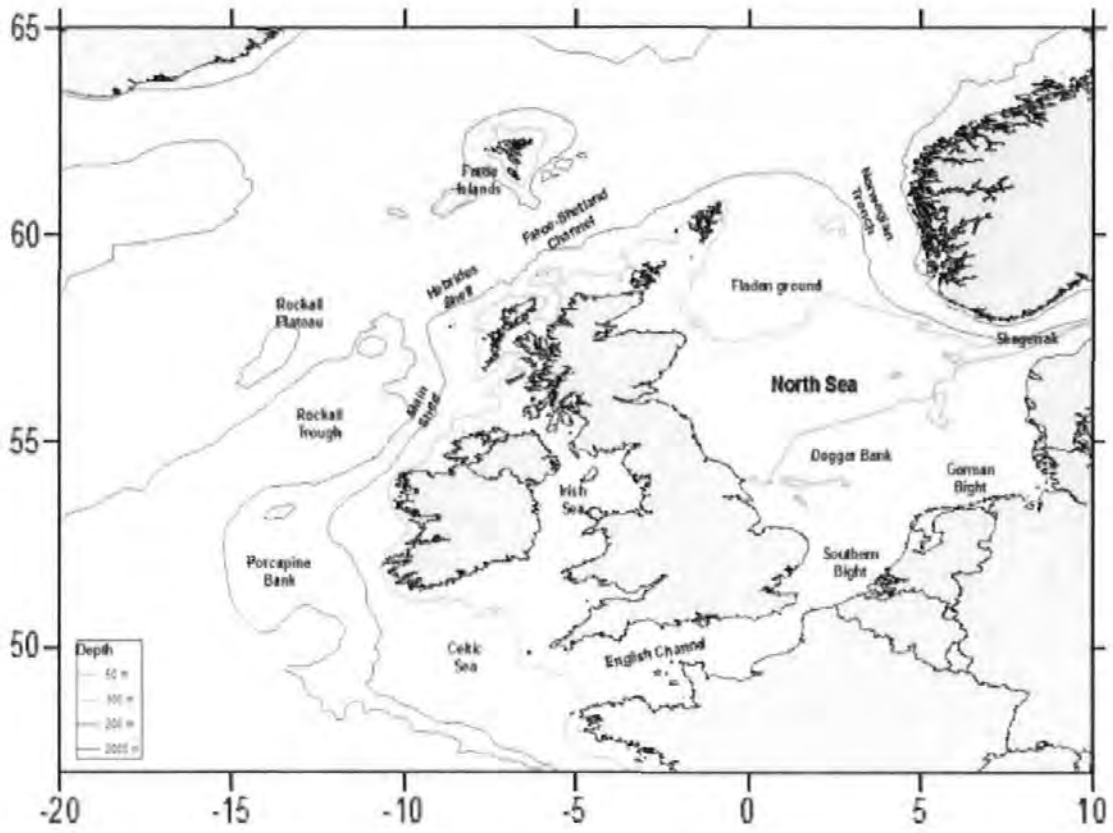


Fig 4

## Reference List

- Alvain S., Moulin C., Dandonneau Y., Breon F.M. (2005). Remote sensing of phytoplankton groups in case 1 waters from global SeaWiFS imagery. *Deep Sea Research Part I*. **52**:1989-2004.
- Armbrust E.V., Berges J.A., Bowler C., Green B.R., Martinez D., Putnam N.H., Zhou S.G., Allen A.E., Apt K.E., Bechner M., Brzezinski M.A., Chaal B.K., Chiovitti A., Davis A.K., Demarest M.S., Detter J.C., Glavina T., Goodstein D., Hadi M.Z., Hellsten U., Hildebrand M., Jenkins B.D., Jurka J., Kapitonov V.V., Kroger N., Lau WWY., Lane TW., Larimer FW., Lippmeier J.C., Lucas S., Medina M., Montsant A., Obornik M., Parker M.S., Palenik B., Pazour G.J., Richardson P.M., Rynearson T.A., Saito M.A., Schwartz D.C., Thamatrakoln K., Valentin K., Vardi A., Wilkerson F.P., Rokhsar D.S. (2004). The genome of the diatom *Thalassiosira pseudonana*: Ecology, evolution, and metabolism. *Science*. **306** (5693): 79-86.
- Balch W.M., Kilpatrick K.A., Holligan P., Harbour D., Fernandez E. (1996a). The 1991 coccolithophore bloom in the central North Atlantic. I. Relating optics to coccolith concentration. *Limnology and Oceanography*. **41** (8): 1684-1696.
- Balch W.M., Kilpatrick K.A., Trees C.C. (1996b). The 1991 coccolithophore bloom in the central North Atlantic .I. Optical properties and factors affecting their distribution. *Limnology and Oceanography*. **41** (8): 1669-1683.
- Balch W.M., Holligan P.M., Acjleson S.G., Voss K.J. (1991). Biological and optical-properties of mesoscale coccolithophore blooms in the gulf of Maine. *Limnology and Oceanography*. **36** (4): 629-643.



- Barnard R., Batten S., Beaugrand G., Buckland C., Conway D.V.P., Edwards M., Finlayson J., Gregory L.W., Halliday N.C., John A.W.G., Johns D.G., Johnson A.D., Jonas T.D., Lindley J.A., Nyman J., Pritchard P., Reid P.C., Richardson A.J., Saxby R.E., Sidey J., Smith M.A., Stevens D.P., Taylor C.M., Tranter P.R.G., Walne A.W., Wootton M., Wotton C.O.M., Wright J.C. (2004). Continuous Plankton Recorder. Continuous plankton records: Plankton atlas of the North Atlantic Ocean (1958-1999). II. Biogeographical charts . *Marine Ecology Progress Series*. 11-75.
- Basile-Doelsch I., Meunier J.D., Parron C. (2005). Another continental pool in the terrestrial silicon cycle. *Nature*. **433** (7024): 399-402.
- Batten S.D., Crawford W.R. (2005). The influence of coastal origin eddies on oceanic plankton distributions in the eastern Gulf of Alaska. *Deep Sea Research Part II*. **52** (7-8): 991-1009 2005
- Batten S. D., Walne A.W., Edwards M., Groom S.B. (2003). Phytoplankton biomass from continuous plankton recorder data: an assessment of the phytoplankton colour index. *Journal of Plankton Research*. **25**: 697-702.
- Beaugrand G. (2004). The North Sea regime shift: evidence, causes, mechanisms and consequences. *Progress in Oceanography*. **60**: 245-262.
- Beaugrand G., Edwards, M. (2001). Differences in performance among four indices used to evaluate diversity in planktonic ecosystems. *Oceanologica Acta*. **24**(5): 467-477.
- Beaugrand G., Ibanez F. (2002). Spatial dependence of calanoid copepod biodiversity in the north Atlantic Ocean. *Marine Ecology Progress Series*. **232**: 197-211.
- Beaugrand G., Reid P.C. (2003). Long-term changes in phytoplankton, zooplankton and salmon related to climate. *Global Change Biology*. **9**: 801-817.

- Beaugrand G., Ibanez, F., Lindley J.A. (2001). Geographical distribution and seasonal and diel changes in the diversity of calanoid copepods in the North Atlantic and North Sea. *Marine Ecology Progress Series*. **219**: 189-203.
- Beaugrand G., Ibanez F., Reid P.C. (2000a). Spatial, seasonal and long-term fluctuations of plankton in relation to hydroclimatic features in the English Channel, Celtic Sea and Bay of Biscay. *Marine Ecology Progress Series*. **200**: 93-102.
- Beaugrand G., Reid P.C., Ibañez F., Planque B. (2000b). Biodiversity of North Atlantic and North Sea calanoid copepods. *Marine Ecology Progress Series*. **204**: 299-303.
- Bigg G. R., Jickells T.D., Liss P.S., Osborn T. J. (2003), The role of the oceans in climate. *International Journal of Climatology*. **23**:1127-1159.
- Bopp L., Aumont O., Cadule P., Alvain S., Gehlen M. (2005). Response of diatoms distribution to global warming and potential implications: A global model study. *Geophysical Research Letters*. **32**: L19606. [doi:10.1029/2005GL023653].
- Brand L.E., Sunda W.G., Guillard R.R.L. (1983). Limitation of marine phytoplankton reproductive rates by zinc, manganese, and iron. *Limnology and Oceanography*. **28**: 1182–1198.
- Broerse A.T.C., Tyrrell T., Young J.R., Poulton A.J., Merico A., Balch W.M., Miller P.I. (2003). The cause of bright waters in the Bering Sea in winter. *Continental Shelf Research*. **23**: 1579–1596.
- Brown C.W., Yoder J.A. (1994). Coccolithophorid blooms in the global ocean. *Journal of Geophysical Research-Oceans*. **99**: 7467–7482.

- Butler M.J.A. (1988). The application of remote sensing technology to marine fisheries: an introductory manual. *FAO Fish, Technical Paper*. 295:165.
- Chambers J.M., Hastie T.J. (1992). *Statistical Models in S-Plus*. Wadsworth & Brooks.
- Clark R.A., Frid C.L.J. (2001). Long-term changes in the North Sea ecosystem. *Environmental Reviews*. 9: 131-187.
- Cloern J.E. (2001). Our evolving conceptual model of the coastal eutrophication problem. *Marine Ecology Progress Series*. 210: 223-253.
- Cokacar T., Oguz T., Kubilay N. (2004). Satellite-detected early summer coccolithophore blooms and their interannual variability in the Black Sea. *Deep Sea Research Part I*. 51 (8): 1017-1031.
- Colebrook J.M. (1960). Continuous plankton records: methods of analysis, 1950–59. *Bulletin of Marine Ecology*. 5: 51–64.
- Colebrook J. M., Robinson G.A. (1965). Continuous plankton records: seasonal cycles of phytoplankton and copepods in the north-eastern Atlantic and North Sea. *Bulletin of Marine Ecology*. 6: 123–139.
- Colebrook J. M., Robinson G. A. (1961). The seasonal cycle of the plankton in the North Sea and the North-eastern Atlantic. *Journal du Conseil international pour l'Exploration de la Mer*. 26: 156–165.
- Cushing D.H. (1990) Recent studies on long-term changes in the sea. *Freshwater Biology*. 23:71-84.

- De Jonge V.N., Bakker J.F., Van Stralen M. (1996). Recent changes in the contributions of river Rhine and North Sea to the eutrophication of the western Dutch Wadden Sea. *Aquatic Ecology*. **30**: 27-39.
- Drinkwater K.F., Belgrano A., Borja A., Conversi A., Edwards M., Greene C.H., Ottersen G., Pershing A.J., Walker H. (2003) The response of marine ecosystems to climate variability associated with the North Atlantic Oscillation. Geophysical Monograph 134:211-234. *American Geophysical Union*. **10**. [1029/134GM10].
- Dytham C. (2000). Choosing and Using Statistics; A Biologist's Guide. Blackwell Science. London, UK.
- Edwards M, Richardson A.J. (2004). Impact of climate change on marine pelagic phenology and trophic mismatch . *Nature*. **430** (7002): 881-884.
- Edwards, M. (2000). Large-scale temporal and spatial patterns of marine phytoplankton and climate variability in the North Atlantic. *PhD dissertation*. University of Plymouth. UK.
- Edwards M., Beaugrand G., Reid P.C., Rowden A.A., Jones M.B. (2002). Ocean climate anomalies and the ecology of the North Sea. *Marine Ecology Progress Series*. **239**: 1-10.
- Edwards M., Reid P.C., Planque B. (2001). Long-term and regional variability of phytoplankton biomass in the Northeast Atlantic (1960-1995). *ICES Journal of Marine Sciences*. **58**: 39-49.
- Ekman V.W. (1905). On the influence of the Earth's rotation on ocean currents. *Arkiv for Matematik, Astronomi, och Fysik*. **2**(11).
- Falciatore A., d'Alcala M.R., Croot P., Bowler C. (2000). Perception of environmental signal by a marine diatom. *Science*. **288** (5475): 2363-2366.

- Falkowski P.G., Katz M.E., Knoll A.H., Quigg A., Raven J.A., Schofield O., Taylor F.J.R. (2004). The evolution of modern eukaryotic phytoplankton. *Science*. **305**: 354-360.
- Flewelling L.J., Naar J.P., Abbott J.P., Baden D.G., Barros N.B., Bossart G.D., Bottein M.Y.D., Hammond D.G., Haubold E.M., Heil C.A., Henry M.S., Jacocks H.M., Leighfield T.A., Pierce R.H., Pitchford T.D., Rommel S.A., Scott P.S., Steidinger K.A., Truby E.W., Van Dolah F.M., Landsberg J.H. (2005). Red tides and marine mammal mortalities. *Nature*. **435** (7043): 755-756.
- Gieskes W.W.C., Kraay G.W. (1997). Continuous Plankton Records: changes in the plankton of the North Sea and its eutrophic Southern Bight from 1948-1975. Netherlands. *Journal of Sea Research*. **11**: 334-364.
- Gregg W.W., Conkright M.E., Ginoux P., O'Reilly J.E., Casey N.W. (2003). Ocean primary production and climate: Global decadal changes. *Geophysical Research Letters*. **30** (15): 1809.
- Harbour D., Davidson R. (2002). Copepod hatching success in marine ecosystems with high diatom concentrations. *Nature*. **419** (6905): 387-389.
- Hastie T., Tibshirani R. (1990). Generalized Additive Models. London: Chapman & Hall.
- Hays G.C., Warner A.J., John A.W.G., Harbour D.S., Holligan P.M. (1995). Coccolithophores and the continuous plankton recorder survey. *Journal of Marine Biological Association of the United Kingdom*. **75**(2): 503-506.
- Holligan P.M. (1987). The physical environment of exceptional phytoplankton blooms in the northeast Atlantic. *Rapport et Proces-Verbaux des Reunions ICES*. **187**: 8-18

- Holligan P.M., Fernandez E., Aiken J., Balch W.M., Boyd P., Burkhill P.H., Finch M., Groom S.B., Malin G., Muller K., Purdie D.A., Robinson C., Trees C.C., Turner S.M., Van der Wal P. (1993). A biogeochemical study of the coccolithophore *Emiliania huxleyi* in the north Atlantic. *Global Biogeochemical Cycles*. **7**: 879-900.
- Hooker S.B., McClain C.R. (2000). The calibration and validation of SeaWiFS data, *Progress in Oceanography*, **45**: 427-465.
- Houghton J.T., Ding Y., Griggs D.J., Noguer M., van der Linden P.J., Dai X., Maskell K., Johnson C.A. (Eds.). (2001). *Climate Change 2001: The Scientific Basis*. 881 pp., Cambridge University Press, New York.
- Iglesias-Rodriguez M.D., Brown C.W., Doney S.C., Kleypas J.A., Kolber D., Kolber Z., Hayes P.K., Falkowski P.G. (2002). Representing key phytoplankton functional groups in ocean carbon cycle models: Coccolithophorids. *Global Biogeochemical Cycles*. **16** [doi: 10.1029/2001GB001454]
- IOCCG. (2000). Remote Sensing of Ocean Colour in Coastal, and Other Optically-Complex Waters, Sathyendranath, S. (Eds.) (2000), Reports of the International Ocean-Colour Coordinating Group, No. 3. *IOCCG*. Dartmouth, Canada.
- Irigoien X., Harris R.P., Verheye H.M., Joly P., Runge J., Starr M., Pond D., Campbell R., Shreeve R., Ward P., Smith A.N., Dam H.G., Peterson W., Tirelli V., Koski M., Smith T., Harbour D., Davidson R. (2002). Copepod hatching success in marine ecosystems with high diatom concentrations. *Nature*. **419** (6905): 387-389.
- Jochem F., Babenerd B. (1989). *Dictyocha speculum*-a new type of phytoplankton bloom in the Western Baltic. *Marine Biology*. **103**: 373-379.

- Jones R.H., Flynn K.J. (2005). Nutritional status and diet composition affect the value of diatoms as copepod prey. *Science*. **307** (5714): 1457-1459.
- Kalnay E., Kanamitsu M., Kistler R., Collins W., Deaven D., Gandin L., Iredell M., Saha S., White G., Woollen J., Zhu Y., Chelliah M., Ebisuzaki W., Higgins W., Janowiak J., Mo K.C., Ropelewski C., Wang J., Leetmaa A., Reynolds R., Jenne R., Joseph D. (1996). The NCEP/NCAR 40-year reanalysis project. *Bulletin of the American Meteorological Society*. **77** (3): 437-471.
- Kohavi R. (1995). The power of decision tables. *Lecture notes in artificial intelligence*. **912**: 174-189.
- Labiosa R.G., Arrigo K.R. (2003). The interplay between upwelling and deep convective mixing in determining the seasonal phytoplankton dynamics in the Gulf of Aqaba: Evidence from SeaWiFS and MODIS. *Limnology and Oceanography*. **48** (6): 2355-2368.
- Lenhart H.J. (2001). Effects of river nutrient load reduction on the eutrophication of the North Sea, simulated with the ecosystem model ERSEM. *Senckenbergiana Maritima*. **31**: 299-311.
- Lessard E.J., Merico A., Tyrrell T. (2005). Nitrate to phosphate ratios and *Emiliania huxleyi* blooms. *Limnology and Oceanography*. **50** (3): 1020-1024.
- Leterme S.C., Edwards M., Reid P.C., John A.W.G., Attrill M.J., Seuront L. (2005). Decadal basin-scale changes in diatoms, dinoflagellates, and phytoplankton color across the North Atlantic. *Limnology and Oceanography*. **50**:1244-1253.
- Lu R. (2005). Impact of Atlantic sea surface temperatures on the warmest global surface air temperature of 1998. *Journal of Geophysical Research*. **110** [doi:10.1029/2004JD005203].

- Maravelias C.D., Haralabous J., Papaconstantinou C. (2003). Predicting demersal fish species distributions in the Mediterranean Sea using artificial neural networks. *Marine Ecology Progress Series*. **255**: 249-258.
- Maravelias C.D. (2001). Habitat associations of Atlantic herring in the Shetland area: influence of spatial scale and geographic segmentation. *Fisheries Oceanography*. **10** (3): 259-267.
- Margaleff R. (1978). Life forms of phytoplankton as survival alternatives in an unstable environment. *Oceanologica Acta*. **1**: 493-509.
- McClain C.R., Cleave M.L., Feldman G.C., Gregg W.W., Hooker S.B., Kuring N. (1998). Science Quality SeaWiFS Data for Global Biosphere Research. *Sea technology*. **39** (9): 10-16.
- Milligan A.J., Morel F.M.M. (2002). A proton buffering role for silica in diatoms. *Science*. **297** (5588): 1848-1850.
- Miralto A., Barone G., Romano G., Poulet S.A., Ianora A., Russo G.L., Buttino I., Mazzarella G., Laabir M., Cabrini M., Giacobbe M.G. (1999). The insidious effect of diatoms on copepod reproduction. *Nature*. **402** (6758): 173-176.
- Mueller J.L. Austin R.W. (1995). SeaWiFS Technical Report Series. *NASA Technical Memorandum*. **25**. [104566].
- Nanninga H.J., Tyrrell T. (1996). Importance of light for the formation of algal blooms by *Emiliana huxleyi*. *Marine Ecology Progress Series*. **136** (1-3): 195-203.
- Nejstgaard J.C., Hygum B.H., Naustvoll L.J., Bamstedt U. (2001). Zooplankton growth, diet and reproductive success compared in simultaneous diatom- and flagellate microzooplankton-dominated plankton blooms. *Marine Ecology Progress Series*. **221**: 77-91.



- Nixon S. (1995). Coastal marine eutrophication: A definition, social causes and future concerns. *Ophelia*. **41**: 199-219.
- Nybakken J.W. (1997). Marine Biology: An ecological approach, 4th ed. Addison-Wesley Educational publishers Inc. pp 1-481, Menlo Park, California.
- Onodera J., Takahashi K. (2005). Silicoflagellate fluxes and environmental variations in the northwestern North Pacific during December 1997-May 2000. *Deep Sea Research Part I*. **52** (2): 371-388.
- O'Reilly J.E., Maritorena S., Mitchell B.G., Siegel D.A., Carder K.L., Garver S.A., Kahru M., McClain C. (1998). Ocean color chlorophyll algorithms for SeaWiFS. *Journal of Geophysical Research*. **103**: 24937-24953.
- Paerl H.W., Valdes L.M., Pinckney J.L., Piehler M.F., Dyble, J., Moisander P.H. (2003). Phytoplankton photopigments as indicators of estuarine and coastal eutrophication. *BioScience*. **53**: 953-964.
- Pickard G.L., Pond. S. (1978). Introductory Dynamic Oceanography. 2nd ed. Pergamon Press, Oxford, England, UK.
- Planque B., Hays G.C., Ibanezod F., Gamble J.C. (1997). Large scale spatial variations in the seasonal abundance *Calanus finmarchicus*. *Deep Sea Research Part I*. **44**: 315-326.
- Platt T., Bouman H., Devred E., Fuentes-Yaco C., Sathyendranath S. (2005). Physical forcing and phytoplankton distributions. *Scientia Marina*. **69**: 55-73.
- Pond S., Pickard G.L. (1983). Introductory dynamical oceanography. Fonte: Oxford; Butterworth-Heinemann. 329 p.

- Pyper B.J., Peterman R.M. (1998). Comparison of methods to account for autocorrelation in correlation analyses of fish data. *Canadian Journal of Fisheries and Aquatic Science*. **55**: 2127.
- Redfield A.C., Ketchum B.H., Richards F.A. (1963). The influence of organisms on the composition of sea water, In M. N. Hill [ed.]. *The Sea*. John Wiley. p. 26-77.
- Reid P.C., Holliday N.P., Smyth T.J. (2001). Pulses in the eastern margin current and warmer water off the north west European shelf linked to North Sea ecosystem changes. *Marine Ecology Progress Series*. **215**: 283-287.
- Reid P.C. (1977). Continuous plankton records: changes in the composition and abundance of the phytoplankton of the north-eastern Atlantic Ocean and North Sea, 1958–1974. *Marine Biology*. **40**: 337–339.
- Reid P.C., Edwards M. (2001). Plankton and climate, in *Encyclopaedia of ocean sciences*. (Eds. Steele, J. H., Thorpe, S. A. & Turekian, K. K.). Academic Press. pp. 2194-2200.
- Reid P.C., Edwards M., Hunt H.G., Warner A.J. (1998). Phytoplankton change in the North Atlantic. *Nature*. **391**: 546.
- Reid P.C., Matthews J.B.L., Smith M.A. (Eds.) (2003). Achievements of the Continuous Plankton Recorder survey and a vision for its future. *Progress in Oceanography*. **58**: 115-358.
- Reid P.C., Borges M.F., Svendsen E. (2001). A regime shift in the North Sea circa 1988 linked to changes in the North Sea horse mackerel fishery. *Fisheries Research*. **50**: 163-171.
- Richardson A.J., Schoeman D.S. (2004). Climate impact on plankton ecosystems in the Northeast Atlantic. *Science*. **305** (5690): 1609-1612.

- Richardson A.J., Walne A.W., John A.W.G., Jonas T.D., Lindley J.A., Sims D.W., Stevens D., Witt M. (2006). Using continuous plankton recorder data. *Progress in Oceanography*. **68** (1): 27-74.
- Richardson A.J., Schoeman D.S. (2004). Climate Impact on Plankton Ecosystems in the Northeast Atlantic. *Science*. **305**: 1609-1612.
- Riebesell U., Zondervan I., Rost B., Tortell P.D., Zeebe R.E., Morel F.M.M. (2000). Reduced calcification of marine plankton in response to increased atmospheric CO<sub>2</sub>. *Nature*. **407**: 364-367.
- Robinson G.A. (1970). Continuous plankton records: variation in the seasonal cycle of phytoplankton in the North Atlantic. *Bulletin of Marine Ecology*. **6**: 333-345.
- Robinson G.A., Hiby A.R. (1978). The Continuous Plankton Recorder survey. In Sournia, A. (ed.). *Phytoplankton Manual*. UNESCO. Paris. p59-63.
- Robinson, G.A., Aiken, J., Hunt H.G. (1986). Synoptic surveys of the western English Channel. The relationships between plankton and hydrography. *Journal of Marine Biological Association of the United Kingdom*. **66**: 201-218.
- Robinson I.S. (1995). *Satellite oceanography: an introduction for oceanographers and remote-sensing scientists*. J. Wiley & Sons Ltd, UK.
- Robinson I.S. (2004). *Measuring the oceans from space*. Praxis Publishing Ltd, Chichester, UK.
- Sabine C.L., Feely R.A., Gruber N., Key R.M., Lee K., Bullister J.L., Wanninkhof R., Wong C.S., Wallace D.W.R., Tilbrook B., Millero F.J., Peng T.H., Kozyr A., Ono T., Rios A.F. (2004). The oceanic sink for anthropogenic CO<sub>2</sub>. *Science*. **305** (5682): 367-371.

SAHFOS official site. (2003): <http://www.sahfos.org> (Last time visited, 15/11/05).

Sathyendranath S., Watts L., Devred E., Platt T., Caverhill C., Maass H. (2004). Discrimination of diatoms from other phytoplankton using ocean-colour data. *Marine Ecology Progress Series*. **272**: 59-68.

Smyth T.J., Tyrrell T., Tarrant B. (2004). Time series of coccolithophore activity in the Barents Sea, from twenty years of satellite imagery. *Geophysical Research Letters*. **31**: (L11302) [doi: 10.1029/2004GL019735].

Sommer U., Stibor H., Katschakis A., Sommer F., Hansen T. (2002). Pelagic food web configurations at different levels of nutrient richness and their implications for the ratio fish production: primary production. *Hydrobiologia*. **484**:11-20.

Specht, D.F. (1991). A general regression neural network. *IEEE transactions on neural networks*. **2** (6): 568-576.

Specht D.F. (1990). Probabilistic neural networks. *Neural Networks*. **3** (1): 109-118.

Specht D.F. (1988). Neural Networks. *IEEE International Conference on: Probabilistic neural networks for classification, mapping, or associative memory*. **1**: 525-532.

StatSoft Inc. (2004). *Electronic Statistics Textbook*, Tulsa, OK, StatSoft. WEB: <http://www.statsoft.com/textbook/stathome.html>

StatSoft. (2003). *Time Series Analysis*. © Copyright StatSoft, Inc., 1984-2003.

Strickland J.D., Parsons T.R. (1972). *A practical handbook of seawater analysis bulletin*. 2nd ed. Fisheries Research Board of Canada. p167.

- Strzepek R.F., Harrison P.J. (2004). Photosynthetic architecture differs in coastal and oceanic diatoms. *Nature*. **431** (7009): 689-692.
- Takahashi K. (1991). Silicoflagellates and Actiniscus vertical fluxes at Pacific and Atlantic sediment trap stations: In: Honjo, S.(Ed.), Ocean Biocoenosis Series No.2. Woods Hole Oceanographic Institution Press 35p.
- Topex/Poseidon,. (2003). NASA official site for Topex/ Poseidon: <http://topex-www.jpl.nasa.gov/mission/tp-launch.html> (Last time visited, 15/11/03)
- Townsend D.W., Cammen L.M., Holligan P.M., Campbell D.E., Pettigrew N.R. (1994). Causes and consequences of variability in the timing of spring phytoplankton blooms. *Deep Sea Research Part I*. **41**:747-765.
- Tucker L.R. (1966). Some mathematical notes on three-mode factor analysis. *Psychometrika*. **31**: 279-311.
- Tyrrell T., Merico A. (2004). *Emiliana huxleyi*: Bloom observations and the conditions that induce them, p. 75-97. In H. R. Thierstein and J. R. Young, [eds.], *Coccolithophores: from molecular processes to global impact*. Springer-Verlag.
- Tyrrell T., Taylor A.H. (1996). A modelling study of *Emiliana huxleyi* in the NE Atlantic. *Journal of Marine Systems*. **9** (1/2): 83-112.
- Tyrrell T., Holligan P.M., Mobley C.D. (1999). Optical impacts of oceanic coccolithophore blooms. *Journal of Geophysical Research-Oceans*. **104** (C2): 3223-3241.
- Uitz J., Claustre H., Morel A., Hooker S.B. (2006). Vertical distribution of phytoplankton communities in open ocean: An assessment based on surface chlorophyll. *Journal of Geophysical Research-Oceans*. **111** (C8).

- Verity P.G., Smetacek V. (1996). Organism life cycles, predation, and the structure of marine pelagic systems. *Marine Ecology Progress Series*. **130**: 277-293.
- Voss K.J., Balch W.M., Kilpatrick K.A. (1998). Scattering and attenuation properties of *Emiliana huxleyi* cells and their detached coccoliths. *Limnology and Oceanography*. **43** (5): 870-876.
- Warner A.J., Hays G.C. (1994). Sampling by the Continuous Plankton Recorder survey. *Progress in Oceanography*. **34**: 237-256.
- Webb D.J, Beverly de Cuevas A., Coward A.C. (1998). The first main run of the OCCAM Global Ocean Model. Southampton Oceanography Centre, Internal document no. 34.
- Weeks S.J., Currie B., Bakun A. (2002). Satellite imaging – Massive emissions of toxic gas in the Atlantic. *Nature*. **415**: 493–494.
- Westbroek P., Brown C.W., Van Bleijswijk J.D.L., Brownlee C., Brummer G.J., Conte M., Egge J.K., Fernandez E., Jordan R.W., Knappertsbusch M., Stefels J., Veldhuis M.J.W., Van der Wal P., Young J. (1993). A model system approach to biological climate forcing: the example of *Emiliana huxleyi*. *Global Planet Change*. **8**: 27–46.
- Wunsch C., Stammer D. (1998). Satellite altimetry, the marine geoid and the oceanic general circulation. *Annual Reviews of Earth and Planetary Sciences*. **26**: 219-254.
- Yelland M., Taylor P.K. (1996). Wind stress measurements from the open ocean. *Journal of Physical Oceanography*. **26** (4): 541–558.
- Zar J.H. (1984). *Biostatistical Analysis*, 2nd ed. Prentice-Hall.

## Extending the SeaWiFS chlorophyll data set back 50 years in the northeast Atlantic

Dionysios E. Raitsos,<sup>1,2</sup> Philip C. Reid,<sup>2</sup> Samantha J. Lavender,<sup>1</sup> Martin Edwards,<sup>2</sup> and Anthony J. Richardson<sup>2</sup>

Received 17 January 2005; accepted 23 February 2005; published 17 March 2005.

[1] Phytoplankton play a key role in biogeochemical cycling and climate processes. Precise quantitative measurements of chlorophyll-*a* (Chl-*a*), a measure of phytoplankton biomass, have only been available globally since 1997 from the Sea-viewing Wide Field-of-view Sensor (SeaWiFS). In the North Atlantic, semi-quantitative measurements of chlorophyll (Phytoplankton Color Index, PCI) for >50 years have been collected by the Continuous Plankton Recorder. Here we demonstrate a significant correlation between PCI and SeaWiFS Chl-*a* from 1997–2002. Combining both time series allows quantification of the stepwise increase in biomass in the mid-1980s; this regime shift corresponded to a 60% increase in Chl-*a*. This was a result of an 80% increase in Chl-*a* during winter, alongside a smaller summer increase. This new high-resolution data set on the monthly variation of Chl-*a* in the North Atlantic since 1948 is now available for the development and validation of climate models, and for interpretation of ecological changes related to climate.

**Citation:** Raitsos, D. E., P. C. Reid, S. J. Lavender, M. Edwards, and A. J. Richardson (2005), Extending the SeaWiFS chlorophyll data set back 50 years in the northeast Atlantic, *Geophys. Res. Lett.*, 32, L06603, doi:10.1029/2005GL022484.

### 1. Introduction

[2] Phytoplankton produce >45% of the primary production of plants on Earth [Falkowski *et al.*, 2004], absorb the greenhouse gas carbon dioxide (CO<sub>2</sub>) from the atmosphere, and contribute to the biological pump, which ensures that the climate of the world is much cooler than would otherwise be the case [Reid and Edwards, 2001]. Changes in phytoplankton composition and abundance may influence the biodiversity of other organisms such as zooplankton, fish, seabirds and marine mammals [Nybakken, 1997]. Despite the significant role of algal production in the oceans, the short time-series of large-scale chlorophyll patterns limits our understanding of the impact of global change on primary productivity and vice versa. Acquiring this information is essential for the further development of global climate change models.

[3] Here we investigate the potential relationship between Sea-viewing Wide Field-of-view Sensor (SeaWiFS) chlorophyll-*a* (Chl-*a*) measurements in the Central Northeast Atlantic and North Sea (1997–2002) and simultaneous in situ

measurements of the Phytoplankton Color Index (PCI). This index of chlorophyll was collected by the Continuous Plankton Recorder (CPR) survey, which is an upper-layer plankton monitoring programme that has operated in the North Sea and North Atlantic Ocean since 1931 [Reid *et al.*, 2003]. By combining data from both instruments, it is now possible to extend the SeaWiFS Chl-*a* data set back more than 50 years.

### 2. Methods

#### 2.1. CPR Plankton Data

[4] For this study, PCI data were extracted from the CPR database for the Central Northeast Atlantic and North Sea. For the period 1948–2002, the CPR survey collected more than 94000 samples (Figure 1a). The methodology of sampling and measurement of PCI has remained consistent since 1948 [Reid *et al.*, 2003]. Samples were collected by a high-speed plankton recorder (~15–20 knots) that is towed behind ‘ships of opportunity’ in the surface layer of the ocean (~10 m depth); one sample represents 18 km of tow. Accumulation of phytoplankton cells on the silk gives it a greenish color [Batten *et al.*, 2003]. Phytoplankton biomass or PCI is based on a relative scale of greenness and determined on the silk by reference to a standard color chart. There are four different ‘greenness’ values: 0 (no greenness), 1 (very pale green), 2 (pale green) or 6.5 (green). Categories of PCI are assigned numerical values based on acetone extracts [Colebrook and Robinson, 1965]. PCI is a unique estimate of phytoplankton biomass, as small phytoplankton cells that cannot be counted under the microscope contribute to the coloration of the filtering silk [Batten *et al.*, 2003].

#### 2.2. Satellite Data

[5] SeaWiFS data were acquired from the NASA GES DAAC and processed using SeaDAS version 4.4. Data used were Level 3 daily products (9 × 9 km<sup>2</sup> resolution) of the near-surface Chl-*a* concentration (mg m<sup>-3</sup>), estimated using the Ocean Chlorophyll 4 - version 4 (OC4-v4) algorithm [O’Reilly *et al.*, 1998]:

$$\text{Chl} - a = 10^{(0.366 - 3.067x + 1.930x^2 + 0.649x^3 - 1.532x^4)},$$

$$\text{where } x = \log_{10} ((R_{rs}443 > R_{rs}490 > R_{rs}510)/R_{rs}555)$$

Processing these data requires a series of radiometric corrections (e.g. atmospheric) to eliminate the presence of clouds, haze and water vapour [Mueller and Austin, 1995].

#### 2.3. Data Analysis

[6] Sixty-four months (September 1997–December 2002) of in situ measurements of PCI and satellite Chl-*a*

<sup>1</sup>School of Earth, Ocean and Environmental Sciences, University of Plymouth, Plymouth, UK.

<sup>2</sup>Sir Alister Hardy Foundation for Ocean Science, Plymouth, UK.

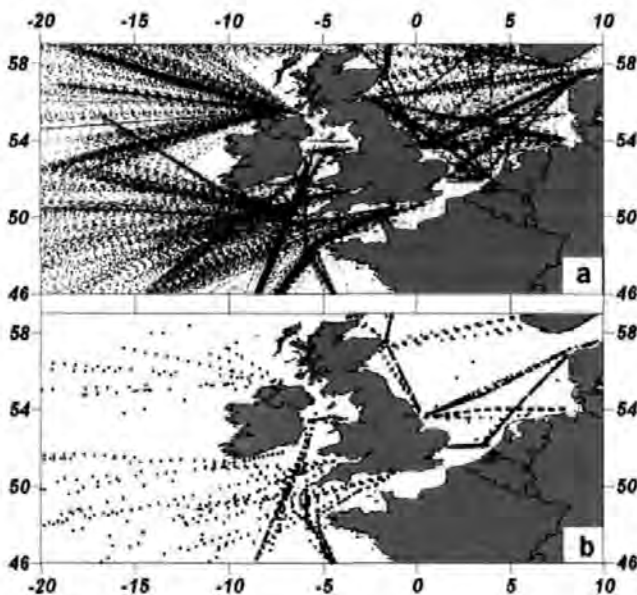


**Figure 1.** (a) Location of Continuous Plankton Recorder samples ( $n = 94,376$ ) in the Central Northeast Atlantic Ocean and North Sea for the period 1948–2002. (b) Distribution of match-ups of CPR/SeaWiFS measurements ( $n = 1585$ ) for the years 1997–2002.

values were compared for the area of the Central Northeast Atlantic and North Sea. Concurrent SeaWiFS and CPR measurements were compared for the same spatial and temporal (daily) coverage. In the area of study, the CPR survey collected 11149 different samples for the 5-year period. After screening the SeaWiFS data set for CPR match-ups, only 1585 samples could be used for comparison (86.7% of data did not have a SeaWiFS match-up, primarily due to cloud coverage) (Figure 1b). PCI data is on a ratio scale (i.e. not only can PCI categories be ranked but differences are quantified). Thus, Pearson correlation (or linear regression) is appropriate to assess the strength of the relationship between SeaWiFS and PCI data (StatSoft, Inc., Electronic Statistics Textbook, <http://www.statsoft.com/textbook/stathome.html>). SeaWiFS data were log-transformed to improve homogeneity of variance and normality [Zar, 1984].

#### 2.4. Potential Biases

[7] Consistency and comparability of the methodology used in the CPR survey has been studied in some depth [Reid *et al.*, 2003]. Although standard methods have been used for more than 50 years in the survey, the PCI has been measured by a number of different analysts during this time. However, measuring greenness is a simple task that is typically undertaken by 2 to 3 people in a year, many of whom have done this work for more than a decade. As well as referring to a standard color chart, apprentices are trained in assessing PCI for a year before they undertake the task on their own.

[8] The study area includes both Case I and Case II waters. In optically-complex Case II waters, Chl-*a* can not readily be distinguished from particulate matter and/or yellow substances (dissolved organic matter) and so global chlorophyll algorithms (such as OC4-v4) are less reliable [International Ocean-Colour Coordinating Group, 2000].

As the majority of the area included in this study comprises Case I water this bias influences only a small proportion of the data points (Figure 1b).

### 3. Results and Discussion

[9] We first examined the overall relationship between PCI and SeaWiFS Chl-*a* for the whole study area (Figure 2a). There is a significant positive relationship ( $r = 0.33$ ,  $p < 0.001$ ). This relationship is confirmed and strengthened when spatial and temporal autocorrelation are considered ( $r = 0.47$ ,  $F = 15.38$ , Adjusted  $df = 53$ ,  $p = 0.0003$ ). (We removed spatial autocorrelation by calculating the monthly average for the entire area of interest for PCI and matched SeaWiFS data. The Pearson correlation between these monthly time series was then calculated, and the degrees of freedom and thus the significance level of this test procedure were adjusted [Pyper and Peterman, 1998]).

[10] As the relationship between SeaWiFS Chl-*a* and PCI is non-linear, we calculated the mean of SeaWiFS Chl-*a* for each PCI category (Figure 2a). There is a relatively small variation in the confidence intervals of Chl-*a* for the first three PCI categories (no green (NG) =  $1.03 \pm 0.21 \text{ mg m}^{-3}$ , very pale green (VPG) =  $1.65 \pm 0.16 \text{ mg m}^{-3}$ , pale green (PG) =  $2.61 \pm 0.29 \text{ mg m}^{-3}$  with maximum variation in the fourth category (green (G) =  $4.25 \pm 0.98 \text{ mg m}^{-3}$ ). There is

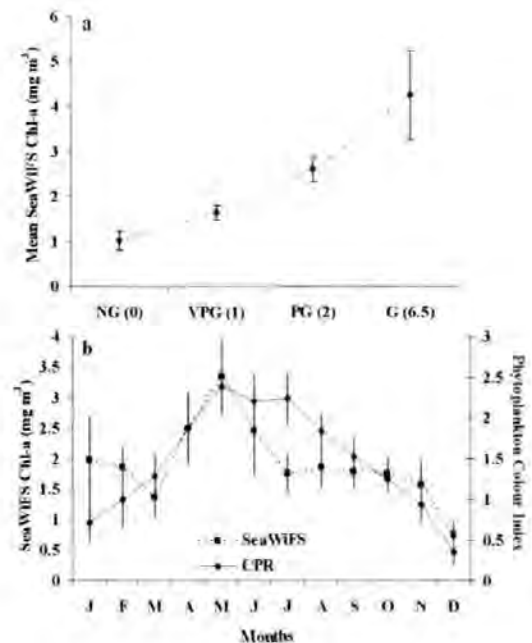


**Figure 2.** (a) Mean Chl-*a* derived from SeaWiFS match-ups with CPR samples plotted against the equivalent values of PCI categories. Standard error bars represent 95% confidence intervals of the mean Chl-*a*. Note there is no overlap between confidence intervals for each PCI category. The number of samples ( $n$ ) for each category is: No Green (NG) = 219, Very Pale Green (VPG) = 723, Pale Green (PG) = 484 and Green (G) = 162 of the 1585 match-ups. (b) The seasonal cycle of Chl-*a* estimated from PCI and SeaWiFS for all match-ups in the area of interest. Error bars represent 95% confidence intervals.



clear differentiation in mean Chl-*a* among PCI categories (95% confidence intervals do not overlap), so these values can be used retrospectively to estimate Chl-*a* from PCI values.

[11] To explore the seasonal patterns of PCI and SeaWiFS, we plotted the monthly means of both data sets (Figure 2b). Seasonal cycles for both show similar patterns, with a peak during late spring (spring bloom) and a decline during autumn and winter. The correlation coefficient implies a significant positive relationship ( $r = 0.79$ ,  $p < 0.01$ ). For all months except July, the 95% confidence intervals overlap, indicating good agreement between the two Chl-*a* measures. It is possible that an increase of dinoflagellates in CPR samples in summer may have contributed to the difference in July, as they are the dominant phytoplankton at this time and give a brownish color to the CPR silks and so could potentially lead to overestimates of Chl-*a* from PCI.

[12] Using the significant relationship between the PCI and Chl-*a* (Figure 2a) and the results of the >94000 CPR samples analysed in the period 1948–2002 (Figure 1a), a retrospective calculation of Chl-*a* averaged for the Central Northeast Atlantic and North Sea has been produced (Figure 3). While the changes shown have been demonstrated previously in a semi-quantitative manner for the PCI [Reid *et al.*, 1998], the current results confirm and quantify the observations. An increasing trend is apparent in mean Chl-*a* for the area of study over the period 1948–2002 (Figure 3). There is clear evidence for a stepwise increase after the mid-1980s, with a minimum of  $1.3 \text{ mg m}^{-3}$  in 1950 and a peak annual mean of  $2.1 \text{ mg m}^{-3}$  in 1989 (62% increase). Post 1986 levels of Chl-*a* have increased systematically during winter (80% increase), with generally higher values in summer as well (Figure 3). The marked increase in chlorophyll seen in the mid 1980s is part of what has been termed a regime shift, a stepwise alteration in the composition and productivity of the whole ecosystem at a regional scale that reflects major hydrographic change [Beaugrand, 2004; Reid *et al.*, 2001]. Changes through time in the PCI are significantly correlated with both sea surface temperature and Northern Hemisphere Temperature [Beaugrand and Reid, 2003]. A climate signal is strongly evident in all trophic levels of the marine system in the North Atlantic and North Sea, although the mechanisms underlying such relationships are not fully understood [Richardson and Schoeman, 2004].

[13] We can develop new insights into decadal changes in phytoplankton standing stock by combining data from SeaWiFS Chl-*a* and PCI, although each have strengths and acknowledged weaknesses. The strength of satellite remote sensing (e.g. SeaWiFS) is its ability to obtain information on phytoplankton distribution and abundance over large spatial scales. For instance, SeaWiFS has been used extensively to assess the role that global oceanic photosynthesis plays in climate and fisheries [McClain *et al.*, 1998]. The PCI is an alternative way of assessing the major temporal and spatial patterns of phytoplankton biomass over almost 60 years in the North Atlantic [Colebrook and Robinson, 1965; Reid *et al.*, 1998]. However, both the PCI and SeaWiFS have limitations. The PCI provides a visual (semi-quantitative) estimate of phytoplankton biomass, which has only previously been coarsely calibrated with chlorophyll acetone extracts [Colebrook and Robinson,

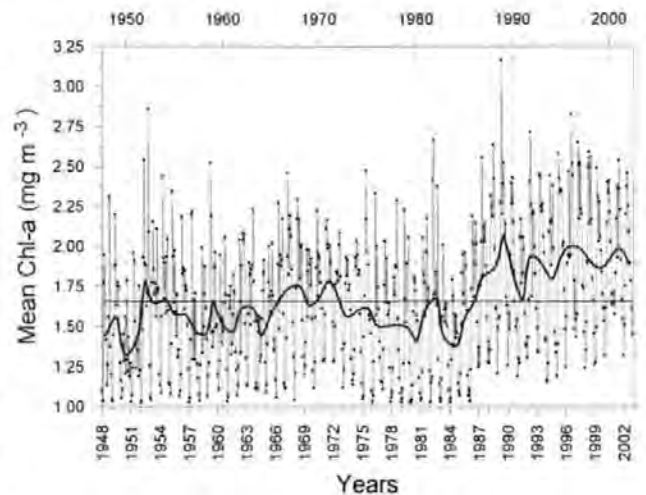


**Figure 3.** Time-series of the new Chl-*a* data set (monthly average) for the period 1948 to 2002 in the Central Northeast Atlantic and North Sea. The annual mean of Chl-*a* is plotted as a bold black line and the overall mean ( $1.678$ ) as a horizontal line.

1965], and its coverage is restricted to shipping routes [Reid *et al.*, 2003]. By contrast, SeaWiFS has limitations due to its limited lifespan, making it impossible to investigate decadal changes in phytoplankton. Problems with SeaWiFS data associated with restricted coverage due to clouds [McClain *et al.*, 1998] are also highlighted in the present study where only 13% of the in situ PCI data could be used for comparison with SeaWiFS, and in a recent comparative study where only about 2–3% could be used [Hooker and McClain, 2000].

[14] The oceans are increasingly recognised as a key component of the climate system [Bigg *et al.*, 2003] and have recently been shown to be the only true sink for anthropogenic  $\text{CO}_2$  over the last 200 years [Sabine *et al.*, 2004]. The same study showed that this oceanic sink of the key greenhouse gas  $\text{CO}_2$  may well be declining, at the same time as the strength of the terrestrial biosphere sink remains constant. If true, this result implies that concentrations of atmospheric  $\text{CO}_2$  are likely to increase at a more rapid rate over the next 100 years than currently predicted. Primary production and phytoplankton composition play a key role in the modulation of radiatively-important gases such as  $\text{CO}_2$  and also produces reactive gases that contribute to the formation of clouds and effect albedo. Increasing levels of atmospheric  $\text{CO}_2$ , which consequently causes significant changes in surface ocean pH and carbonate chemistry, impact phytoplankton with calcareous body parts such as coccolithophores [Riebesell *et al.*, 2000]. Given this background and the fact that primary production is at present not included in global climate models emphasises the importance of obtaining appropriate temporal-spatial data on phytoplankton.

#### 4. Conclusion

[15] Our results make available for the first time data on the monthly variation of plant biomass (Chl-*a*) in the NE Atlantic and North Sea since 1948. This now allows quantification of the stepwise increase in plant biomass in the mid-1980s; this regime shift corresponded to a 60%

increase in Chl-*a*. This increase is mainly due to the 80% increase in Chl-*a* during winter since the mid-1980s, alongside a smaller increase during summer. This new chlorophyll data set (based on >94000 stations), along with physical, biological and chemical parameters, can now be assimilated into the next generation of climate models. This will not only open up new possibilities for modelling marine ecosystems on a regional and oceanic scale, but should also advance our understanding of biogeochemical cycling and improve our predictive capability of the impacts of climate change.

[16] **Acknowledgments.** We are grateful to present and past staff of SAHFOS who have contributed to the maintenance of the CPR time series. We also acknowledge the important co-operation received from agents, owners, masters and crew of the towing vessels. The survey is supported by a consortium comprising IOC, the European Commission, and agencies from Canada, France, Faroes, Iceland, Ireland, the Netherlands, Portugal, Spain, the United Kingdom and the USA. Finally we would like to acknowledge the assistance of Gregory Beaugrand, Christos Maravelias, Yaswant Pradhan, Anthony Walne and Helena Oikonomou. D. E. Raitsos is supported by a scholarship from the University of Plymouth. This study was also supported by the UK Natural Environment Research Council through the Atlantic Meridional Transect consortium (NER/O/S/2001/00680) and Centre for Observation of Air-Sea Interactions and Fluxes (CASIX). This is contribution number 89 of the AMT programme and number 34 for CASIX. The authors would like to thank the SeaWiFS Project (Code 970.2) and the Goddard Earth Sciences Data and Information Services Center/Distributed Active Archive Center (Code 902) at the Goddard Space Flight Center, Greenbelt, MD 20771 for the production and distribution of the SeaWiFS Level 3 data. These activities are sponsored by NASA's Earth Science Enterprise.

## References

- Batten, S. D., A. W. Walne, M. Edwards, and S. B. Groom (2003), Phytoplankton biomass from continuous plankton recorder data: An assessment of the phytoplankton colour index, *J. Plankton Res.*, **25**, 697–702.
- Beaugrand, G. (2004), The North Sea regime shift: Evidence, causes, mechanisms and consequences, *Prog. Oceanogr.*, **60**, 245–262.
- Beaugrand, G., and P. C. Reid (2003), Long-term changes in phytoplankton, zooplankton and salmon related to climate, *Global Change Biol.*, **9**, 801–817.
- Bigg, G. R., T. D. Jickells, P. S. Liss, and T. J. Osborn (2003), The role of the oceans in climate, *Int. J. Climatol.*, **23**, 1127–1159.
- Colebrook, J. M., and G. A. Robinson (1965), Continuous plankton records: Seasonal cycles of phytoplankton and copepods in the north-eastern Atlantic and North Sea, *Mar. Ecol.*, **6**, 123–139.
- Falkowski, P. G., et al. (2004), The evolution of modern eukaryotic phytoplankton, *Science*, **305**, 354–360.
- Hooker, S. B., and C. R. McClain (2000), The calibration and validation of SeaWiFS data, *Prog. Oceanogr.*, **45**, 427–465.
- International Ocean-Colour Coordinating Group (2000), Remote sensing of ocean colour in coastal, and other optically-complex waters, *Rep. Int. Ocean-Colour Coord. Group 3*, edited by S. Sathyendranath, Dartmouth, N. S., Canada.
- McClain, C. R., et al. (1998), Science quality SeaWiFS data for global biosphere research, *Sea Technol.*, **39**(9), 10–16.
- Mueller, J. L., and R. W. Austin (1995), Ocean optics protocols for SeaWiFS validation, revision 1. SeaWiFS Technical Report Series, *NASA Tech. Memo.*, **104566**(25), 67 pp.
- Nybakken, J. W. (1997), *Marine Biology: An Ecological Approach*, 4th ed., 481 pp., Addison-Wesley, Boston, Mass.
- O'Reilly, J. E., et al. (1998), Ocean colour chlorophyll algorithms for SeaWiFS, *J. Geophys. Res.*, **103**, 24,937–24,953.
- Pyper, B. J., and R. M. Peterman (1998), Comparison of methods to account for autocorrelation in correlation analyses of fish data, *Can. J. Fish. Aquat. Sci.*, **55**, 2127.
- Reid, P. C., and M. Edwards (2001), Plankton and climate, in *Encyclopedia of Ocean Sciences*, edited by J. H. Steele, S. A. Thorpe, and K. K. Turekian, pp. 2194–2200, Elsevier, New York.
- Reid, P. C., M. Edwards, H. G. Hunt, and A. J. Warner (1998), Phytoplankton change in the North Atlantic, *Nature*, **391**, 546.
- Reid, P. C., M. F. Borges, and E. Svendsen (2001), A regime shift in the North Sea circa 1988 linked to changes in the North Sea horse mackerel fishery, *Fish. Res.*, **50**, 163–171.
- Reid, P. C., J. B. L. Mathews, and M. A. Smith (Eds.) (2003), Achievements of the Continuous Plankton Recorder survey and a vision for its future, *Prog. Oceanogr.*, **58**, 115–358.
- Richardson, A. J., and D. S. Schoeman (2004), Climate impact on plankton ecosystems in the northeast Atlantic, *Science*, **305**, 1609–1612.
- Riebesell, U., et al. (2000), Reduced calcification of marine plankton in response to increased atmospheric CO<sub>2</sub>, *Nature*, **407**, 364–367.
- Sabine, C. L., et al. (2004), The oceanic sink for anthropogenic CO<sub>2</sub>, *Science*, **305**, 367–371.
- Zar, J. H. (1984), *Biostatistical Analysis*, 2nd ed., Prentice-Hall, Upper Saddle River, N. J.

M. Edwards, P. C. Reid, and A. J. Richardson, Sir Alister Hardy Foundation for Ocean Science, The Laboratory, Citadel Hill, Plymouth, PL1 2PB, UK.

S. J. Lavender and D. E. Raitsos, School of Earth, Ocean and Environmental Sciences, University of Plymouth, Drake Circus, Plymouth, PL4 8AA, UK. (dionysios.raitsos-exarcho@plymouth.ac.uk)

## Coccolithophore bloom size variation in response to the regional environment of the subarctic North Atlantic

*Dionysios E. Raitsos*

School of Earth, Ocean and Environmental Sciences (SEOES), University of Plymouth, Drake Circus, Plymouth PL4 8AA, United Kingdom; Sir Alister Hardy Foundation for Ocean Science (SAHFOS), The Laboratory, Citadel Hill, Plymouth PL1 2PB, United Kingdom

*Samantha J. Lavender and Yaswant Pradhan*

School of Earth, Ocean and Environmental Sciences (SEOES), University of Plymouth, Drake Circus, Plymouth PL4 8AA, United Kingdom

*Toby Tyrrell*

School of Ocean and Earth Science, Southampton Oceanography Center, University of Southampton, Southampton SO14 3ZH, United Kingdom

*Philip C. Reid and Martin Edwards*

Sir Alister Hardy Foundation for Ocean Science (SAHFOS), The Laboratory, Citadel Hill, Plymouth PL1 2PB, United Kingdom

### Abstract

Several environmental/physical variables derived from satellite and in situ data sets were used to understand the variability of coccolithophore abundance in the subarctic North Atlantic. The 7-yr (1997–2004) time-series analysis showed that the combined effects of high solar radiation, shallow mixed layer depth (<20 m), and increased temperatures explained >89% of the coccolithophore variation. The June 1998 bloom, which was associated with high light intensity, unusually high sea-surface temperature, and a very shallow mixed layer, was found to be one of the most extensive (>995,000 km<sup>2</sup>) blooms ever recorded. There was a pronounced sea-surface temperature shift in the mid-1990s with a peak in 1998, suggesting that exceptionally large blooms are caused by pronounced environmental conditions and the variability of the physical environment strongly affects the spatial extent of these blooms. Consequently, if the physical environment varies, the effects of these blooms on the atmospheric and oceanic environment will vary as well.

### Acknowledgments

We thank present and past staff of SAHFOS who have contributed to the maintenance of the continuous plankton recorder (CPR) time series, and especially to the senior analyst of the CPR survey (Anthony Jones) for his assistance in the analysis of the archived CPR samples. We also thank Anthony J. Richardson, Christos D. Maravelias (regarding the analysis of generalized additive models), and Tim Smyth for useful discussions. Special thanks to Marian Scott, Department of Statistics, University of Glasgow. We acknowledge Norman Kuring, for providing the true color image of the bloom (Created by the SeaWiFS Project, NASA/Goddard Space Flight Center, and ORBIMAGE). Reanalysis data was provided by the National Oceanic and Atmospheric Administration/Cooperative Institute for Research in Environmental Sciences Climate Diagnostics Center, Boulder, Colorado, from their Web site at <http://www.cdc.noaa.gov/>. The authors thank the anonymous reviewers for their helpful comments and suggestions.

D. E. Raitsos is supported by a scholarship from the University of Plymouth. This study was also supported by the U.K. Natural Environment Research Council through the Atlantic Meridional Transect consortium (NER/O/S/2001/00680) and Center for Observation of Air-Sea Interactions and Fluxes (CASIX).

This is contribution 113 of the AMT program and 38 for CASIX.

*Emiliana huxleyi* is a relatively small (about 5–10 µm diameter) phytoplankton species belonging to the taxonomic group of coccolithophores, which is capable of forming spatially extensive blooms greater than the size of the United Kingdom. As the species can be visually detected, by turning dark-blue oceanic waters milky-turquoise in color (because of scattering caused by the coccoliths), the extensive blooms that it forms are visible from space (via satellites). That is why more is known about the spatial distribution of this phytoplankton species than any other (Tyrrell and Merico 2004). Blooms exceeding 250,000 km<sup>2</sup> in size, like the 1991 North Atlantic bloom (based on the advanced very high resolution radiometer [AVHRR], Holligan et al. 1993), may have significant effects on the oceanic as well as atmospheric environment (Tyrrell and Merico 2004). Also, coccolithophores are major producers of several substances (e.g., dimethyl sulfide, calcium carbonate, and organic carbon) that are thought to affect the climate (Holligan 1993).

Although satellites have been characterized as excellent tools for detecting and mapping *E. huxleyi* (Tyrrell and Merico 2004), several cases have shown that not all bright waters are caused by this species. Examples of water conditions that mimic *E. huxleyi*, or in other words mimic

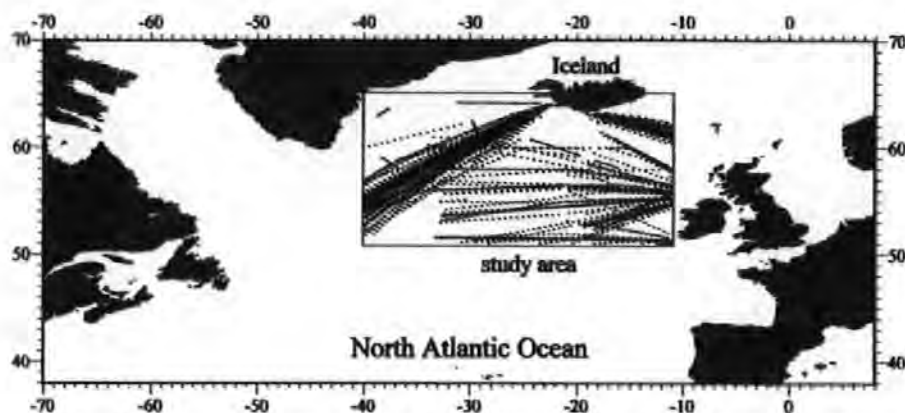


Fig. 1. Study area of the subarctic North Atlantic defined by the coordinates 51°–66°N and 11°–40°W. The black dots represent the CPR samples taken from January 1998 to December 2002 ( $n = 3,977$ ).

the highly reflective characteristics of coccolithophore blooms with significant numbers of liths, include broken-up diatom frustules (Broerse et al. 2003), shallow carbonate shelves (Brown and Yoder 1994), and suspended sulfur particles (Weeks et al. 2002). Generally, it is only very infrequently that open ocean turquoise waters should be ascribed to species other than *E. huxleyi* (Weeks et al. 2004); however, it is essential that in situ verification is obtained before significant conclusions are drawn (Tyrrell and Merico 2004). This in situ verification can be acquired from the Continuous Plankton Recorder (CPR) survey, which has been running in the North Atlantic Ocean and North Sea for approximately 50 years (Reid et al. 2003) and contains details of the plankton from >170,000 samples taken since 1946.

Several environmental, physical, and chemical factors can induce *E. huxleyi* blooms; although one factor alone is unlikely to trigger a bloom. Briefly, this coccolithophore species inhabits the subsurface layer (mixed layer depth ~20 m; Balch et al. 1991) in highly stratified waters (caused by sunny and calm weather) where light intensity is high (Nanninga and Tyrrell 1996). An environmental parameter that may have an indirect effect on coccolithophores (through stratification) is wind stress, which is responsible for vertical mixing in the water column. It was thought (Tyrrell and Taylor 1996) that *E. huxleyi* blooms are favored by inorganic phosphate being more limiting than nitrate, but a recent review showed that the Bering Sea and other blooms occurred in nitrate-scarce, phosphate-replete waters (Lessard et al. 2005). *E. huxleyi* is also found in waters where carbonate saturation is high (Tyrrell and Merico 2004), silicate concentration is low (Brown and Yoder 1994), and iron concentration is low (Brand et al. 1983). In addition, positive temperature and negative salinity anomalies (associated with strong haline stratification) have been correlated with coccolithophore blooms in the Barents Sea (Smyth et al. 2004). Iglesias-Rodriguez et al. (2002) reported that water temperature combined with other factors, such as high light intensity, critical irradiance (stratification relative to light level), and declining nitrate concentrations appeared to be a good predictor of *E. huxleyi*. However, it is thought to be due to secondary

effects, i.e., water stratification (Tyrrell and Merico 2004). Although many attempts have been made to study the biogeochemistry of these blooms, little information is known on the effect of the physical environment in the subarctic North Atlantic.

The purpose of this paper was to examine the causative physical factors and/or environmental extremes that induce extensive coccolithophore blooms, detected by the sea-viewing wide field-of-view sensor (SeaWiFS), in the subarctic North Atlantic. The geophysical variables used in the analysis are solar radiation, sea surface temperature (SST) and its anomaly (SSTA), mixed layer depth (MLD), and wind stress. Particular attention was paid to a massive *E. huxleyi* bloom that occurred in June 1998.

#### Data and methods

All satellite, in situ, and modeled data sets were for the same study area. The area of study, the subarctic North Atlantic, was defined by a 51°N–66°N latitude range and 40°W–11°W longitude range (Fig. 1).

#### Satellite data

**SeaWiFS**—The current reprocessed version (v5.1) produced by the Ocean Biology Processing Group was acquired from the NASA OceanColor web site (<http://oceancolor.gsfc.nasa.gov/>). The data were Level 3 monthly composite products (9 × 9 km<sup>2</sup> resolution) of the normalized water-leaving radiance (nLw) at 555 nm ([nLw<sub>555</sub>] mW cm<sup>-2</sup> μm<sup>-1</sup> sr<sup>-1</sup>) for the period from September 1997 to December 2004 (>7 years of data). These data were used as the temporal and spatial variability of coccolithophore blooms, which has been routinely followed using SeaWiFS imagery (Cokacar et al. 2004). The size of the 1998 coccolithophore bloom (15 June 1998, Fig. 2A) detected by SeaWiFS was calculated by recording the number of pixels where nLw<sub>555</sub> was >0.9 mW cm<sup>-2</sup> μm<sup>-1</sup> sr<sup>-1</sup> (Cokacar et al. 2004).

**AVHRR**—The nighttime AVHRR Pathfinder 5 (P5) monthly mean SSTs at 9 × 9 km<sup>2</sup> resolution were obtained

from the NASA PO.DAAC web site (<http://poet.jpl.nasa.gov>). Then, the monthly mean climatologies were computed from 1985–2004, and the SSTA was the deviation of the SST from the mean climatology. The nighttime SST products were used so that the solar radiation bias (the diurnal fluctuation in SST) that can occur during the daytime could be avoided.

*The NCEP/NCAR (National Center for Environmental Prediction/National Center for Atmospheric Research) reanalysis data*—Monthly composites of mean wind speed ( $\text{m s}^{-1}$ ) data were obtained ( $2.5^\circ \times 2.5^\circ$  spatial resolution) from which the wind stress (Pa) was calculated (September 1997 to December 2004). The stress exerted by the surface wind (at 10 m above the sea surface) is derived as a function of wind speed, nondimensional drag coefficient, and boundary layer air density (Pickard and Pond 1978):

$$\tau = \rho_a C_D |W|W$$

Where  $\rho_a$  is the average air density ( $\sim 1.3 \text{ kg m}^{-3}$ ),  $W$  is the wind speed over the sea surface (for most practical purposes, a 10-m height wind speed,  $W_{10}$ , is acceptable), and  $C_D$  is the dimensionless drag coefficient that varies with wind speed as (Yelland and Taylor 1996):

$$C_D = \left( 0.29 + \frac{3.1}{W_{10}} + \frac{7.7}{W_{10}^2} \right) 10^{-3} \quad \text{for } (3 \leq W_{10} < 6 \text{ m s}^{-1})$$

$$C_D = (0.60 + 0.07 W_{10}) 10^{-3} \quad \text{for } (6 \leq W_{10} \leq 26 \text{ m s}^{-1})$$

Sea surface wind stress drives the dynamics of the boundary layer and is therefore expected, on physical grounds, to be closely related to the generation of surface waves, production of wind-driven ocean surface currents, and the stirring processes that keep the upper ocean well mixed down to the thermocline. The spatial variation of wind stress over the ocean causes surface divergence of horizontal flow that in turn gives rise to vertical mass flux through Ekman pumping (Ekman 1905). Because coccolithophores are likely to be found in highly stratified waters, the wind stress (as well as MLD, *see below*) was used to confirm the presence of these conditions.

Monthly composites of mean downward solar radiation flux ( $\text{W m}^{-2}$ ) data were obtained for the period of 1997–2004 ( $2.5^\circ \times 2.5^\circ$  spatial resolution). We used the NCEP/NCAR reanalyzed surface downward solar radiation flux, which was estimated at the bottom of the atmosphere (Kalnay et al. 1996) and therefore considered as the solar radiation received at the earth's surface. Reanalysis data were provided by the National Oceanic and Atmospheric Administration/Cooperative Institute for Research in Environmental Sciences Climate Diagnostics Center, Boulder, Colorado, from their web site (<http://www.cdc.noaa.gov>).

### OCCAM model data

The MLD data set was obtained from the Ocean Circulation and Climate Advanced Modeling Project (OCCAM) that runs a high-resolution global ocean model. The monthly mean MLD (m) product ( $0.25^\circ \times 0.25^\circ$  resolution) for the North Atlantic and Arctic Ocean model

domain was used. Then, an averaged time series was created for the period from September 1997 to December 2003.

Generally, the modeled MLDs are based on a variety of physical variables such as wind speed, wind stress, and latent heat fluxes, thus the estimation of MLDs are most consistent with a large number of data sources. For instance, the primary OCCAM model variables were potential temperature, horizontal velocity, and sea surface elevation (Webb et al. 1998). More technical details of the OCCAM model can be found elsewhere (Webb et al. 1998). The data were ordered from the official web site of the OCCAM model (<http://www.noc.soton.ac.uk/JRD/OCCAM/EMODS/>).

### In situ data

In situ measurements of coccolithophore numbers were derived from the CPR survey, which is an upper-layer plankton monitoring program that has operated in the North Sea and North Atlantic Ocean since 1946. However, from the beginning of the CPR survey until 1993 sample analysis consisted of recording only the presence/absence of coccolithophores, whereas beginning in 1993 the number of cells was also recorded (Hays et al. 1995). Samples were collected by a high-speed plankton recorder ( $\sim 27$ – $37 \text{ km h}^{-1}$ ) that is towed behind “ships of opportunity” in the surface layer of the ocean ( $\sim 6$ – $10$ -m depth); one sample represents  $\sim 18 \text{ km}$  of tow (Reid et al. 2003). Plankton are filtered onto a constantly moving (powered by an impeller) band of silk mesh (mesh size  $270 \mu\text{m}$ ).

Although *E. huxleyi* is only  $5$ – $10 \mu\text{m}$  in diameter, it is reported that this species has been identified repeatedly in the CPR samples (Hays et al. 1995). Hays et al. (1995) suggested two possible reasons why this small coccolithophore species is present on CPR samples: plankton clogging up the filter and its capture on the finer threads of silk that constitute the mesh-weave.

The CPR analysis does not identify coccolithophores to the species level, but the archived samples are available for re-examination. Therefore, archived samples were reanalyzed to confirm if the bloom observed from a satellite was *E. huxleyi*. Data (number of coccolithophore cells per tow) for the North Atlantic were extracted from the CPR database between 1998 and 2002 (Fig. 1). The CPR took 95 samples within 6 days (1, 20, 21, 27, 28, and 29) of June 1998, and 30 of those appeared to be dominated by coccolithophores. These archived CPR samples (preserved in buffered formalin) were re-examined, and *E. huxleyi* was identified.

### Data analysis

Generalized additive models (GAMs) were used to investigate potential relationships between an index of coccolith abundance ( $\text{nLw}_{555}$ ) and various environmental parameters (solar radiation, SST, SSTA, MLD, and wind stress). GAM is a flexible regression technique; its advantage over traditional regression methods, such as general linear models, is its ability to model nonlinearities using non-

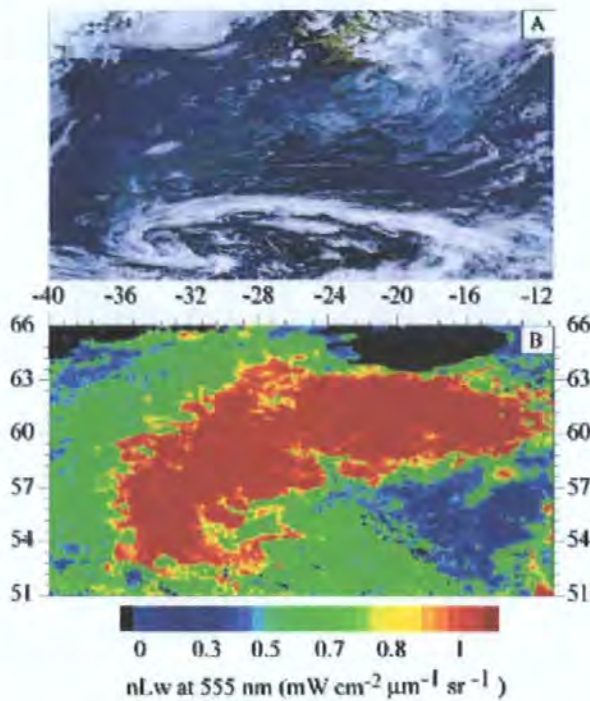


Fig. 2. (A) True color image of the coccolithophore bloom taken by SeaWiFS on 15 June 1998 in the study area of the subarctic North Atlantic. Provided by the SeaWiFS Project, NASA/Goddard Space Flight Center (GSFC), and ORBIMAGE. (B) Pseudocolor image presenting monthly mean of SeaWiFS nLw\_555 for June 1998.

parametric smoothers (Hastie and Tibshirani 1990). However, the algorithm that fits the curve is usually iterative and nonparametric, masking a great deal of complex numerical processing. A detailed description of GAMs can be found elsewhere (Hastie and Tibshirani 1990).

Seventy-six (number of monthly averages) data points were employed to develop the relationships for each parameter. The least squared weighted smoother (loess) was used to estimate the nonparametric function, and the Gaussian error distribution was assumed after consideration of diagnostic residual plots (Hastie and Tibshirani 1990; Maravelias 2001). To construct the GAM, a forward and backward stepwise model fitting approach was used based on the Akaike's information criterion (AIC) statistic (Chambers and Hastie 1992). All predictors in the model were included as smoothed terms. By using the AIC, the significance of each term in the model could be assessed. Also, the stepwise approach enabled the removal of the nonsignificant variables (predictors) from the final model. Hence, the final models showed the combined effect of each predictor (physical variable) on response (nLw\_555).

## Results

To explore the seasonal cycle of coccolithophores, the monthly means of both time series data (CPR and SeaWiFS nLw\_555) were plotted against time for the

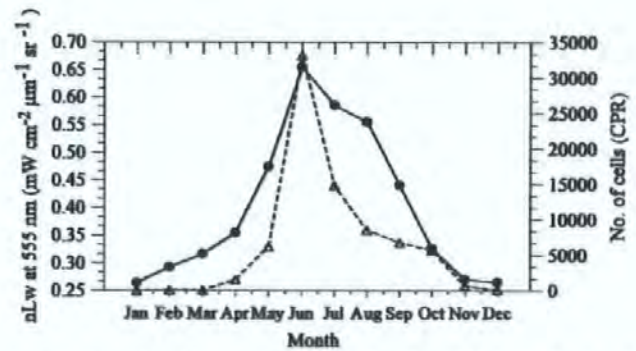


Fig. 3. Monthly mean of SeaWiFS nLw\_555 (solid line) and CPR coccolithophore numbers (dashed line) from January 1998 to December 2002 (3,977 samples) in the study area. The spatial distribution of the samples can be seen in Figure 1.

period 1998–2002 (Fig. 3). A clear visual agreement can be seen, and the results suggest that both patterns exhibit seasonal cycles with similar trends: increasing during early summer (both peaked during June) and gradually decreasing during autumn/winter. However, there is a noticeable difference from July to September when the CPR values drop off rapidly while the nLw\_555 values remain high. Once the coccolithophore bloom starts to decline, the coccoliths are detached from the cells and float separately in the water. Therefore, the satellite still detects the reflectance resulting from these blooms (for optical properties of coccoliths see Voss et al. 1998), whereas the CPR is counting only the live cells and not the empty liths. It has been reported that when the coccolithophore bloom of 1991 aged, the number of the detached coccoliths increased (Balch et al. 1996a) and that suspended coccoliths were causing up to 80% of the total backscattering in the center of the bloom (Balch et al. 1996b). However, Figure 3 clearly shows that in the subarctic North Atlantic the favorable month for coccolithophores is June.

The time series composed of >7 years monthly nLw\_555 data indicated that the highest values (primarily from coccolithophores) occurred during the summer months and specifically June (Fig. 4A). The highest nLw annual mean occurred during 1998, and June appeared to have the highest nLw mean (~0.8) in this 7-yr time series; it showed an increase of ~25% when compared to the overall mean of the remaining June months. In addition, June 1998 appeared to occupy the largest aerial extent. Figure 2B shows that the spatial extent of the June 1998 coccolithophore bloom, and the calculated size (based on SeaWiFS) of this extensive bloom was >995,000 km<sup>2</sup> (15 June 1998). Also, an analysis of the archived in situ samples confirmed that this bloom was primarily composed of coccolithophores; *E. huxleyi* was present in almost all the samples. Coccolithophore blooms also occur in the other years, but their spatial extent appeared to be less pronounced (Fig. 4A).

Several environmental/physical parameters were plotted to examine their importance on coccolithophores (Fig. 4).

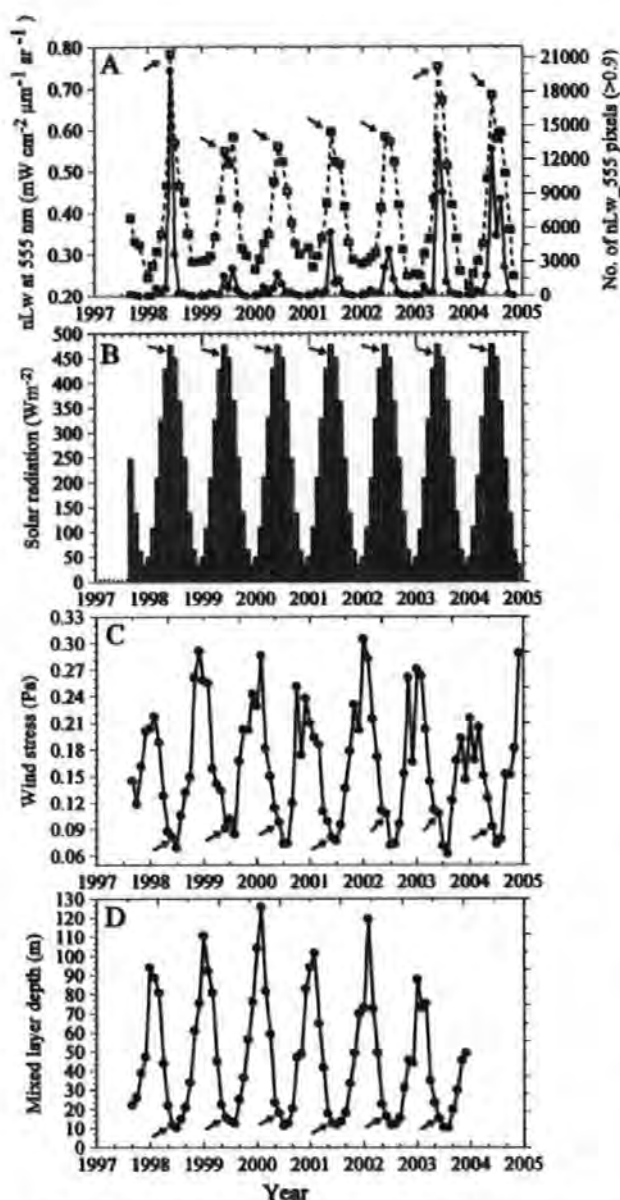


Fig. 4. Satellite time series: (A) The dashed line presents the nLw<sub>555</sub> (coccolithophore abundance) from September 1997 to December 2004, and the solid line presents the number of nLw<sub>555</sub> pixels  $>0.9 \text{ mW cm}^{-2} \mu\text{m}^{-1} \text{ sr}^{-1}$  (blooms areal extent). (B) solar radiation from September 1997 to December 2004. (C) Wind stress from September 1997 to December 2004. (D) MLD from September 1997 to December 2003. The arrows represent June of every year.

The incoming solar radiation time series indicated that the highest light intensity occurred during the summer months and peaked in June every year (mean of  $477 \text{ W m}^{-2}$ ), whereas the lowest light occurred during the winter months, with the lowest values during December (mean of  $35 \text{ W m}^{-2}$ ) (Fig. 4B).

Figure 4C shows that overall, July appeared to have had the lowest wind stress every year. The wind stress shows the

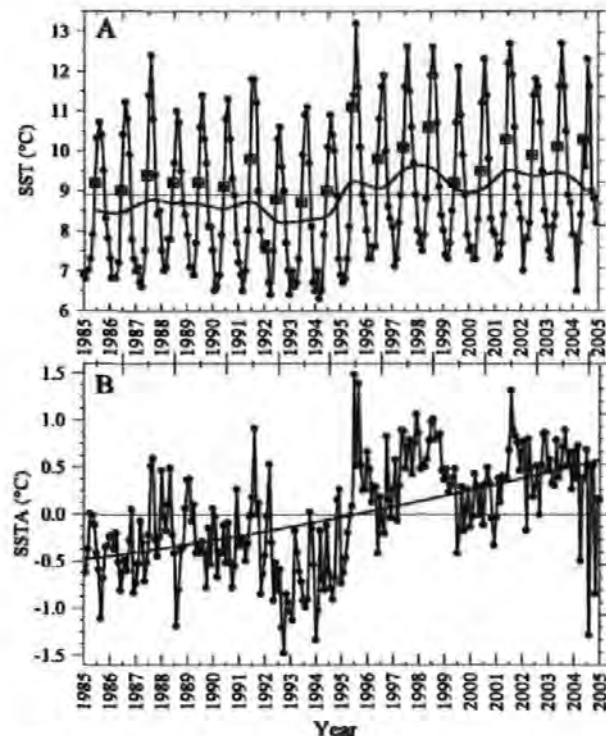


Fig. 5. (A) SST from January 1985 to December 2004. The thin horizontal line is the overall mean, and the thick line is the annual mean. The open boxes surrounding the dots represent June of every year. (B) SSTA from January 1985 to December 2004 (the black curve is a second order polynomial).

opposite pattern (negatively related) to SST (Fig. 5A); it is high during the autumn and winter months and decreases rapidly during the summer months, enabling summer stratification (favorable conditions for *E. huxleyi*). June 1998 and 2001 appeared to have the lowest mean wind stress (0.08 Pa) in comparison with the Junes of other years. However, the overall average for all Junes (0.095 Pa) does not differ considerably from the monthly mean of June 1998.

Figure 4D indicates that during autumn–winter months the MLD reaches the highest values, whereas during the summer months the MLD is decreasing rapidly (lowest in July). During June months (highest nLw<sub>555</sub> values), the overall MLD mean for the study area is 14.6 m, whereas the shallowest MLD of this time series appeared during June 1998 (11.6 m). These results confirm the presence of highly stratified and shallow mixed layer depth waters within the study area (during June months) that favor *E. huxleyi*. Note that the x-axis scale is different in Figure 4D than the preceding plots in Figure 4, because the MLD data was not available for 2004.

Figure 5A shows AVHRR SST (1985–2004) that has a pronounced change in this 20-yr time series, with evidence for a stepwise increase in 1996. It can be clearly seen that after this year the annual SST mean remains above the overall mean, whereas the opposite occurred before 1996. The annual mean showed that 1998 was the warmest year

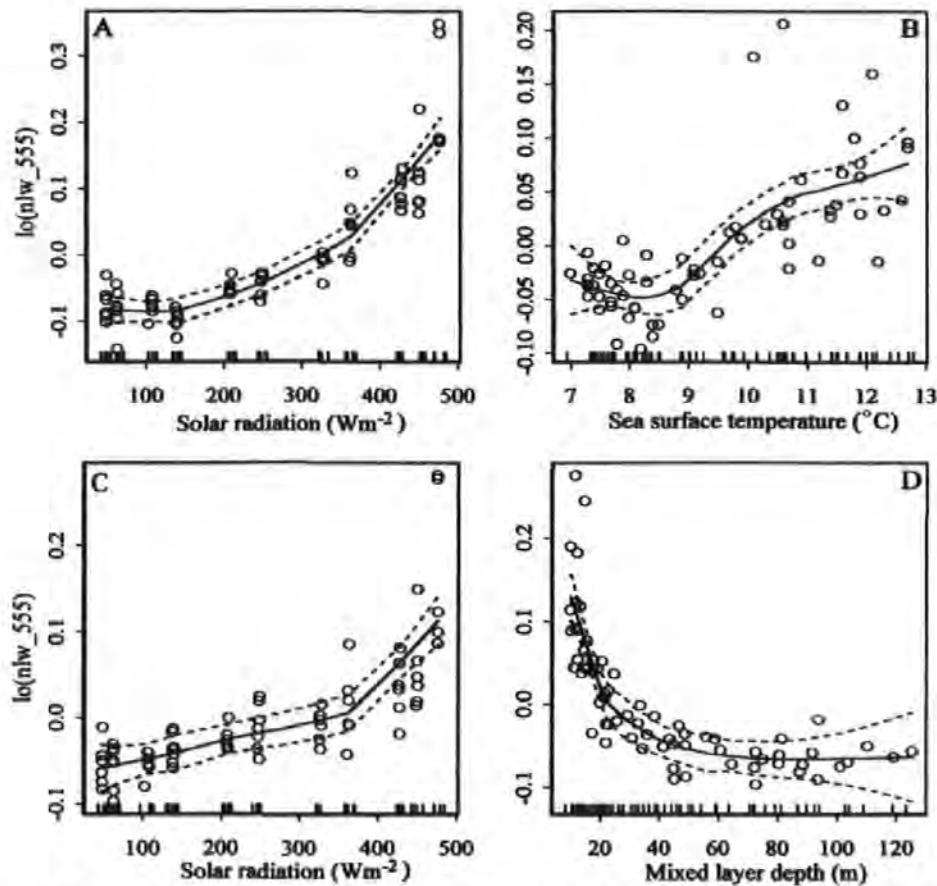


Fig. 6. GAM plots illustrate nonlinear relationships between the nLw\_555 variable (lo stands for loess smoother) and each predictor. Circles represent the raw data, the connected line is the spline, and the dashed lines are the 95% confidence intervals. (A) and (B) illustrate the final product of model 1 ( $r^2 = 0.896$ ), which incorporated solar radiation (A) and SST (B). (C) and (D) illustrate the final result of model 2 ( $r^2 = 0.894$ ), which incorporated solar radiation (C) and MLD (D).

(9.6°C) and June 1998 (when the extensive coccolithophore bloom occurred) and June 1995 appeared to be the warmest Junes of the 20-yr time series. Overall, the average temperature during all June months was 9.6°C, whereas in 1998 the monthly mean was 10.6°C (1°C above the mean).

It should be noted that *E. huxleyi* may trap light near to the surface layer; consequently, surface waters that are dominated with this species tend to have increased temperatures. In other words, the temperature might be increased because of *E. huxleyi* presence rather than the bloom benefiting from an already present increased temperature. The subarctic North Atlantic 1998 monthly SST data were warmer than the monthly SST data from other years for both the area within and outside of the bloom, which suggests that the temperature influenced the size of the bloom rather than the other way around in this particular case. In addition, it has been reported that 1998 was the warmest year in the record of instrumental measurements (Lu 2005). SSTA confirmed the SST

observations and also showed that 1998 was the most anomalous SST year, with June 1998 and 1995 being the most positively anomalous Junes of the time series (Fig. 5B); note that the spike in 2001 is July. In the study area, another extensive bloom was reported (based on AVHRR) during the summer of 1991 (Holligan et al. 1993). In Fig. 5 it can be seen that this year was relatively warm, with a high positive temperature anomaly and generally higher than average temperature (July 1991).

GAMs were also used to identify relationships between nLw\_555 and the environmental/physical parameters. It has to be noted that if two predictors (parameters) are highly correlated with each other, i.e., are not independent, then they can cause a problem in fitting a model involving both of them. The problem is usually that the parameter estimates are unstable and the model cannot be fitted (Scott pers. comm.). To avoid this, two different models should be used that will have all the independent variables. In our case, MLD and SST were highly negatively correlated (Spearman rank order correlation coefficient:  $r_s = -0.85$ ,



$p < 0.0001$ ); probably because of the fact that MLD was derived from temperature (see *Methods*). Consequently, model 1 (Fig. 6A,B) incorporated solar radiation, SST, SSTA, and wind stress, whereas model 2 (Fig. 6C,D) incorporated solar radiation, MLD, SSTA, and wind stress.

Using a stepwise approach, which enabled the removal of nonsignificant variables, model 1 indicated that the parameters to predict coccolithophore abundance (nLw\_555) should be solar radiation and SST (Fig. 6A,B). Both parameters were highly significant and explained 89.6% of the variation in coccolithophore abundance. Figure 6A indicated that coccolithophore abundance increased as the solar radiation (insolation) increased with this significant relationship ( $p < 0.00001$ ) exhibiting an early exponential increase that became linear after  $370 \text{ W m}^{-2}$  of solar radiation. For SST (Fig. 6B), the significant model ( $p = 0.0185$ ) showed that the coccolithophore abundance was low and reasonably constant until  $\sim 8.5^\circ\text{C}$  of SST, after which it increased rapidly as SST increased and then reached an optimal reflectance (nLw\_555) at  $12.5^\circ\text{C}$ . Although both parameters appeared to be significant, solar radiation explained the nLw\_555 variability more than SST.

Model 2 indicated that coccolithophore abundance should be predicted using solar radiation and MLD (Fig. 6C,D) and that the other factors were not significantly related to bloom formation; the combination of these two parameters explained 89.4% of the variation in coccolithophore abundance. As expected, solar radiation ( $p = 0.0002$ ) in Fig. 6C exhibited a similar pattern as in model 1, where it increased progressively along with coccolithophore abundance until the relationship increased rapidly and became linear after  $370 \text{ W m}^{-2}$  of solar radiation. The MLD appeared to be highly significantly negatively related ( $p < 0.00001$ ) with coccolithophore abundance. As can be seen from Fig. 6D, the coccolithophore abundance increased as the MLD values decreased. Specifically, below 20 m of MLD (shallow mixed layer) the relationship was linearly negative, whereas after that an exponential decay can be observed until it became stable below 65 m of MLD. In terms of significance, model 2 indicated that MLD was the most important parameter, because it explained the nLw\_555 variability more than solar radiation.

## Discussion

During June 1998 an extensive coccolithophore bloom occurred in the North Atlantic, and to our knowledge, this bloom is the most extensive coccolithophore bloom recorded by SeaWiFS ( $>995,000 \text{ km}^2$ ). This bloom has been compared to blooms reported in the literature and exceeds their size by a considerable margin, but these were analyzed with AVHRR (at least until 1997), which has a reduced sensitivity and broad waveband in the visible region of the electromagnetic spectrum.

In situ and satellite measurements indicated that coccolithophores in the subarctic North Atlantic occur at their highest abundance during late spring/early summer

and peak in June. The environmental variables used in the analysis suggested that the solar radiation was very high during June 1998 (as it was during every June), while the MLD was shallow (11.6 m). These results are in agreement with those of Balch et al. (1991) who mentioned that the MLD within coccolithophore blooms is shallow ( $\sim 20 \text{ m}$ ). In addition, June 1998 together with 1995 were the warmest and most positively anomalous Junes of the last 20 years.

Using the results of the time series, GAMs were used to identify which environmental/physical parameters were the most important for the formation of coccolithophore blooms. The two GAM models supported the observations and indicated that the combined effect of high solar radiation, shallow MLD, and increased SST were highly correlated with coccolithophore abundance (nLw\_555). Compared to other phytoplankton groups, such as diatoms, this coccolithophore species has an unusual tolerance for high light intensity (i.e., lacks photoinhibition) (Nanninga and Tyrrell 1996). Both models also indicated that wind stress was not a major factor contributing to bloom formation.

The 7-yr time series (Fig. 4C) indicated that there are no anomalous fluctuations (relatively stable seasonal cycle, at least during June months) that can be related to the bloom occurrence; nevertheless, it is suggested that the typical low wind stress (vertical mixing) during all Junes indirectly benefits bloom formation as it contributes to water-column stability. However, it must be noted that whenever high SST anomalies occur it does not mean that a bloom will be formed, but when it co-occurs with the timing of coccolithophores it will probably benefit the bloom. For instance, November 1997 (Fig. 5B) appeared to be the most positively anomalous month during 1997, but the nLw was very low because it was the wrong time of the year in terms of other parameters (Fig. 4A).

The in situ measurements (CPR) confirmed that the 1998 bloom was *E. huxleyi*, and the area of study is a well known region where large coccolithophore blooms and their relationships to the biogeochemical environment have been reported in the past (Holligan et al. 1993). Although the subarctic North Atlantic can be characterized as ideal for studying *E. huxleyi* blooms, information regarding the link between the extensive blooms of this species and the physical environment are limited. The use of physical/environmental data sets in the present study suggested that large blooms may be caused by distinct environmental conditions, i.e., high light intensities, very shallow MLDs, and positive SST anomalies. Also, our understanding of the coccolithophore bloom distribution pattern can be improved by learning more about their ecology. Knowing the effect of the physical as well as biogeochemical environment on this species, we may convey additional knowledge on the potential impact of climate change on coccolithophores.

It is thought that increasing levels of atmospheric carbon dioxide, which consequently cause significant changes in surface ocean pH (acidification), will be responsible for a reduction in calcifying phytoplankton such as coccolithophores (Riebesell et al. 2000). An indirect effect of

climate warming is that increasing temperatures alone or by contributing to ice melting (freshwater runoff) and consequently decreased salinity can lead to increased stratification in surface waters and stabilize the water column for longer (favorable conditions for *E. huxleyi*). Positive temperature and negative salinity anomalies have been correlated with *E. huxleyi* bloom occurrence in the Barents Sea (Smyth et al. 2004). In addition, a potential *E. huxleyi* bloom was detected in the Barents Sea in June 1998 that was less intense than other years. In the same study it was reported that the frequency of coccolithophore blooms in the Barents Sea may be increased if global warming persists and stimulates warming and increased runoff. Our results, based on a 20-yr time series (AVHRR), showed that there was a pronounced temperature shift from 1996 to 2004 in the subarctic North Atlantic. The results also suggested that coccolithophores are probably favored by anomalously warm temperatures, when this increase co-occurs with their seasonal peak (usually June in the area of study). A possible reaction of coccolithophore blooms to this warmth is an increase in their abundance. If the latter is true, it can have a major affect on the oceanic and atmospheric environment of the North Atlantic as these blooms are thought to play a key role in biogeochemical cycling and contribute in a major way to climatic processes (Tyrrell et al. 1999; Holligan et al. 1993; Westbroek et al. 1993). However, the short time series of SeaWiFS (1997–present) does not allow us to draw any significant conclusions on the decadal changes of coccolithophores. Nevertheless, if their spatial extent varies significantly, then their contribution to these cycles or the impacts to the environment will vary too.

### References

- BALCH, W. M., P. M. HOLLIGAN, S. G. ACILESON, AND K. J. VOSS. 1991. Biological and optical-properties of mesoscale coccolithophore blooms in the gulf of Maine. *Limnol. Oceanogr.* 36: 629–643.
- , K. A. KILPATRICK, P. HOLLIGAN, D. HARBOUR, AND E. FERNANDEZ. 1996a. The 1991 coccolithophore bloom in the central North Atlantic. I. Relating optics to coccolith concentration. *Limnol. Oceanogr.* 41: 1684–1696.
- , ———, AND C. C. TREES. 1996b. The 1991 coccolithophore bloom in the central North Atlantic. I. Optical properties and factors affecting their distribution. *Limnol. Oceanogr.* 41: 1669–1683.
- BRAND, L. E., W. G. SUNDA, AND R. R. L. GUILLARD. 1983. Limitation of marine phytoplankton reproductive rates by zinc, manganese, and iron. *Limnol. Oceanogr.* 28: 1182–1198.
- BROERSE, A. T. C., T. TYRRELL, J. R. YOUNG, A. J. POULTON, A. MERICO, W. M. BALCH, AND P. I. MILLER. 2003. The cause of bright waters in the Bering Sea in winter. *Cont. Shelf Res.* 23: 1579–1596.
- BROWN, C. W., AND J. A. YODER. 1994. Coccolithophorid blooms in the global ocean. *J. Geophys. Res. Oceans.* 99: 7467–7482.
- CHAMBERS, J. M., AND T. J. HASTIE. 1992. Statistical models in S-plus. Wadsworth & Brooks.
- COKACAR, T., T. OGUZ, AND N. KUBILAY. 2004. Satellite-detected early summer coccolithophore blooms and their interannual variability in the Black Sea. *Deep-Sea Res. Part I. Oceanogr. Res. Pap.* 51: 1017–1031.
- EKMAN, V. W. 1905. On the influence of the Earth's rotation on ocean currents. *Arkiv for Matematik, Astronomi, och Fysik* 2: 1–53.
- HASTIE, T., AND R. TIBSHIRANI. 1990. Generalized additive models. Chapman & Hall.
- HAYS, G. C., A. J. WARNER, A. W. G. JOHN, D. S. HARBOUR, AND P. M. HOLLIGAN. 1995. Coccolithophores and the continuous plankton recorder survey. *J. Mar. Biol. Assoc. U.K.* 75: 503–506.
- HOLLIGAN, P. M., AND OTHERS. 1993. A biogeochemical study of the coccolithophore *Emiliania huxleyi* in the north Atlantic. *Global Biogeochem. Cycles* 7: 879–900.
- IGLESIAS-RODRIGUEZ, M. D., AND OTHERS. 2002. Representing key phytoplankton functional groups in ocean carbon cycle models: Coccolithophorids. *Global Biogeochem. Cycles.* 16, 1100, doi: 10.1029/2001GB001454.
- KALNAY, E., AND OTHERS. 1996. The NCEP/NCAR 40-year reanalysis project. *Bull. Amer. Meteorol. Soc.* 77: 437–471.
- LESSARD, E. J., A. MERICO, AND T. TYRRELL. 2005. Nitrate to phosphate ratios and *Emiliania huxleyi* blooms. *Limnol. Oceanogr.* 50: 1020–1024.
- LU, R. 2005. Impact of Atlantic sea surface temperatures on the warmest global surface air temperature of 1998. *J. Geophys. Res.* 110, D05103, doi: 10.1029/2004JD005203.
- MARAVELIAS, C. D. 2001. Habitat associations of Atlantic herring in the Shetland area: influence of spatial scale and geographic segmentation. *Fish. Oceanography.* 10: 259–267.
- NANNINGA, H. J., AND T. TYRRELL. 1996. Importance of light for the formation of algal blooms by *Emiliania huxleyi*. *Mar. Ecol. Prog. Ser.* 136: 195–203.
- PICKARD, G. L., AND S. POND. 1978. Introductory dynamic oceanography. 2nd ed. Pergamon Press.
- RIEBESELL, U., I. ZONDERVAN, B. ROST, P. D. TORTELL, R. E. ZEEBE, AND F. M. M. MOREL. 2000. Reduced calcification of marine plankton in response to increased atmospheric CO<sub>2</sub>. *Nature* 407: 364–367.
- REID, P. C., J. B. L. MATTHEWS, AND M. A. SMITH [EDS.]. 2003. Achievements of the Continuous Plankton Recorder survey and a vision for its future. *Prog. Oceanogr.* 58: 115–358.
- SMYTH, T. J., T. TYRRELL, AND B. TARRANT. 2004. Time series of coccolithophore activity in the Barents Sea, from twenty years of satellite imagery. *Geophys. Res. Lett.* 31, L11302, doi: 10.1029/2004GL019735.
- TYRRELL, T., AND A. MERICO. 2004. *Emiliania huxleyi*: Bloom observations and the conditions that induce them, p. 75–97. In H. R. Thiertein and J. R. Young [eds.], *Coccolithophores: from molecular processes to global impact*. Springer-Verlag.
- , P. M. HOLLIGAN, AND C. D. MOBLEY. 1999. Optical impacts of oceanic coccolithophore blooms. *J. Geophys. Res. Oceans.* 104: 3223–3241.
- , AND A. H. TAYLOR. 1996. A modelling study of *Emiliania huxleyi* in the NE Atlantic. *J. Mar. Syst.* 9: 83–112.
- VOSS, K. J., W. M. BALCH, AND K. A. KILPATRICK. 1998. Scattering and attenuation properties of *Emiliania huxleyi* cells and their detached coccoliths. *Limnol. Oceanogr.* 43: 870–876.
- WEBB, D. J., A. BEVERLY DE CUEVAS, AND A. C. COWARD. 1998. The first main run of the OCCAM Global Ocean Model, internal document 34. Southampton Oceanography Centre.
- WEEKS, S. J., B. CURRIE, AND A. BAKUN. 2002. Satellite imaging—massive emissions of toxic gas in the Atlantic. *Nature* 415: 493–494.

- , G. C. PITCHER, AND S. BERNARD. 2004. Satellite monitoring of the evolution of a coccolithophorid bloom in the southern Benguela upwelling system. *Oceanography* 17: 83–89.
- WESTBROEK, P., AND OTHERS. 1993. A model system approach to biological climate forcing: The example of *Emiliana huxleyi*. *Global Planet Change* 8: 27–46.
- YELLAND, M., AND P. K. TAYLOR. 1996. Wind stress measurements from the open ocean, *J. Phys. Oceanogr.* 26: 541–558.

*Received: 3 October 2005*

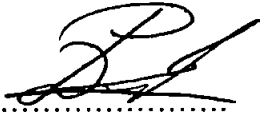
*Accepted: 9 February 2006*

*Amended: 10 April 2006*

## COPYRIGHT STATEMENT

*This copy of the thesis has been supplied on condition that anyone who consults it is understood to recognise that its copyright rests with its author and that no quotation from the thesis and no information derived from it may be published without the author's prior consent.*

Signed.....



24 . 11 . 06.

**Raitos D.E.**